

School of Medicine
Systems Immunity Research Institute

*Ysgol Meddygaeth
Sefydliad Ymchwil Systemau Imiwedd*



MOLECULAR AND CELLULAR BASIS OF T-CELL RESPONSES TO MELANOMA ANTIGENS

VALENTINA BIANCHI

A thesis submitted to Cardiff University
in candidature for the degree of
Doctor of Philosophy

April 2016

CANCERRESEARCHWALES
YMCHWILCANSERCYMRU



DECLARATION

This work has not been submitted in substance for any other degree or award at this or any other university or place of learning, nor is being submitted concurrently in candidature for any degree or other award.

Signed Date

STATEMENT 1

This thesis is being submitted in partial fulfilment of the requirements for the degree of PhD.

Signed Date

STATEMENT 2

This thesis is the result of my own independent work/investigation, except where otherwise stated. Other sources are acknowledged by explicit references. The views expressed are my own.

Signed Date

STATEMENT 3

I hereby give consent for my thesis, if accepted, to be available online in the University's Open Access repository and for inter-library loan, and for the title and summary to be made available to outside organisations.

Signed Date

Acknowledgments

Several colleagues and collaborators have contributed to my research in Cardiff, which has been funded by **Cancer Research Wales**. Firstly, I would like to acknowledge my main supervisor, **Andrew Sewell**, for giving me the opportunity to carry out this interesting project in his research group. Thank you for taking time to read my thesis and for your guidance during postdoc applications. A special mention to **Garry Dolton**, whose support went above and beyond his duties as my co-supervisor. Thank you for your help in experimental design and for always demonstrating patience and enthusiasm throughout my time as your student. I am also grateful to **David Cole** for his supervision in the Gp100 project and for his crucial advice during the paper-writing process.

I would like to acknowledge all the help received from: **Anna Bulek**, **Anna Fuller** and **Andrew Trimby** for protein expression and purification; **Mateusz Legut**, **Sarah Theaker**, **Cristina Rius Rafael** and **Sarah Galloway** for their precious support with T-cell cloning and tissue culture; **Angharad Lloyd** for lentivirus production and molecular biology; **Katie Tungatt** for tetramer staining; **Catherine Naseriyan** (CBS Flow Cytometry Facility, Cardiff) for cell sorting; **Barbara Szomolay** for the computational analysis and use of the PI-CPL webtool. **Meriem Attaf** performed the TCR clonotyping of T-cell clones, optimised PCR conditions and greatly contributed to the TCR repertoire study. Thank you to **Pierre Rizkallah** for introducing me to X-ray crystallography and helping with diffraction data collection and analysis. I also acknowledge **Diamond Light Source** (Oxfordshire) for providing facilities and technical support at the synchrotron. Patient samples and melanoma cell lines used in this thesis were kindly provided by **Inge Marie Svane**, **Per thor Straten** and **Marco Donia** from the Cancer Centre of ImmunoTherapy (CCIT, Copenhagen, Denmark) who have been precious research collaborators. Thank you for your hospitality in Copenhagen and for providing invaluable feedback.

All the members of the **T-cell Modulation group** at the Henry Wellcome Building have greatly contributed to my professional and personal time in Cardiff. On a personal note, I would like to thank the present and past members of the **2F04 office** (Mike, Juneid, Angharad, Katie, Alicia, Sarah and Amandine) for the Janeway's study groups, 'Review crew', monthly bakes and the non-scientific conversations. A special mention goes to Angharad and Katie for being such awesome friends inside and outside the lab. Thank you also to Anna Rita, Diana and Andrea for the lunch breaks away from the laptop and their support during thesis writing.

Finally, I would like to add personal thanks to **Phil Taylor**, **Matthias Eberl** and **Kathy Trantafilou** for taking the time to read my annual progress reports; **Alan Parker**, **David Gilham** and **Zsuzsanna Tabi** for accepting to be my viva examination panel.

Summary

Background — Malignant melanoma is an aggressive form of skin cancer with poor prognosis. Current immunotherapies targeting melanoma using the patient's immune system can achieve long-term melanoma clearance in some patients. T-cells are the main effectors of this anti-melanoma immunity and can specifically recognise and lyse tumour cells. T-cells express unique surface T-cell receptors (TCR) which recognise tumour-derived peptide antigens bound to a Human Leukocyte Antigen (HLA) molecule on melanoma cells. My research aimed at studying anti-melanoma T-cell responses from both a molecular and cellular level.

Results — Initially, I analysed the first crystallographic structure of a TCR in complex with a peptide from the melanoma protein Glycoprotein(gp)100 bound to HLA-A2. I show that an unanticipated molecular switch of the position(P)4-5 peptide bond by substitution of the P3 residue could abrogate recognition by host TCRs. I then dissected successful T-cell responses, restricted to specific HLA alleles, in melanoma infiltrates from two complete responder (CR) patients after Tumour Infiltrating Lymphocyte (TIL) therapy. The antigen specificity and phenotype of anti-melanoma TILs were evaluated, and a panel of TIL clones capable of lysing autologous melanoma cell targets was characterised. Interestingly, in each patient studied, melanoma-specific clonotypes detected in the TILs persist in the blood after TIL therapy and recognise T-cell epitopes shared by other patients and other tumour types.

Conclusions — I demonstrate that structural studies should be considered when designing improved peptide cancer vaccines as even single substitutions in residues not heavily engaged by the TCR can have important, unpredictable knock-on effects that impair T-cell recognition. Understanding the key antigen-specificities of anti-tumour TILs from CR patients, will improve the efficacy of T-cell based therapies. Validated antigens could be applied as biomarkers of, or targets for, cancer immunotherapy. Dominant shared antigens targeted in CR patients may make promising candidates for therapeutic vaccination.

Published work incorporated in this thesis:

V. Bianchi, A. Bulek, A. Fuller, A. Lloyd, M. Attaf, P. J. Rizkallah, G. Dolton, A. K. Sewell and D. K. Cole. (2016). *A molecular switch abrogates gp100 TCR-targeting of a human melanoma antigen*. Journal of Biological Chemistry 291, 8951–8959

Other papers published during my PhD:

Dolton, G., K. Tungatt, A. Lloyd, **V. Bianchi**, S. M. Theaker, A. Trimby, C. J. Holland, M. Donia, A. J. Godkin, D. K. Cole, P. T. Straten, M. Peakman, I. M. Svane, and A. K. Sewell. (2015). *More tricks with tetramers: a practical guide to staining T cells with peptide-MHC multimers*. Immunology 146, 11–22

Tungatt, K., **V. Bianchi**, M. D. Crowther, W. E. Powell, A. J. Schauenburg, A. Trimby, M. Donia, J. J. Miles, C. J. Holland, D. K. Cole, A. J. Godkin, M. Peakman, P. T. Straten, I. M. Svane, A. K. Sewell, and G. Dolton. (2015). *Antibody stabilization of peptide-MHC multimers reveals functional T cells bearing extremely low-affinity TCRs*. J. Immunol. 194, 463–474

Presentations of the results described in this thesis:

Cancer Research Wales 50th Anniversary Symposium, poster presentation (Cardiff, 01/03/16)

Ludwig Centre for Cancer Research, invited speaker (Lausanne, 14/01/16)

Infection and Immunity seminar series, oral presentation (Cardiff 18/05/15)

Symposium on Molecular Aspects of Biology, oral presentation (Cardiff 15/04/15)

School of Medicine, Postgraduate Research Day 2014, oral presentation (Cardiff 12/12/14)

British Society of Immunology (BSI) annual congress, poster presentation (Brighton 1-4/12/14)

Institute of Infection and Immunity annual meeting 2014, oral presentation (Cardiff 20/11/14)

South West Structural Biology Consortium (SWSBC) conference, oral presentation (Bath 23-24/6/14)

British Society for Gene and Cell Therapy (BSGCT) conference, poster presentation (London 28/3/14)

Cardiff Institute of Infection and Immunity annual meeting 2014, (Cardiff 26/9/13)

SWSBC annual conference, poster presentation (Bristol 1-2/7/13)

Abbreviations

β2m	Beta2-microglobulin
Ab	Antibody
ACT	Adoptive cell transfer
APC	Allophycocyanin
ATCC	American-type culture collection
BSA	Bovine serum albumin
C	Celsius
CD	Cluster of differentiation
cDNA	Complementary deoxyribonucleic acid
CDR	Complementarity determining region
CLIP	Class II-associated Invariant-chain Peptide
CTL	Cytotoxic T lymphocyte
Cr	Chromium
CRISPR	Clustered Regularly-Interspaced Short Palindromic Repeats
DAMP	Damage-associated molecular pattern
DC	Dendritic cell
DMEM	Dulbecco modified eagle's minimal essential media
DMSO	Dimethyl sulphoxide
DNA	Deoxyribonucleic acid
<i>E. coli</i>	<i>Escherichia coli</i>
EDTA	Ethyl-enediaminetetra acetic acid
ELISA	Enzyme-Linked Immunosorbent Assay
ELISpot	Enzyme-Linked ImmunoSpot
ER	Endoplasmic reticulum
FACS	Fluorescence-activated cell sorting
FBS	Foetal bovine serum
FDA	Food and Drug Administration
FITC	Fluorescein isothiocyanate
FPLC	Fast protein liquid chromatography
GEM	Germline-Encoded Mycolyl-reactive cell
GF	Gel filtration
HLA	Human Leukocyte Antigen
HLA-I	Human Leukocyte Antigen class-I
HLA-II	Human Leukocyte Antigen class-II
HRP	Horseradish peroxidase
IFN	Interferon
IE	Ion exchange
IL	Interleukin
IPTG	Isopropyl β-D-1-thiogalactopyranoside
ITAM	Immuno-receptor tyrosine-based activation motif
ITC	Isothermal Titration Calorimetry
ITIM	Immuno-receptor tyrosine-based inhibition motif
IU	International Units
MAA	Melanoma associated antigen
mAb	Monoclonal antibody
MAIT	Mucosal-Associated Invariant T-cell
MAPK	Mitogen-Activated Protein Kinase
MHC-I	Major Histocompatibility Complex class-I
MHC-II	Major Histocompatibility Complex class-II
MIP	Macrophage Inflammatory Protein
mRNA	Messenger Ribonucleic Acid
N	Non-germline

NKT	Natural Killer T-cell
NGS	Next Generation Sequencing
PBMC	Peripheral blood mononuclear cell
PBS	Phosphate buffered saline
PCR	Polymerase Chain Reaction
PE	Phycoerythrin
PFA	Paraformaldehyde
PI	Protease inhibitor
PKI	Protein Kinase Inhibitor
RACE	Rapid Amplification of cDNA Ends
RAG	Recombinase-Activating Gene
RNA	Ribonucleic Acid
RT	Reverse Transcriptase
SDS-PAGE	Sodium Dodecyl Sulphate-Polyacrylamide Gel Electrophoresis
SPR	Surface Plasmon Resonance
TAA	Tumour-Associated Antigen
TAP	Transporter associated with antigen processing
TAPI	TNF- α Protease Inhibitor
TCR	T-cell receptor
TIL	Tumour Infiltrating Lymphocyte
TNF	Tumour Necrosis Factor
VDJ	Variable, Diversity, Joining region
UV	Ultraviolet

All units of measure and their abbreviations used in this thesis, follow the International System of Units, unless otherwise specified.

Amino acids are designated by the single-letter or three-letter nomenclature.

Table of contents

1	INTRODUCTION.....	1
1.1	Cutaneous melanoma.....	1
1.1.1	Melanocytes and melanoma progression.....	1
1.1.2	Therapy options: past, present and future.....	3
1.2	$\alpha\beta$ T-cell immunity and cancer.....	5
1.2.1	Antigen presentation to $\alpha\beta$ T-cells.....	6
1.2.1.1	<i>MHC structure.....</i>	<i>6</i>
1.2.1.2	<i>Antigen processing.....</i>	<i>8</i>
1.2.2	T-cell receptor (TCR).....	9
1.2.3	Generation of diversity.....	10
1.2.4	T-cell development and selection.....	12
1.2.5	The production of effector T-cells.....	13
1.2.5.1	<i>CD8+ cytotoxic T-cells.....</i>	<i>15</i>
1.2.5.2	<i>CD4+ T-cells.....</i>	<i>16</i>
1.3	T-cells and melanoma.....	17
1.3.1	Melanoma cells are antigenic.....	17
1.3.1.1	<i>Differentiation antigens.....</i>	<i>17</i>
1.3.1.2	<i>Cancer-testis antigens.....</i>	<i>17</i>
1.3.1.3	<i>Over-expressed antigens.....</i>	<i>18</i>
1.3.1.4	<i>Neo-antigens.....</i>	<i>18</i>
1.3.2	CD8+ T-cell responses in melanoma.....	19
1.3.3	CD4+ T-cell responses in melanoma.....	20
1.4	T-cell based immunotherapy approaches for metastatic melanoma.....	21
1.4.1	Improving antigenic peptide vaccines.....	21
1.4.2	Adoptive Cell Transfer (ACT) for the treatment of metastatic melanoma.....	24
1.4.2.1	<i>Tumour Infiltrating Lymphocyte (TIL)-based therapy.....</i>	<i>24</i>
1.4.2.2	<i>TIL isolation and production.....</i>	<i>24</i>
1.4.2.3	<i>Lessons from using genetically redirected T-cells.....</i>	<i>27</i>
1.4.3	T-cell checkpoint inhibitors.....	29
1.4.4	Towards personalised approaches.....	31
1.5	Project aims.....	32
2	MATERIALS AND METHODS.....	33
2.1	Protein expression, refolding and purification.....	33
2.1.1	Vectors for protein expression.....	33
2.1.2	Protein sequences.....	33
2.1.3	Culture media and buffers used for protein expression, refolding and purification	34
2.1.4	Transformation of competent E. coli cells.....	35
2.1.5	Expression of inclusion bodies in Rosetta E. Coli.....	35
2.1.6	Estimating protein concentration by spectrophotometry.....	35
2.1.7	Sodium Dodecyl Sulphate-Polyacrylamide Gel Electrophoresis (SDS-PAGE).....	36

2.1.8	Soluble pMHC-I and TCR	36
2.1.9	Fast Protein Liquid Chromatography (FPLC)	36
2.1.10	Biotinylation of pMHC	37
2.2	Surface Plasmon Resonance (SPR) analysis	37
2.3	Isothermal Titration Calorimetry (ITC).....	38
2.4	Crystallisation, diffraction data collection and model refinement	38
2.5	TCR lentiviral transduction of primary human CD8+ T-cells	40
2.5.1	293T cells CaCl ₂ transfection for lentivirus particles production	40
2.5.2	Lentiviral transduction of primary CD8+ T-cells.....	40
2.6	Cell culture media and buffers	41
2.7	Cell culture	42
2.7.1	Cell count	42
2.7.2	Cryopreservation and thawing of cell lines.....	43
2.8	Generation of TILs and melanoma cell lines	43
2.8.1	Patient samples.....	43
2.8.2	HLA typing.....	44
2.9	Maintenance and expansion of T-cell cultures	44
2.9.1	Isolation of peripheral blood mononuclear cells (PBMCs).....	44
2.9.2	Expansion and culture of T cells.....	44
2.10	Functional T-cell assays.....	45
2.10.1	Peptides	45
2.10.2	IFN- γ Enzyme-Linked ImmunoSpot (ELISpot) assay	45
2.10.3	⁵¹ Chromium (⁵¹ Cr) release cytotoxicity assay	46
2.10.4	Peptide activation assay by Enzyme Linked Immunosorbent Assay (ELISA).....	46
2.10.5	MIP-1 β /TNF- α ELISA	46
2.10.6	Combinatorial peptide library (CPL) scans	47
2.10.6.1	<i>Epitope identification</i>	<i>48</i>
2.11	Flow cytometric analysis.....	49
2.11.1	Labelling cells with fluorescence conjugated antibodies.....	49
2.11.2	Intracellular cytokine staining (ICS) assay	50
2.11.3	Blocking antibody assay	50
2.11.4	pMHC tetramer staining	51
2.11.4.1	<i>“Boosted” pMHC tetramer staining.....</i>	<i>51</i>
2.11.5	Viable sorting of tumour reactive T cells	52
2.12	Analysis of human TCR Vβ CDR3 repertoire.....	53
2.12.1	Total RNA extraction	53
2.12.2	SMARTer™ RACE cDNA amplification	53
2.12.2.1	<i>First strand cDNA synthesis</i>	<i>53</i>
2.12.2.2	<i>First PCR amplification.....</i>	<i>55</i>
2.12.2.3	<i>Second PCR amplification</i>	<i>55</i>
2.12.2.4	<i>Agarose gel electrophoresis.....</i>	<i>56</i>
2.12.2.5	<i>DNA extraction from gel bands and purification for cloning.....</i>	<i>56</i>
2.12.3	Molecular cloning and bacterial transformation	56

2.12.3.1	<i>Zero Blunt® TOPO® PCR Cloning</i>	56
2.12.3.2	<i>Transformation of One Shot® TOP10</i>	57
2.12.3.3	<i>Colony PCR</i>	57
2.12.4	Sequence analysis	58
2.13	Figures and data analysis	58
3	A MOLECULAR SWITCH IN A GP100 HUMAN MELANOMA ANTIGEN ABROGATES T-CELL RECOGNITION	59
3.1	Background	59
3.1.1	Aims	60
3.2	Results	61
3.2.1	Production of soluble TCR and pHLA ectodomains	61
3.2.2	Two distinct anti-gp100 TCRs share similar binding hotspots	64
3.2.3	The PMEL17 TCR utilizes a peptide-centric binding mode to engage A2-YLE-9V ...	66
3.2.4	The PMEL17 CDR loops focus on YLE residues Pro4, Val7 and Thr8	69
3.2.5	Binding thermodynamics and affinity of the GP100 TCR/A2-YLE complex.....	71
3.2.6	Peptide substitutions can induce perturbation at adjacent peptide residues abrogating T-cell recognition	73
3.2.7	Alanine substitutions in YLE positions 3 and 5 abrogate T-cell activation	75
3.3	Discussion	78
4	DISSECTION OF T-CELL RESPONSES IN AN HLA-A2+ REMISSION MELANOMA PATIENT AFTER TIL-THERAPY	80
4.1	Background	80
4.1.1	TIL-therapy at the CCIT (Copenhagen, Denmark)	80
4.1.2	Aims	81
4.2	Results	82
4.2.1	Patient characteristics and experimental approach	82
4.2.2	Anti-melanoma reactivity of TILs MM909.24	84
4.2.3	Multiple clonotypes mediate an HLA-A2-restricted Melan-A specific anti-tumour response in patient MM909.24.....	87
4.2.4	Unexpected cross-recognition by MM909.24 Melan-A-specific clone ST8.24	93
4.2.5	Tumour-reactive T-cell clones persist in the patient's blood after TIL-therapy.....	98
4.3	Discussion	103
4.3.1	Antigen specificity of tumour reactive TILs.....	103
4.3.2	Cross-reactive potential of T-cell responses in melanoma TILs.....	105
4.3.3	Tracking the fate of tumour-reactive TIL clones	106
5	DISSECTION OF T-CELL RESPONSES IN A NON-HLA-A2+ MELANOMA PATIENT WITH COMPLETE REMISSION AFTER TIL-THERAPY	108
5.1	Aims	108
5.2	Results	108
5.2.1	Anti-tumour responses of MM909.15 TILs	108
5.2.2	CD4+ T-cell response in TILs from patient MM909.15.....	114

5.2.3	Peptide specificity of the dominant clone in the patient blood after cure.....	116
5.3	Discussion.....	120
5.3.1	Heterogeneous cellular composition of TIL infusion products	120
5.3.2	T-cell responses to the TAG cancer-testis antigen.....	121
5.3.3	Persistence of T-cell clones in the blood after cure	122
6	GENERAL DISCUSSION AND CONCLUSIONS.....	124
6.1	Discussion.....	124
6.2	Future perspectives in melanoma immunotherapy	126
6.2.1	The role of the tumour microenvironment	126
6.2.2	The future of peptide cancer vaccines.....	126
6.2.3	Improvement of TIL therapy and future questions.....	127
6.2.3.1	<i>Extension to other tumour types</i>	<i>128</i>
6.3	Concluding remarks	129
7	APPENDIX	130

List of Figures

Figure 1.1. Schematic representation of melanoma progression	2
Figure 1.2. Antigen presentation by MHC class-I and MHC class-II molecules.....	7
Figure 1.3. The $\alpha\beta$ TCR structure and CDR loops	9
Figure 1.4. Human TCR α - and β -chain gene rearrangement and expression.....	11
Figure 1.5. Simplified diagram of T-cell development and selection	12
Figure 1.6. Schematic diagram of a successful anti-tumour T-cell immune response	14
Figure 1.7. Signatures of mutational processes in melanoma compared to other human cancers (from Alexandrov et al., 2013)	19
Figure 1.8. Mechanism of action of an effective peptide cancer vaccine	22
Figure 1.9. Examples of peptide enhancement strategies for melanoma vaccines	23
Figure 1.10. Schematic diagram of TIL isolation and expansion for ACT.....	25
Figure 1.11. Checkpoint blockade antibodies	29
Figure 2.1. Schematic representation of the SPR system.....	37
Figure 2.2. Example of MIP-1 β standard curve	47
Figure 2.3. Schematic diagram of a 10mer combinatorial peptide library.....	48
Figure 2.4. Schematic representation of the 'boosted' pMHC tetramer staining protocol used.....	51
Figure 2.5. Experimental workflow of the SMARTer RACE approach to TCR- β profiling	54
Figure 2.6. Agarose gel analysis of SMARTer RACE cDNA products	56
Figure 3.1. PMEL17 TCR protein purification	62
Figure 3.2. HLA-A2-YLE protein purification.....	63
Figure 3.3. Binding affinity analysis (25°C) of A2-YLE variants	65
Figure 3.4. Overview of the PMEL17 TCR/A2-YLE complex.....	67
Figure 3.5. The PMEL17 CDR loops focus on peptide residues Pro4, Val7 and Thr8.....	70
Figure 3.6. PMEL17 TCR equilibrium-binding responses to A2-YLE at 5, 12, 18, 25 and 37°C.....	72
Figure 3.7. Thermodynamic analysis of the PMEL17 TCR/A2-YLE interaction	73
Figure 3.8. Conformational comparison of YLE, YLE-3A and A2-YLE-5A peptides presented by HLA-A*0201	74
Figure 3.9. Gp100 TCR expression by transduced primary CD8+ human T-cells.....	76
Figure 3.10. Production of MIP-1 β , TNF α and cytotoxicity by gp100 TCR transduced CD8 ⁺ T-cells in response to stimulation with YLE peptide ligands	77
Figure 4.1. Patient MM909.24 characteristics, TIL composition and autologous tumour HLA expression	83
Figure 4.2. MM909.24 TILs reactivity to autologous tumour is mediated by CD8+ T-cells and is HLA class-I restricted	85
Figure 4.3. MM909.24 TIL tumour reactivity is predominantly HLA-A2 restricted	86

Figure 4.4. Schematic outline of the experimental strategy used to dissect anti-melanoma TILs from patient MM909.24	87
Figure 4.5. Melan-A T-cell epitope (ELAGIGILTV) recognition by TILs MM909.24	88
Figure 4.6. ELA-specific TIL population increases during in vitro culture with autologous tumour	90
Figure 4.7. Melan-A specific clones from TILs MM909.24 exhibit differing sensitivity to antigen and express unique TCRs.....	91
Figure 4.8. ST8.24 reacts towards C1R-A2 cells but fails to recognise EBV-immortalised B-cell lines .	93
Figure 4.9. ST8.24 recognises multiple cancer cell types	94
Figure 4.10. Decamer CPL scan of the ST8.24 clone.....	96
Figure 4.11. ST8.24 peptide cross-reactivity	98
Figure 4.12 CDR3 sequences in the TCR beta repertoire of TILs and PBMC from patient MM909.24	100
Figure 4.13 T-cell clone VB8#8 from TILs MM909.24 is ELA-specific	102
Figure 5.1. Patient MM909.15 characteristics, TIL composition and autologous tumour HLA expression.	109
Figure 5.2. MM909.15 TILs reactivity against autologous tumour (gated on CD8 and CD4)	111
Figure 5.3. MM909.15 TILs reactivity against partially matched panel of melanoma cell lines.....	112
Figure 5.4. ELISpot response to 16 known A3-restricted melanoma antigens.....	113
Figure 5.5. CD4+ TILs reactivity against a panel of partially matched melanoma cell lines	114
Figure 5.6. ML30.15 CD4+ cytotoxic clone	115
Figure 5.7. TCR β repertoire diversity in tumour-reactive TILs and PBMC from patient MM909.15..	117
Figure 5.8. Dominant clone ML33.15 (TRBV5-1) is specific for a A3-restricted TAG peptide (RLS)....	119
Figure 6.1. A strategy for dissecting unknown T-cell clones from anti-melanoma TIL and PBMC samples	125
Figure 7.1. Density plot analysis.....	130
Figure 7.2. MM909.24 TIL reactivity against a panel of semi-matched HLA-A2+ melanoma cell lines	132
Figure 7.3. CD8+ TILs MM909.15 reactivity against a panel of melanoma cell lines.....	137
Figure 7.4. CD4+ TILs MM909.15 reactivity against a panel of melanoma cell lines.....	138
Figure 7.5. TAG T-cell reactivity detected in a complete remission HLA-A3, HLA-A1+ melanoma patient (MM909.11).....	139
Figure 7.6. CDR3 sequences in the TCR beta repertoire of TILs and PBMC MM909.11.....	140

List of Tables

Table 1.1. Treatment protocols and clinical results in TIL-based ACT trials	26
Table 1.2. Published reports of genetically redirected T-cells in melanoma	27
Table 2.1. Data collection and refinement statistics (molecular replacement)	39
Table 3.1. Alanin scan mutagenesis	65
Table 3.2. PMEL17 TCR-A2-YLE-9V contact table	68
Table 3.3. Alignment of TCR CDR3 regions of four gp100-specific TCRs	79
Table 4.1. Peptides sequences resulting from ST8.24 CPL scan ranked in order of recognition likelihood	97
Table 7.1. Panel of melanoma cell lines	131
Table 7.2. List of A2-restricted melanoma-associated peptides (from Andersen et al., 2012)	133
Table 7.3 List of A1- or A3-restricted melanoma associated peptides (from Andersen et al., 2012)	135
Table 7.4. Overview of T-cell clones isolated from MM909.24 TIL cultures	136

1 Introduction

1.1 Cutaneous melanoma

Cutaneous melanoma, a cancer derived from the epidermal melanocytes of the skin, is a disease of major public health significance. Although it is the least common form of skin cancer, melanoma is by far the most lethal due to its tendency to metastasize to a number of vital organs (Leung et al., 2012). Global estimates of mortality for melanoma show that the disease is responsible for over 65,000 deaths annually (Berwick et al., 2016). Moreover, data collected by the Cancer Statistics Review Program show that melanoma incidence rates have continued to increase over the past 40 years¹. Cutaneous melanoma incidence rates vary up to 100-fold throughout different populations, with the highest rates reported in Australia and New Zealand (60 cases per 100,000 inhabitants per year) (Erdmann et al., 2012). In Europe, the rate is of approximately 20 cases per 100,000 per year (Garbe et al., 2012). Clinically, melanoma occurs most commonly in individuals between the age of 40 and 60, but it can affect adolescents and the elderly (> 80 years). The median age at diagnosis is 57 years, which is almost one decade before most solid tumours typically arise (Garbe et al., 2012).

Excessive sun exposure is the major risk factor for cutaneous melanoma (Lawrence et al., 2013). UV-mediated damage induces genetic transitions (C>T or G>T) that are frequently observed in melanomas, leading to an extremely high mutation rate compared to other tumours (Alexandrov et al., 2013; Hodis et al., 2012). Other major risk factors include a family history of melanoma, the presence of atypical, large or numerous moles and sun sensitivity (Boniol et al., 2012; FitzGerald et al., 1996; Gandini et al., 2005).

1.1.1 Melanocytes and melanoma progression

In the human skin, melanocytes are specialised pigmented cells in the basal layer of the epidermis, where they form melanin-producing units (Fitzpatrick et al., 1961). Mature melanocytes are characterised by cytoplasmic organelles (i.e. melanosomes) which are responsible of melanin synthesis (reviewed by Raposo and Marks, 2007). The close network between neighbouring keratinocytes and the dendritic processes of melanocytes is essential to transfer newly synthesised

¹ Howlader et al. (eds). *SEER Cancer Statistics Review, 1975-2012*, National Cancer Institute. Bethesda, MD, http://seer.cancer.gov/csr/1975_2012/, based on November 2014 SEER data submission, posted to the SEER web site, April 2015.

melanin into keratinocytes, and is involved in determining skin colour and photo-protection (Plonka et al., 2009).

The transformation of normal melanocytes into melanoma is a multistep process during which pigmented cells acquire distinct phenotypic features, schematically illustrated in **Figure 1.1**. The first event in melanoma development is the formation of benign *nevi* (commonly known as moles) due to the proliferation of structurally normal melanocytes (Alonso et al., 2004; Clark et al., 1984). These primary lesions are flat or slightly raised, with a uniform pigmentation. The next step is the aberrant growth of atypical cells within a pre-existing *nevus* or in a new location. Changes in the symmetry, diameter and colour of benign *nevi*, or the appearance of a new growth, are all important warning signs of atypical lesions evolving (Boland and Gershenwald, 2016). Due to the presence of melanin pigment, melanoma can be accurately diagnosed earlier at these primary stages, compared to most other malignancies.

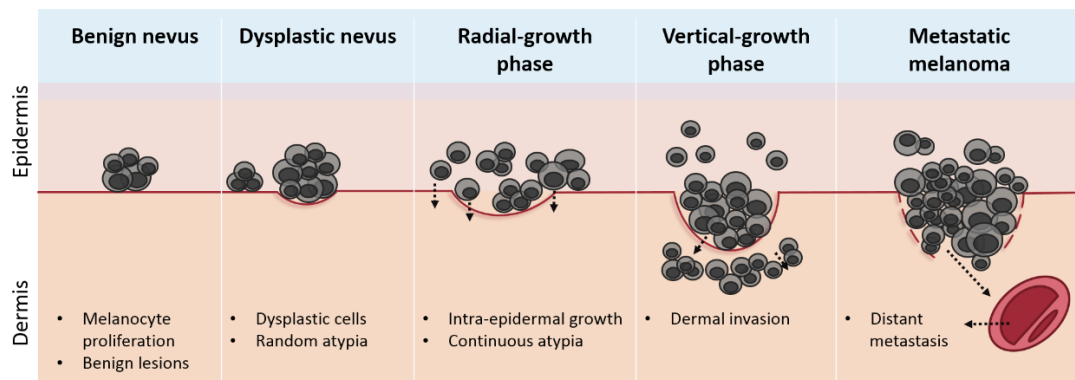


Figure 1.1. Schematic representation of melanoma progression

Normal melanocytes progressively develop a malignant phenotype through the acquisition of various phenotypic features. Clinical and histological features are shown in the insert.

During a later stage (i.e. radial-growth phase), melanocytes become dysplastic and acquire the ability to proliferate in small intra-epidermal nests. Lesions that progress to the following vertical-growth phase, also acquire the ability to invade the dermis and form an expansive nodule, widening the papillary dermis. The final step of melanoma transformation consists of the successful spread of melanoma cells into other areas of the skin and/or vital organs (most commonly the brain, lungs and liver), where tumour cells successfully proliferate and establish metastatic foci (Alonso et al., 2004; Clark et al., 1984). Of note, metastatic spread can also be initiated at earlier stages even during primary lesion formation (Damsky et al., 2014).

Cutaneous melanoma classification involves distinct stages that take into account the depth and thickness of the lesion, and whether or not the tumour has spread to other sites² (Balch et al., 2009; Gershenwald et al., 2010). Stages 0 and I tumours (early melanomas) are mostly *in situ*, meaning that they are small, localised and non-invasive. Stage II tumours (intermediate melanomas), although still localised, are larger (> 1 mm), have penetrated below the surface of the skin and have a greater mitotic rate. Once a melanoma has progressed beyond Stage II, it is likely to have spread beyond the original site. More advanced melanomas metastasise to the regional lymph nodes (Stage III) and/or to other parts of the body (Stage IV), through tissues, the lymphatic system or the blood.

1.1.2 Therapy options: past, present and future

The staging classification described above is also used to determine melanoma treatment. Surgical resection is still considered the primary option at all stages, in particular early diagnosed benign or localised melanoma lesions (Koshenkov et al., 2016). On the other hand, melanomas with deep invasion or that have spread to lymph nodes may be treated with chemotherapy and/or radiation therapy. Standard chemotherapy induces objective responses in less than 20%, rarely leads to complete remission, and benefits last only months (Howard and Mehnert, 2016). Despite significant breakthroughs in understanding the pathobiology of melanoma, which has resulted in new therapies, metastatic (or Stage IV) melanoma, until recently, was still associated with a poor prognosis and a median survival of 6 to 12 months. Because of the difficulty of targeting the disseminated phenotype, advanced stages of the disease are less sensitive to conventional therapeutic regimens. Until 2010, no randomized clinical trial had shown evidence for improved survival for those with Stage IV melanoma. Before then, the only two drugs that had been approved in the USA for the treatment of metastatic melanoma patients were the chemotherapeutic agent dacarbazine and the immunomodulator IL-2, both of which did not increase the median overall survival. Dacarbazine treatment yielded a low clinical response rate with short duration (Rosenberg et al., 1999; Serrone et al., 2000); high-dose IL-2 resulted in durable complete responses (6%) plus severe toxicity (Atkins et al., 1999; Phan et al., 2001).

² Revisions to the Melanoma Staging System were published in the 7th edition of the American Joint Committee on Cancer (AJCC) in 2009, and implemented January, 2010 (Balch et al., 2009).

The treatment of advanced melanoma has changed since 2011 with the Food and Drug Administration (FDA) approval of new 'targeted' drugs. These molecules were designed with the aim of interfering with genetic mutations in specific enzymatic pathways that drive melanoma growth, while leaving normal cells intact. In particular, Vemurafenib (Zelboraf®), Dabrafenib (Tafinlar®), and Trametinib (Mekinist™) target specific mutations in genes encoding for the BRAF protein (shared by nearly 50% of melanomas) or MEK protein (Huang et al., 2013; Solit and Rosen, 2011). BRAF and MEK are both key proteins in the mitogen-activated protein kinase (MAPK) pathway, which helps promote melanoma growth when defective (Davies et al., 2002). Even though BRAF inhibitors result in excellent early disease control for patients with BRAF V600E/K mutations, duration of the responses is limited to less than a year because of the development of multiple molecular mechanisms of resistance (Emery et al., 2009; Nazarian et al., 2010).

Against this background, in the past twenty years, melanoma has been the focus for the research and application of new treatment options, with the help of European guidelines that recommended stage IV melanoma patients to be preferentially enrolled on new trials (reviewed by Garbe et al., 2010). Additional characteristics of cutaneous melanoma, such as the accessible location of lesions on the skin and the adaptability of melanoma cells to *in vitro* culture conditions, have contributed to its role as a 'model tumour' for cutting-edge immunotherapies. Immunotherapy refers to all those approaches that aim to harness the patient's own immune system to eliminate autologous tumour cells. The underlying concept of immunotherapy is that tumours are characterised by several genetic and epigenetic alterations which provide the immune system with a set of antigens to distinguish transformed cells from their healthy counterparts (Burnet, 1970; Thomas, 1982). Of note, the journal *Science* named cancer immunotherapy its 2013 Breakthrough of the Year (Couzin-Frankel, 2013), to acknowledge this rising tide of treatments in melanoma, where they were first tested. My work is focused around the current spectrum of immunotherapies that engage T-cells to fight melanoma (discussed in Section 1.4); therefore, I will first introduce T-cell immunity in the following section.

1.2 $\alpha\beta$ T-cell immunity and cancer

Cells from both the innate arm (dendritic cells, natural killer cells, macrophages, mast cells, neutrophils and myeloid derived suppressor cells) and the adaptive arm (B and T lymphocytes) of the immune system are present within the tumour and interact with the malignant cells, either directly or through the production of soluble factors, therefore shaping tumour progression and its response to therapy (Janeway and Murphy, 2011). As my work focuses on the adaptive immune response to tumours mediated by T-cells, the rest of my thesis will focus on these cells in particular.

T-cells are lymphocytes derived from the bone marrow which undergo maturation within the thymus. The human T-cell population consists of several heterogeneous subsets, which contribute to the overall immune surveillance with distinct functions. Broadly speaking, T-cells can be divided into $\alpha\beta$ and $\gamma\delta$ T-cells, according to the somatically rearranged TCR heterodimer expressed on their cell surface ($\alpha\beta$ or $\gamma\delta$ TCR, respectively). $\alpha\beta$ T-cells are by far the most abundant and best characterised circulating human T-cells. Conventionally, the $\alpha\beta$ TCR is 'MHC-restricted', in that it recognises antigen in the form of foreign (or self) peptide bound to a Major Histocompatibility Complex (MHC) molecule on the surface of antigen-presenting cells. However, a significant fraction of $\alpha\beta$ T-cells that can reside at high frequencies in specific human tissues, does not fit this paradigm. These cells include: (i) invariant natural killer T (NKT) cells, (ii) mucosal-associated invariant T (MAIT) cells; and (iii) germline-encoded mycolyl-reactive (GEM) T-cells (reviewed by Godfrey et al., 2015). Collectively, these $\alpha\beta$ T-cells are named 'unconventional', because they are not MHC-restricted and can recognise lipids, small-molecule metabolites or specially modified peptides. It is becoming clear that these subsets play a role in recognising pathogens and orchestrating inflammatory responses (reviewed by Liuzzi et al., 2015). $\gamma\delta$ T-cells, which represent 1-10% of circulating T-cells, are also considered 'unconventional' as they are not MHC-restricted and do not appear to recognise peptide antigens. Several studies in mouse models have established the protective immune surveillance and antitumor activity of the $\gamma\delta$ lineage (Silva-Santos et al., 2015). These aspects fall beyond the scope of this introduction, therefore, unless otherwise stated, I will provide an overview of conventional $\alpha\beta$ T-cell immunity.

$\alpha\beta$ T-cells can be divided into CD4+ T-cells and CD8+ T-cells and then further fall under specific subsets depending on their effector functions. Broadly speaking, CD4+ T-cells are involved in helping and regulating immune responses, while CD8+ T-cells are responsible for inducing targeted killing of infected or transformed cells (Janeway and Murphy, 2011).

1.2.1 Antigen presentation to $\alpha\beta$ T-cells

MHC restriction is critical for $\alpha\beta$ T-cell function because it enables T lymphocytes to identify target cells expressing intracellular, foreign proteins or genetic mutations in cancer cells (Cole et al., 2007; Zinkernagel and Doherty, 1997). In humans, MHC molecules are encoded within the Human Leukocyte Antigen (HLA) locus, which is the most polymorphic region of the human genome (Potts and Slev, 1995). The HLA locus is located on the short arm of chromosome 6 and spans a region of about four million bp. It encodes more than 7,000 allelic variants across the population, with a large number of these variants present at appreciable frequencies (Robinson and Marsh, 2003).

The *mhc* genes encode two homologous types of proteins, MHC molecules of class-I (MHC-I) and class-II (MHC-II), which are expressed differentially on human cells. MHC-I molecules, generated from the HLA-A, -B or -C loci, are expressed by all nucleated cells and platelets (Germain, 1994). However, expression levels differ between tissues; high levels can be found in lymphocytes whereas cells in the brain or kidney express lower levels. MHC-II molecules, generated from the HLA-DR, -DP or -DQ loci, are expressed in a tissue-specific manner; with constitutive expression normally restricted to cells of the immune system (i.e. activated B cells, macrophages, and Langerhans-dendritic cells of the skin and lymphoid organs) and the thymus epithelium (Mendez et al., 2009; Radka et al., 1986; Reith et al., 2005). Several cytokines, especially interferons, are known to upregulate MHC-I and MHC-II expression (Steimle et al., 1994). MHC-I molecules present peptide antigens to CD8+ cytotoxic T-cells, whereas MHC-II molecules present peptides to CD4+ helper T-cells.

1.2.1.1 MHC structure

MHC-I molecules consist of two polypeptide chains: a highly-variable 44 kDa membrane-spanning heavy chain associated with a conserved 12 kDa β_2 microglobulin (β_2m) domain (**Figure 1.2**). The heavy chain is composed of three domains named α_1 , α_2 and α_3 . Only the membrane-distal α_1 and α_2 domains are polymorphic; these form the antigen-binding groove, a group of eight β -strands supporting two α -helices. The closed-end conformation of the $\alpha_1\alpha_2$ binding groove restricts the length of peptides presented to 8-13 amino acids. Most commonly, MHC-I accommodates a 9mer or 10mer peptide (Bouvier and Wiley, 1994; Rammensee et al., 1995; Rudolph et al., 2006). It is known, however, that longer peptides can also bind MHC-I (Burrows et al., 2008; Probst-Kepper et al., 2001); these will be fixed at both termini and, as a result, adopt a bulging conformation out of the cleft (Speir et al., 2001).

MHC-II are polypeptides of approximately 35 kDa, formed by an α - and β -chain, both of which are anchored to the plasma membrane. Each chain folds into a membrane-distal polymorphic domain followed by an Ig-like domain (Rudolph et al., 2006; Stern and Wiley, 1994). Despite structural similarities, the two MHC classes present peptides in a distinct manner that depends on the composition of their binding groove (**Figure 1.2**). Unlike MHC-I, the $\alpha 1\beta 1$ binding groove of MHC-II molecules is characterised by an open-end conformation, allowing longer peptides to bind (Lippolis et al., 2002; Stern and Wiley, 1994). The 9mer peptide core contains the motif for binding to the particular MHC-II heterodimer, but eluted and sequenced peptides reveal families of processed peptides 12–20 aa (namely, ‘nested’ peptide sets) that share the core binding region (Carson et al., 1997; Holland et al., 2013; Rudolph et al., 2006). The peptide flanking regions (i.e. the amino acids outside of the peptide core) can also interact with the MHC-II and influence peptide stability (Godkin et al., 1997). It is becoming increasingly clear that these regions may have a more specific role in T-cell recognition and TCR activation (Carson et al., 1997; Moudgil et al., 1998).

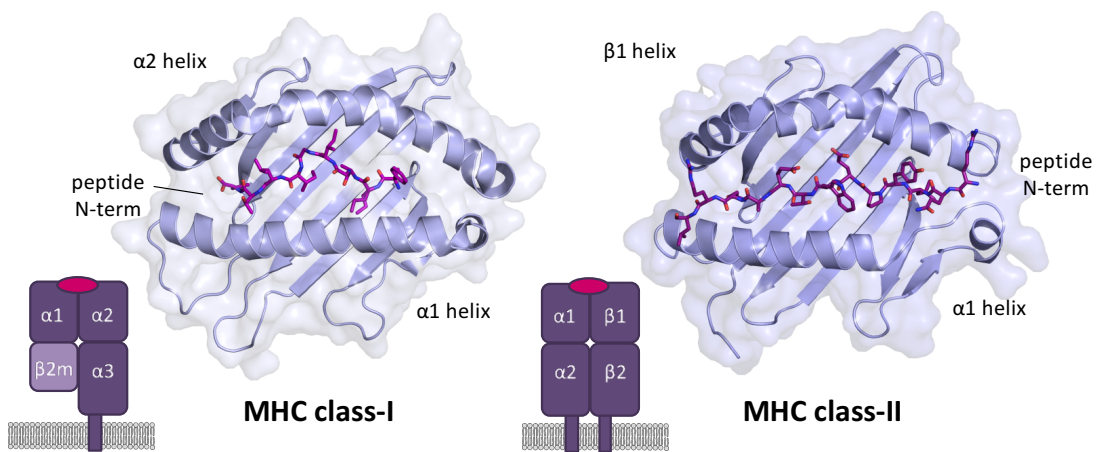


Figure 1.2. Antigen presentation by MHC class-I and MHC class-II molecules

Combined ribbon and surface representation (blue) of the human MHC-I molecule (PDB-code: 4WJ5) and MHC-II molecule (PDB-code: 4IS6) peptide binding groove. The peptide is shown in pink sticks. Schematic representations of MHC class-I and class-II domains are also shown.

1.2.1.2 Antigen processing

Two distinct intracellular pathways deliver the peptide ligands that are presented on MHC-I or MHC-II molecules at the cell surface. Intracellular self and foreign peptides presented by MHC-I are produced from the degradation of intracellular proteins by the proteasome, a large proteolytic complex in the cytosol (Kloetzel, 2004; Vigneron and Van den Eynde, 2014). Most cells in the steady state contain a standard proteasome which includes constitutive catalytic subunits ($\beta 1$, $\beta 2$, and $\beta 5$). In lymphoid tissues and under inflammatory condition, the proteasome catalytic machinery is replaced by inducible subunits ($\beta 1i$, $\beta 2i$, and $\beta 5i$) which have different cleaving specificities (Aki et al., 1994; Macagno et al., 1999). In addition, some tumour tissues process peptide antigens exclusively through intermediate proteasomes made of a mixed assortment of catalytic subunits (Guillaume et al., 2010). Peptide precursors produced by the proteasome can be further trimmed to an optimal length for MHC-I presentation by other peptidases, mainly in the ER by the endoplasmic reticulum aminopeptidase ERAP1 (Hammer et al., 2007; Serwold et al., 2002). Peptides are translocated to the ER lumen by a transporter associated with antigen processing (TAP). In the ER, the assembly of a stable pMHC complex is assisted by chaperone proteins. This MHC-I complex finally exits the ER via the constitutive secretory pathway to the cell surface for presentation (Harding and Unanue, 1990; Pamer and Cresswell, 1998).

MHC-II molecules generally bind peptides generated by lysosomal proteolysis in the endocytic and phagocytic pathways (Lechler et al., 1996; Théry et al., 1998). During their maturation, MHC-II molecules are prevented from binding to endogenous antigens in the ER by associating with an invariant chain (Ii). MHC II-Ii complexes translocate through the Golgi to the MIIC/CIIV compartment where the invariant chain is degraded to CLIP (Class II-associated Invariant-chain Peptide) (Riberdy et al., 1992). Finally, the CLIP peptides is removed from the MHC-II complex and exchanged for the antigenic peptide which is presented on the cell surface. However, both MHC-I and MHC-II can present peptides generated from endogenous and exogenous antigens. For example, MHC-I can bind peptides derived from exogenous proteins that have been internalised by endocytosis or phagocytosis, a process known as 'cross-presentation' (reviewed by Heath and Carbone, 2001).

1.2.2 T-cell receptor (TCR)

The $\alpha\beta$ TCR is a disulphide-linked heterodimer consisting of an α - and β -chain (**Figure 1.3A**). The two chains are composed of an Ig-like variable and constant domains, each with an intra-chain disulphide bond, joined by a hinge region (Chothia et al., 1988; Rudolph et al., 2006). The constant domains are N-terminal to the transmembrane region, while the hypervariable loops from the variable domains ($V\alpha$ and $V\beta$) are distal from the cell surface. The TCR binds the peptide-MHC via six complementarity-determining regions (CDR) loops, three from the $V\alpha$ domain and three from $V\beta$ (Rudolph et al., 2006) (**Figure 1.3B**). CDR1 and CDR2 are germline-encoded, while the hypervariable CDR3 region consists of both germline and non-germline-encoded segments (Chothia et al., 1988).

X-ray crystallographic studies of TCR–pMHC complexes (in their bound and/or free state) published to date, show similarities in the overall binding mode of the TCR, independently of MHC-restriction (reviewed by Gras et al., 2012; Rudolph et al., 2006). Nevertheless, as the number of TCR structures increases, it is now accepted that TCR-peptide-MHC interactions are not rigidly conserved but allow for flexibility. TCRs are indeed intrinsically flexible and can undergo large conformational changes in order to bind their ligands (Borbulevych et al., 2009). Apart from structural features (Garcia et al., 2009; Marrack et al., 2008), other characteristics of the TCR-pMHC interaction can be analysed, including thermodynamic properties (Krogsgaard et al., 2003; Willcox et al., 1999), kinetic on-/off-rates and affinity (Aleksic et al., 2012; Bridgeman et al., 2011). Interestingly, compared to antibody recognition, the TCR-pMHC interaction is of low affinity, with a dissociation constant in the low micromolar range (van der Merwe and Davis, 2003), and is characterised by slow association rates and fast dissociation rates (Boniface et al., 1999).

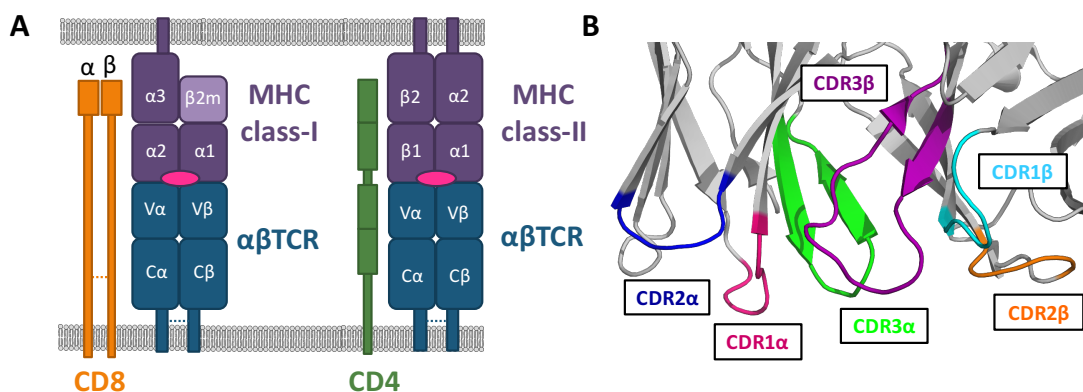


Figure 1.3. The $\alpha\beta$ TCR structure and CDR loops

A) MHC (purple), TCR (blue) and peptide (pink) structure schematic representation. Co-receptor CD8 binds the $\alpha 3$ domain of MHC class-I, while CD4 binds the $\beta 2$ domain of MHC-class II. **(B)** Ribbon model of an $\alpha\beta$ T-cell receptor (TCR) showing the positions of the six variable complementarity-determining region (CDR) loops (PDB-code: 4QOK).

1.2.3 Generation of diversity

Approximately 4×10^{11} T-cells circulate in the adult human body. Many different TCRs are generated by genetic recombination during T-cell development, such that each T-cell generally expresses a single type of TCR (Janeway and Murphy, 2011). The set of cells with a same TCR defines a T-cell clonotype, and the set of T-cells in the body can be thought of as a repertoire of clonotypes. $\alpha\beta$ TCR diversification mainly occurs in the thymus by stochastic V(D)J recombination of non-contiguous gene segments (Davis and Bjorkman, 1988; Yui and Rothenberg, 2014). **Figure 1.4A** shows the gene segment composition for both the α -chain and β -chain locus. During thymocyte development in the thymus, the variable domains of *tcr α* and *tcr β* genes are assembled following rearrangement of the variable (V), diversity (D), and joining (J) gene segments by a multistep process called V(D)J recombination. The enzyme pair RAG1 and RAG2 selectively targets recombination signal sequences that flank the V, D, and J segments (Oettinger et al., 1990; Schatz et al., 1989). V(D)J recombination events first bring together one of many V segments and a J segment to form the N-terminal variable domain of the TCR (Tonegawa, 1983); an additional D segment is included in the case of the TCR β -chain (Born et al., 1985). The C gene contains separate exons encoding for the constant and hinge domains, and a single exon for the transmembrane and cytoplasmic regions. The V(D)J process is such that TCR CDR1 α , CDR1 β , CDR2 α and CDR2 β loops are entirely encoded by germline DNA segments.

In contrast, the CDR3 loops are generated from the joining of recombined V, (D) and J segments. Joining at these sites is imprecise and results in the CDR3 loop hyper variability, in that template and non-template nucleotides can be randomly added and/or deleted by the DNA-repair machinery (**Figure 1.4B**). Therefore, TCR diversity can be mainly attributed to the pairing of different TCR- α and - β chains (i.e. combinatorial diversity), and is further enhanced by imprecise joining of coding nicked gene segments (i.e. junctional diversity).

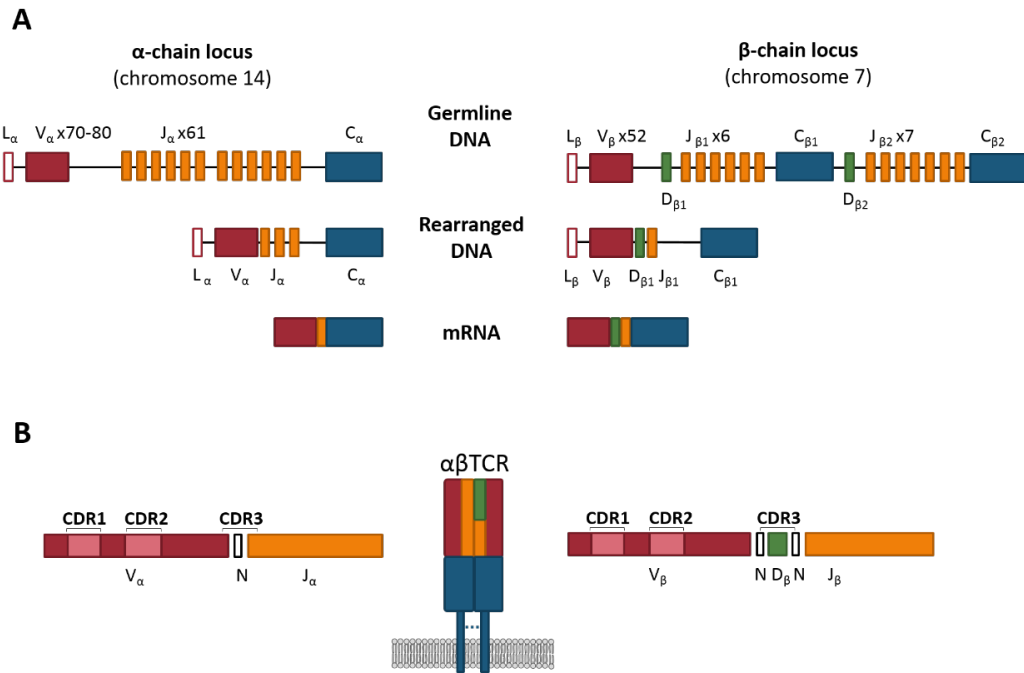


Figure 1.4. Human TCR α- and β-chain gene rearrangement and expression

(A) The germline organisation of the human TCRα locus (chromosome 14) and TCRβ locus (chromosome 7) is shown in the top panel. The TCRα- and β-chain genes are composed of discrete segments that are joined by somatic recombination. The TCRα locus consists of 70–80 V_α gene segments, each preceded by an exon encoding the leader sequence (L), a cluster of 61 J_α gene segments, followed by a single C gene. The TCRβ locus consists of a cluster of 52 functional V_β gene segments and two separate clusters each containing a single D gene segment; 6-7 J gene segments and a single C gene segment. Rearrangement of V(D)J gene segments generates a functional V-region exon for both chains, that is transcribed and spliced to join to the corresponding C-region. The resulting mature mRNA is translated to the T-cell receptor α- and β-chain. **(B)** V(D)J recombination produces three TCR CDR loops. CDR1 and CDR2 are entirely germline-encoded and lie in the V region. The hypervariable CDR3 loop is formed at the junction between recombined V(D)J segments. Combinatorial diversity is further enhanced by addition and deletion of nucleotides (N) at the junctions between segments.

The theoretical number of different αβ TCRs that could be generated, in principle, by the V(D)J recombination system alone is around 10^{18} (Davis and Bjorkman, 1988; Zarnitsyna et al., 2013). However, these estimates are limited because each individual can only possess a smaller subset of possible TCRs at one time, $\sim 10^{11}$ at most. This number is sufficient to recognise at least one antigen from any given pathogen. This also implies that TCRs must be able to respond to distinct pMHC ligands (Mason, 1998); the notion of TCR ‘cross-reactivity’ is consistent with a large body of experimental evidence which includes studies of T-cell clones responding to several distinct peptide antigens (Sewell, 2012; Wooldridge et al., 2012). Given the excess thymic TCR diversity described above, one would also expect that individuals hardly ever share the same TCR recombination. Nevertheless, several studies have shown that ‘public’ TCRs (i.e. identical clonotypes) to defined antigens can be found in different MHC-matched individuals (Li et al., 2012; Venturi et al., 2008).

1.2.4 T-cell development and selection

In human adults, thymocyte development begins with the migration of multipotent precursors from the bone marrow into the cortico-medullary junction of the thymus via chemotactic attraction (Haynes and Heinly, 1995; Lind et al., 2001). T-cell development and repertoire selection is a highly regulated multi-step process that requires the relocation of thymocytes (i.e. developing lymphocytes) within microenvironments in the thymus (Bevan, 1977; Miller, 1961). The thymic stroma not only structurally supports migrating thymocytes but also provides guidance through chemokines produced by distinct subsets of cells in the stroma (Takahama, 2006). Following their entry into the thymus, lymphoid progenitor cells gradually lose multi-potency which defines their T-cell lineage commitment (Rothenberg et al., 2008). The development of thymocytes is commonly divided into major stages based on the expression of surface markers: the $CD4^- CD8^-$ double negative (DN) stage; the $CD4^+ CD8^+$ double positive (DP) stage and the $CD4^+ CD8^-$ or $CD8^+ CD4^-$ single positive (SP) stage (**Figure 1.5**). For most of the $\alpha\beta$ T-cell lineage, development is made of selection steps that are MHC-induced and result in the complete differentiation of ($CD4^+$ or $CD8^+$) SP thymocytes that are direct precursors of mature T-cells (reviewed by Carpenter and Bosselut, 2010).

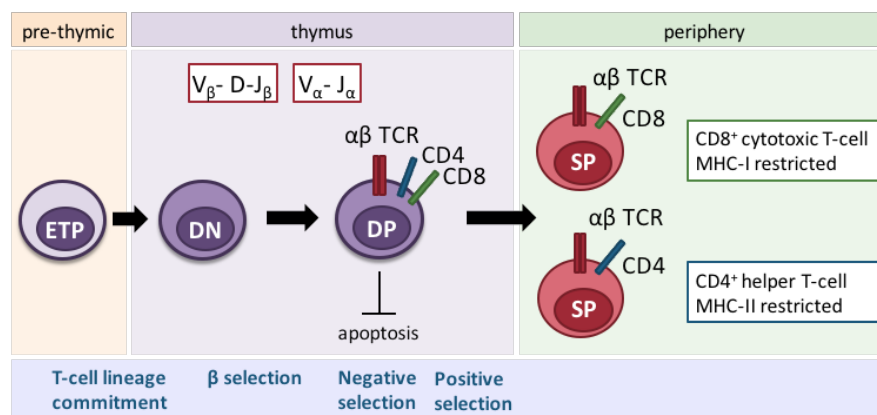


Figure 1.5. Simplified diagram of T-cell development and selection

On the basis of CD4 and CD8 co-receptor surface expression, several stages of thymocyte differentiation can be distinguished. In the thymus, double-negative (DN) thymocytes progress to the double-positive (DP) stage. During the DP to single-positive (SP) transition, the T-cell repertoire is formed by a process known as positive selection. DP thymocytes that express a potentially harmful (autoreactive) T-cell receptor (TCR) are deleted by negative selection at this stage, whereas DP thymocytes that express TCRs that do not recognize self-peptide–MHC complexes are eliminated in a process that is known as 'death by neglect' (not shown). Positive selection correlates with commitment to the $CD4^+$ or $CD8^+$ T-cell subsets. Decision checkpoints in the thymus are shown in blue in the bottom panel.

After T-cell lineage commitment, multiple checkpoints during thymic development ensure that thymocytes expressing a non-functional (or autoreactive) TCR are deleted, and that a functional T-cell repertoire is generated and ready to translocate to the periphery. The first checkpoint for committed thymocytes, known as β selection, verifies that a correct TCR β gene rearrangement has occurred and that a functional receptor is expressed on the T-cell surface. β selection requires thymocytes to signal through a pre-TCR (i.e. a correctly rearranged TCR β -chain, CD3 chains and a pre-T α) (Boehmer, 2005; Yamasaki et al., 2006). The second checkpoint verifies the interaction of the $\alpha\beta$ TCR with self-peptide-MHC complexes presented by thymic epithelial cells and dendritic cells, determining the fate of the developing T-cell (Anderson et al., 2000). T-cells with TCRs that don't bind self pMHC complexes, fail to transduce signals required for survival and die by neglect. Thymocytes bearing interacting TCRs result in positive selection and develop into single positive CD8+ or CD4+ T-cells, which are capable of recognising foreign antigens presented by self MHC-I or MHC-II molecules, respectively (Anderson et al., 1994; Hogquist et al., 1994; Hu et al., 1997). However, those bearing a TCR that binds with high affinity for the selecting pMHC ligand are eliminated (negative selection) through apoptotic cell death (Rammensee et al., 1984). However, via a process known as receptor editing, thymocytes with a high-affinity TCR for self pMHC can avoid clonal deletion by undergoing a secondary TCR α gene rearrangement, therefore changing their antigen specificity (McGargill et al., 2000). Overall, the selection process in the thymus, known as 'central tolerance', has evolved to limit potential self-reactivity of the final T-cell repertoire, by ensuring that only those T-cells expressing a TCR within a narrow affinity range for self peptide-MHC are rescued from clonal deletion (Alam et al., 1996; Ashton-Rickardt and Tonegawa, 1994). Although central tolerance mechanisms are efficient, they cannot eliminate all potential self-reactive T-cells, in part because not all self-antigens are expressed in the thymus, the primary site of T-cell development (Kyewski and Derbinski, 2004). Therefore, various mechanisms operate to ensure that self-reactive T-cells after thymic output become functionally unresponsive or are deleted by apoptosis after self-antigen encounter in peripheral tissues (Xing and Hogquist, 2012).

1.2.5 The production of effector T-cells

Once completed their maturation in the thymus, naïve T-cells enter the periphery and recirculate throughout the secondary lymphoid compartment, moving between lymph nodes, blood and spleen (Janeway, 2011). For the T-cell arm of the immune system to lead to the effective killing of tumour cells, a series of steps must be initiated (schematically represented in **Figure 1.6**). Signals with immunogenic potential are exposed at the cell surface or released from stressed and damaged tumour cells (reviewed by Hernandez et al., 2016).

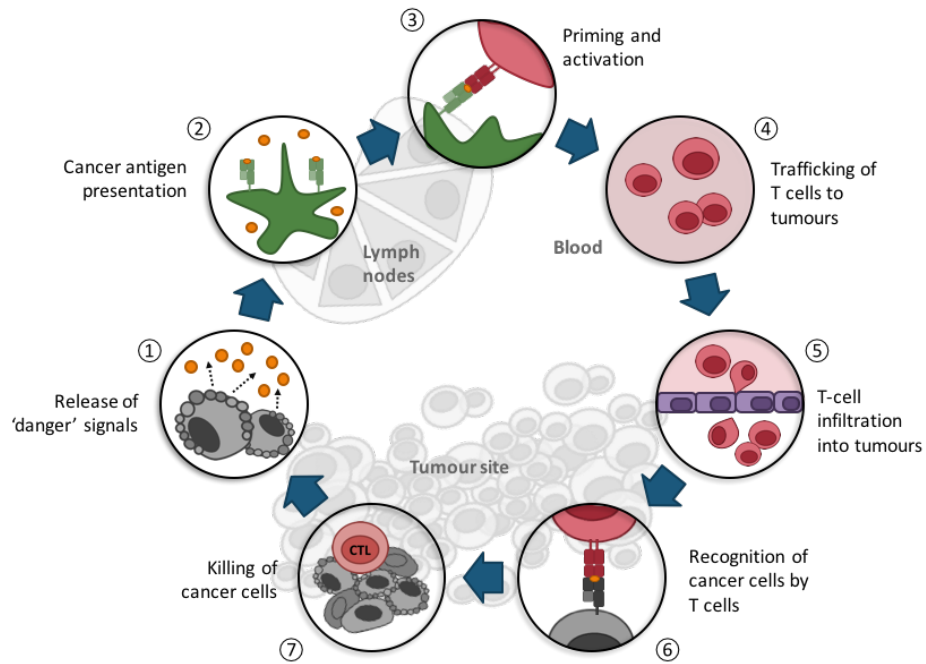


Figure 1.6. Schematic diagram of a successful anti-tumour T-cell immune response

The immune surveillance of cancer by T-cells requires local uptake of tumour-specific antigen followed by the activation and expansion of tumour specific effector T-cells, such as CTLs. Each step is described above, with the primary cell types involved and the anatomic location of the activity listed. Adapted from Chen and Mellman et al., 2013.

Such damage-associated molecular patterns (DAMPs) include a large range of molecules, such as surface proteins (eg. heat shock proteins), secreted proteins (eg. HMGB1), as well as nucleic acid degradation products and lipids (eg. Phosphatidylserine residues exposed on the outer layer of the plasma membrane) (reviewed by Kroemer et al., 2013; Li et al., 2003; Scaffidi et al., 2002). The release of these molecules alerts the immune system to the presence of dying tumour cells, therefore enhancing their immunogenicity. An increasing number of DAMPs are being reported as candidate ligands of Toll-like receptors (TLRs), in particular TLR4 (Fang et al., 2011; Apetoh et al., 2007). DAMPs can bind to the TLR, promoting an inflammatory response and providing dendritic cells (DCs) with 'danger signals' (Fang et al., 2014). Overall, this immunogenic form of cancer cell death contributes to the triggering of tumour-specific T-cell responses by assisting the activation and maturation of DCs, the antigen processing and presentation on MHC-I or MHC-II molecules on mature DCs and, eventually, T cell activation (Hernandez et al., 2016).

T-cell activation is a finely regulated process that includes mobilisation of Ca^{2+} , new transcription, release of pre-processed and retained surface receptors, internalisation of surface receptors and the release of granules or cytokines (reviewed by Malissen et al., 2014). To achieve maximal expansion, CD8+ T cells need to integrate multiple signals, including the TCR, co-stimulatory signals, and inflammatory cytokines (Mescher et al., 2006; Parish and Kaech, 2009). Activated T-cells are induced to proliferate and differentiate into armed CD4+ or CD8+ primed T-cells; they leave the

lymph nodes via the circulation and are recruited to the tumour site, providing that the vascular endothelium expresses the correct homing ligands. Finally, tumour-specific T-cells bind to the target pMHC on malignant cells, and are able of clearing the autologous cancer cells through several effector mechanisms, such as cell-mediated cytotoxicity. Lysis of the tumour cells results in the release of further tumour-associated antigens which can be taken up by resident dendritic cells (Mellman et al., 2011). In tumour patients with progressing disease, one or more steps described above fail to occur correctly. For example, tumour-associated antigens may not be detected because of a down-regulation of MHC molecules on tumour cells; T regulatory cell responses may be elicited rather than effector responses, because of the self origin of tumour antigens; T-cells may not home to the tumour site and can be inhibited by an immunosuppressive tumour microenvironment (reviewed by Joyce and Fearon, 2015; Lanitis et al., 2015).

1.2.5.1 *CD8+ cytotoxic T-cells*

Traditionally, effector cytotoxic CD8+ T-cells have been thought to be the major mediators of effective anti tumour T-cell responses. CD8+ T-cells represent a population of cytotoxic lymphocytes (CTLs) that are able to induce targeted killing of both infected and malignant cells (Andersen et al., 2006; Henkart, 1994). They can contribute to promote tumour rejection also by changing the micro-environment of the tumour cells to inhibit further growth (Andersen et al., 2006; Barry and Bleackley, 2002). Direct killing is mediated by cytolytic factors that are compartmentalized into acidified secretory lysosomes commonly known as 'lytic granules'. Cytolytic factors include perforin (a toxin that forms pores in the target cell plasma membrane), serine proteases such as granzymes (in particular granzyme B), and chemokines (such as MIP-1 α , MIP-1 β and RANTES) which promote the recruitment of additional cells to the immune response (Thiery et al., 2011; Voskoboinik et al., 2010). Granzymes enter the target cell through newly formed pores and, by cleaving aspartate residues, activate the caspase cascade which leads to apoptosis of the target tumour cell (Ewen et al., 2012). Advanced confocal and electron microscopy have provided super high-resolution images of secreting CTLs, showing how these cells polarise the Golgi and microtubule apparatus in order to focus the lytic granules release only on the point of contact with the target cell, therefore leaving the neighbouring cells intact (Ritter et al., 2015). CTLs can also secrete TNF- α family members (such as TNF- α , FasL and TRAIL) which induce the multimerisation of the cognate receptors on the target cell and induce apoptosis (Ratner and Clark, 1993). IFN- γ can enhance Fas levels on target cells, thus increasing the sensitivity to CD8+ T-cell killing (Seliger et al., 2008). Whereas perforins and granzymes are produced constitutively in effector cells delivering immediate cytotoxic effect, cytokines are produced upon relevant stimulation and are released on a time scale of hours (Sanderson, 1976; Slifka et al., 1999). In fact, unlike lytic factors, cytokines are newly produced after TCR stimulation by either upregulation of gene transcription or translation of pre-existing mRNA transcripts. The lysosomal-associated membrane glycoproteins

(LAMPs), CD107a and CD107b are also transiently expressed on the T-cell surface upon degranulation of lytic granules (Betts et al., 2003). Finally, although IL-2 doesn't have a direct cytolytic effect, antigen-specific CD8+ T-cells can use IL-2 secretion as an autocrine growth factor promoting their survival and further proliferation after second antigen encounter (Cox et al., 2013).

1.2.5.2 CD4+ T-cells

Although CD8+ T cells are important mediators of anti-tumour immunity, the contribution of CD4+ T cells has also been appreciated. CD4+ T-cells represent a heterogeneous population of lymphocytes with effector and regulatory functions (Kim and Cantor, 2014). Following antigen recognition, naïve CD4+ T-cells have the potential to differentiate into a wide array of effector T helper (Th1, Th2, Th17, Th22 and Tfh) and regulatory cell types (Tregs), capable of differentially orchestrating immune responses. The cytokine environment and the induction of specific transcription factors drive the polarisation of recently activated CD4+ T cells (Jiang and Dong, 2013; Zhu and Paul, 2008).

CD4+ T cells are mainly known for their ability to provide a helper function to tumour-reactive cytotoxic and memory CD8+ T-cells responses (Antony et al., 2005; Gao et al., 2002; Janssen et al., 2003; Nishimura et al., 1999). A primary helper mechanism involves the 'licensing' of DCs to induce optimal expansion and activation of cytotoxic CD8+ T cells ('licence to kill'). Licensing of DCs is mediated by the CD40-CD40L interaction between the DC and cognate CD4+ T cell, respectively (Bennett et al., 1998). DCs require antigen-specific CD4+ T-helper cell to mature and increase their antigen-presenting and co-stimulatory activity. Functionally mature DCs can subsequently induce a robust CD8+ effector T cell response, with both the CD8+ and CD4+ T cells binding an antigen presented by the same DC (Bennett et al., 1997).

1.3 T-cells and melanoma

1.3.1 Melanoma cells are antigenic

Proteins expressed by melanoma cells may contain one or more peptide epitopes presented by MHC molecules and bound by autologous T-cells (Boon et al., 2006). Melanoma peptide antigens were among the first tumour-associated antigens to be identified in humans (Traversari et al., 1992; van der Bruggen et al., 1991), leading to a wave of research in the identification of other T-cell targets which provided the basis for antigen-specific cancer immunotherapy (**Section 1.4.1**). Several melanosome antigens, including tyrosinase (Brichard et al., 1993), MART-1/Melan-A (Kawakami et al., 1994c), gp100 (Kawakami et al., 1994b), TRP1 (Wang et al., 1995) and TRP-2 (Bloom et al., 1997) have been identified by screening cDNA libraries with tumour-reactive CD8+ T-cells which exhibited antitumor functions. Tumour-associated peptide antigens that are expressed by melanoma cells are listed in an online, open-access database³, which is regularly updated (Vigneron et al., 2013). Depending on their tissue distribution, T-cell defined melanoma associated antigens fall into the broad groups listed below.

1.3.1.1 Differentiation antigens

The first group of tumour antigens includes those encoded by differentiation genes. After transformation, melanoma cells generally continue to express antigens that are characteristic of their tissue site of origin. Melanocyte differentiation antigens are usually overexpressed by most melanoma tumours but are also expressed by normal melanocytes in the *stratum basale* of the skin, in the retinal pigmented epithelium in the eyes, and in the inner ear, where they are associated with melanin production in melanosomes (Overwijk and Restifo, 2000; Overwijk et al., 1998). Prototypes of melanoma differentiation antigens include proteins such as Glycoprotein (gp)100, MART-1/Melan-A, tyrosinase, TYRP1 and TYRP2. Gp100 will be the focus of **Chapter 3**.

1.3.1.2 Cancer-testis antigens

MAGE-I, MAGE-3, BAGE, GAGE and NY-ESO-1 belong to a second group of tumour-specific antigens (Gillespie et al., 1998; Jäger et al., 1998; van der Bruggen et al., 1991; 1994). This group of antigens are called cancer-testis (CT) antigens because of their predominant expression in many tumours (including melanomas) and male germline cells, but not in other normal adult tissues (Simpson et al., 2005).

³ <http://www.cancerimmunity.org/peptidedatabase/Tcellepitopes.htm> (*Peptide database: T cell-defined tumour antigens. Cancer Immunology*)

Male germline cells do not express MHC molecules on their surface, and therefore do not express antigens that can be recognized by CT antigen-specific T-cells. Whereas melanoma differentiation antigens are expressed at very high frequencies that do not differ between early and late stage disease, several CT antigens are increasingly expressed with disease progression (Barrow et al., 2006; Hodi, 2006).

1.3.1.3 Over-expressed antigens

In contrast to CT antigens, which have the potential to be strictly tumour-specific, a third group of cancer antigens, namely overexpressed antigens, are also present in many normal cells. Survivin (Schmidt et al., 2003), PRAME (Ikeda et al., 1997) and telomerase (Vonderheide et al., 1999) are prototypes of this category. Overexpressed antigens are heterogeneous in their distribution in normal tissues and in terms of their biological function. In some cases, over-expressed antigens are critical for cancer cell survival (e.g. the anti-apoptotic activity of Survivin), suggesting highly stable expression of these antigens in tumour cells. Widespread expression of these antigens and the essential nature of such gene expression for the survival of malignant neoplasms has made them particularly attractive targets for immunotherapy.

1.3.1.4 Neo-antigens

A fourth group of tumour-associated antigens, known as 'neo-antigens', has recently raised considerable interest in the scientific community (McGranahan et al., 2016; Ophir et al., 2015; Schumacher and Schreiber, 2015). Neo-antigens result from the large number of somatic mutations found in human cancer cells and therefore are by definition tumour (and patient) specific. Such gene mutations can produce new antigenic peptides by changing one amino acid, by altering the phase of the reading frame or by extending the coding sequence beyond the normal stop codon. Massive parallel sequencing can now reveal with precision the mutational spectrum of individual tumours (i.e. the mutanome) (**Figure 1.7**). Most human melanomas have a mutational load above 10 somatic mutations per megabase (Mb) of coding DNA, and this is apparently sufficient to lead to the frequent formation of neo-antigens (Alexandrov et al., 2013; Vogelstein et al., 2013). Identification of tumour-associated antigens (TAA) peptides expressed by human melanomas provided the basis for antigen-specific active immunotherapy and facilitated the design of new vaccination clinical trials (**section 1.4.1**).

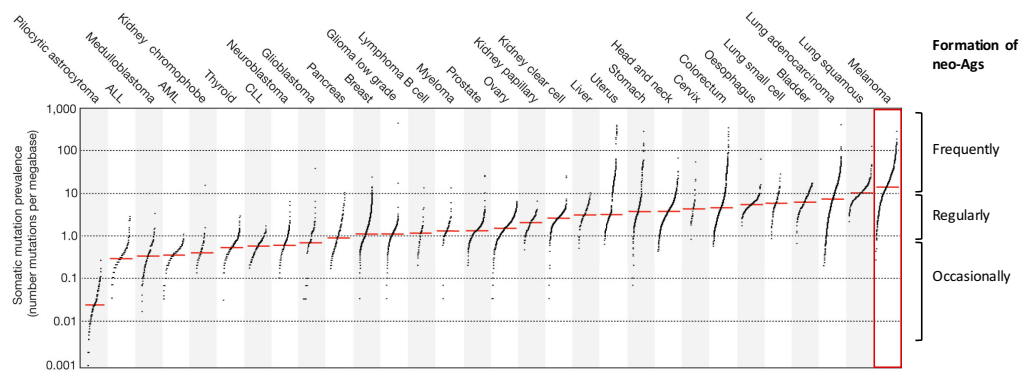


Figure 1.7. Signatures of mutational processes in melanoma compared to other human cancers (from Alexandrov et al., 2013)

Estimate of the neo-antigen repertoire in human cancer. Data depict the number of somatic mutations in individual tumour types. Every dot represents a sample whereas the red horizontal lines are the median numbers of mutations in the respective cancer types. The y axis (log scaled) shows the number of mutations per megabase, whereas the different cancer types are ordered on the x axis based on their median numbers of somatic mutations. A value of 10 somatic mutations per Mb of coding DNA corresponds to ~150 non-synonymous mutations within expressed genes.

1.3.2 CD8+ T-cell responses in melanoma

A number of studies regarding the role of the immune system in melanoma, provide evidence that CD8+ T-cells can naturally recognise and help control melanoma, therefore justifying the use of T-cell based immunotherapies in the clinic. First, spontaneous regression, which occurs in 13.8-50% of primary melanomas, is a result of a successful immune response against melanoma cells (Kalialis et al., 2009), with infiltration of CD4+ and CD8+ T-cells observed in melanomas samples (Wenzel et al., 2005). One of the major goals was to demonstrate that melanoma patients harbour CD8+ T-cell clones that could selectively recognise autologous melanoma cells in cytotoxicity assays (Kawakami et al., 2000; Knuth et al., 1984; Mukherji and MacAlister, 1983). These studies also reported that the frequency of melanoma-specific CTL precursors was higher in tumour infiltrates and affected lymph nodes, compared to the circulating population (Mazzocchi et al., 1994; Romero et al., 1998). T-cell cloning techniques (from tumour tissues, draining lymph nodes or peripheral blood) allowed further questions to be addressed regarding the effector functions and antigen specificity of melanoma-reactive T-cells. Beside cytotoxicity, melanoma-specific CTLs are known to produce a number of cytokines such as TNF- α , IFN- γ and IL-2 (reviewed by Boon et al., 2006). T-cell specificity is not always restricted to autologous cell lines; many CD8+ T-cell clones recognise allogeneic cell lines, supporting the notion that some melanoma peptides may represent shared antigens. Overall it seems that despite the mechanisms of central and peripheral T-cell tolerance against self-antigens, spontaneous immune responses against melanoma antigens are not uncommon.

The best studied CTL melanoma peptide target to date is Melan-A/MART-1₂₆₋₃₅ (EAAGIGILTV), which is recognized by CD8+ T-cells in the context of HLA-A2 (Romero et al., 2002). The EAAGIGILTV epitope (EAA hereafter) is located within the putative transmembrane region of the Melan-A protein (118 aa), where most of Melan-A encoded T-cell antigens have been identified (Kawakami et al., 1994c).

High frequencies (0.1%) of Melan-A-specific CD8+ T-cells are found in the blood and in invaded lymph nodes of most HLA-A2+ melanoma patients (Romero et al., 1998). In particular, HLA-A2+ healthy individuals show about 0.07% of EAA-specific CD8+ T-cells in their blood, a frequency which is two orders higher than anti-MAGE precursors (Marincola et al., 1996; Romero et al., 2002). An interesting paper suggests the transcription of the protein in the thymus could explain the observed high frequency of circulating anti-Melan-A T-cells (Pinto et al., 2014). The authors show that medullary thymic epithelial cells lack the immunodominant EAA epitope because they express a truncated form of the Melan-A transcript, therefore precluding central tolerance to this antigen. In contrast, melanoma cells and normal melanocytes almost exclusively express a full-length Melan-A transcript, providing the HLA-A2 restricted antigen for efficient recognition by CTLs. In addition, the recognition of this peptide by germline-encoded residues within the CDR1 region of the TRAV12-1 gene segment, is further thought to vastly increase the potential to generate T-cells specific for this HLA-A2-restricted, melanoma-derived peptide (Cole et al., 2009; Trautmann et al., 2002; Wieckowski et al., 2009).

1.3.3 CD4+ T-cell responses in melanoma

Most tumour cells express only MHC-I molecules ensuring that the majority of interest has focused on CD8+ T-cell responses in cancer immunotherapy. However, melanoma cells commonly constitutively express MHC-II molecules *de novo* (Altomonte et al., 2003; Fossati et al., 1986; Mendez et al., 2009). While melanocytes are usually MHC-II negative, class-II expression appears in early melanoma lesions as a possible bystander effect of transformation and invasion (Moretti et al., 1990; Ruitter et al., 1984; van Vreeswijk et al., 1988). MHC-II expression in melanoma has been also linked to patient survival (Anichini et al., 2006; van Duinen et al., 1988; Zaloudik et al., 1988). Expression of MHC-II by melanoma cells allows direct recognition by tumour-antigen specific CD4+ T-cells (Donia et al., 2013; Friedman et al., 2012). Initial studies using prediction algorithms identified an MHC-DR4-restricted epitope in the Melan-A protein (Zarour et al., 2000). Since these early findings, several other MHC-II restricted melanoma-associated antigens have been characterised (Andersen et al., 2012; Ayyoub et al., 2010; 2005; Gnjatic et al., 2003). Several early studies demonstrated that T-cell infiltrates of melanoma lesions contained not only CD8+ T-cells, but also CD4+ T-cells, capable of recognising melanocyte differentiation antigens (Robbins et al., 2002; Topalian et al., 1996). While direct cytotoxicity by CD4+ T-cells may play a role in tumour clearance (Quezada et al., 2010), the more canonical effector mechanism of producing cytokines such as IFN- γ or TNF- α that could mitigate the immune-suppressive tumour microenvironment might be more important (Brady et al., 2000; Braumüller et al., 2013). Interestingly, a few examples of clinical tumour regression possibly associated with CD4+ lymphocytes have been reported (Friedman et al., 2012; Hunder et al., 2008). Is it important to underline though that CD4+ T-cells can also downregulate immune responses to melanoma (Sakaguchi, 2004). CD4+ TILs with a regulatory T-cell phenotype have been isolated and expanded from melanoma tumours (Wang et al., 2004; Wang, 2006; Yao et al., 2012).

1.4 T-cell based immunotherapy approaches for metastatic melanoma

Melanoma has been the focus of extensive research in tumour immunotherapies for several decades. Due to the breath and pace of development of this field, a truly exhaustive review of all this literature is beyond the scope of this introduction. Here, I will instead introduce the main T-cell based immunotherapy approaches that are relevant to my own studies. Some expansion of this background will be provided in the introduction to specific results chapters. In this respect, peptide vaccination for melanoma treatment will be discussed in **Chapter 3** while Tumour Infiltrating Lymphocyte (TIL)-based immunotherapy will be the focus of **Chapters 4** and **5**.

1.4.1 Improving antigenic peptide vaccines

The field of tumour vaccination comprises a broad array of approaches that aim to generate and amplify cancer-specific immune responses. Cancer vaccines include full length proteins, short peptides, DNA, pulsed dendritic cells, viruses, whole tumour cells and cell lysates (reviewed by Blanchard et al., 2013). Peptide cancer vaccines are attractive compared to other immunotherapy approaches because they have low production costs, are easy to use as an 'off-shelf' reagent and have shown low toxicities in preclinical settings. Following the molecular identification of a large collection of melanoma-associated antigens, several peptide vaccines have been (and are being) used for the immunisation of advanced melanoma patients. However, although cancer vaccines can extend survival (by months, not years), broad reviews of clinical trials have shown that objective cancer regression is achieved in less than 4% of patients (Blanchard et al., 2013; Klebanoff et al., 2011; Rosenberg et al., 2004).

As shown in **Figure 1.8**, an effective therapeutic peptide cancer vaccine delivers a target antigen to both MHC-I and MHC-II molecules of antigen presenting cells at the site of intradermal injection, promoting both CD4+ and CD8+ T-cell responses. A non-specific adjuvant component can be added to activate dendritic cells and augment vaccine potency (Melief et al., 2015). Immunisation with peptide epitopes can be quite effective in inducing tumour-specific T-cells that can be detected among circulating lymphocytes of vaccinated patients (Cormier et al., 1997; Lee et al., 1999; Pittet et al., 2001; Scheibenbogen et al., 2000).

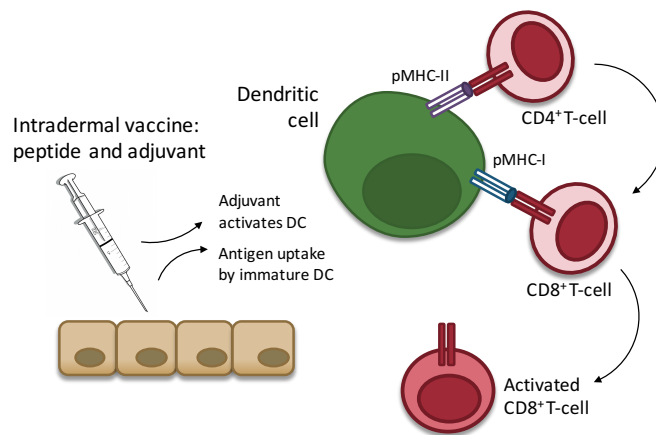


Figure 1.8. Mechanism of action of an effective peptide cancer vaccine

Adjuvant molecules in the vaccine preparation activate dendritic cells (DCs), which respond by up-regulating molecules needed to interact with T-cells in the lymph nodes. Activated DCs present antigen to T-cells; if the T-cell recognises its cognate antigen in the proper context, it is activated. Upon activation, CD4+ T cells produce cytokines that support CD8+ T-cells maturation (Adapted from (Drake et al., 2014).

Melanoma vaccination clinical trials have frequently shown that the detection of T-cell responses in patient blood may not correlate with outcome. These suboptimal clinical responses may relate to the quality of the induced T-cell response (for instance, TAA tolerance induced by a sub-optimal antigen presentation) or to melanoma escape mechanisms that might influence the tumour susceptibility to treatment (Marincola et al., 2000). Among other reasons, the insufficient immune response to control melanoma growth *in vivo* can be caused by the poor immunogenicity of natural epitopes expressed by tumour cells. Many of these self-antigens are expressed in the thymus, resulting in deletion of the highly reactive T-cell repertoire and development of suppressive T-regulatory cells. With the exception of the immunodominant melanoma antigens Melan-A and gp100, which readily activate specific T-cells *in vitro* (Rivoltini et al., 1995) and *in vivo* (Cormier et al., 1997; Salgaller et al., 1996), generation of most T-cell responses requires repeated *in vitro* stimulation with TAA epitopes and shows limited immunogenicity when used as vaccines for melanoma patients (Marchand et al., 1999; Weber et al., 1999). Multiple strategies have been designed with the aim of enhancing peptide immunogenicity (Berzofsky et al., 2015; Tsang et al., 2015). One approach involves the use of peptide substitutions aimed at increasing the affinity for cognate TCRs or presenting MHC molecules. Such peptides are referred to as 'altered peptide ligands' (APL) or 'heteroclitic peptides' (Figure 1.9).

Single amino acid modifications can improve the peptide stability in the MHC binding groove by introducing higher affinity primary or secondary 'anchor' residues (Rammensee et al., 1995; Ruppert et al., 1993). Another strategy to improve immunogenicity involves modifying residues of the peptide that protrude out of the binding groove and interact with the TCR CDR loops. The best-studied system in this respect is probably the HLA-A2 restricted immunodominant Melan-A/MART-1 antigen EAAGIGILTV (EAA) (Valmori et al., 1998).

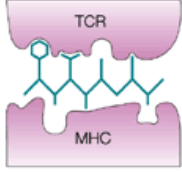
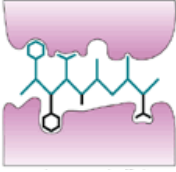
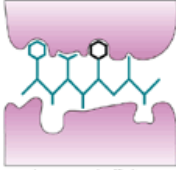
Wild type		Epitope enhancement		
A		B	C	
				
		Improve pMHC binding	Increase TCR triggering	<i>Mechanism</i>
		Substitution of an MHC 'anchor' residue	Modification of individual amino acids that contact the TCR	<i>Approach</i>
		Melan-A (26-35) 2L Gp100 (209-217) 2M Gp100 (280-288) 9V	Melan-A (27-35) 1L	<i>Examples using melanoma antigens</i>
		<i>Valmori et al., 1998</i> <i>Parkhurst et al., 1996</i>	<i>Rivoltini et al., 1999</i>	<i>Reference</i>

Figure 1.9. Examples of peptide enhancement strategies for melanoma vaccines

(A) A wild-type tumour-associated peptide antigen is presented on a MHC molecule and bound by a TCR. (B) The affinity for binding to the MHC molecule can be increased by modifying the anchor peptide residues that affect the interaction with the MHC binding groove. (C) The peptide affinity for a particular TCR can be increased by modifying those residues that interact with the CDR loops of the TCR. Schematic representation of TCR and peptide-MHC was adapted from Berzofsky et al., 2001. Amino acid position is indicated in brackets; mutations are designated by the residue number in the the wild type sequence and the single-letter amino acid code of the substitution.

The anchor-modified 'heteroclitic' version of this peptide, ELAGIGILTV (ELA hereafter), has been shown to induce a far greater expansion of T-cells compared to the wild type EAA, when used in vaccine trials (Romero et al., 2002). It has been shown that APLs can strongly stimulate T-cells and achieve more potent immune responses than native peptide epitopes. It is critical that the T-cells elicited by the enhanced vaccine also recognise the wild-type sequence actually expressed on the melanoma cell surface. This was the main caveat of using ELA for therapeutic melanoma vaccination; ELA-based vaccines may prime T-cells that do not optimally recognise the wild type EAA epitope (Cole et al., 2010; Madura et al., 2015; Speiser et al., 2008). Preclinical studies have confirmed that, with carefully design, heteroclitic peptides are indeed capable of inducing T-cells with capacity of tumour cell recognition and killing (Ayyoub et al., 2003; Parkhurst et al., 1996; Rivoltini et al., 1999; Speiser et al., 2005; Valmori et al., 1998). Overall, these studies highlight that even when peptide modifications are selected very conservatively to avoid changes in antigenic structure, APLs may prime T-cells bearing TCRs that are unable to recognize tumour cells (Clay et al., 1999; Pass et al., 1998; Tsang et al., 2015). Therefore, use of APLs to break cancer tolerance requires careful evaluation for each specific peptide-MHC combination to reduce the risk of activating T-cells that do not recognise tumour (Berzofsky et al., 2015; Boon et al., 2006).

1.4.2 Adoptive Cell Transfer (ACT) for the treatment of metastatic melanoma

Adoptive cell transfer (ACT) lies at the other end of the immunotherapy spectrum from peptide vaccines. This cell-based approach in which autologous T-cells are expanded, manipulated *ex vivo*, and then re-infused into the patient to exert an anti-tumour response involves multiple technical challenges.

1.4.2.1 Tumour Infiltrating Lymphocyte (TIL)-based therapy

Tumour Infiltrating Lymphocytes (TILs) represent a heterogeneous population of T-cells within a tumour and can be associated with killing malignant cells. The rationale of TIL-based therapy is to enhance the natural anti-tumour immune response by removing cells with anti-tumour potential from an immunosuppressive tumour microenvironment, to an *in vitro* setting where autologous T-cells can be expanded and then re-infused. TILs should be returned in high enough numbers to allow trafficking to tumour sites and selective killing of tumour targets (possibly along with other cell targets that sustain the tumour, such as vascular endothelial cells). In 1988 Rosenberg and colleagues, at the Surgery Branch at the NIH, pioneered this new approach by publishing the first human study that showed how TILs could induce cancer regression when administered to patients with metastatic melanoma (Rosenberg et al., 1988). Since then, there has been considerable effort, at the NIH and other institutions worldwide, towards the improvement of these first promising results by modifying both the TIL generation and selection protocols, and the preparative regimens given prior to ACT that allow TIL to engraft.

1.4.2.2 TIL isolation and production

TIL manufacturing is a technically complex and resource-consuming process which needs to be carried out following cGMP compliant rules. A general diagram of TIL isolation and production is shown in **Figure 1.10**, although protocols may vary between research institutes. Tran and colleagues established a “Young TILs” protocol that shortened the time in culture and eliminated the step of screening for tumour recognition (Tran et al., 2008). The first use of young TILs for patient treatment was reported a few years later, resulting in 15 objective responders (48%) out of 31 treated patients (Itzhaki et al., 2011). Other groups supported the notion that ‘young/unselected’ TILs were simpler and more reliable than selected TILs (Dudley et al., 2010). Svane and colleagues in Denmark performed a side-by-side comparison of ‘standard’ TIL and ‘young’ TIL in 2011 and also found a higher expression of CD27+ T-cells with longer telomeres (Donia et al., 2012). The introduction of the bioreactor (i.e. GMP compliant closed systems) to TIL manufacture has allowed high-density T-cell expansions by more than 5,000-fold at considerably reduced costs (Donia et al., 2014b; Somerville et al., 2012).

Currently TIL therapy is being undertaken at several different institutions worldwide using a number of varied protocols (Besser et al., 2009; Dudley et al., 2010; Goff et al., 2010; Joseph et al., 2011). The use of ‘Young TIL’ has reduced the time from tumour resection to TIL infusion to <5 weeks and ensured that most patients can be treated.

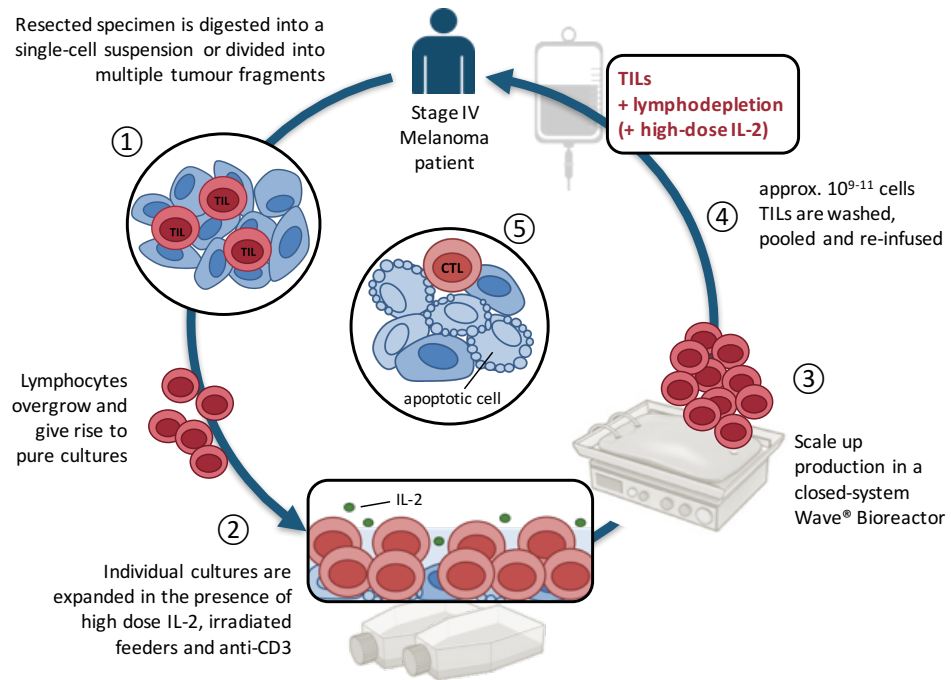


Figure 1.10. Schematic diagram of TIL isolation and expansion for ACT

Melanoma lesions, which often contain diverse cell types, can be surgically resected and fragmented; the cells can be placed in wells into which a T-cell growth factor, such as interleukin-2 (IL-2), is added. T-cell populations can be isolated and expanded, and then adoptively transferred into patients. Prior to T-cell adoptive transfer, hosts are immunodepleted by either chemotherapy alone or in combination with total-body irradiation. The combination of a lymphodepleting preparative regimen, adoptive cell transfer and a T-cell growth factor (such as IL-2) can lead to prolonged tumour eradication in patients with metastatic melanoma.

The addition of a lymphodepleting conditioning regimen has resulted in considerable improvement of TIL-based ACT. Creating a lymphopenic environment prior to TIL infusion is believed to eliminate other lymphocytes (i.e. immunosuppressive regulatory T-cells and myeloid derived suppressor cells) that may compete for homeostatic cytokines IL-7 and IL-15 (Gattinoni, 2005). Therefore, lymphodepletion provides both a physical and biologic “space” for TILs and other potential effectors (such as NK cells) to proliferate and survive. Total body irradiation contributes to lymphodepletion but also appears to increase the function of antigen-presenting cells by activating the innate immune system, in part due to bacterial translocation from gut mucosal damage, which provides activation signals to antigen presenting cells through their Toll-Like Receptors (Paulos et al., 2007).

In 2008, Dudley *et al* presented an interesting analysis which described three sequential trials with increasing intensities of myeloablation prior to TIL infusion (Dudley et al., 2008). Results suggest that the overall response rates and complete response rates were progressively higher with the greater intensity of lympho- and myeloablation. Building on this success, ACT with tumour infiltrating lymphocytes, T-cells grown from resected metastatic tumour deposits, has resulted in high response rates and reproducible complete and durable responses in metastatic melanoma. As shown in **Table 1.1**, most TIL-based clinical trials achieved overall response rates and complete response rates for metastatic melanoma were around 50% and 20% respectively, independent of the cancer centre. 95% of complete responses are ongoing, all at least with 5 years of follow-up. In Europe, TIL therapy is currently performed in three European research institutions: CCIT, Denmark; Netherlands Cancer Institute–Anthoni van Leeuwenhoek Hospital, Amsterdam, The Netherlands. In the United Kingdom, a GMP compliant TIL production process has been established in Manchester in partnership with groups overseas (reviewed by Gilham et al., 2015).

Table 1.1. Treatment protocols and clinical results in TIL-based ACT trials

NMA, non myeloablative; TILs, tumour-infiltrating lymphocytes; TBI. Total body irradiation

Protocol	Institution	# patients treated	Response rate	CR rate	Reference
Unselected TILs + high-dose IL-2	NCI	86	34%	6%	(Rosenberg et al., 1994)
NMA + selected TILs + high-dose IL-2	NCI	43	49%	12%	(Dudley, 2005; Rosenberg et al., 2011)
NMA + 2-Gy TBI + selected TILs + high-dose IL-2	NCI	25	52%	20%	(Dudley et al., 2008; Rosenberg et al., 2011)
NMA + 12-Gy TBI + selected TILs + high-dose IL-2	NCI	25	72%	40%	(Dudley et al., 2008; Rosenberg et al., 2011)
NMA + young TILs + high-dose IL-2	Sheba Medical Center	42	40%	10%	(Itzhaki et al., 2011)
NMA + CD8+ enriched young TILs + high-dose IL-2	NCI	33	58%	9%	(Dudley et al., 2010)
NMA + 6-Gy TBI + CD8+ enriched young TILs + high-dose IL-2	NCI	23	48%	9%	(Dudley et al., 2010)
NMA + modified young TILs + two cycles high-dose IL-2	MD Anderson	31	42%	6%	(Radvanyi et al., 2012)
NMA + selected TILs + high-dose IL-2	H Lee Moffitt	13	38%	15%	(Pilon-Thomas et al., 2012)
NMA + modified selected TILs + 14 days low-dose IL-2	Herlev Hospital	6	33%	33%	(Ellebæk et al., 2012)
NMA + selected TILs + prolonged low-dose IL-2	Uppsala University	24	21%	4%	(Ullenhag et al., 2011)

1.4.2.3 Lessons from using genetically redirected T-cells

T-cells that are reactive against melanoma cells can also be generated *ex vivo* prior to infusion using genetic engineering approaches, which involve the transduction of TAA-specific surface receptor genes. The rationale of infusing genetically-modified T-cells in melanoma patients, is that the endogenous repertoire of potent tumour-specific T-cells has been compromised as a consequence of central tolerance. Comparative analyses have demonstrated that tumour-specific TCRs have substantially lower antigen affinity compared with those directed against virus-derived antigens (Bridgeman et al., 2011), therefore partially explaining the lack of clinical efficacy of some approaches.

There are two main types of antigen surface receptors used in genetic redirection of autologous T-cells (reviewed by Hinrichs and Rosenberg, 2013). The first uses the native α - and β -chains of a TAA-specific TCR; the second, termed a chimeric antigen receptor (CAR), is usually composed of an extracellular TAA-specific single-chain antibody variable fragment (scFv) linked to an intracellular signalling domain via a hinge and transmembrane domains. Of note, because CARs are derived from antibodies, their TAAs recognition is not MHC-restricted; CAR-based redirection represents a near universal ‘off-the-shelf’ method to generate large numbers of antigen-specific helper and cytotoxic T-cells. Following the achievements in preclinical settings, in which established melanomas were eradicated using genetically engineered T-cells, these approaches have been tested in patients (Vonderheide and June, 2013). **Table 1.2** summarises the key published reports in the field for melanoma treatment.

Table 1.2. Published reports of genetically redirected T-cells in melanoma

(HMW-MAA, high molecular weight melanoma-associated antigen).
Clinical trial ID number and phase in brackets

Antigens targeted by TCR	<i>Ref (Trial ID number)</i>
MAGE-A1	<i>Willemsen et al., 2005</i>
MAGE-A3	<i>Morgan et al., 2013 (I/II; NCT01273181)</i>
HMW-MAA	<i>Burns et al., 2010</i>
gp100	<i>Johnson et al., 2009 (II; NCT00509496)</i> <i>Rosenberg et al., 2010 (I; NCT01176461)</i>
Melan-A	<i>Morgan et al., 2006; Burns et al., 2009 (II; NCT00706992)</i> <i>Johnson et al., 2009 (II; NCT00509288)</i>
NY-ESO1	<i>Robbins et al., 2011 (II; NCT00670748)</i>
p53	<i>Davis et al., 2010 (II; NCT00393029)</i>
Antigens targeted by CARs	<i>Ref</i>
Ganglioside GD2	<i>(Gargett et al., 2015) (I; NCT02107963)</i>
VEGFR2	<i>(Chinnasamy et al., 2010) (I/II; NCT01218867)</i>

Genetically modified T-cells expressing melanoma-specific TCRs can be applicable to a wider range of patients when suitable TILs cannot be isolated or grown, but they can be less effective than TIL-based therapy (Johnson et al., 2009; Morgan et al., 2006). Efforts have been made to increase the effectiveness by generating modified high-affinity TCRs for clinical studies (Chinnasamy et al., 2011; Robbins et al., 2008; 2011). However, the correlation between TCR affinity and anti-tumour activity is still controversial: high-affinity TCRs have been shown to lead to stronger (Varela-Rohena et al., 2008), plateaued (Schmid et al., 2010), or even attenuated (Irving et al., 2012; McMahan, 2006) T-cell responses. A recent study from my own laboratory compared a range of enhanced TCRs specific for three different tumour antigens in an attempt to reconcile previous disparate findings (Tan et al., 2015). This study showed that responses could be improved in all systems by modest enhancement of anti-tumour TCR affinity (~10-fold). Greater enhancements reduced tumour recognition and/or resulted in target recognition without the need for cognate antigen. Further unpublished studies have demonstrated that the optimal affinity of MHC-I-restricted anti-tumour TCRs is higher in CD4+ T-cells than in CD8+ T-cells. This difference is presumed to be due to the lack of help from the CD8 co-receptor, which binds to invariant parts of MHC-I to aid TCR stability and intracellular signalling, in CD4+ T-cells (Tan et al., unpublished).

An important issue with TCR- or CAR-modified T-cells is that the receptor antigen specificity has to be chosen so that the transduced T-cells selectively target tumour cells and not healthy tissues. Despite the promising results emerging from early phase clinical trials, a couple of studies targeting members of the MAGE family have reported safety concerns associated with the potency of TCR-engineered T-cell therapy (van den Berg et al., 2015). In one trial, T-cells were engineered to express a TCR generated in HLA-A2 transgenic mice that recognized an epitope shared between MAGE-A3, MAGE-A9, and MAGE-A12. Five out of nine patients showed objective clinical responses, but three reported neural toxicities, including two deaths (Morgan et al., 2013). *Post-mortem* analysis revealed rare and previously unknown expression of MAGE-A12 in brain tissues. A second trial, which evaluated the use of the affinity enhanced MHC-A*01-restricted TCR, specific for MAGE-A3, was aborted due to unexpected toxicity (Linette et al., 2013). A patient experienced encephalopathy associated with cardio-toxicity and died within 7 days after T-cell infusion. Extensive and detailed retrospective analysis demonstrated that the affinity enhancement of the TCR resulted in the off-target recognition of a related epitope from the protein titin, which is expressed in cardiomyocytes (Linette et al., 2013; van den Berg et al., 2015). My own laboratory have recently visualised the interaction between this TCR and the titin and MAGE-A3 peptides (Raman et al., 2016) and shown that it is possible to reverse engineer out the dangerous cross-reaction with titin.

1.4.3 T-cell checkpoint inhibitors

Immune checkpoint inhibitors have also been successfully used to treat advanced melanoma. This form of immunotherapy exploits a naturally occurring feedback mechanism that prevents excess T-cell activation through the expression of negative costimulatory molecules. T-cell negative regulatory signals can be initiated through membrane receptors, following the binding of cognate ligands, either soluble or membrane-bound (Janeway, 2011). These inhibitory receptors, also known as ‘checkpoints’, such as cytotoxic T-lymphocyte antigen 4 (CTLA-4), programmed death 1 (PD-1), T-cell immunoglobulin 3 (TIM-3) and lymphocyte-activation gene 3 (LAG-3), act as ‘brakes’ on T-cell activation (reviewed in Pardoll, 2012). In patients with advanced cancer, inhibitory ligands and receptors that regulate T-cell tissue effector functions are often overexpressed on tumour cells (or non-malignant cells in the tumour microenvironment). This can allow the development of tumour resistance and immune escape, which prevents the induction of an optimal anti-tumour response. Therefore, membrane-bound T-cell immune checkpoints are considered attractive drug targets using inhibitory monoclonal antibodies (Pardoll, 2012). Of note, unlike most antibodies approved for cancer therapies which target tumour cells directly, mAbs blocking T-cell immune checkpoints target inhibitory receptors (or their ligands) in order to enhance endogenous anti-tumour activity. As of 2010, three new mAbs have been approved for advanced melanoma by the US Food and Drug Administration (FDA), which target T-cell checkpoints PD-1 and CTLA-4. **Figure 1.11** schematically shows their mechanism of action.

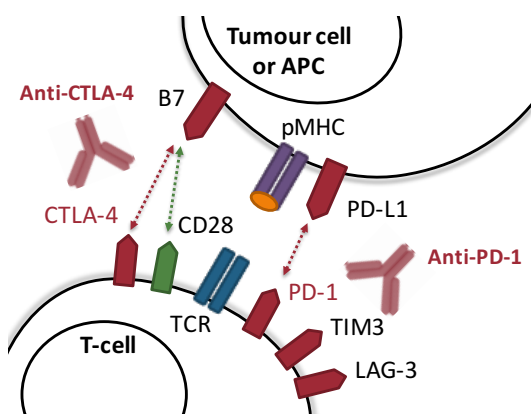


Figure 1.11. Checkpoint blockade antibodies

This approach to immunotherapy is exemplified by antibodies directed against CTLA-4, which block the immune suppression mediated by the interaction between B7 family members (on antigen presenting cells) and CTLA-4 (on CD8+ and CD4+ T cells). A second major checkpoint, mediated by the interaction between PD-1 (on T-cells) and its ligand PD-L1 (on antigen presenting cells or tumours), has been the subject of several recent clinical trials (adapted from Drake et al., 2014). Other inhibitory receptors on T-cells are TIM3 and LAG3. The bottom panel shows a few example of commercially available antibodies. Commercial names are indicated in brackets.

<i>Treatment</i>	<i>Action</i>	<i>Example</i>	<i>Drug modality</i>	<i>Target</i>	<i>Reference</i>
immunotherapy drugs	target T-cell "brakes"	Ipilimumab (<i>Yervoy</i>)	antibody	CTLA-4	Hodi et al., 2010
		Pembrolizumab (<i>Keytruda</i>)	antibody	PD-L1	Robert et al., 2014
		Nivolumab (<i>Opdivo</i>)	antibody	PD-1	Weber et al., 2015

CTLA-4 was the first immune-checkpoint receptor to be clinically targeted in melanoma. Its expression is primarily restricted to T-cells where it mainly regulates the amplitude of the early stages of T-cell activation (Brunet et al., 1987; McCoy and Le Gros, 1999). In a milestone publication, more than 600 stage III or IV melanoma patients were treated with Ipilimumab (anti-CTLA-4 mAb), gp100 peptide vaccine or a combination of both; the best overall response rate (10.9%) was achieved by Ipilimumab alone, and long-term responses (>2 years) were reported in 60% of patients (Hodi et al., 2010).

PD-1 has a broader expression compared to CTLA-4; it is minimally expressed in resting immune cells, however, upon activation, it can be induced in other immune cells (including B and NK cells) where it limits their lytic functions (Ishida et al., 1992; Keir et al., 2008). In activated and 'exhausted' T-cells, the interaction between PD-1 and its ligands, PD-L1 or PD-L2, dampens T-cell function in non-lymphoid organs and lymphoid organs, respectively (Keir et al., 2008). PD-L1 is expressed by several tumour cell types, including melanoma; PD-L1 can engage PD-1 on tumour infiltrating cells and inhibit their function, therefore shielding the tumour from immune-mediated killing. Results from a large phase I clinical trial led to the FDA approval of Pembrolizumab (anti-PD-1) in September 2014 for the treatment of patients with metastatic or unresectable melanoma (Robert et al., 2014). Nivolumab, another anti-PD-1, was approved in December 2014 with the same indication (Weber et al., 2015). More recently, another molecule, V-domain Immunoglobulin Suppressor of T-cell Activation (VISTA), has been characterised as a potential T-cell immune checkpoint target (Márquez-Rodas et al., 2015; Wang et al., 2011). VISTA and PD-1/PD-L1 share expression profiles in haematopoietic cells, but their immune-regulatory pathways are non-redundant, therefore VISTA and PD-1 can be targeted in synergy (Lines et al., 2014; Liu et al., 2015). Preclinical studies in murine cancer models have also shown that VISTA blockade leads to inhibition of melanoma growth and (Liu et al, 2015).

Overall, treatment with T-cell checkpoint inhibitors produces long-term responses, but in a minority of patients. Treatment response and improved survival is often also associated with autoimmune side effects (Hodi et al., 2010; Robert et al., 2011; Topalian et al., 2012). In addition to their use in monotherapy, a few T-cell checkpoint inhibitors are now being tested in combination with other treatments (such as TIL-based therapy) in clinical trials, which showed promising response rates (Kim et al., 2014).

1.4.4 Towards personalised approaches

Although a number of studies provided early evidence for the immunogenicity of mutation-derived neo-antigens, the technology to analyse T-cell reactivity against these antigens only became available very recently. Identification of neo-antigens can be achieved by eluting the peptides from MHC molecules derived from the tumour tissue of a patient (i.e. MHC ligandome), followed by reversed phase HPLC fractionation and mass spectrometry (MS). Results are integrated with cancer genome data in order to identify mutations that may lead to candidate peptides (Haen and Rammensee, 2013; Trajanoski et al., 2015). Sahin and colleagues were the first to demonstrate how whole-exome sequencing data could be used to identify neo-antigens recognized by CD8⁺ T-cells in the B16F10 murine melanoma models (Castle et al., 2012). In recent promising case studies, cancer exome information was used to identify mutations in human melanomas, and T-cell reactivities against melanoma neo-antigens was demonstrated in both CD8⁺ and CD4⁺ T-cell compartments (Kreiter et al., 2015; Linnemann et al., 2014; Tran et al., 2014). Robbins and colleagues have shown responses in melanoma patients that correlated with neo-antigen specific T-cells in *in vitro* expanded and infused TILs (Robbins et al., 2013). Another study presented the case of a melanoma patient with partial tumour regression following anti-CTLA-4 antibody treatment, which correlated with expansion of neo-antigen specific T-cells after treatment (van Rooij et al., 2013). Durable complete tumour regression was achieved infusing T-cells specific for the mutated PP1R3B protein in a further patient (Lu et al., 2013). Finally, three patients were recently treated with autologous DC pulsed with a pool of 7 private peptides, showing a robust increase in the frequency of neo-antigens-specific T-cells following vaccination (Carreno et al., 2015). T-cells specific for neo-antigens were also shown to possess functional sensitivity equivalent to that of anti-viral T-cells (Lennerz et al., 2005). In contrast, T-cell reactivity toward self-antigens is lower by definition and is achieved only when tolerance to these antigens is not fully developed. The identification of neo-antigens on a patient-specific basis could be the way forward to design personalised immunotherapy programs aimed to induce (or boost) melanoma-specific adaptive immunity. However, such personalised approaches are highly expensive and it is unlikely that they will become routine for the majority of patients.

1.5 Project aims

Melanoma is generally accepted as being an antigenic tumour capable of eliciting T-cell responses. However, in most cases immune surveillance is suboptimal and fails to control melanoma growth. As a result, several T-cell based immunotherapy approaches, which aim at harnessing the patient's own anti-melanoma adaptive immune response are being developed. My thesis mainly focuses on two of these therapeutic approaches: cancer peptide vaccines and TIL-based therapy. In particular, I aimed to analyse human anti-melanoma T-cell responses from both a molecular and cellular point of view.

- In **Chapter 3** my studies focus on the melanoma differentiation antigen gp100, which encodes for several T-cell peptide epitopes that have been extensively tested in cancer vaccination. Despite the interest in these antigens, they have never before been viewed by X-ray crystallography. My main goal was therefore to build a molecular picture of how a gp100-specific TCR interacted with its cognate antigen and to provide a detailed binding analysis of this important anti-melanoma molecular interaction.
- In **Chapters 4 and 5**, I focus on successful T-cell responses against melanoma and, in particular, I aimed to dissect the tumour reactivity of human TIL cultures associated with *in vivo* tumour clearance. I was fortunate to be given privileged access to samples from patients who had undergone successful TIL-based therapy for metastatic melanoma at the Centre for Cancer Immune Therapy (CCIT) in Copenhagen, Denmark. Having access to T-cell infiltrates and autologous melanoma cells from cured melanoma patients after TIL-therapy, the main goal was to provide cellular profiling of anti-melanoma TILs in both an HLA-A2+ (Chapter 4) and an HLA-A2- patient (Chapter 5). Both studies aim to examine the phenotype and antigen specificity of the tumour-reactive populations. In addition, I hypothesised that the dominant anti-melanoma responses in the patient's blood following successful TIL therapy, could be those contributing to *in vivo* tumour clearance. I therefore investigated whether anti-melanoma T-cell clones persist in both patient's blood after TIL therapy and attempted to map the antigen specificity.

2 Materials and Methods

2.1 Protein expression, refolding and purification

2.1.1 Vectors for protein expression

The pGMT7 expression plasmid (Banham and Smith, 1993; Studier et al., 1990) was used as a vector for bacterial protein expression, conferring a resistance to carbenicillin. It contains a sequence encoding the protein of interest inducible with IPTG (Isopropyl β -D-1-thiogalactopyranoside) under the control of the T7 RNA polymerase promoter, the sequence being cloned between BamHI and EcoRI restriction sites. pGMT7 expression were used to produce the extracellular domain of α -chain and the β -chain soluble domains of the gp100-specific TCRs, and HLA-A*0201 (HLA-A2 from hereon) heavy chain. Human β 2m was also expressed from pGMT7. The sequences that encode for the α -chain of HLA-A2 and β 2m chain were designed according to previous work performed by Boulter and colleagues (Boulter et al., 2003). The N-terminus of the α -chain of HLA-A2 was tagged with a 15 aa biotinylation sequence (GLNDIFEAQKIEWHE) (AviTag™, Avidity) allowing tetramerisation of pMHC monomer or adherence to streptavidin BIAcore chips (see section below). Proteins were expressed without the biotinylation tag for crystallisation studies. A cysteine residue was added to the TCR α - and β -chain extracellular domains in order to introduce potential for a non-native disulphide bond to enhance potential for $\alpha\beta$ chain-pairing during the refolding process (Boulter et al., 2003) as described below.

2.1.2 Protein sequences

Expression constructs were used that expressed the following sequences:

PMEL17 TCR soluble alpha chain

```
KQEVTVQIPAAALSVPEGENLVLNCSFTDSAIYNLQWFRQDPGKGLTSLLLIQSSQREQTSGRNLNASLDKSSGRSTLYIAASQPGDS  
ATYLCAVLSSGGSNYKLTFGKGTLLTVNPNIQNPDPVAVYQLRDSKSSDKSVCLFTDFDSQTNVVSQSKSDVYITDKCVLDMRSMDFKSN  
SAVAWSNKSDFACANAFNNSIIPEDTFFPSPSS
```

PMEL17 TCR soluble beta chain

```
MGAGVSTPSPNKVTEKGYVELRCDPISGHTALYWYRQSLGQGPEFLIYFQGTGAADDSGLPNDRFFAVRPEGSVSTLKIQRTER  
GDSAVYLCASSFIGGTDYQYFGPGTRLTVLEDLKNVFPPEVAVFEPSEAEISHTQKATLVCLATGFYDPDHVELSWVNGKEVHSG  
VCTDPPQLKEQPALNDSRYALSSRLRVSATFWQDPRNHFRQVQFYGLSENDEWTQDRAKPVTVIWSAEAWGRAD
```

Gp100 TCR soluble alpha chain

```
MSQQGEEDPQALSIQEGENATMNCYSYKTSINNLLQWYRQNSGRGLVHLILIRSNEREKHSGRRLRVTLDTSKKSSLLITASRAADT  
ASYFCATDGDTPLVFGKGRSLVIANIQKPDPAVYQLRDSKSSDKSVCLFTDFDSQTNVVSQSKSDVYITDKCVLDMRSMDFKSN  
SAVAWSNKSDFACANAFNNSIIPEDTFFPSPSS
```

Gp100 TCR soluble beta chain

MDGGITQSPKYLFRKEGQNVTLSCQNLNHDAMYWYRQDPGQGLRLIYYSQIVNDFQKGDIAEGYSVSREKKESEFPLTVTSAQKN
PTAFYLCASSIGGPYEQYFGPGTRLTVTEDLKNVFPPEVAVFEPSEAEISHTQKATLVCLATGFYPDHVELSWVNGKEVHGVCT
DPQPLKEQPALNDSRYALSRLRVSATFWQDPRNHFRQVQFYGLSENDEWTQDRAKPVTVQIVSAEGLG

HLA-A2 heavy chain (with/without biotin tag):

MGSHSMRYFFTSVSRPGRGEPFRFIAVGYVDDTQFVRFDSDAASQRMEPRAPWIEQEGPEYWDGETRKYVKAHSQTHRVDLGLTRGY
YNQSEAGSHTVQRMYGCDVGSQDWRFLRGYHQYAYDGKDYIALKEDLRSWTAADMAAQTTKHKWEAAHVAEQLRAYLEGTCVEWLR
RYLENGKETLQRTDAPKTHMTHHAVSDHEATLRCWALSFYPAEITLTWQRDGEDQTQDTELVEVTRPAGDGTQKWAAVVPSGQE
QRYTCHVQHEGLPKPLTLRWEPLNDIFEAQKIEWHE

β 2-microglobulin:

MIQRTPKIQVYSRHPAENGKSNFLNCYVSGFHPSDIEVDLLKNGERIEKVEHSDLSFSKDWFSFYLLYYTEFTPTKDEYACRVNH
VTLSQPKIVKWRDMD

2.1.3 Culture media and buffers used for protein expression, refolding and purification

<i>Buffer</i>	<i>Composition</i>
LB medium	10 g/L tryptone (Fisher Scientific), 5 g/L yeast extract (Fisher Scientific), 5 g/L NaCl (Fisher Scientific) and supplemented with 50 mg/L carbenicillin (Carbenicillin Direct)
LB agar plate medium	15 g/L agar bacteriological (Oxoid), 10 g/L tryptone (Fisher Scientific), 5 g/L yeast extract (Fisher Scientific), 5 g/L NaCl (Fisher Scientific) and supplemented with 50 mg/L carbenicillin
TYP medium	16 g/L tryptone, 16 g/L yeast extract, 5 g/L potassium phosphate dibasic (Acros Organics)
Lysis buffer	10 mM Tris pH 8.1 (Fisher Scientific), 10 mM MgCl ₂ , 150 mM NaCl, 10% glycerol.
Triton wash buffer	0.5% Triton X, 50 mM Tris pH 8.1, 100 mM NaCl, 2 mM EDTA (Fisher Scientific).
Resuspension buffer	50 mM Tris pH 8.1, 100 mM NaCl, 2 mM EDTA.
Guanidine buffer	6 M guanidine, 50 mM Tris pH 8.1, 100 mM NaCl, 2 mM EDTA.
pMHC I refold buffer	50 mM Tris pH 8, 2 mM EDTA pH 8, 400 mM L-arginine (SAFC), 0.74 g/L cysteamine and 0.83 g/L cystamine
TCR refold buffer	50 mM Tris pH 8, 2 mM EDTA pH 8, 2.5 M Urea (Fisher scientific), 0.74 g/L cysteamine and 0.83 g/L cystamine
Ion exchange buffer A	10 mM Tris
Ion exchange buffer B	10 mM Tris, 1 M NaCl
Biomix A	0.5 M Bicine buffer pH 8.3
Biomix B	100 mM ATP, 100 mM MgO(Ac) ₂ , 500 μ M Biotin.
Biacore buffer-HPS	10 mM HEPES pH7.4, 150 nM NaCl, 3 mM EDTA and 0.005% (v/v) Surfactant P20 (GE Healthcare)
Crystal buffer	10 mM Tris pH 8.1 and 10 mM NaCl.
ITC buffer	20 mM Hepes pH 7.4, 150 mM NaCl
Reducing sample buffer	125 mM Tris pH 6.8, 4% SDS, 20% glycerol, 20 μ g/mL bromophenol blue, 10% DTT
Non-reducing sample buffer	125 mM Tris pH 6.8, 4% SDS, 20% glycerol, 20 μ g/mL bromophenol blue

2.1.4 Transformation of competent *E. coli* cells

Competent Rosetta (DE3) pLysS *E. coli* cells (Invitrogen) were used to produce TCR α - and β -chains, and MHC-I α and β_2m chains in the form of inclusion bodies. Transformation of competent Rosetta *E. coli* cells was performed by thawing 20 μ L of competent cells on ice for 5 min. 50-100 ng of plasmid DNA were added to the bacterial aliquot and incubated for 5min on ice. The cells were then heat-shocked at 42 °C for 2min and placed directly on ice for a 5min recovery period. Cells were then plated onto a LB agar medium plate (supplemented with 50 μ g/mL carbenicillin) and grown overnight at 37 °C.

2.1.5 Expression of inclusion bodies in Rosetta *E. Coli*

A starter culture was set up to verify the expression of the protein by picking and culturing a single colony in 30 mL of TYP media supplemented with 50 μ g/mL of carbenicillin. The starter culture was grown at 37 °C and shaken at 220 rpm (Sanyo, Leics, UK; MIR-222U) until the suspension reached an optical density (OD_{600nm}) approx. 0.5. The starter culture was then inoculated in 1 L carbenicillin (50 μ g/mL) supplemented TYP medium and incubated in a shaker at 37 °C, 220 rpm (Sanyo, Leics, UK) for 3h (or until OD_{600nm} was approx. 0.5). Protein expression was induced by adding 0.5 mL of 1 M IPTG and incubating at 37 °C for 3h in an orbital shaking incubator. A 0.5 mL sample was taken before and after IPTG induction to record the OD_{600nm} and run on a SDS-PAGE gel (**Section 2.1.7**) in order to verify the quality and quantity of protein expression. Cells were harvested and centrifuged at 3450 xg for 20 min. The cell pellet was resuspended in 40 mL of lysis buffer and sonicated on ice at 20% power for 20 min using 2 sec intervals using a MS73 probe (Bandelin). The sonicated pellet was incubated with 200 μ L of 20 mg/mL DNAase (Sigma) for over 30 min RT, resuspended with 100 mL of Triton wash buffer and centrifuged for 20 min at 15,180 xg. The supernatant was discarded and the pellet was scraped and resuspended into 100 mL of triton wash buffer following homogenization (VWR VD25, 17,500/min). Pellets were then resuspended in 10 mL resuspension buffer and centrifuged for 20 min at 15,180 xg. Finally, pellets were dissolved in the smallest volume possible (e.g. 5-10 mL) of guanidine buffer and stored in 15 mL tubes at -20°C. The concentration of inclusion bodies was determined using 1-3 μ L of each sample and guanidine buffer as a blank (**Section 2.1.6**).

2.1.6 Estimating protein concentration by spectrophotometry

To determine the concentration of pMHC-I and TCR proteins, samples were diluted 1/100 in PBS or appropriate buffer. Using a spectrophotometer (NanoPhotometer®, Geneflow) the machine was blank referenced using appropriate buffer (e.g. guanidine buffer for inclusion bodies). Readings at 280 nm wavelength were recorded and the protein concentration was calculated using the dilution factor and extinction co-efficient (calculated from the amino acid sequence using ProtParam tool, <http://web.expasy.org/protparam/>) following Beer's Law formula: $A_{280nm} = \epsilon \cdot I \cdot C$.

2.1.7 Sodium Dodecyl Sulphate-Polyacrylamide Gel Electrophoresis (SDS-PAGE)

SDS-PAGE (Life Technologies X-Cell SureLock™ system) was used to verify purity and quantity of proteins. Each sample was centrifuged at 15.7 xg for 1 min, prepared by diluting 1:4 in 5X non-reducing sample buffer (or 5X reducing buffer with the addition of 10% DTT) and then incubated at 90 °C for 5min. 20 µL of each sample were analysed by loading onto a pre-cast 10% Bis/Tris gel (NuPAGE®, Invitrogen). The running chamber was filled using 1X running buffer (NuPAGE®, Invitrogen). The pre-stained protein ladder (BLUeye, 10-245 kDa range, Geneflow Ltd.) was loaded in a separate lane. Gels were run at 180 V for 45 min at 200 mA, stained with Quick Coomassie stain (Generon) and de-stained in dH₂O for band visualisation.

2.1.8 Soluble pMHC-I and TCR

For a 1 L refold, 30 mg of TCR α-chain inclusion bodies were incubated at 37 °C for 15 min with 10 mM DTT and added to cold refold buffer. After 15 min, 30 mg of TCR β-chain, incubated for 15 min at 37 °C with 10 mM DTT, were added. For a 1 L pMHC-I refold, 30 mg of HLA-A2 α-chain inclusion bodies was mixed with 30 mg of β₂m and 4 mg of synthetic peptide at 37°C for 15 min, and then added to cold refold buffer. Refolds were mixed at 4°C for >1h. Dialysis was conducted twice using against 10 mM Tris pH 8.1 until the conductivity of the refolds was <2 mS/cm. All buffers and refolds were filtered, firstly through a 0.22 µm filter (Fisher Scientific) and then a 0.45 µm (Sartorius) filter, before further FPLC purification steps.

2.1.9 Fast Protein Liquid Chromatography (FPLC)

The refolded proteins were purified initially using an anion exchange column (POROS® 50HQ, Life Technologies), previously equilibrated in buffer A and washed with buffer B. Protein sample was loaded at a flow rate of 20 mL/min (5 MPa pressure) and eluted using buffer A into FPLC tubes (Greiner Bio-One) on a Frac-920 rack. Fractions were analysed for protein purity by SDS-PAGE, pooled and concentrated at 3000 xg until sample volume <1 mL (approx. 10-15 min) using a 4 mL Vivaspin® (10 kDa molecular weight cut-off, Sartorius) concentrator tube. Buffer exchange and removal of aggregates was achieved by gel filtration using a Superdex™ HR 200 size-exclusion column (Amersham Pharmacia), previously equilibrated with appropriate buffer (i.e. crystal buffer, BIAcore buffer, ITC buffer or PBS). Samples were carefully loaded with a 1 mL syringe to avoid air bubbles, and eluted into FPLC tubes (Greiner Bio-One). Fractions containing correctly folded TCR or pMHC-I proteins were identified by SDS-PAGE, pooled, concentrated as described above, and stored at -20 °C. For BIAcore experiments, refolded and purified pMHC-I were biotinylated (**section 2.1.10**) before gel-filtration.

2.1.10 Biotinylation of pMHC

Refolded and purified pMHC-I proteins were concentrated to a volume of 700 μL using a 20 mL Vivaspin® concentrator tube (10 kDa molecular weight cut-off, Sartorius). The biotinylation process included the addition of 100 μL Biomix A, 100 μL Biomix B, 100 μL d-Biotin 500 μM (Avadin) and 2 μL BirA enzyme (Avadin) to the concentrated pMHC-I at 37 °C for 4 h (or overnight at RT). Excess biotin was removed by following gel filtration purification step.

2.2 Surface Plasmon Resonance (SPR) analysis

The binding analysis was performed using a BIAcore™ 3000 or BIAcore™ T100 equipped with a CM5 sensor chip as previously reported (Wyer et al., 1999). **Figure 2.1** illustrates a schematic representation of the SPR system used. Briefly, biotinylated pMHC complexes were immobilized to streptavidin (500-600 response units [RUs]), which was chemically linked to the chip surface by amine coupling. The pMHC was injected at a slow flow rate (10 $\mu\text{L}/\text{min}$) to ensure a uniform distribution of pMHC on the chip surface.

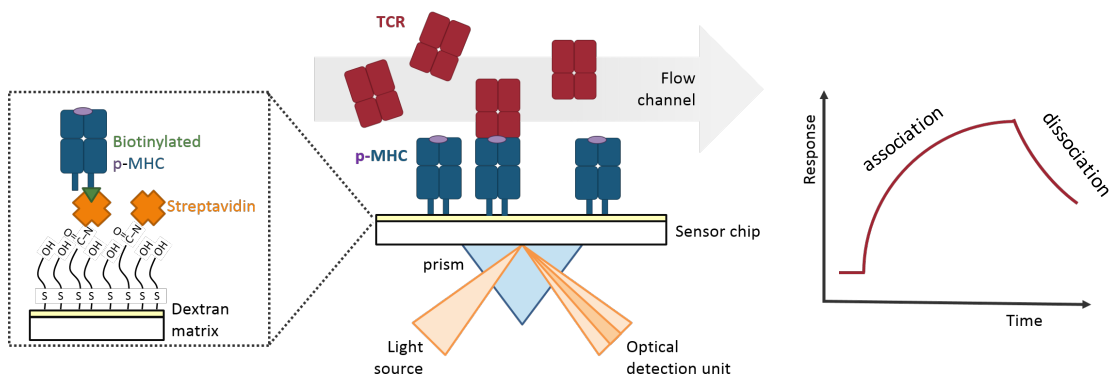


Figure 2.1. Schematic representation of the SPR system

A typical SPR immunoassay setup uses microfluids to flow controlled amounts of purified TCR protein across the sensor chip surface to which the pMHC is immobilised. The system includes a light source, a prism and an optical detection unit, all coupled to a gold-coated sensor microfluidic chip. SPR detection monitors the variations in refractive index close to the gold layer of the sensor chip surface. The intensity of the reflective light is measured to determine the occurrence of binding between the two interacting proteins. **Left panel)** The surface of the sensor chip carries a dextran matrix to which streptavidin has been covalently attached. The biotinylated pMHC protein is captured to the surface of the chip through the high affinity binding with streptavidin. **Right panel)** Schematic illustration of an SPR sensorgram, which plots the response against time. A sensorgram shows in real-time the progress (association and dissociation) of the interaction between the TCR and pMHC proteins.

A flow cell with an irrelevant pMHC was used for each chip for background correction. Combined with the small amount of pMHC bound to the chip surface, this reduced the likelihood of mass transfer being in effect during these experiments. TCRs were purified and concentrated to 100 μM on the same day of SPR analysis to reduce the likelihood of TCR aggregation affecting the results.

For equilibrium analysis, 10 serial TCR dilutions were carefully prepared in triplicate for each sample and injected over the relevant sensor chip at 25 °C. The maximum concentration for all soluble TCR dilution series was in the range of 200-250 µM. The equilibrium-binding constant (K_D) values were calculated using a nonlinear curve fit ($y = (P_1x)/(P_2 + x)$). For thermodynamic experiments, the above-mentioned method was repeated at the following temperatures: 5 °C, 12 °C, 18 °C, 25 °C, and 37 °C. The thermodynamic parameters were calculated according to the Gibbs-Helmholtz equation ($\Delta G = \Delta H - T\Delta S$). The binding free energies, ΔG ($\Delta G = -RT\ln KD$) were plotted against temperature (K, Kelvin) using nonlinear regression to fit the three-parameter equation ($y=dH+dCp*(x-298)-x*dS-x*dCp*\ln(x/298)$). Results were analysed using BIAevaluation 3.1™, Microsoft Excel™ and Origin 6.0™.

2.3 Isothermal Titration Calorimetry (ITC)

ITC experiments were performed using a Microcal VP-ITC (GE Healthcare) as previously described (Armstrong and Baker, 2007), with 30 µM pMHC-I in the calorimeter cell and 210 µM soluble PMEL17 TCR in the syringe. ITC buffer was used and twenty 2 µL-volume injections were performed. Results were processed and integrated with the Origin 6.0™ software distributed with the instrument.

2.4 Crystallisation, diffraction data collection and model refinement

All protein crystals were grown at 18 °C by vapour diffusion via the hanging drop technique. 200 nL of 1:1 molar ratio TCR and pMHC-I (10 mg/mL) in crystallization buffer was added to 200 nL of reservoir solution. PMEL17 TCR/A2-YLE-9V crystals were grown in 0.2 M sodium sulphate, 0.1M Bis/Tris propane pH 6.5, 20% w/v PEG 3350 (Bulek et al., 2012). Crystals of pMHC complexes were grown at 18 °C by seeding into hanging drops of 0.5 µL of seeding solution, 1 µL of complex and 1 µL of reservoir solution. In particular, 0.1 M HEPES pH 7.5, 0.2 M Ammonium Sulphate, 25% PEG 4000 was used for A2-YLE and A2-YLE-5A; 0.1 M Tris pH 8.0, 15% Glycerol, 20% PEG 4000 for A2-YLE-3A (Bulek et al., 2012).

Data were collected at -180 °C at the Diamond Light Source (Oxfordshire, UK). All datasets were collected at a wavelength of 0.976 Å using an ADSC Q315 CCD detector. Reflection intensities were estimated with the XIA2 package (Winter, 2010) and the data were scaled, reduced and analysed with SCALA and the CCP4 package (Bailey, 1994). Structures were solved by molecular replacement using PHASER (McCoy et al., 2007). Sequences were adjusted with COOT (Emsley and Cowtan, 2004) and the models refined with REFMAC5 (Murshudov et al., 1997). Graphical representations were prepared with PYMOL (DeLano Scientific, LLC). Data reduction and refinement statistics are shown in **Table 2.1**. X-ray structures were deposited in the Protein Data Bank (PDB) (<http://www.rcsb.org/pdb/>).

Table 2.1. Data collection and refinement statistics (molecular replacement)

One crystal was used for solving each structure. Values in parentheses are for the highest resolution shell.

Parameters	PMEL17 TCR-A2-YLE-9V	A2-YLE	A2-YLE-3A	A2-YLE-5A
PDB code	<i>5EU6</i>	<i>5EU3</i>	<i>5EU4</i>	<i>5EU5</i>
Dataset statistics				
Space group	P1	P1 21 1	P1	P1 21 1
Unit cell parameters (Å)	a= 45.5, b= 54.4, c= 112.1	a= 52.8, b= 80.4, c= 56.1	a= 56.1, b= 57.6, c= 79.9	a= 56.3, b= 79.6, c= 57.7
Radiation source	DIAMOND I03	DIAMOND I03	DIAMOND I02	DIAMOND I02
Wavelength (Å)	0.9763	0.9999	0.9763	0.9763
Measured resolution range (Å)	51.87 – 2.02	45.25 – 1.97	43.39 – 2.12	43.42 – 1.54
Reflection observed	128191	99442	99386	244577
Unique reflections	64983	30103	49667	67308
Completeness (%)	97.3	98.5	97.4	99.6
Multiplicity	2	3.3	2	3.6
I/Sigma(I)	5.5	7.2	6.7	13
R _{merge} (%)	7.8	9.8	8.7	5
Refinement statistics				
Resolution (Å)	2.02	1.97	2.12	1.54
No reflections used	61688	28557	47153	63875
No reflection in Rfree set	3294	1526	2514	3406
R _{cryst} (no cut-off) (%)	18.1	19.7	17.2	17.0
R _{free}	22.2	25.5	21.1	20.1
Root mean square deviation from ideal geometry				
Bond lengths (Å)	0.018 (0.019)	0.019 (0.019)	0.021 (0.019)	0.018 (0.019)
Bond angles (°)	1.964 (1.939)	1.961 (1.926)	2.067 (1.927)	1.914 (1.936)
Overall coordinate error (Å)	0.122	0.153	0.147	.055

2.5 TCR lentiviral transduction of primary human CD8+ T-cells

2.5.1 293T cells CaCl₂ transfection for lentivirus particles production

Prior to transfection, 2×10^7 293T cells (ATCC®) were plated in a T175 flask in 50 mL transfection medium, and incubated overnight at 37 °C, 5% CO₂ until 80% confluent.

The following media were prepared and 0.2 µm filtered:

<i>Medium</i>	<i>Composition</i>
transfection medium (TFM)	DMEM (Life Technologies), 100U/mL Penicillin, 100µg/mL Streptomycin, 2mM L-Glutamine, 10% FBS
pH 7.1 medium	DMEM, 25mL HEPES, pH 7.1
pH 7.9 medium	TFM, 25mL HEPES, pH 7.9

Lentivirus particles were generated using a 3rd generation plasmid biosafe system. The lentiviral vector plasmid (15 µg) bearing the IMC TCR construct (Immunocore Ltd., UK) was combined in pH 7.1 medium with packaging plasmids pMDL (18 µg), pVSV-G (7 µg) and pRSV (18 µg) in a 15mL tube (final volume 2.85 mL). 150 µL of 1 M CaCl₂ solution were added to the DNA transfection mix. The transfection mix was incubated at room temperature for 30 min to allow precipitates to form, briefly vortexed and added dropwise to the flask. 293T cells were incubated overnight. at 37 °C, 5% CO₂. Supernatant was replaced 16 hours post transduction and collected after 48 and 72h incubations, kept at 4 °C and filtered through a 0.45 µm filter. The 48h and 72h lentivirus particle collections were concentrated as a pool by ultracentrifugation (150,000 xg for 2 hours) in sterilised pollyallomer ultracentrifuge tubes (Beckham Coulter). After centrifugation, the medium was discarded and the lentiviral pellet was resuspended in 300 µL of complete T-cell media. The lentiviral aliquots were snap frozen on dry ice into cryovials and stored at -80 °C.

2.5.2 Lentiviral transduction of primary CD8+ T-cells

Lymphocytes were isolated from PBMCs by standard density gradient as described in **section 2.9.1**. CD8+ T cells were positively selected using human CD8 MicroBeads (Miltenyi Biotec) following manufacturer's instructions. Briefly, magnetically labelled CD8+ cells were eluted from a MACS L-column as the positively selected cell fraction, and resuspended in T-cell complete medium. Cells were activated overnight with anti-CD3/CD28 Human T cell activator Dynabeads® (Invitrogen) at a bead to cell ratio of 1:1 before lentiviral transduction. Activated primary CD8+ T cells (1×10^6 in 100 µL) were transduced with lentiviral constructs (100 µL) expressing the IMC TCR specific for the HLA-A2-restricted melanoma differentiation antigen gp100 (YLEPGPVTA).

Polybrene® (Santa Cruz Biotechnology, CA) was added at a final concentration of 500 µg/mL in order to increase binding between the viral particle and the cellular membrane and plates were incubated at 37 °C, 5% CO₂. After 72 hours, transduction efficiency was determined by flow cytometry after staining with the relevant pMHC-I tetramer (as described in **section 2.11.4**) or anti-Vβ17 TCR (FITC-conjugated) antibody. Dynabeads® were removed by magnet separation five days after transduction. Non transduced cells and MEL5 TCR transduced cells (kindly provided by Angharad Lloyd) were used as controls.

2.6 Cell culture media and buffers

All reagents and buffers, with the exception of those supplied as part of commercial kits, used for T-cell culture are listed below.

<i>Media and reagents</i>	<i>Composition</i>
R0	RPMI-1640 (Life Technologies) 100 U/mL Penicillin (Life Technologies), 100 µg/mL Streptomycin (Life Technologies) 2 mM L-Glutamine (Life Technologies)
R5	R0 with 5% Heat-Inactivated Fetal Bovine Serum (FBS) (Life Technologies)
R10	R0 with 10% FBS
T-cell culture medium	R10 10 mM HEPES (Life Technologies) 1 mM Sodium Piruvate (Life Technologies) 1X MEM Non-essential amino acids (NEAA) solution (Life Technologies) 25 ng/mL IL-15 (PeproTech) 200 IU/mL IL-2 (Aldesleukin, brand name Proleukin; Prometheus)
T-cell expansion medium	R10 10 mM HEPES 1 mM Sodium Piruvate 1X MEM Non-essential amino acids (NEAA) solution 25 ng/mL IL-15 20 IU/mL IL-2 1 µg/mL purified PHA (Phytohemagglutinin) (Alere)
Freezing buffer	90% FBS 10% DMSO (Dimethyl sulfoxide) (Sigma Aldrich)
RBC lysis buffer	155 mM NH ₄ Cl, 10 mM KHCO ₃ , 0.1 mM EDTA (pH 7.2-7.4)
PBS-EDTA	PBS, 2 mM EDTA
FACS buffer	PBS, 2% FBS

All media and buffers used for tissue culture were filtered using 0.2 µm syringe or filter bottle filters (Stericup®, Merck Millipore). T25, T75 and T175 flasks (Greiner Bio-One) and 24-, 48-, 96-multi well plates (Greiner Bio-One) were used for tissue culture, unless otherwise stated. Cell lines were regularly screened for Mycoplasma infection (MycoAlert™ kit, Lonza) following manufacturer’s instructions. Cells were washed in serum-free media (R0 medium) and adherent cell cultures were detached with PBS-EDTA. R5 medium was used to rest T cells overnight and to perform most of the *in vitro* assays (ELISA, ELISPOT, etc).

2.7 Cell culture

Cell lines were grown at 37 °C with 5% CO₂ in R10 medium, unless otherwise stated. Every 2 to 3 days, cells were split and a portion thereof seeded into fresh media. Care was taken to ensure the cells did not exceed 80-90% confluence and/or turned the media yellow, indicating a decrease in pH level due to the accumulation of waste products. For adherent cell lines, the whole content of the tissue culture flask was transferred into a 50 mL centrifuge tube and the flask washed with PBS to remove all remains of the media. PBS-EDTA was added to detach the cells from the inner surface of the flask. The flask was then incubated at 37 °C for 2 min and then rinsed with an equal volume of R10 media. The bulk cell suspension was transferred to the 50 mL centrifuge tube, centrifuged at 400 xg for 5 min and resuspended in R10 medium for counting. Cells were plated into a new flask at the recommended seeding density. For suspension cultures, cells were resuspended thoroughly and counted if required. Cells were then split into fresh R10 medium in a new flask.

The following cell lines were used throughout my studies:

<i>Cell line:</i>		<i>Grown in:</i>	<i>Used as:</i>
melanoma cell lines	adherent	R10	target cells
T2 (HLA-A2+)	suspension	R10	antigen presenting cells
C1R-A2 (HLA-A2+)	suspension	R10	antigen presenting cells

2.7.1 Cell count

Cells were thoroughly resuspended, 10 µL of cell suspension was mixed 1:1 with trypan blue 0.4% solution (Sigma-Aldrich) in a single well of a 96-well round bottomed plate. 10 µL were loaded onto a counting chamber and live cells were counted based on trypan blue exclusion according to the following formula: (number of cells in one section) x (trypan blue dilution factor) x10⁴ = number of cells/mL.

2.7.2 Cryopreservation and thawing of cell lines

Cells were centrifuged at 400 xg for 5 min to remove culture media, and resuspended in freezing buffer. Viable cell numbers were enumerated by trypan blue exclusion and 1 mL aliquots (typically from 1 to 1×10^7 cells) were frozen in internal thread cryovials (Nunc) at -80°C using a controlled-rate freezing device (either Mr. Frosty® freezing pot, Nalgene, or CoolCell freezing pot, Biocision) following manufacturer's instructions. Once frozen, cells were stored short- or long-term in liquid nitrogen. Vials of cryopreserved cells were removed from liquid nitrogen storage and thawed at 37°C in a water bath. Immediately upon thawing, cells were transferred into a 15 mL centrifuge tube containing 10 mL pre-warmed R10 medium. Cells were centrifuged at 400 xg for 5 min and the supernatant discarded. The cell pellet was resuspended in 1 mL R10 media, counted and transferred to flasks or plates.

2.8 Generation of TILs and melanoma cell lines

Expanded TILs and autologous melanoma cell lines used in this study were generated by collaborators at the Center for Cancer Immune Therapy (CCIT) Herlev Hospital, Copenhagen, Denmark) with protocols extensively described in other studies (Donia et al., 2012; Ellebæk et al., 2012). Briefly, TILs were initially isolated from surgically resected tumour fragments and minimally expanded in high doses of IL-2 (6000 IU/mL IL-2, Proleukin; Novartis). When a minimum of 5×10^7 TILs were obtained (typically about 14-28 days after surgical resection), expansion was further achieved by a standard 14-days Rapid Expansion Protocol (REP), in which TILs are non-specifically expanded with a 200-fold excess of allogeneic irradiated PBMCs from at least three different healthy donors and 30 ng/mL anti-CD3 antibodies. Autologous melanoma cell lines were generated separately from TILs either from tumour fragments or from a combination of cells recovered from suspension in transport medium or after mincing, as previously described (Donia et al., 2012).

2.8.1 Patient samples

All the procedures were approved by the Scientific Ethics Committee for the Capital Region of Denmark. Written informed consent was obtained from patients before any procedure according to the Declaration of Helsinki. Tumour specimens of at least 1 cm were obtained from patients with melanoma stage III or IV undergoing standard-of-care surgical procedures or specimen collection for enrolment in a clinical trial (phase II identifier: NCT00937625). Throughout the text, patients sample ID is referred to as MM909.24, MM909.11 and MM909.15⁴.

⁴ *J Clin Oncol* 31, 2013 (suppl; abstract 3028)

2.8.2 HLA typing

HLA typing of TIL samples was performed by either Pure Transplant Solutions, LLC (Oklahoma) or Welsh Transplantation and Immunogenetics Laboratory (UK).

2.9 Maintenance and expansion of T-cell cultures

2.9.1 Isolation of peripheral blood mononuclear cells (PBMCs)

Fresh blood samples were obtained from (EDTA-treated) buffy coats via the Welsh Blood Service (WBS, Cardiff) in accordance with the appropriate ethical approval. Samples were confirmed seronegative for HIV-1, HBV and HCV. PBMCs were isolated from whole blood by Lymphoprep™ (Stemcell™ Technologies Inc.) density gradient centrifugation. Tubes were centrifuged at 900 xg for 20 min without brake at RT. Using a sterile pasteur pipette, the mononuclear interface layer was removed, transferred into a new 50 mL tube and washed in R10 (700 xg for 10 min). The pellet was resuspended in 25 mL red blood cell lysis buffer and incubated at 37°C for 10 min. A further wash was performed at 200 xg for 10 min to remove platelets. PBMC were finally resuspended in R10 medium, counted and kept in the incubator at 37 °C, 5% CO₂ for further processing.

2.9.2 Expansion and culture of T cells

The following antigen-independent expansion protocol was used to generate large numbers of T-cell lines and clones. Up to 1×10^6 T cells were seeded into a T25 tissue culture flask with 15 mL of T-cell expansion medium and 15×10^6 irradiated (3000 rad) PBMC feeders (from 3 pooled donors as described in **section 2.9.1**). The flask was placed at 37 °C, 5% CO₂ tilted at approx. 45°, so as to enhance cell-to-cell contact. On day 5 of the expansion, half the medium was replaced with the same volume of T-cell expansion medium. Cells were resuspended and incubated for a further 2 days in upright position. Cells were then harvested on day 7 of the expansion, counted and plated in fresh T-cell culture medium at $3-4 \times 10^6$ cells/well in 24 well plates (2 mL/well) or $1-2 \times 10^6$ cells/well in 48 well plates (1 mL/well). The plate was incubated at 37 °C, 5% CO₂ and left until the wells were confluent. Every 2-3 days half the media was replaced, when media turned yellow, with fresh T-cell complete medium. After 14 days from expansion, T-cells could be used for experiments, maintained for up to 4 weeks in culture or frozen until further use.

2.10 Functional T-cell assays

2.10.1 Peptides

Crude (50-60% purity) and pure (> 90% purity) peptides used throughout this study were synthesized by GL Biochem Ltd. (Shanghai, China) and Peptide Protein Research Ltd. (Hampshire, UK), respectively. Lyophilised peptides (4 mg) were reconstituted in DMSO to a final stock concentration of 20 mg/mL and stored at -80 °C. Reconstituted peptides were thawed last minute on ice and a working dilution was prepared in R0 medium. HLA-A2-restricted viral peptides used as controls in this thesis are: GILGFVFTL (designated as GIL) from Influenza viruses M1 matrix protein (Bednarek et al., 1991) and NLVPMVATV (designated as NLV) from CMV virus (Diamond et al., 1997). The full list of tumour-associated antigens used is provided in the Appendix.

2.10.2 IFN- γ Enzyme-Linked ImmunoSpot (ELISpot) assay

Mouse anti-human IFN- γ antibody 1-D1K (Mabtech) was diluted to 10 μ g/mL with PBS, and 50 μ L were added to each well of an ELISpot plate (PVDF-backed plate, Millipore). Coated plates were incubated for 4 h at 37 °C wrapped in cling film, washed thoroughly 5 times with 250 μ L PBS/well, and blocked with 100 μ L of R10 medium for 1 h at RT. Rested T cells (overnight at 37°C in R5) were added to the wells (10^5 cells) in 100 μ L of R5 medium. The peptide was added at the desired concentration (10^{-5} M) to appropriate wells in 20 μ L of R0 medium. The final volume (200 μ L/well) was made up in R5 medium. Phytohaemagglutinin (PHA) (Sigma Aldrich) 2 μ g/mL was added to the positive control wells; T cells only were added to the negative control wells. ELISpot wells were set up in duplicate. Control wells that did not require peptide received media alone, so that the total volume is 200 μ L. The plate was then wrapped in silver foil and incubated at 37 °C for 16-18 hours. Plates were washed 3 times with 150 μ L PBS and incubated with 100 μ L sterile water for 10 min at room temperature (therefore lysing the remaining bound cells). The plate was further washed twice with 150 μ L/well PBS. Secondary biotinylated antibody 7-B6-1-Biotin (Mabtech) (1:1000 in PBS) was added at 50 μ L/well and incubated in the dark at room temperature for 2 hours. The plate was washed 5 times with PBS, and 50 μ L of Streptavidin-Alkaline phosphatase (1:1000 in PBS) was added to each well. The plates were incubated for 2 hours in the dark at RT, followed by 5 washes with 150 μ L PBS. Developing solution was made fresh using 25X AP colour development buffer (Bio-Rad), AP-conjugate substrate A and B solutions (Bio-Rad), and sterile water. The solution was added at 50 μ L/well and left to develop in the dark between 10 to 20 min, until spots were clearly visible. Developing reaction was stopped by washing plates with tap water; plates were then air dried in the dark before spot counting using an automated ELISpot counting system (AID ELISpot reader, Cadama Medical).

2.10.3 ⁵¹Chromium (⁵¹Cr) release cytotoxicity assay

Functional assays to determine specific T-cell killing of target cells were carried out by ⁵¹Cr release cytotoxicity assay. Effector T cells were rested overnight in R5 when supernatant was harvested for ELISA the following day. Assays were performed in duplicate for each sample in a 96-well round-bottomed plate. Briefly, target cells (2000/well) were labelled for 1 hour at 37 °C with 30 µCi ⁵¹Cr (sodium chromate in normal saline, Perkin Elmer) per 1x10⁶ cells, washed with R10 and allowed to leach for a further hour at 37 °C in R10 to remove any excess ⁵¹Cr from the cells. After ⁵¹Cr labelling, target cells were washed, resuspended in R5, and plated with effector T cells at the desired effector-to-target (E/T) ratio in a final volume of 150 µL of R10. Target cells were also incubated with 5% Triton X-100 detergent or alone to give the total and spontaneous ⁵¹Cr released from the target cells respectively. After a 5- and/or 18-hour incubation at 37 °C, 5% CO₂, the supernatants were harvested (15 µL), mixed with 150 µL of Optipahse Supermix Scintillation Cocktail (Perkin Elmer) in 96-well polyethylene terephthalate plates (Perkin Elmer) and sealed. The amount of released ⁵¹Cr was measured indirectly on a 1450-MicrobetaTM counter (Perkin Elmer). The percent-specific target cell lysis by T cells was calculated according to the following formula: (experimental release – spontaneous release) / (maximal release – spontaneous release) *100 = % specific lysis.

2.10.4 Peptide activation assay by Enzyme Linked Immunosorbent Assay (ELISA)

T-cells were washed with R0 medium and rested in R5 medium overnight before being used in an activation assay. In a single well of a 96 round bottom-well plate, 3x10⁴ T-cells were primed with 6x10⁴ antigen presenting cells per 100 µL of R5 medium and a titration of peptide from 10⁻⁵ to 10⁻¹² M for 13 h at 37 °C, 5%CO₂. The plate was centrifuged at 300 xg 3 min to sediment cells to the bottom of the well. 50 µL/well of supernatant was harvested and diluted with 70 µL of R0 medium. Supernatants were analysed by ELISA (described in **section 2.10.5**).

2.10.5 MIP-1β/TNF-α ELISA

MIP-1β/TNF-α ELISA were performed using DuoSet® human ELISA kit following manufacturer's instructions (R&D Systems). All washes were performed with 190 µL of 0.05% Tween 20-PBS (wash buffer) using an automated microplate washer. Briefly, a half-well flat bottom ELISA microplate (Corning Costar) was coated with 50 µL of mouse anti-human MIP-1β/TNF- α capture antibody (1.5 µg/mL) and incubated overnight at RT. The plate was washed 3 times, 150 µL of 1% BSA-PBS (reagent diluent) solution was added to each well and the plate was incubated for 1 h at RT. Following 3 washes, 50 µL of cell supernatant collected from an activation assay was added to each well and incubated 1 h and 15 min at RT. A recombinant human MIP-1β (or TNF-α) standard (R&D Systems) was titrated from 1,000 to 15.6 pg/mL in reagent diluent and plated 50 µL to produce a standard curve (**Figure 2.2**).

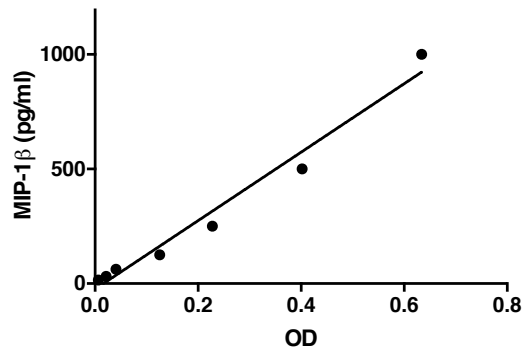


Figure 2.2. Example of MIP-1 β standard curve

The linear regression line equation ($y = m \cdot x$) was calculated and used to interpolate MIP-1 β concentrations for each sample.

The plate was washed 3 times and coated with 50 μ L biotinylated goat anti-human MIP-1 β (or TNF- α) (50 ng/mL) detection antibody. After 1h and 15 min incubation at RT, the plate was washed 3 times and HRP-conjugated streptavidin (50 μ L) was added to the wells. The plate was incubated in the dark for 20 min at room temperature followed by 3 final washes. 50 μ L of a 1:1 ratio colour reagents A and B (R&D Systems) were added to each well and incubated for a maximum of 15 min at RT. The reaction was blocked by adding 25 μ L of stop solution (R&D Systems). The OD_{450nm} of each well was read using a Bio-rad iMark microplate reader with correction set to 570 nm.

2.10.6 Combinatorial peptide library (CPL) scans

T cells were challenged with either a 9-mer or 10-mer combinatorial peptide library (CPL) in positional scanning format (Pepscan Presto Ltd) and their activation towards each mixture was evaluated by the release of MIP-1 β chemokine by ELISA (described in **section 2.10.5**). The decamer CPL contains a total of 9.36×10^{12} ($= (10+19) \times 19^9$) different decamer peptides and is divided into 200 different peptide mix. In every peptide mixture, one position has a fixed L-amino acid residue and all other positions are degenerate, with the possibility of any one of 19 natural L-amino acids being incorporated in each individual position. The cysteine residue was omitted from the random positions to avoid formation of disulphide bonds between peptides within the mixture and peptide aggregation. Each peptide mix consists of 3.2×10^{11} (19^9) different decamer peptides in approximately equimolar concentrations. **Figure 2.3** depicts a 10-mer CPL.

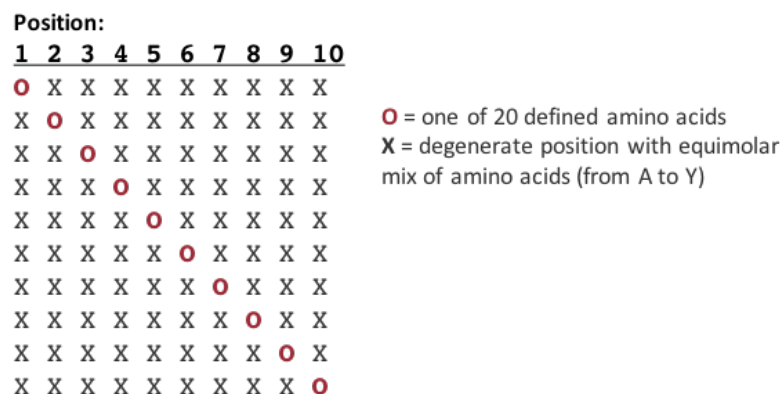


Figure 2.3. Schematic diagram of a 10mer combinatorial peptide library

Each of the 20 natural proteogenic amino acids at each position and all possible combinations of the other amino acids in the other positions. For instance, sub-library 1 has an Alanine at P1 and an equimolar mix of amino acids at all the other positions. Sub-Library 200 has Tyrosine at P10 and an equimolar mix at other positions. Each sub-library contains 3.2×10^{11} different peptides.

CD8+ T cells were washed with R0 medium and rested in R5 medium overnight. Antigen presenting cells were plated in single well of a 96 round bottom-well plate at a concentration of 6×10^4 cells per 45 μ L and pulsed with 5 μ L of peptide mixture from a decamer peptide library at a final concentration of 100 μ M for 1 hour at 37 °C, 5% CO₂; 3×10^4 CD8+ T cells (50 μ L) were added to pulsed antigen presenting cells. Plates were incubated overnight at 37 °C, 5% CO₂ and centrifuged at 300 xg for 5 min. Subsequently, the supernatant (50 μ L) was harvested and assayed for MIP-1 β by ELISA according to the manufacturer's instructions (R&D Systems) (**Section 2.10.5**).

2.10.6.1 Epitope identification

A novel webtool (PI CPL) developed by Dr Barbara Szomolay in Cardiff, was used to link the raw data of CPL scans to the likelihood of the peptide to bind the cognate T-cell clone (Szomolay et al., 2016). The webtool is integrated into the WSBC webtools and is accessible at <http://wsbc.warwick.ac.uk/wsbcToolsWebpage>. Human self databases were compiled on the basis of public available protein sequence databases provided by NCBI (National Center for Biotechnology Information), UniProt (Universal Protein Resource), and PDB (Protein Data Bank).

2.11 Flow cytometric analysis

Samples were acquired on a BD FACSCanto™ II flow cytometer (BD Biosciences) using the FACSDiva software (BD Biosciences). Data analysis was performed on FlowJo version 5.7 (Tree Star Inc, US). Anti-mouse Igk antibody capture beads (BD Biosciences) were used to prepare individual compensation tubes for each mAb used in the experiment.

2.11.1 Labelling cells with fluorescence conjugated antibodies

Cells were washed in FACS buffer (700 xg 3 min), counted by trypan blue exclusion and transferred to either a 96 well plate or 5mL FACS tube (Elkay Laboratory Products Ltd, UK) and washed in FACS buffer (700 xg for 3 min). Cells were washed in PBS and stained 5min at room temperature with LIVE/DEAD® Violet (Life Technologies) (diluted 1:40 in PBS) for dead cell exclusion before surface staining (20 min on ice and in the dark) with relevant mouse anti-human mAb.

The following mouse-anti human mAbs were used depending on each experiment:

<i>mAb specificity</i>	<i>Fluorochrome</i>	<i>Clone</i>	<i>Supplier</i>
CD3	PerCP	BW264/56	Miltenyi Biotec
CD8	APC-Vio770 APC PE	BW135/80	Miltenyi Biotec
CD4	PE-Vio770 FITC APC	VIT4	Miltenyi Biotec
$\alpha\beta$ TCR	PE FITC APC	IP26	Biolegend
INF- γ	APC	45-15	Miltenyi Biotec
CD107a	PE	H4A3	BD Bioscience
TNF- α	PE-Vio770	MAB11	Bioscience
CD19	Pacific Blue	HIB19	Biolegend

The following mouse-anti human TCRBV mAbs (Beckman Coulter), PE- or FITC-conjugated, were used for TCR β -chain scanning: (Arden et al., 1995; Folch and Lefranc, 2000)

<i>Vβ</i>	<i>IMGT nomenclature</i>	<i>Clone</i>	<i>Fluorochrome</i>
1	TRBV9	BL37.2	FITC
2	TRBV20-1	MPB2D5	FITC/PE
3	TRBV28	CH92	FITC
4	TRBV29-1	WJF24	PE
5.1	TRBV5-1	IMMU 157	FITC
5.2	TRBV5-6	36213	FITC
5.3	TRBV5-5	3D11	PE
7.1	TRBV4-1	ZOE	FITC

7.2	TRBV4-3	ZIZOU4	PE
8	TRBV12	56C5.2	FITC
9	TRBV3	FIN9	PE
11	TRBV25	C21	FITC
12	TRBV10	VER2.32.1	FITC
13.1	TRBV6-5	IMMU 222	FITC
13.2	TRBV6-2	H132	PE
13.6	TRBV6-6	JU74.3	FITC
14	TRBV27	CAS1.1.3	FITC
16	TRBV14	TAMAYA1.2	FITC
17	TRBV19	E17.5F3.15.13	FITC
18	TRBV18	BA62.6	PE
20	TRBV30	ELL1.4	PE
21.3	TRBV11-2	IG125	FITC
22	TRBV2	IMMU 546	FITC
23	TRBV13	AF23	PE

Cells were washed twice in FACS buffer and finally resuspended in 100-200 μ L of PBS.

Cells were kept on ice in the dark (or fixed in 2% PFA) until flow cytometric analysis.

2.11.2 Intracellular cytokine staining (ICS) assay

Cells were washed from culture medium and rested overnight in R5 prior to activation. Subsequently, cells were incubated at 37 °C, 5% CO₂ for 4 h, with and without target cells, at a 1:1 ratio, in R5 containing GolgiStop™ and GolgiPlug™ (BD Biosciences), according to manufacturer's instructions. Cells were then stained with LIVE/DEAD® Violet (Life Technologies) and Abs against desired cell surface markers. Cells were prepared for ICS by incubation with Cytofix/Cytoperm™ (BD Biosciences) according to manufacturer's instructions, before staining for 20 min on ice with mouse anti-human IFN γ -APC mAb (Miltenyi Biotec). Cells were resuspended in PBS (or fixed with 2% PFA and stored overnight at 4 °C in the dark) before flow cytometry and data analysis.

2.11.3 Blocking antibody assay

HLA-restriction of CTL-mediated killing was achieved by pre-incubating the target cells with HLA specific antibodies for 1 h at 37 °C, 5% CO₂ before addition of effector cells. The following monoclonal antibodies were used for blocking assays: anti-HLA-A, B, C (clone W6/32, Biolegend) and anti-HLA-DR, DP, DQ (clone Tü39, Biolegend) at a final concentration of 10 μ g/mL.

2.11.4 pMHC tetramer staining

Soluble biotinylated pMHC-I were produced as previously described in **Section 2.1.8**. Peptide-MHC-I tetramers were assembled over five separate 20 min steps with the successive addition of streptavidin, APC or PE conjugates (Life Technologies) to monomeric pMHC at a molar ratio of 1:4. The desired number of cells, typically $0.5\text{--}1 \times 10^5$ of a T-cell clone or $1\text{--}3 \times 10^6$ TILs, was transferred to flow cytometry tubes and cells washed with FACS buffer (700xg 3 min). Cells were treated with the PKI (protein kinase inhibitor) (Dasatinib, Axon Medchem, Reston) at a final concentration of 50 nM for 30 min at 37 °C and then stained with tetramer without washing. Treatment with PKI prevents TCR triggering and internalization of the TCR and any pMHC tetramer bound to it. PKI is unstable when stored at 4 °C, so 1 mM DMSO aliquots of PKI were stored at -80 °C and working aliquots of 100 nM were prepared in PBS for each experiment. Tetramer concentrations ranged from 0.02 to 2.4 mg (0.4–48 mg/mL with respect to the monomeric pMHC concentration) per stain in 50 μ L FACS buffer, and typically 0.5mg was used. Following tetramer addition, cells were placed on ice and in the dark for 30 min. All subsequent Ab staining of the cells was performed for 20 min on ice and in the dark. Cells were washed first in FACS buffer and then PBS before LIVE/DEAD[®] Violet stain (Life Technologies). Following a 5 min incubation at room temperature in the dark, mAbs against cell-surface markers were added directly without washing and incubated on ice for 20 min in the dark. Samples were prepared for flow cytometry by washing twice in FACS buffer and resuspended in PBS or 2% PFA.

2.11.4.1 “Boosted” pMHC tetramer staining

A “boosted” protocol was used to enhance tetramer staining intensity of T-cell populations and T-cell clones described in Chapter 4. A schematic diagram is shown in **Figure 2.4** (Tungatt et al., 2015).

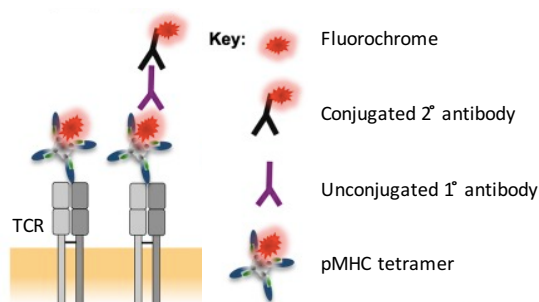


Figure 2.4. Schematic representation of the ‘boosted’ pMHC tetramer staining protocol used

(adapted from Tungatt et al., 2015).

Alongside a standard pMHC tetramer, the staining protocol includes the binding of a mouse anti-fluorochrome unconjugated primary (1°) antibody to the pMHC multimer associated fluorochrome, followed by a goat anti-mouse conjugated secondary (2°) Ab.

Briefly, post-pMHC tetramer staining, the cells were washed in FACS buffer (700 xg 3 min) and labelled with anti-fluorochrome unconjugated primary Ab for 20 min on ice in the dark. Following two washes in FACS buffer, the anti-Ab conjugated secondary Ab was added and incubated for 20 min on ice in the dark. Primary (1°) unconjugated mAbs were used at a concentration of 10 mg/mL (0.5 mg/test). A goat anti-mouse conjugated secondary (2°) Ab was used at 2 mg/mL (0.1 mg/test). The fluorochrome conjugated to the 2° Ab was matched to the one used for the initial pMHC multimer staining. Both anti-fluorochrome and anti-Ab antibodies were spun at maximum speed in a micro-centrifuge for 1 min to remove any aggregates before staining cells.

The following primary and secondary antibodies were used in Chapter 4:

<i>Primary (1°) unconjugated</i>	<i>Fluorochrome</i>	<i>Clone</i>	<i>Supplier</i>
Mouse anti-PE		PE001	BioLegend
Mouse anti-APC		APC003	BioLegend
<i>Secondary (2°) conjugated</i>			
Goat anti-mouse	PE APC	polyclonal	BD Biosciences

2.11.5 Viable sorting of tumour reactive T cells

Autologous tumour cells were plated 1×10^6 /well in a 24 multi-well plate in R10 the day before sorting. TIL samples or autologous PBMC were rested overnight in R5 medium. Cells were then stimulated with autologous tumour (1:1) in the presence of 15 μ L of anti-TNF- α PE-Cy7 (clone Mab11, BD Biosciences), 15 μ L CD107a PE (clone H4A3, BD Biosciences) and 10 μ M of TAPI-0 (Calbiochem) for 4h at 37 °C, 5% CO₂. Note that following the 5-hour incubation period with anti-TNF- α mAb, cells were *not* re-stained with anti-TNF- α in any subsequent steps. Following incubation, cells were LIVE/DEAD® Violet stained and surface stained with anti-CD3 PerCP (clone BW264/56, Miltenyi Biotec), anti-CD8 APC Vio770 (clone BW135/80, Miltenyi Biotec), anti- α TCR FITC (clone IP26, Biolegend) and anti- γ TCR APC (clone 11F2, Miltenyi Biotec) mAbs. Cells from each experimental condition were washed and sorted directly into microfuge tubes containing 350 μ L lysis buffer (Qiagen) and stored at -80 °C until RNA extraction.

2.12 Analysis of human TCR V β CDR3 repertoire

2.12.1 Total RNA extraction

RNA from reactive TILs and PBMC was extracted using the RNeasy Micro Kit (Qiagen), following the manufacturer's instructions. Briefly, samples were first lysed and then homogenized. Ethanol was added to the lysates to provide ideal binding conditions. The lysates were then loaded onto a RNeasy silica membrane, to which RNA binds while all contaminants are efficiently washed away. Pure, concentrated RNA were eluted in 14 μ L water. Isolation of total RNA was performed shortly after cell sorting, in order to minimize loss of RNA. Standard RNA sample handling precautions (i.e. filtered tips and certified RNAase free reagents) were used to avoid RNA degradation. All RNA isolation, cDNA synthesis and PCR preparation steps were carried out in a clean RNAase free room to prevent contamination. RNA samples were stored at -80 °C.

2.12.2 SMARTer™ RACE cDNA amplification

SMARTer™ (Switching Mechanism At 5' end of RNA Transcript) RACE (Rapid Amplification of cDNA Ends) kit (Clontech) was used for generating full-length cDNAs from TCR- β RNA (Zhu et al., 2001). **Figure 2.5** provides a schematic representation of the experimental workflow described in this section.

2.12.2.1 First strand cDNA synthesis

Samples and reagents were kept on ice at all times. RNA samples were thawed at room temperature. The following mix was prepared for each sample:

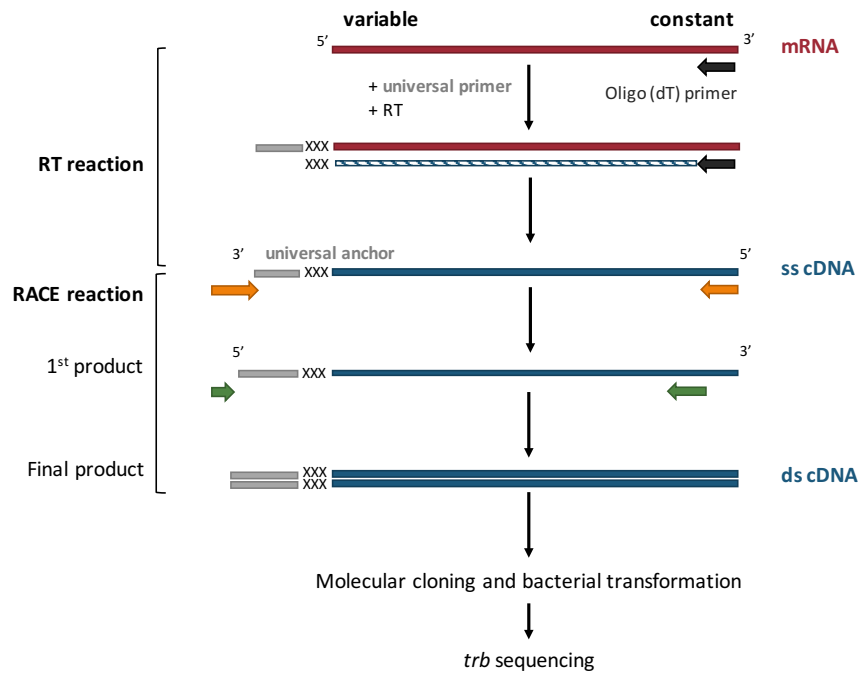
<i>Reagent</i>	<i>Amount</i>
RNA	10 μ L
Oligo-dT	1 μ L
Final volume	11 μ L

The reaction tubes were placed in a thermal cycler and incubated at 72 °C for 3 min, then at 42 °C for 2 min to anneal the synthesis primer. After incubation, tubes were spun briefly. The following master mix for n reactions was prepared and 8 μ L added to each tube:

<i>Reagent</i>	<i>Amount</i>
5X First Strand buffer	4 μ L
DTT (100 mM)	0.5 μ L
dNTP (20 mM)	1 μ L
RNase Inhibitor (20 U)	0.5 μ L
SMARTScribe RT (100 U)	2 μ L
Final volume	8 μ L

1 μ L of SMARTer II oligo A was added to each tube. In a thermal cycler, the tubes were incubated at 42 °C for 90 min, then 70 °C for 10 min cDNA samples were directly stored at -20 °C or used for the following PCR amplification step.

A



B

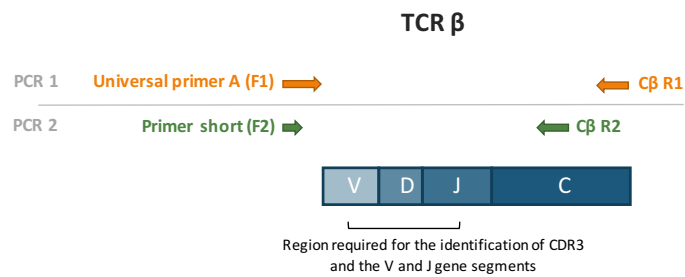


Figure 2.5. Experimental workflow of the SMARTer RACE approach to TCR-β profiling

Abbreviations: Ss, single-stranded; ds, double-stranded; F, forward primer; R, reverse primer; RT, reverse transcriptase.

(A) Schematic diagram of the reverse transcription and PCR amplification of TCR-β chain mRNA sequences (adapted from Clontech Laboratories Inc. website). Single-stranded cDNA from a mRNA template was generated by reverse transcription using an oligo dT primer (located in the constant gene of the TCR-β chain) and a MMLV-derived RT. When the RT reaches the end of the mRNA template, it adds several non-templated nucleotides (indicated as “xxx”). The universal primer anneals to the tail of the cDNA and serves as an extended template for the RT. The “universal anchor” appended to the target during cDNA synthesis, allows subsequent PCR amplification steps (PCR 1 and 2) using a 5′ universal primer (forward) and a 3′ Cβ-specific primer. The final product was cloned into a commercial vector and transformed into bacterial cells. **(B)** Semi-nested PCR approach for amplification of TCR-β subunits. The primer pair (orange) used for the first PCR captures the entire variable region and some of the constant region of the TCR-β cDNA. The primer pair (green) used in the second PCR retains the entire TCR-β cDNA variable region and a smaller portion of the constant region. The expected size of final TCR-β library cDNA (which include the inserts and the universal adapters) is of approximately 600 bp.

2.12.2.2 First PCR amplification

The first PCR amplification captures the entire variable region and some of the constant region of the TCR- β cDNA. A PCR mastermix was prepared as shown below:

<i>Reagent</i>	<i>Amount</i>
Phusion® 5X Green buffer	10 μ L
DMSO (100 mM)	0.5 μ L
dNTPs (20 mM)	1 μ L
10X Universal Primer A (F)	5 μ L
Primer C β -R1 (R)	1 μ L
Phusion® HF DNA polymerase	0.25 μ L
H ₂ O	29.75 μ L
cDNA sample	2.5 μ L
Final volume	50 μ L

The following cycling conditions were used:

4°C; initial denaturation	
94°C; 30 s	30 cycles
63°C; 30 s	
72°C; 3 m	
72°C; final extension	

2.12.2.3 Second PCR amplification

The second PCR amplification used the DNA from the first round of amplification as template. It captures the entire variable region and a smaller region of the constant TCR- β cDNA. A PCR mastermix was prepared as shown below:

<i>Reagent</i>	<i>Amount</i>
Phusion® 5X Green buffer	10 μ L
DMSO (100 mM)	0.5 μ L
dNTPs (20 mM)	1 μ L
Primer A Short (F)	1 μ L
Primer C β -R2 (R)	1 μ L
Phusion® HF DNA polymerase	0.25 μ L
H ₂ O	33.75 μ L
DNA sample	2.5 μ L
Final volume	50 μ L

The following cycling conditions were used:

94°C; initial denaturation	
94°C; 30 s	30 cycles
66°C; 30 s	
72°C; 3 m	
72°C; final extension	

2.12.2.4 Agarose gel electrophoresis

Electrophoresis gels were prepared with 1% agarose powder (Invitrogen) dissolved in (Tris-acetate EDTA) TAE buffer. For DNA visualisation, Midori Green nucleic acid staining solution (GeneFlow) was added before allowing the gels to set. Samples were allowed to run at 80V for 45 min on the gel, along with 5 μ L of 1 Kb DNA HyperLadder™ (Bioline). Gels were visualised under a LED-based illuminator (FastGene) and bands cut out using a disposable scalpel (**Figure 2.6**).

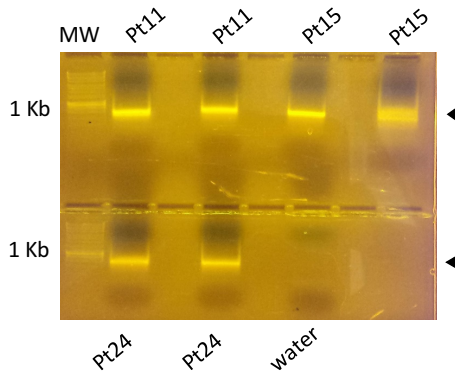


Figure 2.6. Agarose gel analysis of SMARTer RACE cDNA products

Representative gel of PCR amplified TCR- β cDNA products from PBMC samples of three melanoma patients (plus and minus stands for the tumour-reactive or non-tumour reactive population, respectively). Lane 1: molecular weight ladder (MW). An empty lane was kept between samples to avoid cross-contamination during gel loading and electrophoretic run. Water was used as a negative control. Arrow heads indicate the expected TCR- β band of approx. 600 bp.

2.12.2.5 DNA extraction from gel bands and purification for cloning

Amplified products were extracted from the agarose gel and purified for subsequent cloning steps. The NucleoSpin® Gel and PCR Clean-up kit (Clontech) was used to extract DNA from gel bands, following manufacturer's instructions. Briefly, the cut-out gel band was mixed with Binding Buffer NT1 (200 μ L/100 mg) and heated at 50 °C for 10 min to dissolve the agarose. In the presence of chaotropic salt, the DNA sample was bound to the silica membrane of a NucleoSpin® column. Contaminations were removed by washing steps with ethanolic Wash Buffer NT3. Finally, pure DNA was eluted under low salt conditions with slightly alkaline Elution Buffer NE (5 mM Tris/HCl, pH 8.5).

2.12.3 Molecular cloning and bacterial transformation

2.12.3.1 Zero Blunt® TOPO® PCR Cloning

Blunt-end PCR products were cloned into a pCR™-Blunt II-TOPO® vector using a Zero Blunt® TOPO® PCR Cloning Kit (Invitrogen), following manufacturer's instructions. Briefly, a topoisomerase I-based 10-minute ligation was performed in order to directly insert the blunt-ended PCR products into a plasmid vector.

The following 6 µL TOPO® Cloning reaction was set up for each sample:

<i>Reagent</i>	<i>Amount</i>
Fresh PCR product	4 µL
Salt solution	1 µL
pCR™-Blunt II-TOPO®	1 µL
Final volume	6 µL

The tubes were incubated for 10 min at room temperature, then placed on ice to stop the reaction. TOPO® Cloning reactions were then transformed into chemically competent One Shot® TOP10 *E. coli* cells (Invitrogen).

2.12.3.2 Transformation of One Shot® TOP10

Chemically competent *E. coli* cells (One Shot® TOP10) were transformed following the manufacturer's instructions (Invitrogen). Briefly, one vial of One Shot® *E. coli* cells was thawed on ice for each transformation. 2 µL of the TOPO® Cloning reaction were added to each vial of cells to be transformed, and mixed gently. The vials were incubated on ice for 30 min and then heat-shocked for 30 sec at 42 °C without shaking. 250 µL of room temperature S.O.C. medium (supplied with the kit, Invitrogen) were added to the cells. The tubes were capped and shaken at 37 °C for 1h. 150 µL from each transformation were spread on pre-warmed LB-Agar plates containing 50 µg/mL kanamycin selective antibiotic. Plates were incubated overnight at 37 °C. An efficient TOPO® Cloning reaction would produce several hundred colonies. Approximately 96 colonies were picked for analysis of transformants. Each colony consists of bacteria transformed with one (and only one) *tr* sequence.

2.12.3.3 Colony PCR

Colonies containing the insert were screened and selected for amplification and sequencing. Single bacterial colony plasmid inserts were amplified in a sealed 96-well plate format (Applied Biosystems) using primers flanking the insertion site (M13F: 5'-TTTCCCAGTCACGAC-3'; M13R: 5'-CAGGAAACAGCTATGAC-3'). Care was taken in order to pick only single colonies and to avoid cross-contamination between wells. Colony PCR reactions were prepared as follows:

<i>Reagent</i>	<i>Amount</i>
Primer M13F	1 µL
Primer M13R	1 µL
DreemTaq Green master mix	23 µL
Final volume	25 µL

Colony PCR reactions were run in a thermocycler as follows:

5 µL of several individual products from plate were run on an agarose gel. Positive colonies were sent for sequencing (Eurofins Genomics, Ebersburg, Germany).

2.12.4 Sequence analysis

TCR- β sequences were visualized in the analysis software BioEdit (<http://www.mbio.ncsu.edu/BioEdit/bioedit.html>) (Hall, 1999) and analysed using IMGT/V-QUEST (http://www.imgt.org/IMGT_vquest), in order to identify the V, D and J segments for human TCR- β (Giudicelli et al., 2011). Grouped sequences for TIL and PBMC samples were ranked in a Microsoft Office™ Excel spreadsheet according to their frequency. Unless otherwise stated, all *tr* and gene segments are described using the ImMunoGeneTics (IMGT) nomenclature (Lefranc et al., 1999). Accordingly, TCR α - and β - chain segments are designated TRA and TRB respectively, followed by the letter V, D or J.

2.13 Figures and data analysis

Unless otherwise stated, figures were made using GraphPad Prism 5 (GraphPad Software Inc., La Jolla, USA) or Microsoft Office™ Excel.

3 A molecular switch in a gp100 human melanoma antigen abrogates T-cell recognition

3.1 Background

Glycoprotein 100 (gp100) has been a widely studied target for melanoma peptide-based vaccines. This 661 amino acid long melanoma differentiation antigen is a melanosome matrix protein involved in melanosome maturation and melanin synthesis (Raposo and Marks, 2007). The gp100 protein has a significantly differential expression between tumour cells, being often over-expressed in all stages of melanoma progression, compared to normal melanocytes (Wagner et al., 1997). It was originally identified by its reactivity with a melanocyte lineage-specific monoclonal antibody used for diagnosis of human melanoma (Kawakami et al., 1994b). Several studies showed that gp100 encoded epitopes can be recognised by tumour-infiltrating and circulating T-cells associated with tumour regression in metastatic melanoma patients after TIL therapy (Kawakami et al., 1994b; 1995; Salgaller et al., 1996). Among these epitopes, the nonamer peptide gp100₂₈₀₋₂₈₈ (YLEPGPVTA) was originally shown to be recognized by HLA-A*0201⁺ TILs from melanoma patients (Kawakami et al., 1994a), and subsequently eluted from HLA-A*0201 molecules on melanoma cells (Skipper et al., 1999). Immunization with YLEPGPVTA peptide (YLE hereafter) has been shown to stimulate an *in vitro* polyclonal T-cell response in the context of HLA-A*0201, present in 49% of Caucasian individuals (Parkhurst et al., 1996).

Collectively, the above findings renewed the interest in the development of gp100-based anti-melanoma vaccines. However, our group and others, have previously shown through direct biophysical measurements that anti-cancer TCRs bind to their cognate peptide-Human Leukocyte Antigen (pHLA) with affinities ~5-fold weaker than pathogen specific TCR (Aleksic et al., 2012; Cole et al., 2007). TCR affinity is crucial for T-cell activation and a 5-fold difference in TCR affinity can result in a marked difference in recognition of tumour epitopes which are often present at low copy number (Tan et al., 2015). Several strategies have been attempted to increase the immunogenicity of tumour antigens. Many tumour-associated epitopes possess suboptimal sequences for HLA anchoring (Cole et al., 2010). Since the binding preferences of common HLA are known, improvements in suboptimal primary HLA anchoring positions are easily made. Altered peptide ligands (APL), with improved primary HLA anchor residues, have been designed for some melanoma-associated antigens (Parkhurst et al., 1996; Salgaller et al., 1996). Among these, the YLE-9V modified version of YLE, in which a Valine replaces Alanine at anchor position 9 to improve binding to HLA-A*0201 (HLA-A2, hereafter) (Miles et al., 2011b), enhanced the induction of melanoma reactive CTLs *in vitro* and has been successfully used in clinical trials (Lesterhuis et al., 2011).

However, studies using another HLA-A2-restricted melanoma-derived epitope have demonstrated that even minor changes in peptide anchor residues can substantially alter T-cell recognition unpredictably by altering TCR binding (Cole et al., 2010; Madura et al., 2015). Thus, a more complete understanding of the molecular mechanisms underlying gp100₂₈₀₋₂₈₈ targeting by specific TCRs is needed to direct the design of improved APLs for use in therapeutic vaccination strategies.

3.1.1 Aims

The gp100₂₈₀₋₂₈₈ epitope YLE presented on the surface of HLA-A2⁺ melanoma cells offers an attractive target for immunotherapy. The YLE-9V APL induces melanoma reactive CTLs *in vitro* and has been successfully used in clinical trials (Lesterhuis et al., 2011), but no structural analysis of T-cell recognition of this peptide has been published to date. Previous studies from my own laboratory have demonstrated that such HLA anchor residue alterations can unpredictably alter the way a peptide is viewed by the TCR on cognate T-cells (Cole et al., 2010) and show that increased HLA binding does not necessarily produce a more potent antigen for tumour-specific TCRs (Madura et al., 2015).

The overall aim of this project was to understand the molecular recognition of gp100₂₈₀₋₂₈₈, by using a combination of structural and biophysical approaches. In particular, my aims were to:

- Solve the first ternary crystal structure of a natural cognate TCR in complex with the YLE-9V epitope
- Complement structural information with a thermodynamic analysis of the TCR-pMHC interaction
- Perform an alanine scan mutagenesis across the wild type YLE peptide backbone and investigate TCR binding hotspots by Surface Plasmon Resonance (SPR)

The results presented in this chapter formed the basis of a publication in *The Journal of Biological Chemistry* entitled “A molecular switch abrogates gp100 TCR-targeting of a human melanoma antigen” (Bianchi et al., 2016).

3.2 Results

3.2.1 Production of soluble TCR and pHLA ectodomains

Two distinct YLE-specific $\alpha\beta$ TCRs were used in this project. The PMEL17 TCR (TRAV21, TRBV7-3) was provided by Thymed and was isolated from a melanoma patient (Cole et al., 2007); the gp100 TCR (TRAV17, TRBV19) was provided by Immunocore Ltd (Oxfordshire, UK) and was isolated from a healthy donor (Aleksic et al., 2012). Structural and biophysical experiments for this study required the manufacture of considerable amounts of soluble, refolded and pure pHLA and TCR proteins. Briefly, the process involved: (i) the expression of the ectodomain of each protein chain in the form of inclusion bodies in *E. coli* bacteria; (ii) the purification of inclusion bodies and refolding by dilution of denaturing conditions; (iii) anion exchange chromatography as a first purification step and (iv) several gel filtration chromatography steps in order to obtain enough pure protein to perform the different experiments. For biophysical analysis using BIAcore® technology, pHLA proteins were biotin-tagged prior to gel filtration (Figure 4.3). The biotin group allowed coupling of the pHLA protein to a streptavidin-coated sensor chip (BIAcore®). **Figure 3.1** and **3.2** provide an example of the final purification steps for the TCR and peptide-HLA-A2 proteins, respectively.

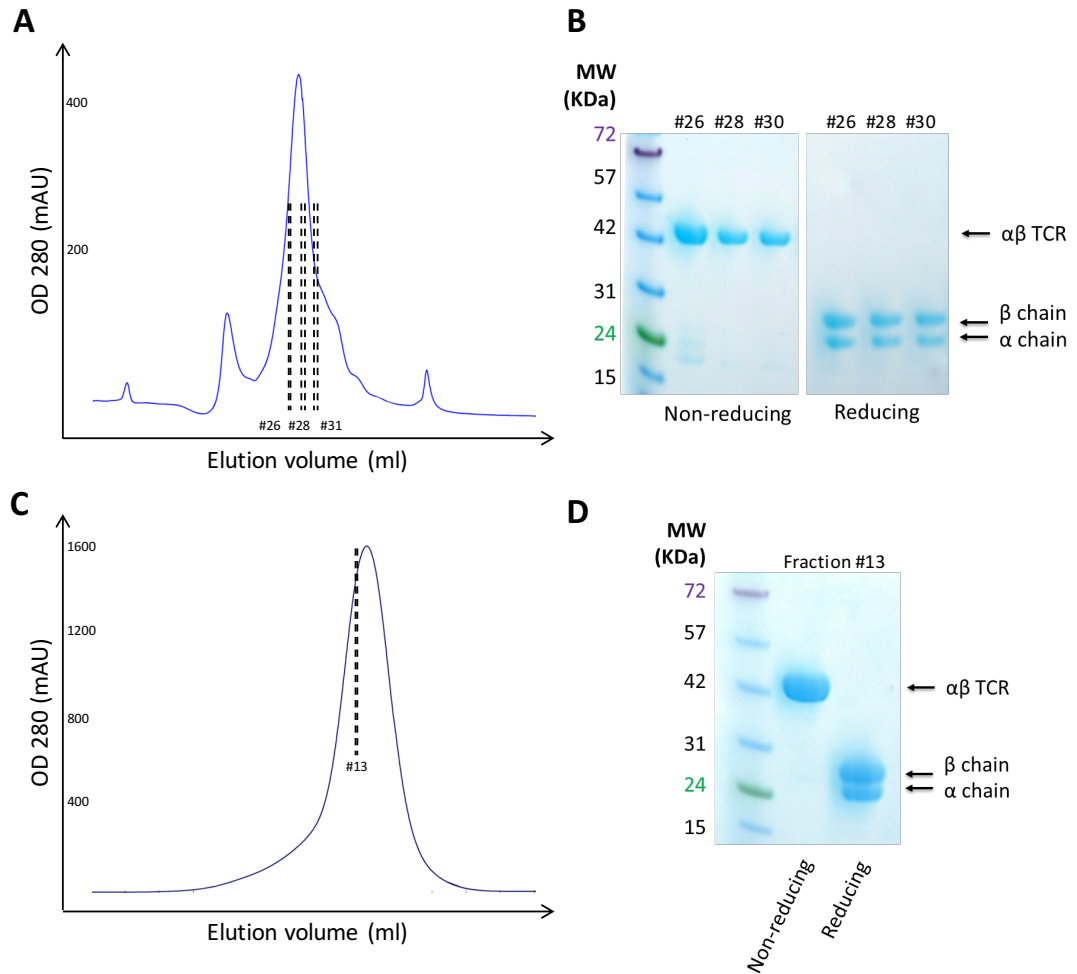


Figure 3.1. PMEL17 TCR protein purification

(A) Representative anion-exchange chromatography of *in vitro* refolded PMEL17 TCR on an 8 ml POROS 50HQ column eluted with a gradient of NaCl. The protein elutes as a single major peak. Fractions corresponding to the main peak were collected and analysed by SDS-PAGE. **(B)** Selected eluted fractions from A were analysed by Coomassie-stained SDS PAGE under non-reducing and reducing conditions. A single band corresponding to the $\alpha\beta$ TCR ectodomain can be seen ~ 45 kDa, which runs as distinct chains of ~ 23 kDa and ~ 28 kDa, under reducing conditions. Lane 1, molecular weight ladder (MW); lanes 2-7, fractions #26, #28 and #30 analysed under both non-reducing and reducing conditions. **(C)** Gel-filtration chromatography (Superdex S200 column) of peak fraction from A, eluted with BIAcore buffer. **(D)** Coomassie-stained SDS-PAGE of pooled fractions from C, to evaluate protein quality. Lane 1, molecular weight ladder (MW); Lane 2-3, fraction #13 (non-reducing and reducing buffer). Fractions were pooled and the TCR was concentrated to 10.3 mg/mL on the same day of SPR analysis to reduce the likelihood of TCR aggregation affecting the results.

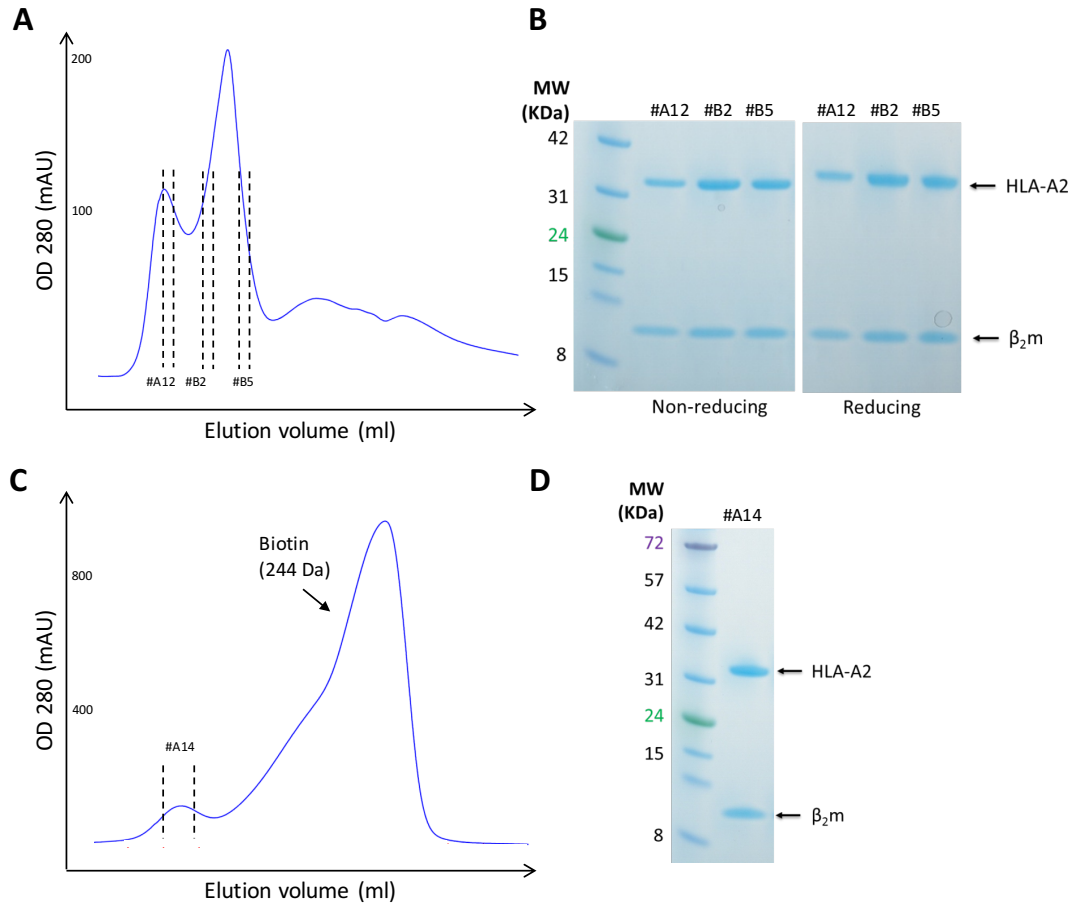


Figure 3.2. HLA-A2-YLE protein purification

(A) Representative anion-exchange chromatography of 500 mL refold of HLA-A2-YLE complex on an 8 ml POROS 50HQ column eluted with a gradient of NaCl. The protein elutes as two peaks (indicated by the arrows). Fractions corresponding to both peaks were collected, analysed by SDS-PAGE and pooled. **(B)** Coomassie-stained SDS-PAGE of fractions to evaluate protein quality. Two distinct bands of ~35 kDa (α -chain) and ~10 kDa (β_2m chain) can be seen in both non/reducing conditions. Lane 1, molecular weight ladder (MW); Lane 2-7, fractions from A analysed under both non-reducing and reducing conditions. **(C)** Gel-filtration chromatography of pooled peaks from A, on a Superdex S200 column eluted with BIAcore buffer. **(D)** Coomassie-stained SDS-PAGE of fraction #A14 from C. Positive A2-YLE fractions were pooled and concentrated to 400 μ L (1.042 mg/mL).

3.2.2 Two distinct anti-gp100 TCRs share similar binding hotspots

In order to study the individual contribution of the YLE peptide residues to TCR-pHLA binding, an “alanine scan” mutagenesis was performed across the peptide backbone. Briefly, each amino acid residue of the peptide was sequentially substituted with an Ala residue, based on the concept that the Ala side chain is a small and uncharged methyl group. Residues P2 and P9, which are known to be important for HLA-A2 binding (Parker et al., 1992), were not assessed; in addition, P9 residue was an Alanine in the native sequence. The ability of the pHLA mutants to bind a YLE-specific TCR was evaluated by Surface Plasmon Resonance (SPR) experiments (**Figure 3.1**). The altered peptide ligand YLE-9V, which has been shown to be a more potent agonist than the wild type sequence (Salgaller et al., 1996), was also included in the experiment. SPR experiments were initially performed with the human YLE-specific PMEL17 TCR (*TRAV21 TRBV7-3*). PMEL17 TCR bound both A2-YLE and A2-YLE-9V with similar affinities ($K_D = 7.6 \mu\text{M}$ and $6.3 \mu\text{M}$, respectively), consistent with the fact that YLE-9V variant was originally designed in such a way to increase HLA binding affinity without significantly altering TCR recognition of the pHLA complex (Parkhurst et al., 1996) (**Table 3.1**). Interestingly, replacement of Glu by Ala in position 3 completely abrogated binding by PMEL17 TCR.

To support the results obtained on PMEL17 TCR, the same experiment was also performed using a previously published anti-cancer TCR specific for the same nonamer (Aleksic et al., 2012). Alanine Scan results on the gp100 TCR (*TRAV17, TRBV19*), showed a similar pattern to those of PMEL17, although at weaker affinities (of $K_D = 26.5 \mu\text{M}$ and $21.9 \mu\text{M}$, for A2-YLE and A2-YLE-9V, respectively). Interestingly, no measurable binding could again be observed with A2-YLE-3A mutant and YLE-5A was confirmed as a very poor ligand, suggesting the importance of these residues for TCR specificity. Overall, these data indicated that both PMEL17 and gp100 TCRs used a similar overall binding mode, focused around peptide residues 3 and 5 with supporting interactions towards the N-terminus of the peptide.

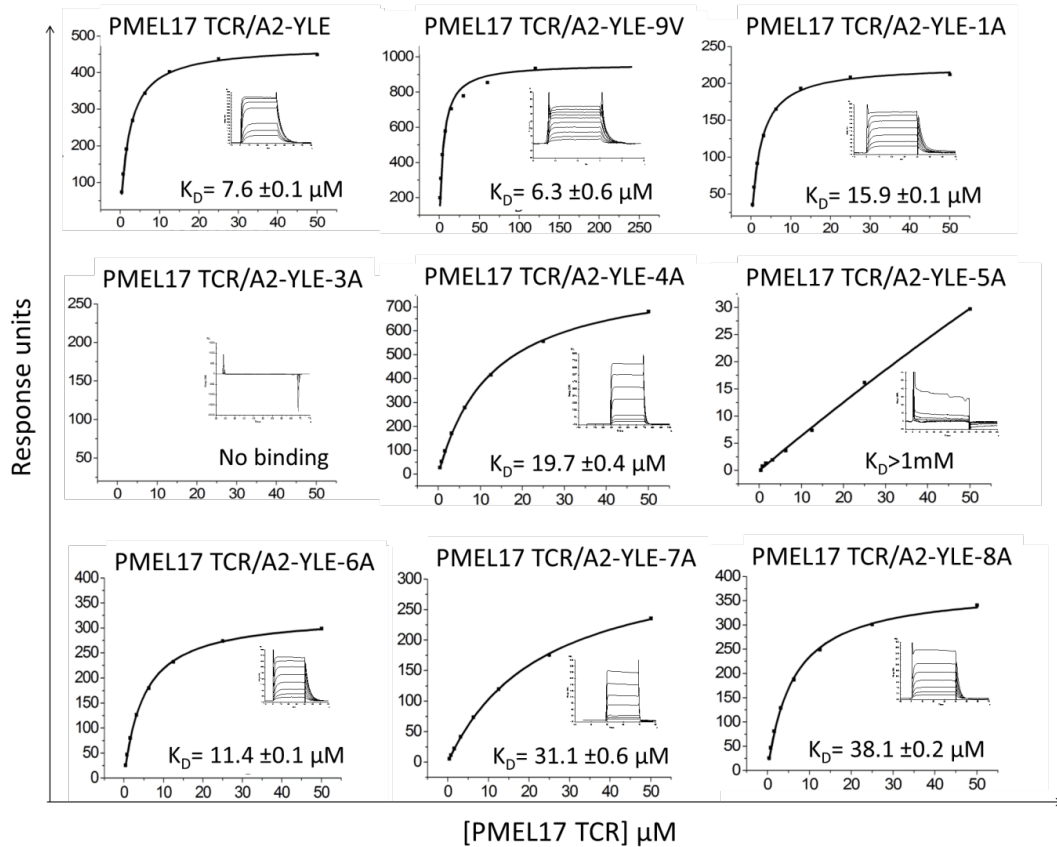


Figure 3.3. Binding affinity analysis (25°C) of A2-YLE variants

PMEL17 TCR equilibrium-binding responses to A2-YLE and altered peptide ligands are shown. Eight serial dilutions were conducted for each equilibrium experiment. Sensorgrams (insert panels) were obtained using BIAevaluation 3.1. The equilibrium-binding constant (K_D) values were plotted using a nonlinear curve fit using Origin 6.0. Sensorgrams and equilibrium-binding plots are representative of a single experiment.

Table 3.1. Alanin scan mutagenesis

<i>Peptide sequence</i>	<i>Peptide</i>	<i>PMEL17 TCR</i> <i>Affinity K_D</i>	<i>gp100 TCR</i> <i>Affinity K_D</i>
YLEPGPVTA	YLE	7.6 μ M	26.5 μ M
YLEPGPV <u>T</u> V	YLE-9V	6.3 μ M	21.9 μ M
<u>A</u> LEPGPVTA	YLE-1A	15.9 μ M	60.6 μ M
YL <u>A</u> PGPVTA	YLE-3A	No binding	No binding
YLE <u>A</u> GPVTA	YLE-4A	19.7 μ M	144.1 μ M
YLEP <u>A</u> PVTA	YLE-5A	> 1mM	> 1mM
YLEPG <u>A</u> VTA	YLE-6A	11.4 μ M	954.9 μ M
YLEPGP <u>A</u> TA	YLE-7A	31.1 μ M	102.0 μ M
YLEPGPV <u>A</u> A	YLE-8A	38.1 μ M	121.0 μ M

3.2.3 The PMEL17 TCR utilizes a peptide-centric binding mode to engage A2-YLE-9V

To understand why TCR recognition of YLE was highly sensitive to some of the substitutions in the native peptide sequence, the crystal structure of the PMEL17 TCR was determined in complex with A2-YLE-9V at 2.02 Å resolution. Data collection and refinement statistics (molecular replacement) are shown in Chapter 2 (**Table 2.1**). Crystallographic $R_{\text{work}}/R_{\text{free}}$ ratios were within accepted limits, as shown in the theoretically expected distribution (Tickle et al., 2000).

Figure 3.4 provides an overview of the PMEL17 TCR/A2-YLE-9V complex. The PMEL17 TCR was centrally positioned over the exposed residues of the peptide (**Figure 3.4A**) and used a conventional diagonal orientation (crossing angle = 46.15°), with the α -chain positioned over the $\alpha 2$ helix of the HLA-I binding groove, and the β -chain over the $\alpha 1$ helix. All but the CDR2 α loop were involved in contacting A2-YLE-9V, with the CDR3 α and CDR3 β “sitting” on the central axis of the antigen-binding cleft, making contacts with both the peptide and α -helices of the HLA (**Figure 3.4B-C**).

The PMEL17 TCR made approximately the same number of peptide-mediated contacts and HLA-A2 interactions; forming 53 of 125 (42.4%) van der Waals contacts and 3 of 8 (37.5%) hydrogen bonds between the TCR and the peptide (**Table 3.2**). The HLA helices were contacted by residues within the CDR3 α , CDR3 β and CDR2 β loops (with additional support of CDR1 α residue Tyr32), which focused on Arg65, Ala69, Gln72 and Gln155 (**Figure 3.4D**). HLA residues at positions 65, 69 and 155 are conserved TCR-mediated contact points in several TCR-pHLA-I structures determined so far, and are referred to as “restriction triad” (Tynan et al., 2005).

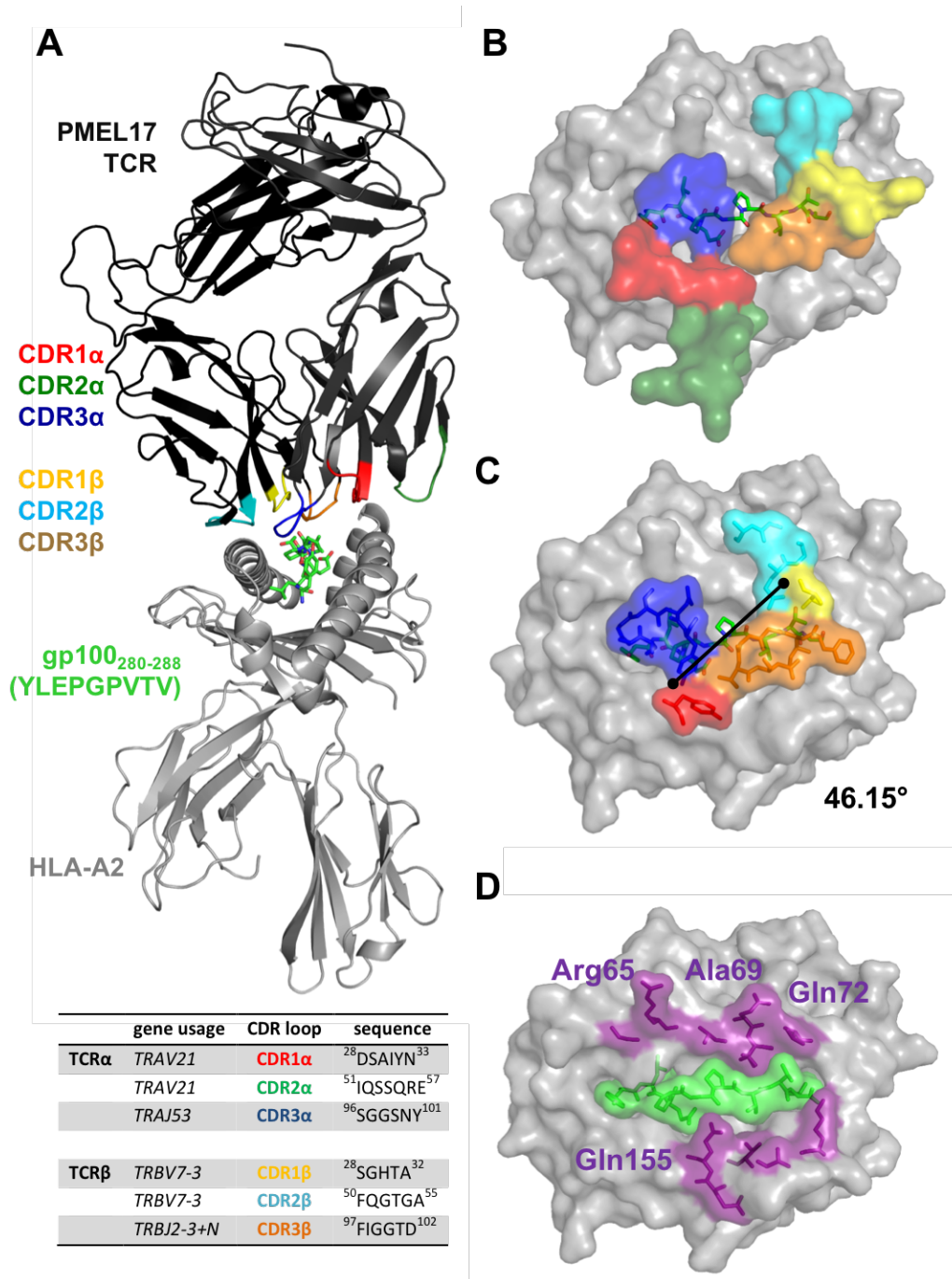


Figure 3.4. Overview of the PMEL17 TCR/A2-YLE complex

(A) Cartoon representation of the PMEL17 TCR-A2-YLE-9V complex. The TCR α -chain and TCR β -chain are dark grey and black, respectively; TCR CDR loops are shown (red, CDR1 α ; dark green, CDR2 α ; blue, CDR3 α ; yellow, CDR1 β ; aqua, CDR2 β ; orange, CDR3 β); the HLA-A*0201 is depicted in grey. The YLE-9V peptide is represented in green sticks. The bottom panel shows the TCR α - and β -chain CDR loops sequences and gene usage. N; nucleotide addition. **(B)** Close-up view of the PMEL17 TCR-A2-YLE-9V interface (colour-coded as in A). The overall position of the PMEL17 TCR CDR loops over both the peptide and the HLA-A2 helices can be observed. **(C)** Surface and stick representation of residues of the PMEL17 TCR CDR loops (colour-coded as in A) that contact the A2-YLE surface (A2, grey; YLE-9V, green sticks). Black diagonal line indicated the crossing angle of the TCR with respect to the long axis of the YLE-9V peptide (46.15°). Crossing angle was calculated as described in Rudolph et al, 2006. **(D)** Contact footprint of the PMEL17 TCR on the A2-YLE-9V surface (A2, grey); purple and green (surface and sticks) indicate HLA-A*0201 and YLE residues, respectively, contacted by the gp100 TCR. Cut-off of 3.4Å for hydrogen bonds and 4Å for van der Waals contacts.

Table 3.2. PMEL17 TCR-A2-YLE-9V contact table

<i>HLA/peptide residue</i>	<i>TCR residue</i>	<i>No. vdW ($\leq 4\text{\AA}$)</i>	<i>No. H-bonds ($\leq 3.4\text{\AA}$)</i>
Gly62	α Gly98	3	
	α Ser99	1	
Arg65	α Ser99	2	
Arg65 ^O	α Asn100 ^{N62}	2	1
Arg65 ^{NH1}	β Asp58 ^{O62}		1
	β Ser59	8	
Lys66	α Gly98	1	
	α Ser99	4	
	α Asn100	4	
Ala69	α Asn100	2	
	β Ala56	2	
Gln72 ^{Ne2}	β Gln51 ^O	3	1
	β Gly54	7	
	β Ala55	1	
Thr73	β Gln51	1	
Val76	β Gln51	3	
	β Gly52	2	
Lys146	β Phe97	3	
	β Ile98	3	
Ala150	β Ile98	1	
	β Asp102	3	
Val152	β Ile98	1	
Glu154	α Tyr32	1	
Gln155 ^N	α Tyr32 ^{OH}	4	1
Gln155 ^{Oe1}	β Thr101 ^N	10	1
Tyr1 ^{OH}	α Gly97 ^O	1	1
	α Gly98	1	
	α Ser96	1	
Glu3	α Tyr101	1	
Pro4	α Ser96	1	
	α Ser99	1	
	α Asn100	4	
Pro4 ^O	α Tyr101 ^N	14	1
Gly5	α Tyr101	3	
	β Gly100	2	
Val7	β Ile98	7	
	β Gly99	2	
	β Gly100	2	
Thr8	β Thr31	5	
	β Gln51	1	
	β Phe97	1	
Thr8 ^N	β Ile98 ^O	6	1

3.2.4 The PMEL17 CDR loops focus on YLE residues Pro4, Val7 and Thr8

The central positioning of the PMEL17 TCR enabled contacts with 6 out of 9 amino acids in the peptide (**Figure 3.5A**). Peptide residues Pro4, Val7 and Thr8 represented the focal points of the PMEL17 TCR. Pro4 made a sizeable network of interactions (1 hydrogen bond and 14 van der Waal contacts) (**Figure 3.5B**). Interestingly, Pro6 was the only central residue that did not interact with the PMEL17 TCR because of its reduced surface exposure. Therefore, the relative insensitivity of the PMEL17 TCR to alanine substitution at position 6 is consistent with its lack of involvement in TCR binding. In contrast, the gp100 TCR seemed to be more sensitive to position 6 mutation, causing a ~40-fold drop in binding affinity compared to the unaltered peptide (**Table 3.1**). This might be explained by the different *TRAV* and *TRBV* gene usage of the two gp100-specific TCRs and the very different residues of the CDR3 loops possibly contacting the central part of the gp100₂₈₀₋₂₈₈ peptide. However, the PMEL17 TCR complex structure did not provide any clear mechanisms to explain the reduction in binding observed when peptide residues 3 and 5 were mutated to alanine.

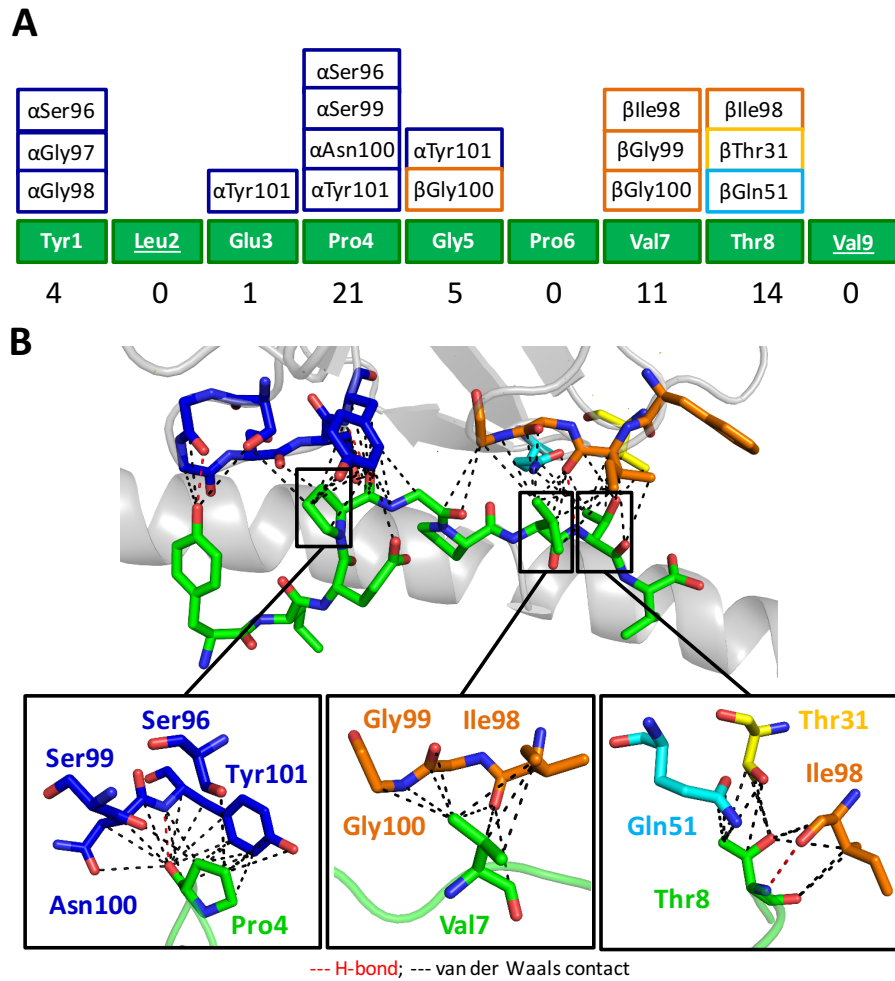


Figure 3.5. The PMEL17 CDR loops focus on peptide residues Pro4, Val7 and Thr8

(A) Schematic representation of contacts between YLE-9V peptide and PMEL17 CDR loop residues (colour coded as in Figure 2A). Number at the bottom of the panel show total contacts between the TCR and peptide. **(B)** Contacts between the PMEL17 TCR and the YLE peptide (green sticks), showing the van der Waals contacts (black dashed lines) and hydrogen bonds (red dashed lines) made by the TCR CDR3 α (blue), CDR1 β (yellow), CDR2 β (aqua) and CDR3 β (orange) loops. In the lower panel, close view of contacts between YLE Pro4, Val7 and Thr8, respectively, and TCR CDR loops residues (sticks colour coded as in Figure 1A). Cut-off of 3.4Å for hydrogen bonds and a cut-off of 4Å for van der Waals contacts.

3.2.5 Binding thermodynamics and affinity of the GP100 TCR/A2-YLE complex

To complement information gained from the crystal structure, the affinity and thermodynamic parameters of the PMEL17 TCR were studied. Affinity data collected from kinetic studies is helpful in understanding the free energy (ΔG) of the TCR-pMHC binding, while thermodynamic parameters (ΔH° , ΔS°) help understanding the molecular forces driving the TCR-pMHC interaction. SPR experiments were performed with purified soluble gp100-specific TCR and immobilized A2-YLE complex. The binding strength of the complex was then measured at 5, 12, 18, 25 and 37 °C (**Figure 3.6**). At 25 °C (the standard temperature for binding measurements), the K_D of the complex was 3.2 μM . The PMEL17 TCR-A2-YLE interaction at 25 °C was characterized by a binding ΔG of -7.5 kcal/mol, which was within the normal range of TCR/pHLA interactions. PMEL17 TCR-A2-YLE binding was characterized by a very small, favourable enthalpy change ($\Delta H = -0.6$ kcal/mol) and a larger, positive entropy change ($T\Delta S = 6.9$ cal/mol); thus, order to disorder drove the interaction, probably through the expulsion of ordered water molecules at the interface (i.e. solvation effects) (**Figure 3.7A**). The thermodynamic properties of the complex at the physiologically relevant temperature of 37 °C were also studied. The binding free energy ($\Delta G = -7.7$ kcal/mol) was very similar to the one observed at 25 °C ($\Delta G = -7.5$ kcal/mol). Interestingly though, at 37 °C, the parameters were reversed; the interaction was driven mostly by enthalpy, thus probably by the formation of non-covalent bonds.

Isothermal calorimetric titration (ITC) was also performed as it provides a direct measure of enthalpy and is therefore considered more accurate than SPR in determining thermodynamic parameters (Armstrong and Baker, 2007). ITC is based on the measurement of heat released or absorbed upon the binding of the TCR to the pHLA. ITC measurements ($\Delta H = -0.3$ kcal/mol and $T\Delta S = 5.6$ cal/mol) confirmed observation made with SPR thermodynamics (**Figure 3.7B**). The favourable enthalpy of this TCR/pHLA system shows that the overall number of formed bonds is equal to number of disrupted ones upon PMEL17 TCR binding.

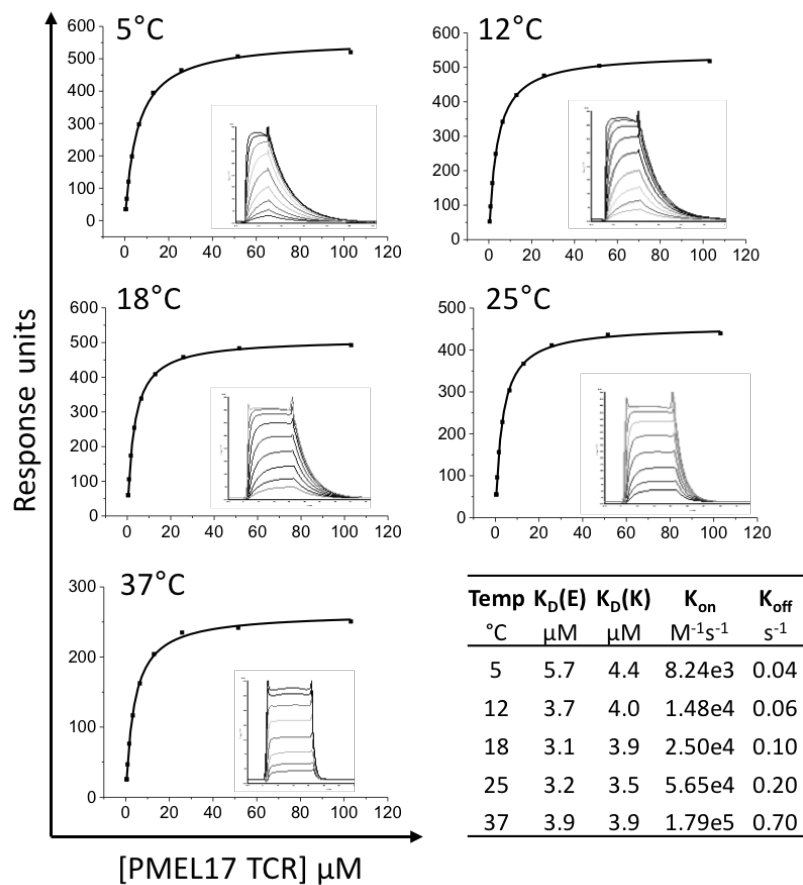


Figure 3.6. PMEL17 TCR equilibrium-binding responses to A2-YLE at 5, 12, 18, 25 and 37°C

PMEL17 TCR equilibrium-binding responses to A2-YLE at 5, 12, 18, 25 and 37°C, respectively. Nine serial dilutions of the PMEL17 TCR were measured at each temperature. The equilibrium binding constant (K_D , μM) values were calculated in each case using a nonlinear fit ($y=(P1x)/(P2+x)$).

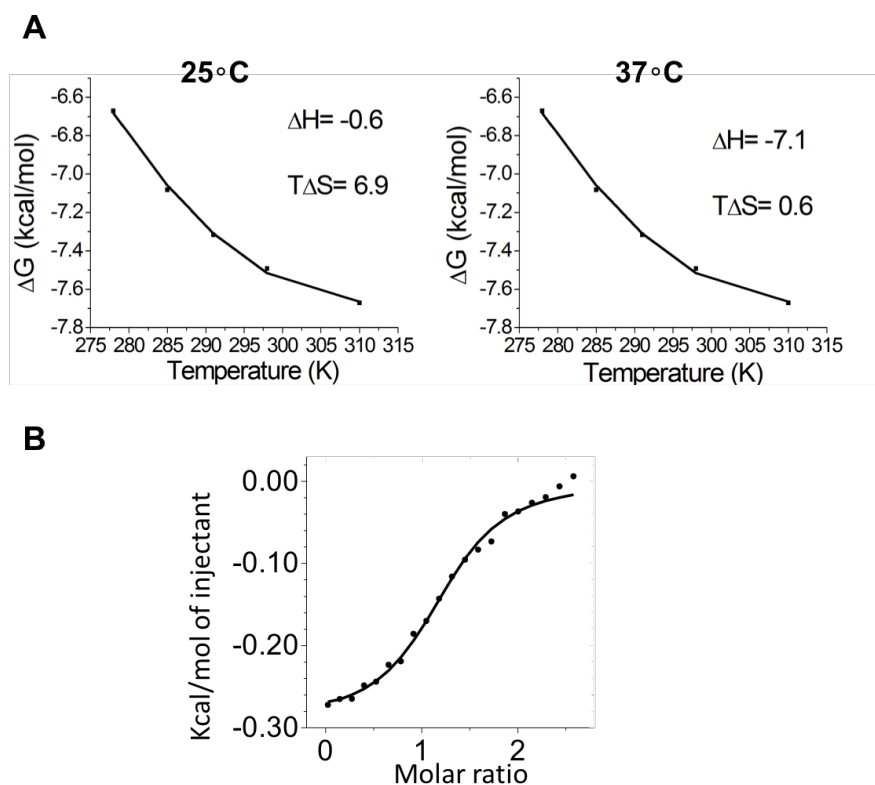


Figure 3.7. Thermodynamic analysis of the PMEL17 TCR/A2-YLE interaction

(A) The thermodynamic parameters were calculated first by SPR, according to the Gibbs-Helmholtz equation ($\Delta G^\circ = \Delta H - T\Delta S^\circ$), at 25°C and 37°C, respectively. The binding free energies, ΔG° ($\Delta G^\circ = -RT \ln KD$), were plotted against temperature (K) using nonlinear regression to fit the three-parameter equation, ($y = dH + dCp \cdot (x - 298) - x \cdot dS - x \cdot dCp \cdot \ln(x/298)$). Enthalpy (ΔH°) and entropy ($T\Delta S^\circ$) at 25°C and 37°C, are shown in kcal/mol, and were calculated by a non-linear regression of temperature (K) plotted against the free energy (ΔG°). **(B)** Isothermal calorimetric titration (ITC) measurements for PMEL17 TCR/A2-YLE interaction. Enthalpy (ΔH°) and entropy ($T\Delta S^\circ$) at 298K (25°C), are shown in kcal/mol

3.2.6 Peptide substitutions can induce perturbation at adjacent peptide residues abrogating T-cell recognition

The alanine scan results regarding position 3 and 5 were quite unexpected, considering that the Glu3 and Gly5 residues in the ternary complex structure were only involved in weak bonds with the PMEL17 TCR (Table 3.2). In order to understand the structural basis underlying the substantial changes in affinity of PMEL17 TCR-A2-YLE-9V binding resulting from Glu3>Ala and Gly5>Ala substitutions, I decided to solve the unbound structures of YLE-3A and YLE-5A alanine mutant peptides in complex with HLA-A2. Data collection and refinement statistics for individual structures are shown in Chapter 2 (Table 2.1). The structures were solved between 1.54 – 2.12 Å resolution with crystallographic R_{work}/R_{free} ratios within accepted limits. Electron density around the peptide was unambiguous (Appendix, Figure 7.1). Comparison of the crystallographic structure of A2-YLE and A2-YLE-3A complexes surprisingly did not show an overall change in the peptide backbone conformation (Figure 3.9).

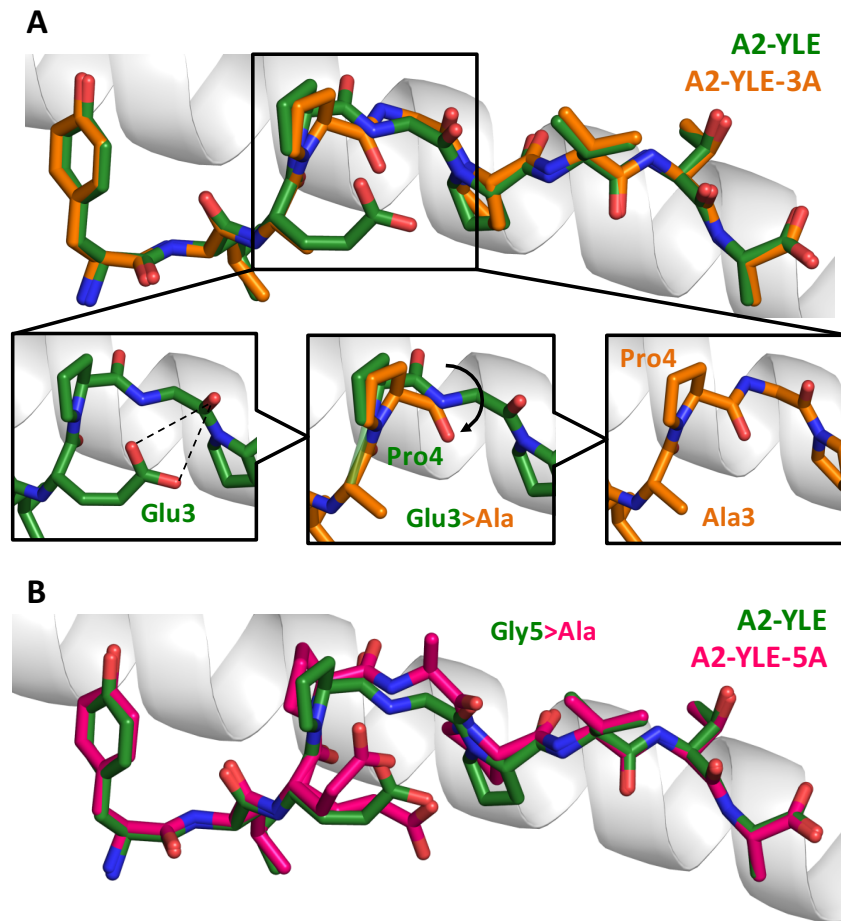


Figure 3.8. Conformational comparison of YLE, YLE-3A and A2-YLE-5A peptides presented by HLA-A*0201

(A) YLE (dark green sticks) and YLE-3A (orange sticks) peptide alignment by superimposition of HLA-A2 α 1 helix (grey cartoon). Boxed residues indicate the mutation of Glu3 into an Alanine. The insets show how the Glu3>Ala substitution, causes a shift in position (black arrow) of neighbour residue Pro4 in the A2-YLE-3A structure compared to the A2-YLE structure. **(B)** YLE (dark green sticks) and YLE-5A (pink sticks) peptide alignment by superimposition of HLA-A2 α 1 helix (grey cartoon). Boxed residues indicate the mutation of Glycine 5 into an Alanine.

Nonetheless, in the A2-YLE structure, Glu3 bridges across to the main chain at position 4-5; the mutation of Glu3 into a shorter side chain (i.e. alanine), which is no longer able to bridge across the void, caused an unusual “knock-on effect” on the central Pro4 residue (**Figure 3.8A**). The Pro4 in the A2-YLE-3A structure lost restraint, causing the oxygen atom to flip in the opposite direction. Because of this unanticipated displacement of the Pro4 oxygen, the outward facing side of the Pro4 residue was no longer in an optimal position to be contacted by the TCR, therefore potentially losing a network of interactions. These findings are consistent with the complete absence of measurable binding of the YLE-3A mutant in the alanine scan (Table 3.1). Gly5 was the only gp100 peptide residue contacted by both CDR3 loops through α Tyr101 and β Gly100 in the PMEL17 TCR/A2-YLE structure. Upon mutation of Gly5 with an alanine residue in A2-YLE-5A structure, steric hindrance in the centre of the peptide may explain the significant fold-increase in binding affinity observed in the alanine scan (**Figure 3.8B**). As with YLE-3A, the substitution did not distort the overall conformation of the YLE nonamer.

3.2.7 Alanine substitutions in YLE positions 3 and 5 abrogate T-cell activation

To determine the effect of YLE altered peptide ligands on the activation of T-cells, the ability of these mutants to induce MIP-1 β , TNF- α production and specific cytotoxicity was determined. These are key effector functions of activated CD8⁺ T-cells, which can be measured over a wide range of peptide concentrations. Human primary CD8⁺ T-cells were transduced with a lentiviral construct carrying the gp100 TCR and enriched for high and equal levels of TCR expression. Flow cytometry analysis with mAb anti-V β 17 TCR (i.e. TRBV19) showed that gp100 TCR expression levels were \geq 30% of total CD3⁺ T-cells in three independent donors (**Figure 3.9**). Transduced CD8⁺ T-cells were stimulated with peptide-pulsed HLA-A2⁺ T2 target cells, across a range of different concentrations of YLE altered peptide ligands.

Antigen-specific responses of gp100 TCR-engineered T-cells were validated at the level of production of MIP-1 β and specific lysis of pulsed targets. Non-transduced CD8⁺ T-cells were used to control for non-specific activation through the endogenous TCR; T-cells transduced with the MEL5 TCR (specific for the HLA-A2 restricted cancer epitope ELA from the Melan-A protein) were used as an irrelevant control in all experiments. Peptide titration experiments showed marked differences in the ability to sensitize target cells for MIP-1 β production by CD8⁺ gp100-specific T-cells (**Figure 3.11A**). In particular, target cells pulsed with YLE and YLE-9V were recognized more efficiently than those pulsed with YLE-1A, YLE-8A, YLE-4A and YLE-7A. No MIP-1 β production was measured with YLE-3A and YLE-5A peptide ligands, even at higher peptide concentrations. TNF- α production was measured by ELISA from the same supernatants (**Figure 3.11C**) and low levels of this cytokine were only detected when cells were pulsed with YLE, YLE-9V, YLE-8A or YLE-6A. **Figure 3.11B** shows specific lysis of target cells pulsed with the same range of peptides and measured by ⁵¹Cr release assay. Similar to the MIP-1 β response curves, the specific lysis induced by these altered YLE ligands was variable. Most importantly, no CTL-mediated lysis was observed when peptides YLE-3A or YLE-5A were used. Taken together, these data are consistent with the molecular analysis demonstrating that the structural and biophysical alterations induced by peptide modifications translate directly to the effects observed upon T-cell recognition.

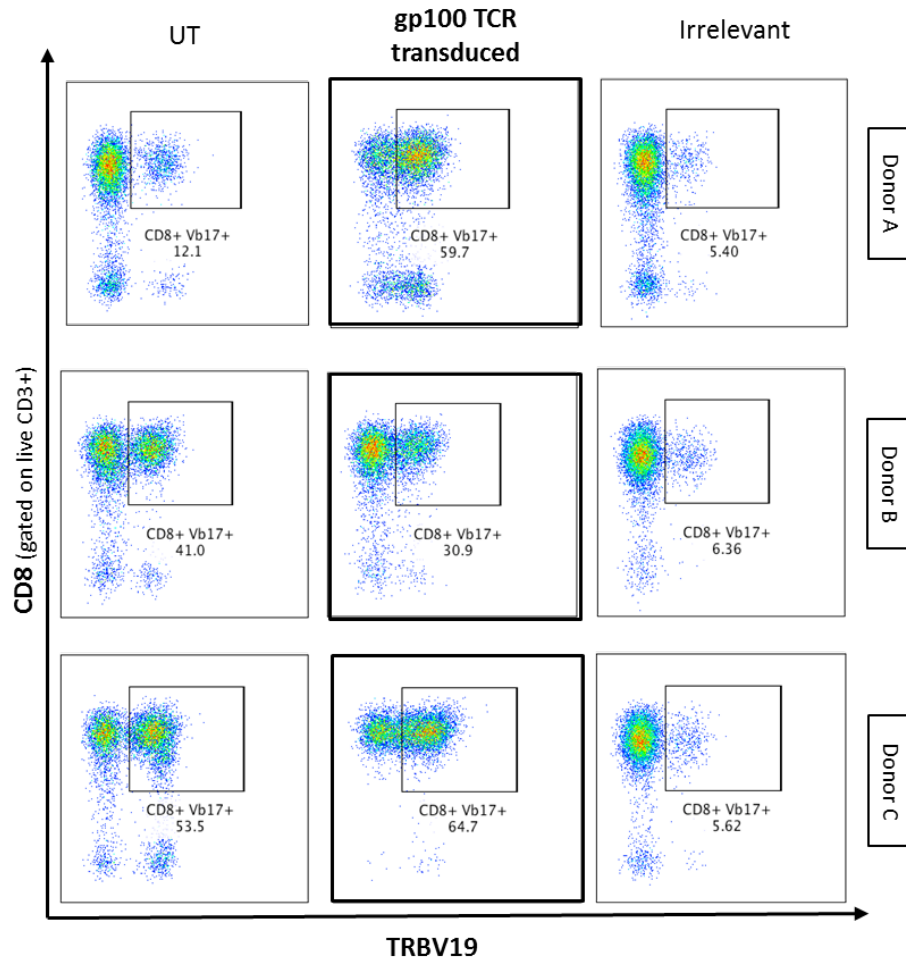


Figure 3.9. Gp100 TCR expression by transduced primary CD8+ human T-cells

Activated primary CD8+ T cells were transduced with lentiviral constructs expressing the gp100 TCR specific for the HLA-A2-restricted melanoma differentiation antigen gp100 (YLEPGPVTA, 280-288). After 72 hours, transduction efficiency was determined by flow cytometry after staining with anti-V β 17 TCR (i.e. TRBV19) FITC-conjugated antibody. Anti-FITC microbeads (MACS) were used to enrich the TRBV+ population before staining. Dot plots show surface expression of gp100 TCR (TRBV19) on primary CD8+ cells (gated on live CD3+ T cells) in three different blood donors (A, B and C). Untransduced (UT) cells or MEL5 TCR (irrelevant) transduced cells were used as controls.

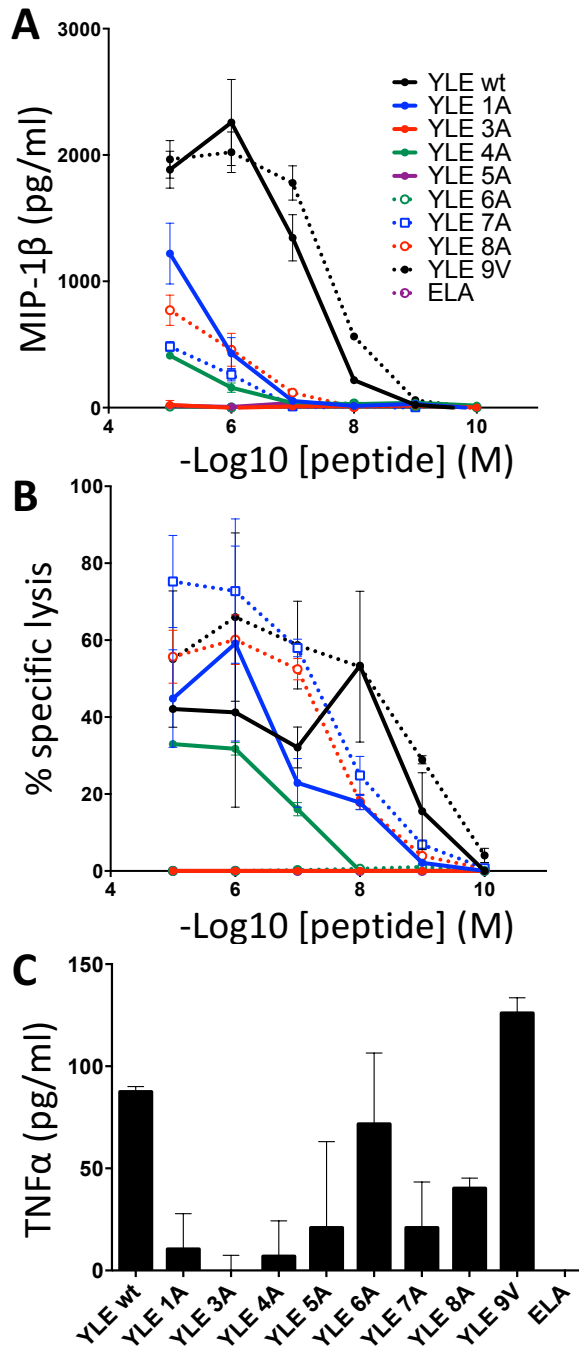


Figure 3.10. Production of MIP-1 β , TNF α and cytotoxicity by gp100 TCR transduced CD8⁺ T-cells in response to stimulation with YLE peptide ligands

A) gp100 TCR transduced CD8⁺ T-cells were stimulated with peptide-pulsed target cells as indicated. Supernatant was assayed for MIP-1 β by ELISA. Negative control (no peptide) was subtracted from each stimulated condition. **(B)** gp100 TCR transduced CD8⁺ T-cells were tested in a standard 4 h ⁵¹Cr-release assay against peptide-pulsed targets. Negative control (no peptide) was subtracted from each stimulated condition. **(C)** gp100 TCR transduced CD8⁺ T-cells were stimulated with peptide-pulsed target cells (10⁻⁵ M peptide) as indicated. Supernatant was assayed for TNF- α by ELISA. Negative control (no peptide) was subtracted from each stimulated condition. ELA (Melan-A/MART-1) 9mer peptide was used as an irrelevant control in all experiments. Results of one (out of three) donor are shown.

3.3 Discussion

TCRs specific for cancer epitopes are generally characterised by low binding affinities (binding K_D s high micromolar range) (Bridgeman et al., 2011). This lower binding affinity is thought to be a result of negative selection of T-cells that bear TCRs with higher affinity for self-ligands in the thymus. Since TCR affinity plays an important role in T-cell activation, the TCR affinity gap between anti-pathogen and anti-cancer T-cells leaves the latter at a distinct disadvantage and makes it more difficult to break self-tolerance to such antigens. One approach to enhance the T-cell response to tumour antigen-derived peptides has been to immunize patients with altered peptide ligands that differ from the native sequence by a single, or multiple, amino acid residues (Lesterhuis et al., 2011). However, such 'heteroclitic' peptides with even single amino acid substitutions that are predicted to only contact the HLA can have unpredictable, yet important, effects on TCR engagement. Despite their extensive application in clinical trials as cancer vaccines, to date only a few X-ray structures of TCRs bound to cognate tumour antigens have been determined (Borbulevych et al., 2011; Chen, 2005; Deng et al., 2007; Madura et al., 2015). I have solved the first crystal structure of a HLA-A2 restricted gp100 peptide antigen bound to a cognate $\alpha\beta$ TCR. In this chapter, I show how the PMEL17 TCR bound with a typical diagonal orientation over the central peptide residues, and mainly contacted residues 4, 7 and 8 of the YLE-9V peptide which protruded out of the HLA-A2 binding groove. Interestingly, the PMEL17 TCR was characterized by a binding affinity (K_D) of 7.6 μ M, a value that falls in the very high end of affinity ranges described so far for cancer TCR and pHLA interactions (Bridgeman et al., 2011; Aleksic et al., 2012). These observations suggest that healthy donors or melanoma patients may harbour T-cells bearing TCRs with reasonable affinity for some tumour associated antigens, which can be preferentially chosen for TCR-based applications. For example, gp100-specific ImmTACs (Immune-mobilising monoclonal TCRs against cancer) are a new class of soluble bi-specific anti-tumour agents that combine a high-affinity TCR-based gp100 recognition domain with a T cell activation domain (Liddy et al., 2012; Bossi et al., 2014). IMCgp100 is being tested as a soluble drug and is showing partial or complete durable responses in Phase I/IIa trial in patients with advanced melanoma (Middleton et al., 2015).

In this chapter I also provide insight into YLE single amino acid contribution to TCR binding by performing an alanine scan mutagenesis across the peptide backbone with two different YLE-specific $\alpha\beta$ TCRs. Interestingly, both PMEL17 TCR and gp100 TCR were most sensitive to mutations at position 3 or 5 of the native YLE peptide sequence despite these TCRs being constructed from completely different $V\alpha$ and $V\beta$ genes. These results are supported by a recent study of YLE altered peptide ligands which described YLE-3A as a null agonist for a different TCR (Shaft et al., 2003; 2013). Overall, along with the two TCRs studied here, the sequences of further two distinct YLE-specific TCRs have been published, demonstrating diverse gene usage and different CDR3 loop sequences (**Table 3.3**).

No structural data supporting these observations have been published to date.

Table 3.3. Alignment of TCR CDR3 regions of four gp100-specific TCRs

PMEL17, gp100, MPD (Schaft et al., 2003) and 296 (Schaft et al., 2003) gp100-specific TCR.

<i>TCR</i>	<i>CDR1α</i>	<i>CDR2α</i>	<i>CDR3α</i>	<i>CDR1β</i>	<i>CDR1β</i>	<i>CDR1β</i>
PMEL17	DSAIYN	IQSSQRE	CAVLSSGGSNYKLTFG	SGHTA	FQGTGA	CASSFIGGTDYQYFG
gp100	TSINN	IRSNERE	CATDGDTPLVFG	LNHDA	SQIVND	CASSIGGPYEQYFG
MPD	KALYS	LLKGGEQ	CGTETNTGNQFYFG	SGHDY	FNNNVP	CASSLGRYNEQFFG
296	DSASNY	IRSNVGE	CAASTSGGTSYGKLTFG	MNHEY	SMNVEV	CASSLGSSYEQYFG

Interestingly, mutation in position 3 in the YLE peptide did not alter the conformation of the peptide backbone itself, but resulted in a ‘knock-on’ effect on the neighbouring residue Pro4 that completely abolished TCR binding and T-cell recognition. This can be explained by the fact that Pro4 was at the centre of a sizeable network of interactions (both vdW and hydrogen bonds) in the PMEL17-A2-YLE-9V structure. In addition, Position 3 in HLA-A2 restricted peptides is known to be a secondary anchor residue (Ruppert et al., 1993), in that it supports the exposed peptide bulge that is normally involved in TCR binding. By mutating the residue in position 3 with a smaller side chain, this support is lost causing a ‘molecular switch in the neighbour Pro4. A similar mechanism in an HIV-1 derived peptide, has recently been described by our group, with important implications for the immune control of HIV infection and patterns of viral escape mutants (Kløverpris et al., 2015). Additionally, the existence of a novel mode of flexible peptide presentation in a diabetes model has been demonstrated, showing the potential dynamic nature of the region surrounding the HLA F-pocket (Motozono et al., 2015; Borbulevych et al., 2009). Taken together, these studies support the notion that peptide-HLA interactions are more plastic and dynamic than previously appreciated, with obvious implications for immune recognition, epitope prediction and structural modelling.

Overall, the results presented here represent the first structural insight into TCR recognition of an important tumour antigen, targeted by many clinical therapies. They reveal that two very different TCRs share a similar pattern of specificity, demonstrated by their near identical sensitivity to different peptide modifications. Finally, I’ve shown that modification to peptide residues outside of the TCR binding motif can have unpredictable knock-on effects on adjacent peptide residues that abrogate TCR binding and T-cell recognition, highlighting that even conservative peptide substitutions can have unexpected consequences for T-cell recognition by different antigen-specific TCRs due to ‘knock-on’ structural changes in the HLA-bound peptide. Such ‘transmitted’ structural changes need to be taken into consideration when designing improved peptides for cancer vaccination. Given the growing evidence that plasticity at the TCR-pHLA interface can influence immune recognition, structural and biophysical studies of binding should be taken into account when attempting to design altered peptide ligands with improved immunogenicity.

4 Dissection of T-cell responses in an HLA-A2+ remission melanoma patient after TIL-therapy

4.1 Background

4.1.1 TIL-therapy at the CCIT (Copenhagen, Denmark)

Tumour infiltrating lymphocytes (TILs) represent a heterogeneous population of lymphocytes that are found within a tumour. TIL-based Adoptive T cell therapy (ACT) is emerging as a promising option to cure treatment-refractory metastatic melanoma. More than 30 patients (between the age of 18 and 70) with progressive metastatic (or locally advanced) cutaneous malignant melanoma have been treated with TIL therapy in a phase I/II clinical trial (identifier: NCT00937625, directed by Professor Inge Marie Svane) at the CCIT and Herlev Hospital (Copenhagen, Denmark) (Ellebæk et al., 2012). Durable complete tumour regressions (>1 year) and an overall response rate of 42% were achieved (Andersen et al., 2016; Ellebæk et al., 2012). A schematic representation of the TIL isolation and expansion process is shown in **Figure 1.9 (Chapter 1)**. Briefly, TIL isolation starts with the surgical resection of suitable melanoma lesions, which are cut into 1-3 mm³ fragments and grown in culture plates with IL-2 supplemented medium. The process involves an initial *in vitro* expansion step of the patient's autologous TILs for a period of 2-4 weeks to at least 5x10⁷ cells, after which cells can be cryopreserved for future use. TILs are then subjected to a Rapid Expansion Protocol (REP) and re-infused into the patient with intravenous moderate dose of IL-2, following a lympho-depleting regimen (Donia et al., 2012; Elleabak et al., 2012).

Although the clinical efficacy of these TIL-based trials is promising, the characterisation of the T-cell responses that mediate tumour recognition and regression *in vivo* has been limited. Previous work has shown that the absolute number of TILs infused, and in particular the number of CD8+ TILs, is a critical factor influencing the outcome of ACT (Itzhaki et al., 2011; Radvanyi et al., 2012). Analysis of the composition of melanoma-restricted T-cell responses among TILs revealed that only small percentages of TILs recognise shared self-antigens (Andersen et al., 2012). Most of the antigen specificities in melanoma TILs associated with long-term complete regressions remain elusive.

4.1.2 Aims

The overall aim of this study, which was carried out in collaboration with the CCIT research team in Denmark, was to dissect melanoma T-cell responses in TIL infiltrates associated with complete *in vivo* tumour regression. I had privileged access to samples (TIL infusion products, autologous melanoma cell lines and blood samples) of metastatic melanoma patients from the Danish trial who achieved complete remission after TIL-based therapy (Ellebaek et al., 2012; Andersen et al., 2016). In this chapter, I have focused on an HLA-A2+ complete responder patient, identified hereafter as patient MM909.24. In the next chapter, I took a similar approach using TILs from a patient that did not express HLA-A2 and the biases associated with this HLA. The HLA-A2 allele is the most common in Northern Asia and North America populations, and is the restricting element that presents the majority of the T-cell epitopes described to date (Andersen et al., 2012).

At the outset, I aimed to address the following research questions:

- Which T-cell subsets contribute to T-cell tumour reactivity?
- To what degree is the autologous tumour targeted through HLA-A2?
- Is the antigen specificity of TILs directed towards known shared melanoma antigens?
- How many clonotypes constitute tumour reactive TILs and do dominant clones persist in the patient's blood after treatment?
- What is the antigen specificity of the dominant anti-tumour T-cell clonotype(s)?

4.2 Results

4.2.1 Patient characteristics and experimental approach

Details of the patient MM909.24 clinical outcome and characteristics of the infused TILs are shown in **Figure 4.1A**. The TIL infusion product was defrosted and cultured in complete T-cell medium, supplemented with 200 IU/mL IL-2 (see section 2.9 of Materials and Methods for details regarding TIL culture maintenance and expansion). The limited sample availability (approximately $2\text{-}3 \times 10^6$ of cells from the original TIL infusion product) required the expansion of TILs to the minimum cell numbers for functional experiments. Repeated *in vitro* expansion and long-term culture of TILs was a potential concern as it could result in a bias toward certain clonotypes that were adapted to growth *in vitro*. Therefore, all the experiments shown in this chapter were performed on TIL cultures that were expanded for a maximum of 2-3 passages. Where possible, the original infusion product itself was studied.

The presence of distinct TCR V β families in TIL cultures was initially analysed by staining with conjugated antibodies directed against individual TRBV gene products. TRBV20-1 and TRBV12 were the most frequent in MM909.24 TILs (26.7% and 9.5% of total CD8+ TILs, respectively) (**Figure 4.1B**). However, commercially available TRBV antibodies cover only about half of the whole TCR V β repertoire, and therefore sometimes fail to label cognate TRBV+ T-cell populations. Furthermore, distinct T-cell clones may share the same TCRV β but have a different CDR3 sequence (i.e. the region that interacts with the cognate peptide-HLA ligand) and therefore different peptide specificities. Therefore, to overcome these limitations and to provide a more complete analysis of the TCR β V gene usage of tumour reactive T-cells in the patient's TIL population, I opted for TCR β clonotyping, which will be discussed in more detail in section 4.2.5 of this chapter.

The HLA expression of the autologous tumour cell line was tested by flow cytometry (**Figure 4.1C**). MM909.24 melanoma cells express high levels of HLA-I molecules, while HLA-II expression could only be induced after a 72-hour treatment with a low dose of IFN- γ . These expression profiles are in accordance with studies from our collaborators and others groups, which have shown a heterogeneous pattern of constitutive or IFN- γ induced HLA-II surface expression in hundreds of human melanomas (Donia et al., 2013; LeibundGut-Landmann et al., 2004; Mendez et al., 2009).

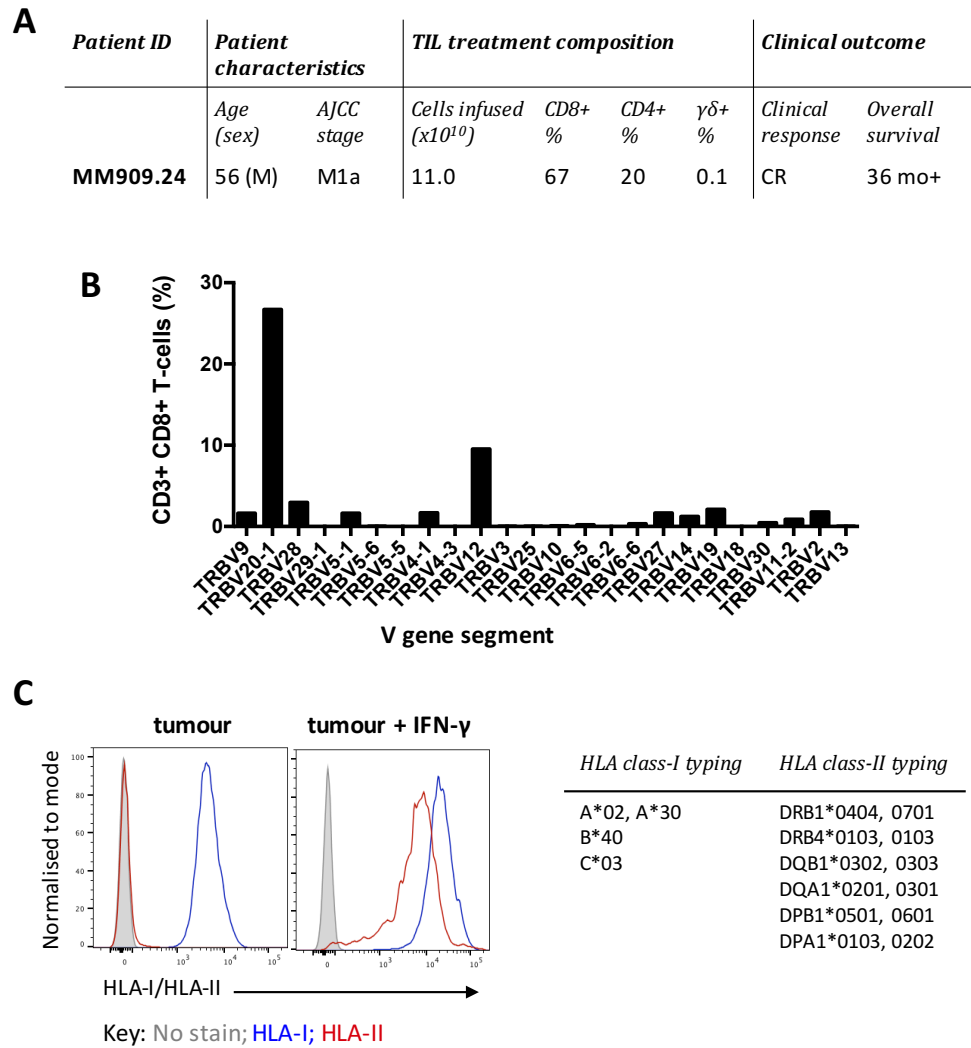


Figure 4.1. Patient MM909.24 characteristics, TIL composition and autologous tumour HLA expression

(A) Patient characteristics, treatment details and clinical outcome. M1a stage (AJCC) (Balch et al., 2009) involves distant metastasis in the skin, subcutaneous tissue, or distant lymph nodes. A complete response (CR) is defined by RECIST guidelines as the “disappearance of all target lesions and any pathological lymph nodes must have reduction to <10 mm (Eisenhauer et al., 2009). **(B)** TRBV antibody surface staining of MM909.24, gated on total CD3+ CD8+ viable T-cells. **(C)** Left panel shows the flow cytometric analysis of HLA-I and HLA-II expression of autologous melanoma cells. Cells were untreated or treated with low dose IFN- γ (100 IU/mL) for 72 hours. Right panel shows full HLA-I and HLA-II typing. HLA-I typing is shown at the 2-digit level, which distinguishes the protein family, whereas HLA-II was performed to the 4-digit level and distinguishes different proteins within a family.

4.2.2 Anti-melanoma reactivity of TILs MM909.24

IFN- γ and TNF- α are among the secreted cytokines that mediate the anti-tumour activity of effector CD8+ T-cells. During the killing process of the target tumour cell the lysosomal-associated membrane protein, CD107a, is also transiently mobilised to the surface membrane of effector CD8+ cells (Betts et al., 2003). The reactivity of cultured MM909.24 TILs against autologous tumour cells was analysed by measuring IFN- γ , CD107a and TNF- α T-cell production by flow cytometry (**Figure 4.2B**). The CD8+ subset of TILs MM909.24 (which represents 96.9% of total CD3+ TILs) produced IFN- γ , TNF- α and CD107a upon stimulation with autologous tumour cells (14.4%, 21.7% and 28%, respectively). When gated on CD4+ TILs (2.49% of total CD3+ cells), only 0.2% of CD4+ CD107a+ cells could be detected (**Figure 4.2C**) and as the number of events acquired for this population is very low, it may not be a true representation of activity. The assay would need to be repeated to validate CD4+ activity using more cells per condition. Alternatively, the CD4+ cells could be cloned and tumour reactivity assessed at the clonal level. Collectively, these data suggest that there is a functional heterogeneity among tumour reactive TILs. The hierarchy seen for the outputs used here may be attributable to T-cell peptide sensitivity (La Gruta et al., 2004; Laugel et al., 2007; Price et al., 1998).

My first attempt at investigating the HLA-restriction of tumour-reactive TILs involved the use of blocking antibodies. Incubation of target melanoma cells with an anti-HLA-I mAb resulted in the inhibition of IFN- γ , TNF- α and CD107a expression, which decreased in turn to 1.02%, 1.15% and 3.04% (**Figure 4.2B**), from 14.4%, 21.7% and 28% respectively. Incubation with an anti-HLA-II mAb resulted in a less marked reduction in IFN- γ , TNF α and CD107a, with a drop of 3.9%, 1.7% and 0.4% respectively. Taken together, these initial results suggest that the major reactivity against autologous tumour in MM909.24 TILs is mediated by the CD8+ TIL subset and expected to be HLA-I restricted.

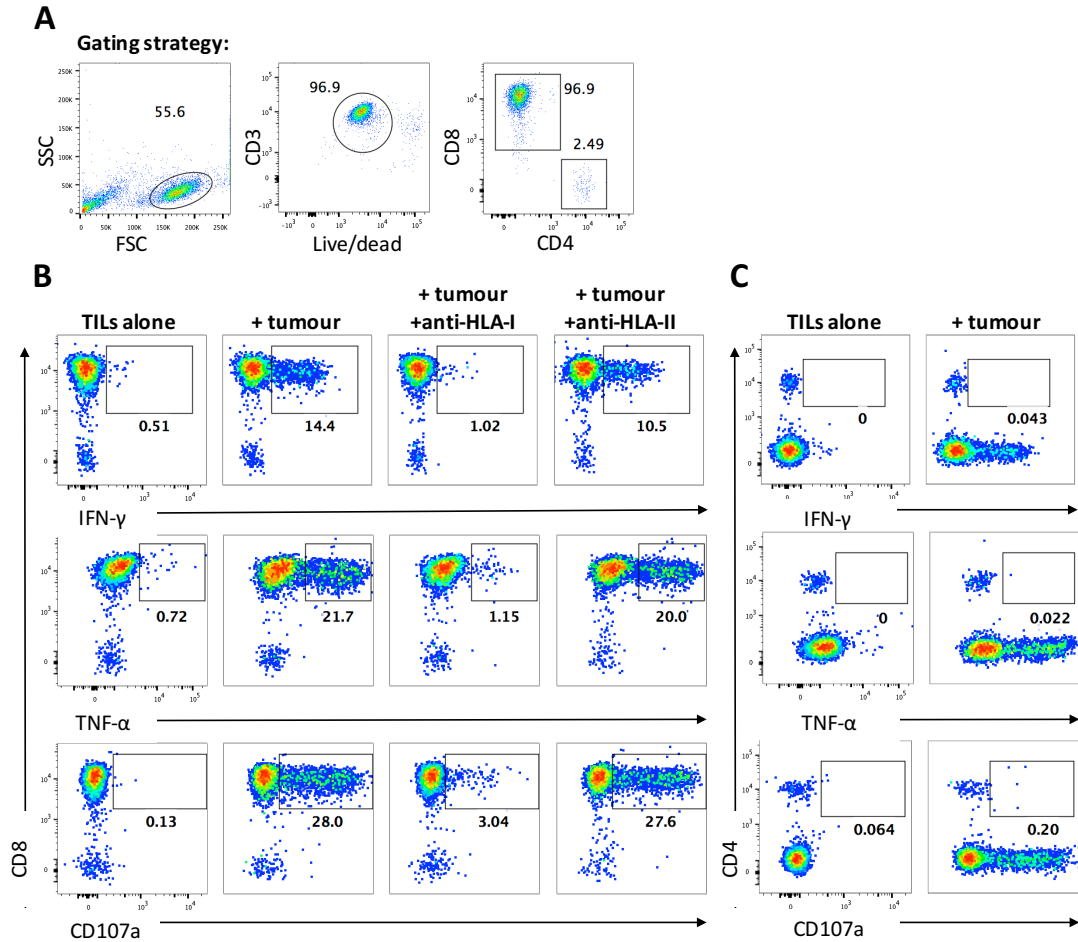


Figure 4.2. MM909.24 TILs reactivity to autologous tumour is mediated by CD8+ T-cells and is HLA class-I restricted

(A) TILs were gated on live CD3+ T-cells and CD8+ and CD4+ subsets analysed separately. **(B)** FACS plots of ICS of CD8+ TILs expressing IFN- γ , TNF- α and CD107a after 5 hour stimulation with autologous tumour cells (E:T ratio 2:1). TILs alone were used as control. Target melanoma cells were also incubated with either an anti-HLA-I or HLA-II mAb to explore HLA-restriction. Gates were set based on Fluorescence Minus One (FMO) sample (i.e. unstimulated TILs stained with surface markers only). **(C)** ICS FACS plots of CD4+ TILs expressing IFN- γ , TNF- α and CD107a upon activation with autologous tumour cells. TILs alone were used as control.

Given the fact that patient MM909.24 is HLA-A2+ (HLA-A30 at the second HLA-A allele), another blocking experiment using an anti-HLA-A2 mAb (BB7.2 clone) was performed and the production of IFN- γ by CD8+ TILs was measured. As shown in **Figure 4.3A**, incubation of melanoma cells with the antibody resulted in a 3-fold reduction of TILs IFN- γ expression, but did not completely inhibit autologous melanoma recognition. An anti-HLA-A1 blocking antibody was used as a negative control and had no effect on tumour recognition as expected. These data suggest that at least 30% of the tumour reactivity in MM909.24 TILs is restricted by HLA-A2.

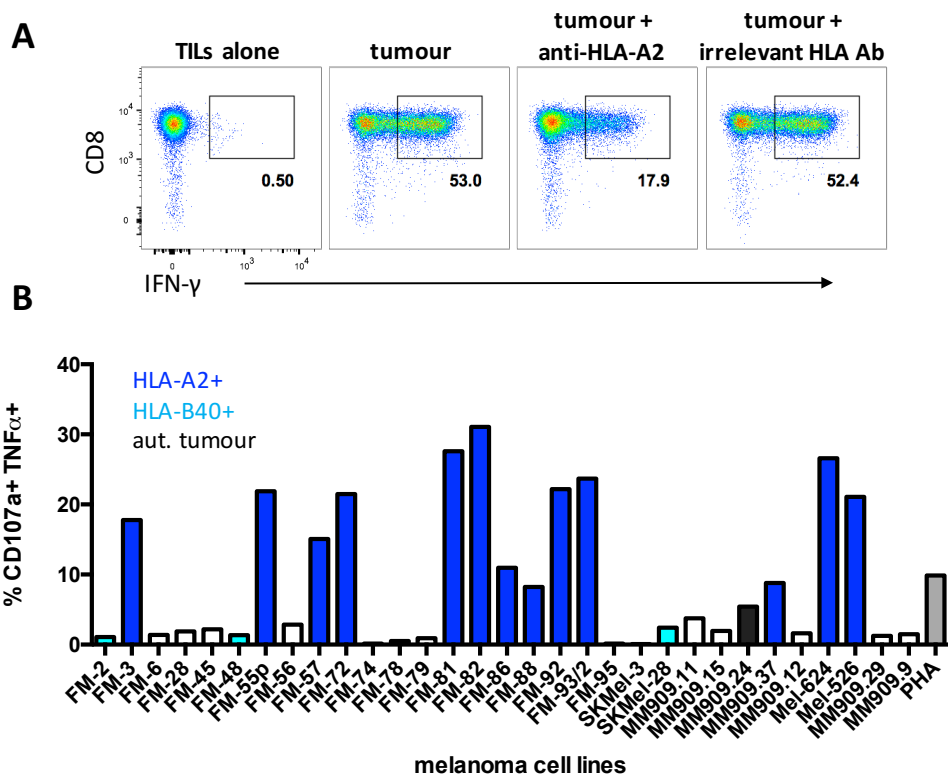


Figure 4.3. MM909.24 TIL tumour reactivity is predominantly HLA-A2 restricted

(A) ICS FACS plots show the percentage of CD8⁺ IFN- γ ⁺ TILs upon 5 hour stimulation with autologous tumour cells (E:T ratio 2:1). Unstimulated TILs were used as negative control. Cells were gated on live CD3⁺ TILs. Target melanoma cells were also incubated with either an anti-HLA-A2 or anti-HLA-A1 (irrelevant control) mAb to explore HLA-A2 restriction. (B) Bar chart shows the percentage of CD107a⁺ TNF- α ⁺ TILs upon stimulation with melanoma cell lines, of which several share the HLA-A2 allele (blue) or HLA-B40 allele (aqua) with the autologous tumour. Stimulation with autologous tumour (black bar) and PHA (3 μ g/mL) (grey bar) were used as positive controls. Reactivity against the autologous tumour was lower than seen in previous experiments. Gates were set on unstimulated TILs samples (negative control). Representative FACS plots are shown in Appendix (Figure 7.2). Cells were gated on viable CD3⁺ CD8⁺ TILs.

Blocking antibodies might not be the optimal tool to inhibit effector T-cell activity, as they can fail to saturate all the available surface HLA molecules. To further explore TILs HLA-A2 restriction and overcome the limitations of using blocking antibodies, I decided to evaluate TILs MM909.24 reactivity against a panel of partially HLA matched (for HLA-A2 or HLA-B40) or mismatched melanoma cells lines, kindly provided by Marco Donia (CCIT, Copenhagen) (Appendix, **Table 7.1A**). As shown in **Figure 4.3B**, TIL reactivity against target cell lines was defined as the percentage of CD107a⁺ and TNF- α ⁺ cells gated on total CD8⁺ TILs. All 13 melanoma cell lines recognised by MM909.24 TILs express HLA-A2, supporting the results previously obtained with the BB7.2 blocking antibody. This experiment also suggests that the HLA-A2-restricted T-cell epitope(s) recognised by MM909.24 TILs are not exclusively displayed by the autologous tumour cells but are shared by other HLA-A2 tumours. Shared antigens are particularly interesting for immunotherapy as they are relevant to many patients, I therefore decided to further explore the antigen specificity of tumour-reactive TILs from this HLA-A2+ patient.

4.2.3 Multiple clonotypes mediate an HLA-A2-restricted Melan-A specific anti-tumour response in patient MM909.24

TIL reactivity against melanoma can be mediated by shared antigens (such as differentiation, overexpressed or cancer testis antigens) and/or neo-antigens derived from private point mutations (Boon et al., 2006). In order to explore peptide dominant specificities in MM909.24 TILs, I decided to examine the TILs at the polyclonal level and also to grow tumour specific T-cell clones. My initial experimental strategy is schematically outlined in **Figure 4.4**.

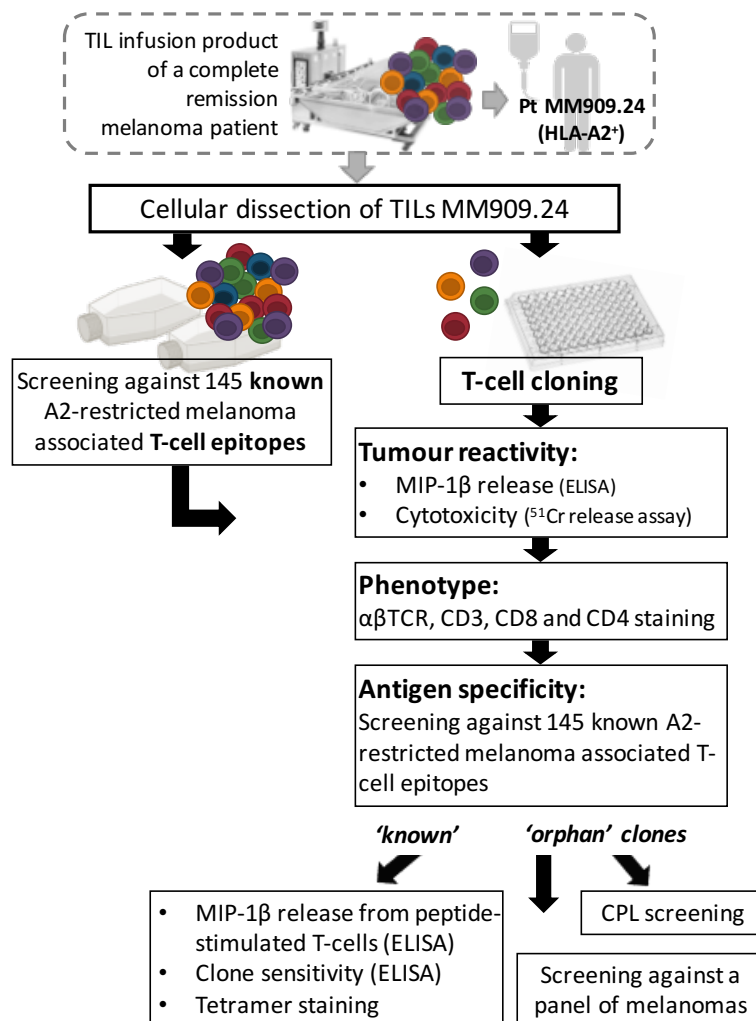


Figure 4.4. Schematic outline of the experimental strategy used to dissect anti-melanoma TILs from patient MM909.24

MM909.24 TILs are associated with *in vivo* long-term tumour clearance. TILs as a bulk population were screened against a panel of known HLA-A2 restricted melanoma T-cell epitopes. Individual T-cell clones were also isolated and selected based on reactivity against the autologous melanoma cell line. HLA-A2 restricted antigen specificity was dissected by screening against a panel of known melanoma T-cell epitopes. T-cell clones with known antigen specificities were validated through tetramer staining and peptide sensitivity experiments. T-cell clones with unknown antigen specificity ('orphan' clones) were screened against a panel of melanoma cell lines. The specificity of orphan clones can be further explored by using Combinatorial Peptide Library scans (CPL) with a positional scanning format, in order to obtain detailed picture of the amino acid landscape preferred by the TCR.

Firstly, I assessed whether known A2-restricted melanoma T-cell responses were present within MM909.24 TILs. To address this question, I selected a large panel of published melanoma-associated T-cell epitopes (Andersen et al., 2012), encoded by proteins that are either exclusively melanoma specific (such as gp100, Melan-A, tyrosinase antigens) or shared with other tumours types (such as p53, Survivin, NY-ESO and the MAGE antigens). The Andersen et al. study (Andersen et al., 2012) combined data from available literature with the Cancer Immunity database (Van den Eynde and van der Bruggen, 1997), the CTpedia database (Almeida et al., 2009) and a previously published antigen list (Novellino et al., 2005). The study was more rigorous than those that preceded it and only included T-cell epitopes with: (i) a defined minimal epitope sequence; (ii) known HLA restriction; and, (iii) evidence that the peptide is processed and presented on tumour cells. A full list of the 145 peptides is provided in the **Appendix (Table 7.2)**. Peptide specific T-cell responses in MM909.24 TILs were quantified by an IFN- γ ELISpot assay.

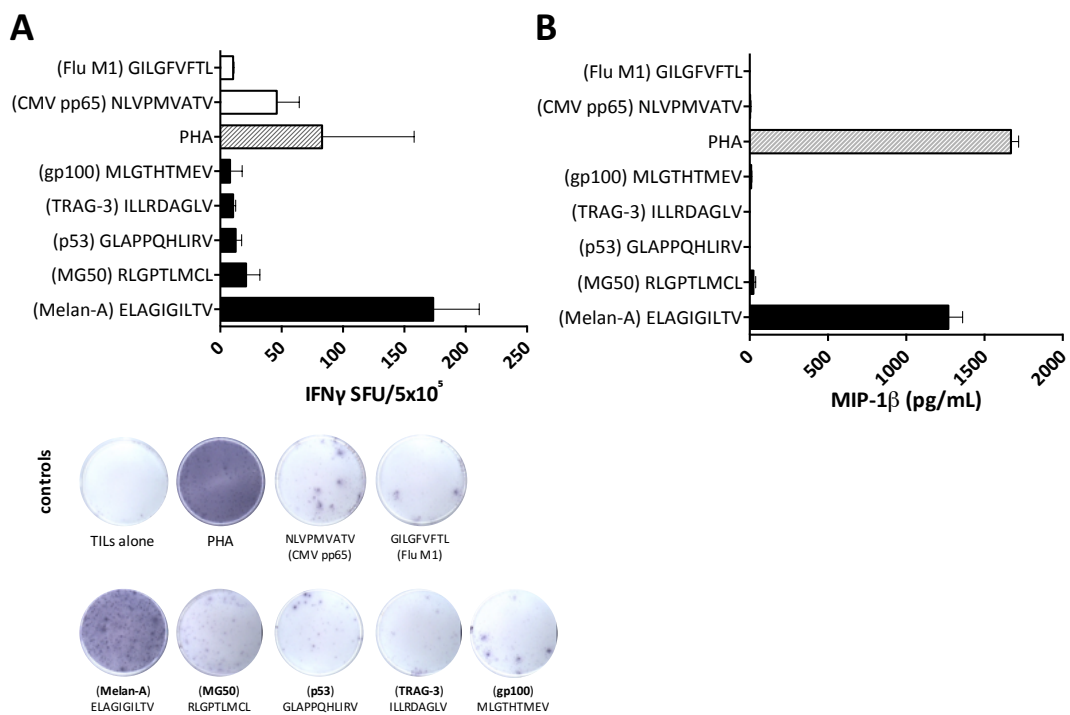


Figure 4.5. Melan-A T-cell epitope (ELAGIGILTV) recognition by TILs MM909.24

(A) IFN- γ ELISpot performed on 5x10⁵ MM909.24 TILs stimulated in duplicate with 145 known HLA-A2 restricted melanoma-associated peptides (10⁻⁶ M) for 24 hours. Data for wells that gave a response above background are shown. Viral peptides NLVPMATV (CMV pp65 protein) and GILGFVFTL (Influenza M1 protein) were also tested. PHA (3 μ g/mL) was used as a positive control. The number of IFN- γ secreting cells per 5 x10⁵ TILs is displayed on the X axis; peptide sequence and protein of origin (in brackets) are displayed on the Y axis. Each bar represents the mean spot count per well (\pm SD). Representative images of ELISpot wells are shown in the bottom panel. **(B)** Supernatants from A) were used to detect MIP-1 β release (ELISA). Background (T-cells alone) was subtracted from each condition. Duplicate mean \pm SD is shown.

Of the 145 known peptides tested, the Melan-A decamer heteroclitic peptide ELAGIGILTV (ELA hereafter) elicited the highest response within MM909.24 TIL (173 ± 37 IFN- γ SFU / 5×10^5 TILs; **Figure 4.5A**). This result is consistent with prior data on melanoma TILs reactivity, showing that T-cell responses against the melanocyte differentiation antigen Melan-A are dominant in HLA-A2+ individuals (Boon et al., 2006; Romero et al., 2006). Other known tumour-associated antigens were not detected or only elicited specific T-cell responses in the range of 10-12 IFN- γ SFU. In concordance with these results, our collaborators showed that 1.8% of the MM909.24 TIL infusion product stained with an A2-ELA tetramer and produced IFN- γ (data not shown; Marco Donia, personal communication). Interestingly, a CMV-derived T-cell epitope also produced a positive result (46 ± 16 IFN- γ SFU) in ELISpot. There was also a smaller response to an immunodominant HLA-A2-restricted influenza-derived epitope. The occurrence of anti-viral T-cells within TIL populations is supported by previous studies in which low frequency virus-specific T-cells were detected in melanoma TIL cultures (Andersen et al., 2012; Kvistborg et al., 2012). Supernatants were also tested by MIP-1 β ELISA, confirming the immunodominance of the Melan-A epitope (**Figure 4.5B**).

I next decided to further explore the dominant ELA T-cell reactivity in MM909.24 TILs. TIL cultures were stained with an A2-ELA tetramer to measure Melan-A reactivity at the population level, and cloning plates were also set up to isolate tumour-specific T-cell clones from these TILs. During the course of my PhD, our research group has developed an improved pHLA tetramer staining protocol that allows the detection of low-affinity or rare T-cells otherwise undetected by standard tetramer staining (Dolton et al., 2015; Tungatt et al., 2015). We showed that the addition of a primary anti-fluorochrome Ab followed by a secondary anti-Ab conjugated secondary Ab substantially improved tetramer staining intensity and flow cytometry detection (Tungatt et al., 2015). This 'boosted' protocol (A2-ELA tetramer + primary Ab + secondary Ab) was used to stain ELA T-cell responses in MM909.24 TIL cultures (**Figure 4.6**). Baseline A2-ELA tetramer staining of unstimulated TILs showed that 5% of CD8+ T-cells were tetramer positive. TILs were then co-cultured with autologous melanoma cells for 7 days. Long-term stimulation with autologous melanoma resulted in the enrichment of the A2-ELA+ population (19.6% of total CD8+ TILs by day 7). No tumour cells were visible in culture or on FACS after 48 hours (data now shown). Overall, these results show that *in vitro* exposure to autologous melanoma leads to a significant expansion of ELA-specific T-cells. Although Melan-A-specific T-cell responses in TILs have been relatively well described, given the dominance of the response shown here, I was interested in studying the clonotypic composition of ELA-specific T-cells in MM909.24 TILs and in dissection of their anti-tumour function at the clonal level. I successfully grew ELA specific clones as part of my strategy as outlined in **Figure 4.4** and described below.

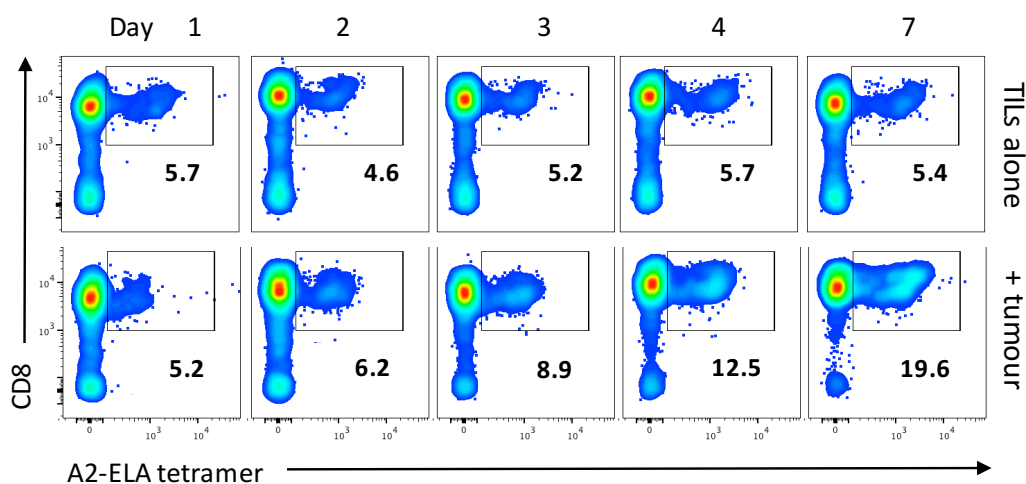


Figure 4.6. ELA-specific TIL population increases during *in vitro* culture with autologous tumour

FACS plots show the percentage of CD8+ TILs that are stained with an A2-ELA (Melan-A) tetramer. TILs were cultured for 7 days *in vitro* with autologous tumour cells. No tumour cells were visible in culture or on FACS after 48 hours. Gates were set based on staining with an irrelevant tetramer A2-ALW (residues 15-24 from preproinsulin) (not shown). All samples were treated with Dasatinib (a protein kinase inhibitor, PKI) to prevent TCR triggering and internalisation of the TCR. Cells were tetramer stained with a 'boosted' protocol using both primary and secondary antibodies (Materials and Methods, section 2.11.4).

Fifty cloning plates (~5000 wells) were set up from MM909.24 TIL cultures, and T-cell clones isolated by limiting dilution. More than one hundred clones were screened and selected based on specific lysis of autologous tumour cells and ability to grow well in culture (**Appendix: Table 7.4**). I opted for cloning straight from the TIL infusion product to minimise further *in vitro* manipulation and potential distortion. I later used flow cytometry based methods to sort viable T-cells producing TNF- α and CD107a after co-culture with tumour. Some clones did not grow after two passages and therefore could not be used for further experiments. I also screened the clones with the peptides from Melan-A, gp100, TRAG-3, p53 and MG50 (**Figure 4.5**), which I previously identified by ELISpot performed on bulk TILs. Overall five unique ELA specific clones were identified, some more than once. No clones were procured from MM909.24 TILs specific for gp100, TRAG-3, p53 or MG50, which may be due to their relatively low frequency in the TILs and the cloning strategy I used. Peptide-based methods could have been used to specifically enrich these cells if desired, but I did not explore this any further due to time constraints.

Figure 4.7 displays the characterisation of the five unique ELA clones isolated. All T-cell clones specifically recognised and lysed the autologous melanoma (**Figure 4.7A**), and showed higher cytotoxic capability when target cells were pre-treated with IFN- γ for 72 hours. Enhanced tumour recognition is likely to be associated with IFN- γ induced expression of HLA complexes on the tumour surface as shown in **Figure 4.1C**, and as previously reported (Donia et al., 2013; Weidanz et al., 2006).

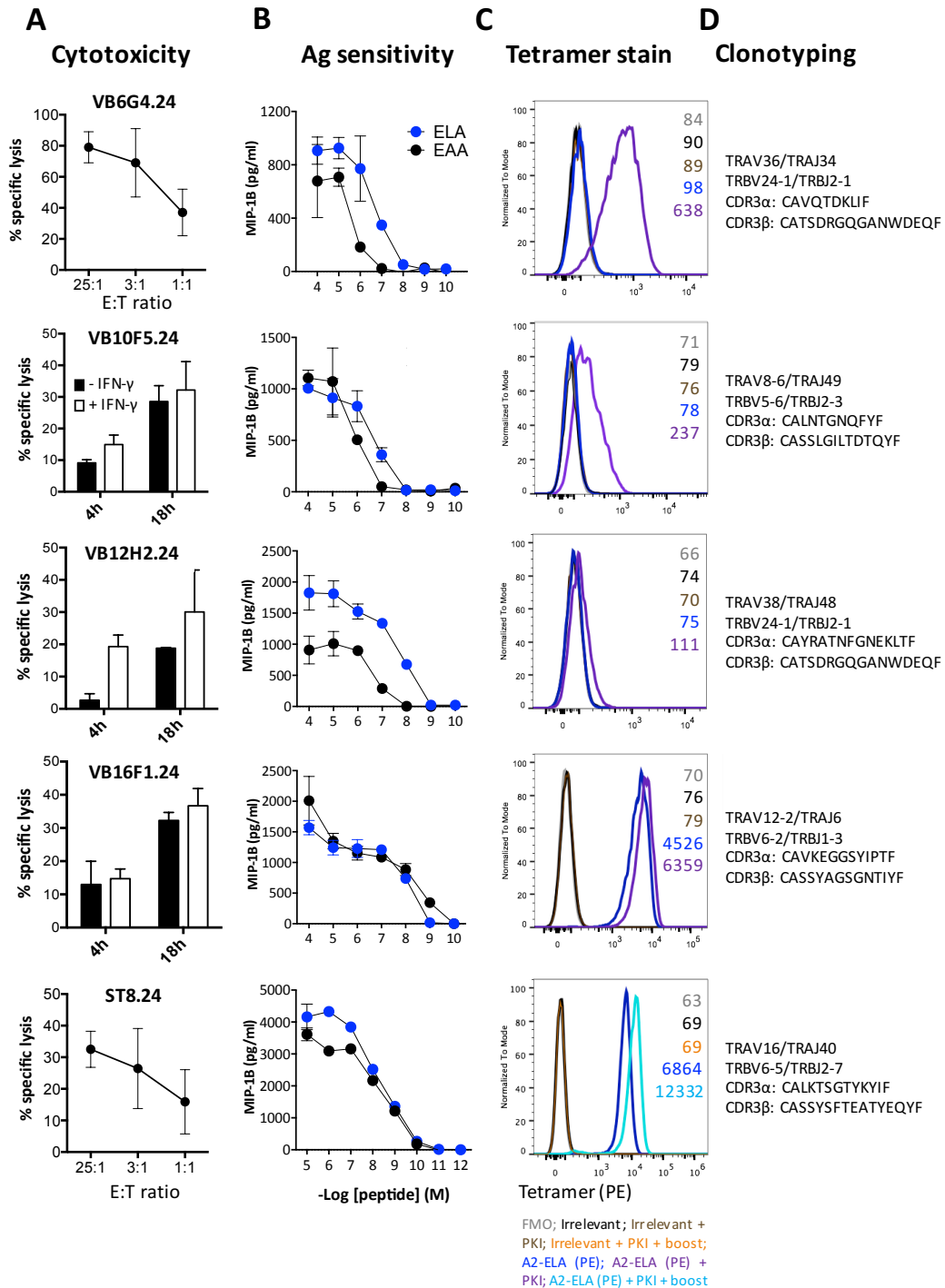


Figure 4.7. Melan-A specific clones from TILs MM909.24 exhibit differing sensitivity to antigen and express unique TCRs

(A) Specific melanoma lysis (%) by T-cell clones was determined in cytotoxicity assays with autologous target cells (E:T ratio 5:1) after 4 and 18 hours. Cytotoxicity of T-cell clones VB6G4.24 and ST8.24 was titrated at different E:T ratios and is displayed after 24 hours. Melanoma cells were left untreated or treated with low dose of IFN- γ (100 IU/mL) for 72 hours, as indicated **(B)** Peptide sensitivity of Melan-A specific CD8+ CTL clones was determined by measuring MIP-1 β (pg/mL) release from peptide-stimulated T-cells. T2 cells were incubated in duplicate with titrated amounts of ELA (blue symbols) or EAA (black symbols) peptide. **(C)** T-cell clones were stained with PE-conjugated A2-ELA tetramer \pm 50 nM Dasatinib (PKI) treatment. Unstained cells and irrelevant tetramer staining (HLA-A2 ALWGPDPAAA: residues 15-24 from pre-proinsulin or HLA-A2 ILAKFLHWL: residues 540-548 from hTERT) were used as negative controls. 'Boost' stands for tetramer staining followed by the addition of a primary anti-fluorochrome antibody. Mean fluorescence intensity (MFI) of PE is shown. **(D)** TCR α and TCR β gene usage and CDR3 amino acid sequences of Melan-A specific CTL clones (courtesy of M. Attaf).

The CTL clone VB6G4.24 was the most sensitive killer among the T-cell clones analysed, displaying an average specific lysis of untreated tumour of 37% at the lowest effector-to-target (E:T) ratio after 18 hours. To further characterise the peptide sensitivity of Melan-A specific clones they were tested in a titration assay by MIP-1 β ELISA using T2 cells pulsed with either the wild type EAA epitope or the ELA analogue (**Figure 4.7B**). This experiment was performed to ensure that the CTL clones recognised the wild type epitope, which is actually processed and presented on melanoma cells. As shown in previous studies (Kawakami et al., 1994c; Romero et al., 1997; Valmori et al., 1998) most of the Melan-A clones analysed displayed a pattern of recognition whereby the ELA analogue was recognised at lower concentrations than the natural EAA decamer. The highest functional sensitivity (recognition at the lowest peptide concentrations) was observed to both ELA and EAA peptides by T-cell clone ST8.24.

Finally, binding to A2-ELA complexes was validated by tetramer staining of T-cells (**Figure 4.7C**). Interestingly, despite all the clones recognising the ELA peptide in ELISA assays, three out of five clones did not stain with the corresponding tetramer using standard protocols. With the exception of CTL clone VB12H2.24, staining intensities were enhanced only when samples were pre-treated with 50 nM of the protein kinase inhibitor (PKI) Dasatinib. Tetramer staining is dependent on the TCR density at the cell surface, therefore Dasatinib-induced staining recovery is likely to be due to an inhibition of tetramer-induced TCR turnover (Dolton et al., 2015; Lissina et al., 2009). As previously reported by our group (Tungatt et al., 2015; Dolton et al., 2015), addition of an anti-tetramer primary antibody and conjugated secondary antibody following A2-ELA tetramer, is likely to boost the staining of the Melan-A clone VB12H2.24.

Clonotypically, the five different Melan-A clones shown here have unique $\alpha\beta$ TCR sequences (**Figure 4.7D**). A TCR repertoire bias in human anti-Melan-A T-cell responses has been reported by previous studies. In particular, A2-restricted CD8⁺ T-cells specific for the EAA antigen, were found to predominantly express TRBV27/TRBJ2-1/TRAV12/TRAJ34 gene segments (Dietrich et al., 2003; Serana et al., 2009; Wieckowski et al., 2009). Interestingly, only T-cell clone VB16F1.24 expresses the TRAV12-2 gene segment, which is commonly used to encode the TCR α in more than 80% of EAA-specific T-cells across multiple individuals (Cole et al., 2009; Trautmann et al., 2002; Wieckowski et al., 2009). Furthermore, despite having different peptide sensitivities, T-cell clones VB6G4.24 and VB12H2.24 use the TRBJ2-1 gene segment and also share the same CDR3 β sequence. Taken together, these results show that Melan-A specific CTL clones isolated from the TIL infusion product of patient MM909.24 exhibit different sensitivity to the immunodominant ELA T-cell epitope and express unique TCRs. My experiments with one of these clones, ST8.24, indicated that it might recognise a further tumour-derived peptide and took my work in an unexpected direction.

4.2.4 Unexpected cross-recognition by MM909.24 Melan-A-specific clone ST8.24

During my experiments with clone ST8.24, I found that this T-cell clone repeatedly recognised the C1R-A2 cell line I was using as a control. C1Rs are a lymphoblastoid cell line that also expresses some Epstein Barr Virus (EBV) proteins, but not Melan-A. Recognition of C1R-A2, but not wild-type C1Rs that lack HLA-A2 expression, by clone ST8.24 suggested that this clone might recognise a further HLA-A2-restricted antigen (**Figure 4.8A**). In order to test for recognition of EBV proteins, I tested ST8.24 against other EBV-immortalised B-cells to assess whether the observed cross-reactivity was due to an EBV epitope. Effector function was assessed by flow cytometry by measuring the expression of CD107a and TNF- α following 5-hour stimulation with target cells (**Figure 4.8B**). ST8.24 failed to recognise other EBV-immortalised B-cell lines suggesting that this mechanism could not account for its reactivity towards C1R-A2 cells.

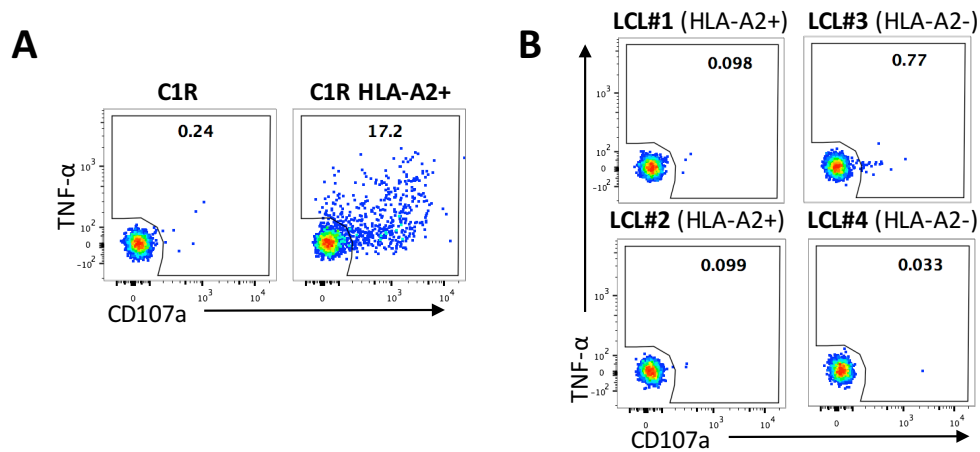


Figure 4.8. ST8.24 reacts towards C1R-A2 cells but fails to recognise EBV-immortalised B-cell lines

(A) ST8.24 was tested against the human leukemic cell line C1R and its HLA-A2+ transfectant. Reactivity was measured as the percentage of TNF- α CD107a+ T-cells by flow cytometry. Cells were gated on live CD8+ T-cells. (B) ST8.24 was tested against EBV immortalised lymphoblastoid cell lines (LCL) that were either HLA-A2+ or HLA-A2-. Reactivity was measured as the percentage of TNF- α CD107a+ T-cells by flow cytometry. Cells were gated on live CD8+ T-cells.

I next screened the ST8.24 clone against a wide panel of HLA-A2+ tumour cell lines to test whether it might recognise a further tumour antigen-derived peptide in addition to Melan-A. Effector function was assessed by flow cytometry by measuring the expression of CD107a and TNF- α following 5-hour stimulation with target cells (**Figure 4.9**). HLA-A2+ and HLA-A2- melanoma cell lines were also included as positive and negative controls, respectively. Surprisingly, several non-melanoma cell lines were recognised by the ST8.24 clone.

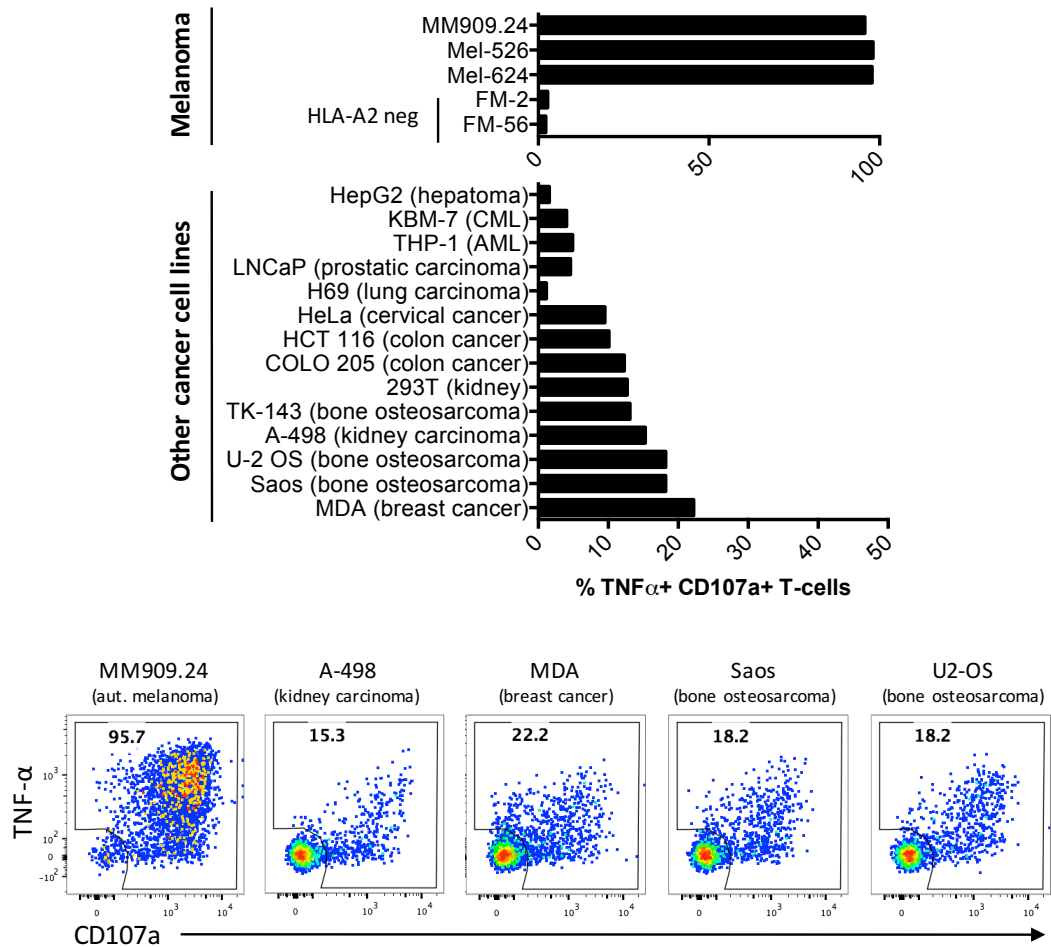


Figure 4.9. ST8.24 recognises multiple cancer cell types

ST8.24 T-cell clone was tested against a panel of HLA-A2+ cell lines from tumour types other than melanoma. The tumour of origin is indicated in brackets. The HLA-A2+ melanoma cell lines Mel-526, Mel-624 and autologous tumour MM909.24 were added as positive control. The HLA-A2- melanoma cell lines FM-2 and FM-56 were added as negative control. Tumour reactivity was measured as the percentage of TNF- α CD107a+ T-cells by flow cytometry. Representative dot plots are shown in the bottom panel. Cells were gated on live CD8+ T-cells.

The interaction between the TCR and pHLA can be highly degenerate, in that a single TCR may recognise huge numbers of peptides in the context of a single HLA-I molecule (Sewell, 2012). T-cell cross-reactivity in TILs, and its potential role in mediating *in vivo* tumour regression has never been investigated. In order to address this, I took a systematic approach using combinatorial peptide libraries (CPL) to screen the ST8.24 clone. CPL libraries are composed a series of sub-libraries in positional-scanning format; in particular, individual peptide sub-libraries have an amino acid fixed in each position and all other positions are made up of an equimolar mix of all remaining amino acids. A schematic diagram is shown in Material and Methods, **Figure 2.3**.

The ST8.24 CD8⁺ T-cell clone was subjected to a decamer CPL library scan. Each sub-library of a decamer library is made of 9.36×10^{12} different decamer peptides. Using this approach, I was able to scan every amino acid at every position of the peptide within a random residue “backbone” and obtain a detailed picture of the amino acid landscape preferred by ST8.24 the TCR. T-cell activation was measured by MIP-1 β ELISA (**Figure 4.10**). The number of amino acids that were recognised by the ST8.24 TCR was limited to the index in the central region of the peptide (residues 5-6, corresponding to I and G of EAAGIGILTV), suggesting that the TCR makes the majority of its peptide contacts with these residues. In contrast, recognition was highly degenerate at the remaining positions at the N-term and C-term of the peptide. The CPL scan results also suggested that the index Melan-A peptide (EAAGIGILTV) is suboptimal in positions 1 and 2. Overall, positional peptide degeneracy is very high at least at 4 out of 10 positions; these results suggest that ST8.24 TCR can potentially recognise a multitude of different amino acid combinations in addition to the EAA peptide. I was interested in testing whether this TCR degeneracy was exclusive to the ST8.24 clone or shared by the other ELA-specific CT clones isolated from MM909.24 TILs. Unfortunately, I wasn't able to grow the other clones in high enough numbers to perform a full decamer CPL assay (approximately 2×10^7 cells are needed). I was thus forced to continue my studies using only the ST8.24 clone.

I next sought to identify the sequence of decamer peptides from human proteins that could be recognised by the ST8.24 cytotoxic T-cell clone. A novel webtool, developed by Dr Barbara Szomolay, was used to link the raw data of the CPL scan to the likelihood of potential peptides from the human proteasome to activate ST8.24 T-cells. During this bioinformatic approach, the CPL scan data were used to search collated human ‘self’ protein database including proteins identified by Andersen et al. (2012). A similar method was recently used to find the specificity of viral CD8⁺ T-cells (Szomolay et al., 2016). This computational approach produced a ranked list of peptides that the ST8.24 clone might recognise. The top ranked peptides are listed in **Table 4.1**, with colour coding depicting the sub-database each peptide was chosen from. The EAA index peptide and its ELA analogue were within the top three scores. Interestingly, two peptides from the Insulin-like growth factor 2 mRNA-binding protein family (IF2B2) resulted in a high score. IF2B2 protein isoforms have been shown to be expressed in several tumour-derived and transformed cell lines, including the osteosarcoma-derived U2-OS cells and melanoma (Bell et al., 2013). A decamer peptide LLLGIGILVL from the Bone marrow stromal antigen 2 protein (BST2) also ranked highly in this bioinformatic analysis. Up-regulation of this interferon-induced anti-viral protein has been reported in the human MCF-7 breast cancer cell line (Cai et al., 2009; Yi et al., 2013). Interestingly, the nonamer version of this BST2 T-cell epitope (LLLIGILV) was first published as an HLA-A2 restricted multiple myeloma-associated antigen (Hundemer et al., 2006). Peptides from other proteins that have been associated with melanoma, such as MC1R and MAGE proteins also ranked highly (**Table 4.1**).

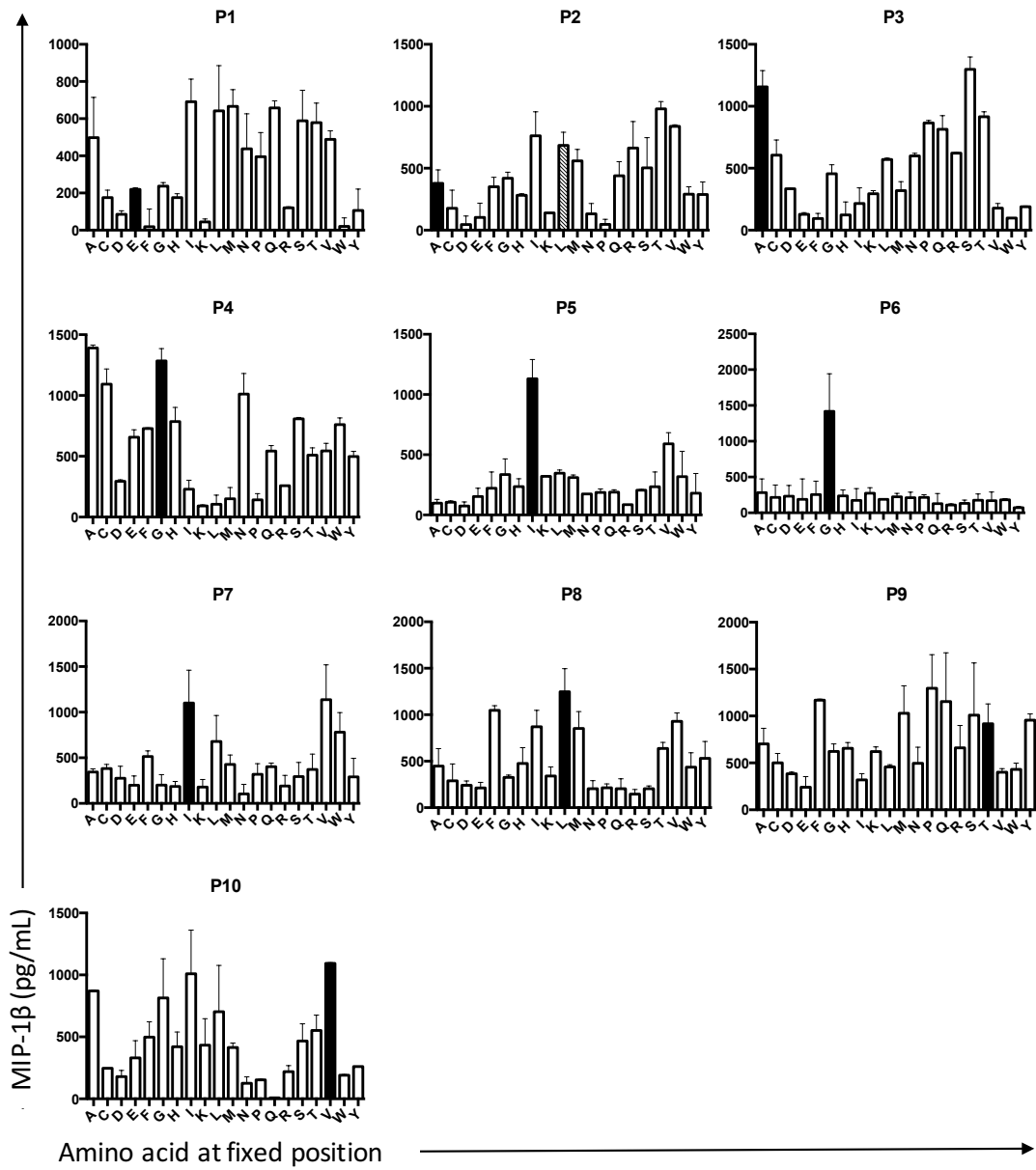


Figure 4.10. Decamer CPL scan of the ST8.24 clone

In each well, 6×10^4 T2 cells were pulsed in duplicate with each mixture from a decamer CPL library (100 g/mL) at 37°C. After 2 hours, 3×10^4 ST8.24 T-cells were added and incubated overnight at 37°C. Supernatants were harvested and assayed for MIP1- β (pg/mL) by ELISA. Results are displayed as histogram plots and SD from the mean of two replicates is shown. The index Melan-A peptide sequence (EAAGIGILTV) is shown in black bars. The L at position 2 in the ELAGIGILTV variant peptide is shown with a hatched bar.

Rank	Peptide	Protein	Abbrev.	UniProt ID	Organism
-22.065	ELAGIGILTV	Melanoma antigen recognized by T-cells 1 (analogue)	Melan-A		Human
-22.488	NLAAVGLFPA	Insulin-like growth factor 2 mRNA-binding protein 1	IF2B2	Q9NZI8	Human
-22.659	EAAGIGILTV	Melanoma antigen recognized by T-cells 1	Melan-A	Q16655	Human
-22.969	LLLGIGILVL	Bone marrow stromal antigen 2	BST2	Q10589	Human
-23.128	NLSALGIFST	Insulin-like growth factor 2 mRNA-binding protein 2	IF2B2	Q9Y6M1	Human
-23.301	VYAALGILQG	Canalicular multispecific organic anion transporter 2	MRP3	O15438	Human
-23.373	LILNIAIFFV	Dermatan-sulfate epimerase	DSE	Q9UL01	Human
-23.418	ATSAMGTISI	Mucin-16	MUC16	Q8WXI7	Human
-23.435	ISAVVGILLV	Tyrosine Kinase-Type Cell Surface Receptor HER2	HER2	P04626	Human
-23.477	TSSAIPIMTV	Mucin-16	MUC16	Q8WXI7	Human
-23.530	TYSCVGVFQH	Heat shock 70 kDa 1A	HS71A	P08107	Human
-23.530	LRLALGLLQL	G-protein coupled receptor 143	GP143	P51810	Human
-23.592	MVSCIIFFFV	Multidrug resistance-associated protein 1	MRP8	Q96J66	Human
-23.692	QLLAEGVLSA	Anoctamin-7	ANO7	Q6IWH7	Human
-23.695	TTLAICLLYV	Canalicular multispecific organic anion transporter 2	MRP3	O15438	Human
-23.794	GVSGIGVTLF	Tyrosine-protein kinase Fgr	FGR	P09769	Human
-23.820	LIAARGIFYG	Canalicular multispecific organic anion transporter 2	MRP3	O15438	Human
-23.836	TSSAIPPLPV	Mucin-16	MUC16	Q8WXI7	Human
-23.840	TIPSMGITSA	Mucin-16	MUC16	Q8WXI7	Human
-23.843	TTQSLGVMSS	Mucin-16	MUC16	Q8WXI7	Human
-23.877	VLNAVGVYAG	Melanoma-associated antigen C2	MAGE-C2	Q9UBF1	Human
-23.893	MISAIPTLAV	Mucin-16	MUC16	Q8WXI7	Human
-23.916	AVAAIWVASV	Melanocyte-stimulating hormone receptor	MC1R	Q01726	Human
-23.917	SVTWIGAAPL	Prostate-specific antigen	PSA	P07288	Human
-23.947	LTSSKGQLQK	Perilipin-2	PLIN2	Q99541	Human
-23.957	AASAIKVIPT	Indoleamine 2,3-dioxygenase 1	IDO1	P14902	Human
-23.984	MVLGIGPVLG	Solute carrier family 45 member 3	SLC45A3	Q96JT2	Human
-23.985	SAAGLGLVAI	Solute carrier family 45 member 3	SLC45A3	Q96JT2	Human
-24.014	QTQAVPLLMA	P protein	P protein	Q04671-2	Human
-24.016	STLNIDLFPFA	Peroxidase homolog	PXDN	Q92626	Human
-24.019	ILNGIKVLKL	Multidrug resistance-associated protein 1	MRP1	P33527-9	Human
-24.024	VLTAMGLIGI	Calcium-activated chloride channel regulator 2	CLCA2	Q9UQC9	Human

Key: [Self protein database](#);
[Tumour-associated protein database \(Andersen et al., 2012\)](#);
[Known A2-restricted melanoma-associated T-cell epitope database \(Andersen et al., 2012\)](#)

Table 4.1. Peptides sequences resulting from ST8.24 CPL scan ranked in order of recognition likelihood

CPL scan data was used to search protein databases and rank peptides in order of likelihood recognition. Peptide ranking is expressed on a natural logarithmic scale. For instance, a ranking value of -22 means that the corresponding peptide is approximately three times more likely to be recognised than a peptide with ranking -23. Computational analysis was performed by Dr Barbara Szomolay (Cardiff). Protein names are colour coded according to the database of origin used for the computational search. All peptides were used for titration assays, with the boxed sequences correspond to the peptides selected for display (Figure 4.11).

I next validated the bioinformatic data in **Table 4.1** by examining whether the ST8.24 clone could recognise the predicted peptides in MIP-1 β ELISA (**Figure 4.11**). ST8.24 recognised the LLLGIGILVL peptide from the Bone Marrow Stromal antigen 2 (BST2) with a similar sensitivity ($-\text{LogEC}_{50} = 8.4$) to the cognate EAAGIGILTV (Melan-A) peptide ($-\text{LogEC}_{50} = 7.9$). Peptide NLSALGIFST (IF2B2) resulted in MIP-1 β production only at the highest peptide concentrations (10^{-5} and 10^{-6} M), whereas peptide NLAAVGLFPA from the same protein was not recognised.

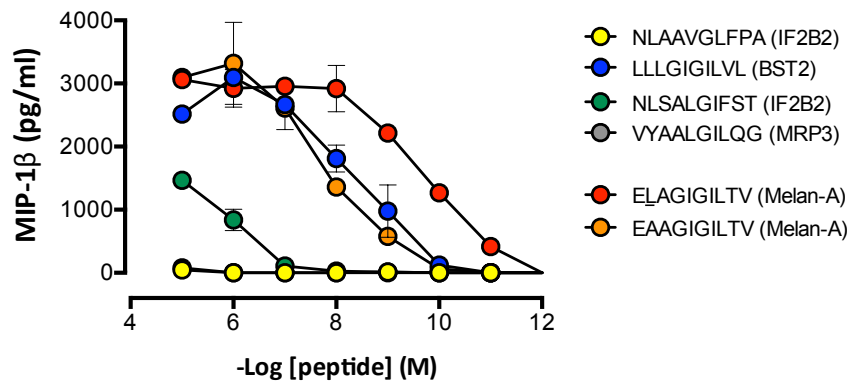


Figure 4.11. ST8.24 peptide cross-reactivity

Antigen sensitivity was measured in peptide titration assays by MIP-1 β ELISA. Briefly, 6×10^4 T2 cells were pulsed with serial dilutions of cognate peptide from 10^{-5} to 10^{-10} M in duplicate for 1 hour at 37 °C. ST8.24 T-cells were added and incubated overnight at 37°C. Supernatants were harvested and assayed for MIP-1 β production by ELISA. The mean \pm SD of two replicate assays is shown.

Taken together, the data obtained from the CPL decamer scan of T-cell clone ST8.24, point towards the possibility that this clone recognises other tumour-associated peptides. However, further experiments are required to validate the recognition of potential agonists.

4.2.5 Tumour-reactive T-cell clones persist in the patient's blood after TIL-therapy

Previous work indicates that the ability of tumour-reactive TILs to persist *in vivo* following adoptive infusion can have a significant impact on the clinical outcome of therapy (Dudley, 2002; Huang et al., 2004; Yee et al., 2002). To better understand which T-cell clones are dominant in MM909.24 TILs and may be important in mediating *in vivo* tumour regression, I decided to analyse the presence and persistence of individual tumour-reactive T-cell clones in the patient's circulation after TIL therapy. In order to address this, TCR clonotyping by sequence analysis was selected as the method of choice to provide a complete analysis of TCR β usage in TILs and PBMC samples.

The experiment was performed directly on a thawed TIL infusion product sample to avoid *in vitro* culture that could bias towards certain clonotypes. Briefly, tumour reactive T-cells from the TIL infusion product and PBMC were live-sorted on their ability to produce TNF- α and CD107a when stimulated with autologous tumour (35.9% and 2.6% of total CD3+ cells, respectively) (**Figure 4.12A**). The TNF- α Processing Inhibitor 0 (TAPI-0) can directly prevent its release from the cell surface therefore effectively 'trapping' TNF on the surface of the effector T-cell (Crowe et al., 1995; Hinrichs et al., 2011). Total mRNA was isolated from sorted cells and used to analyse the TCR β repertoire of both samples by SMARTer™ RACE technique.

Figure 4.12B shows the comparison of the TRBV gene segment usage between infused TILs and PBMC (after therapy) from the patient MM909.24. TRBV20-1 and TRBV12-4 are the most frequent TCR β families amongst tumour reactive TILs (50% and 14% respectively). These results are in accordance with the data obtained by initial surface staining of total TILs with TRBV antibodies (Figure 4.1B). Interestingly, TRBV20-1 is still detected in the matched PBMC sample post TIL therapy, however it is present at lower frequency (4.5% of total tumour reactive T-cells). TRBV12-4, on the other hand, is the most frequent TCR β family in circulation of patient MM909.24 six months after therapy (51% of total tumour reactive PBMC). TRBV24-1, TRBV7-9 and TRBV4-3 are represented amongst the tumour-reactive cells in the TIL infusion product and the patient blood 6 months after treatment. In contrast, TRBV5-6 and TRBV6-1 (7.8% and 3.5% in TIL infusion product, respectively) did not persist within the tumour-reactive T-cell population in patient blood 6 months after treatment.

The analysis of the composition of CDR3 sequences, which are unique to each TCR- β variant, was used to further quantify TCR diversity in TILs and PBMC samples. The pie charts in **Figure 4.12C** show the distinct CDR3 sequences detected in the TCR β repertoire of the infusion product and blood from patient MM909.24. Overall, both samples are characterised by a polyclonal T-cell response against autologous tumour. Strikingly, a single T-cell clone represents 34% of the total tumour-reactive T-cells present in the original TIL infusion product, and is still present in the circulation after therapy (1.14%). A second tumour-specific T-cell clone present at much lower frequency in the TILs (4.9%) persists in the PBMC (1.13%). Interestingly, the clonotype that represents 40% of the tumour-reactivity in PBMC was not present in the infusion product suggesting that this is a new T-cell response. Deep sequencing of all TCR β in these samples will be required to confirm this finding.

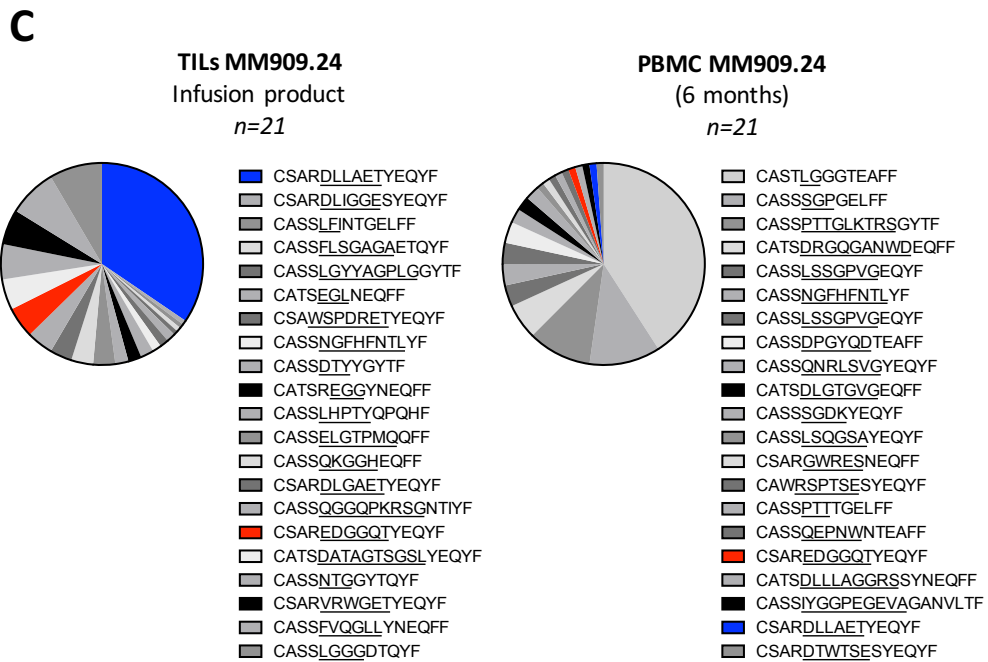
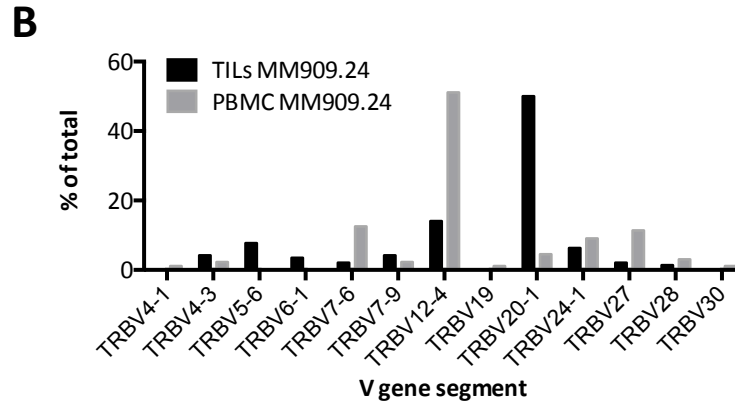
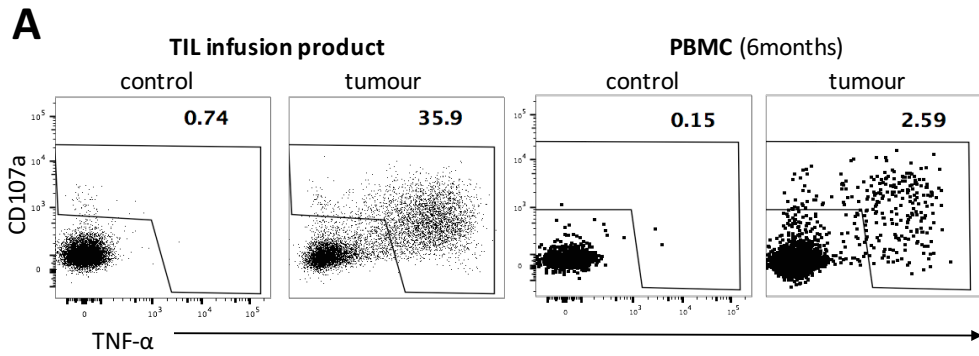


Figure 4.12 CDR3 sequences in the TCR beta repertoire of TILs and PBMC from patient MM909.24

(A) Tumour reactive T-cells from TIL and PBMC were viably sorted based on the expression of both CD107a and TNF- α (after gating on live CD3+ cells). T-cells were stimulated with autologous tumour for 5 hours in the presence of TAPI-0 (30 μ M), anti-CD107a and anti-TNF- α mAb. Control cells were incubated with tumour. (B) Comparison of TCRBV gene usage between tumour reactive T-cells in TILs and PBMC. (C) Each pie chart represents the distribution of unique CDR3 sequences detected in the TCR β repertoire of TIL infusion product and PBMC from patient MM909.24. Each pie segment represents the share of a distinct CDR3 β clonal sequence, thus reflects the respective frequency of each clonotype. Several grey scales are used repeatedly for different sequences because of the high level of diversity. Shared CDR3 amino acid sequences between matched TIL and PBMC samples are indicated by coloured pie segments.

Further experiments are ongoing aimed at cloning the dominant T-cell from the infusion product and/or the patient's blood. If we can isolate these clones, we intend to dissect their antigen specificity and HLA-restriction. Preliminary studies were performed on the TRBV12-4+ T-cell population that is one of the dominant V β families in MM909.24 TILs. I aimed at cloning tumour-reactive T-cells from live-sorted TRBV12-4+ TILs and map their antigen recognition. Tumour reactive TRBV12-4+ CD8+ T-cells were sorted in bulk from TILs MM909.24 based on TNF- α and CD107a expression and cloned by limiting dilution in 96 multi-well plates. Individual clones were re-tested for CD8+ and TRBV12-4+ expression (**Figure 4.13A**). The tumour-reactive T-cell clone VB8#8 was selected based on *in vitro* expansion and used for further experiments. **Figure 4.13B** shows that the clone recognizes many HLA-A2+ melanomas. Unsurprisingly, VB8#8 was found to be an HLA-A2-restricted Melan-A-specific clone, as confirmed by ICS (**Figure 4.13C**) and tetramer staining (**Figure 4.13D**).

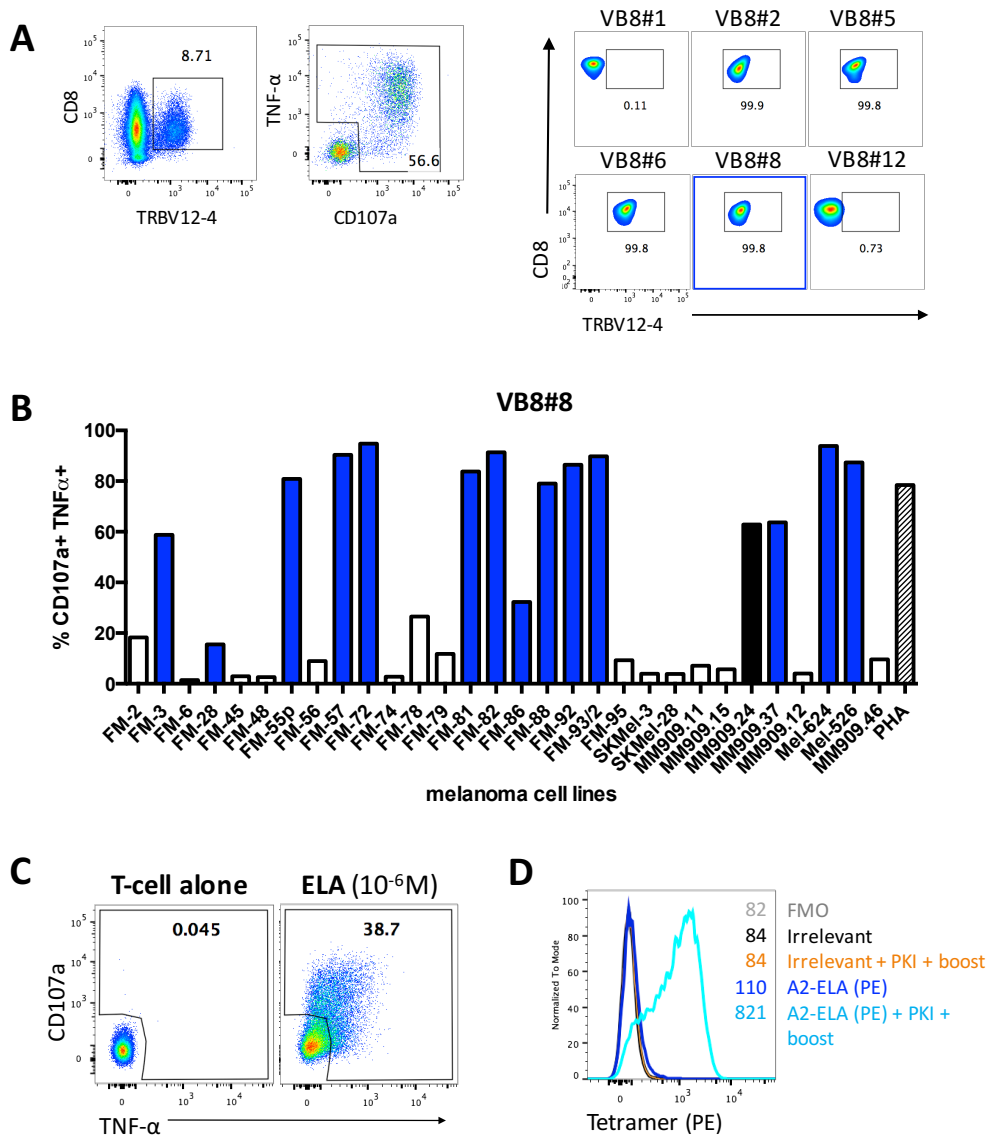


Figure 4.13 T-cell clone VB8#8 from TILs MM909.24 is ELA-specific

(A) Tumour reactive and TRBV12-4+ CD8+ T-cells were sorted in bulk from TILs MM909.24 (left panel) and cloned by limiting dilution in 96 multi-well plates. Individual clones were then re-tested for CD8+ and TRBV12-4+ expression (right panel). The VB8.8 clone is boxed in blue. **(B)** Partially matched HLA-A2+ melanoma cell lines are indicated by blue bars. Cells were gated on live CD3+ CD8+ T-cells. Co-culture conditions with autologous tumour (black bar) and PHA (3 µg/mL) (grey bar) were used as positive controls. **(C)** Reactivity of the VB8#8 T-cell clone towards the Melan-A analogue peptide ELA was assessed by flow cytometry by measuring the production of TNF-α and CD107a. T-cell alone were used as negative control. Cells were gated on viable CD3+ CD8+ T-cells. **(D)** T-cells were stained with PE-conjugated A2-ELA tetramer ± 50 nM Dasatinib (PKI) treatment. Unstained cells and irrelevant tetramer staining (HLA-A2 ILAKFLHWL: residues 540-548 from hTERT) were used as negative controls. 'Boost' stands for tetramer staining followed by the addition of a primary anti-fluorochrome antibody. Mean fluorescence intensity (MFI) of PE is shown.

4.3 Discussion

TIL-ACT for stage IV melanoma is based on the re-infusion of *ex vivo* expanded autologous tumour reactive T-cells. This relatively new form of immunotherapy provides onco-immunology the proof of principle that natural tumour specific CD8+ T-cells present within the tumour can mediate long-lasting cancer regression. TIL samples associated with *in vivo* tumour regression provide a good experimental system to explore T-cell reactivity and antigen specificity of successful T-cell responses in melanoma. In this chapter, I analysed naturally occurring T-cell responses to melanoma-associated peptide antigens in TILs from an HLA-A2+ CR melanoma patient. I showed that TILs expanded from patient MM909.24 were mainly CD8+ T-cells. These results are in accordance with most of the existing literature, which suggests that the clinical efficacy of TIL therapy is mainly associated with the CD8+ T-cell subset of melanoma infiltrates (Dudley et al., 2011; Besser et al., 2012; Radvanyi et al., 2012).

4.3.1 Antigen specificity of tumour reactive TILs

The individual antigen specificity of T-cell clones present in infused TIL populations is likely to vary and could be another factor that influences clinical outcome. Melanoma TIL antigens that have been identified to this date include both widely expressed non-mutated antigens as well as neo-antigens derived from point mutations, which are generally expressed only by the autologous tumour. In this chapter, I began to dissect the antigen reactivity of the TILs administered to an HLA-A2+ patient, who subsequently achieved a long-lasting complete remission. My results show that CD8 T-cells specific for the Melan-A epitope (EAAGIGILTV, residues 26-35) dominate the anti-melanoma response in this patient. Melan-A is a melanocyte-expressed melanoma differentiation antigen that is also over-expressed in more than 90% of melanomas (Kawakami et al., 1994c). Among the relatively large number of known melanoma-associated antigens recognised by human CD8 T cells, Melan-A is one of the most immunodominant in HLA-A2 melanoma patients (Boon et al., 2006). The Melan-A nonamer (AAGIGILTV, residues 27-35) was originally described as the antigenic peptide (Kawakami et al., 1994); however, it was subsequently shown that the ELA 'heteroclitic' decamer bound more efficiently to HLA-A2 and was substantially more immunogenic (Romero et al., 1997; Valmori et al., 1998).

Overall, my results show that multiple clonotypes mediate the anti-Melan-A response in TILs from patient MM909.24. I also showed that individual ELA-specific CTL clones had different sensitivities. Previous papers in the literature have shown that CD8+ T-cells specific for the A2-EAA Melan-A epitope are characterised by a common TCR gene usage pattern (Miles et al., 2011a; Turner et al., 2006). In particular, there is a remarkable bias in the TRAV segment usage, whereby more than 80% of CD8+ EAA-specific T-cell isolated from multiple HLA-A2+ donors expressed a TRAV12-2+ TCR (Dietrich et al., 2003). Interestingly, only one out of five of the unique Melan-A clonotypes described in this chapter used the TRAV12-2 gene segment.

I also examined the Melan A-specific T-cell response in patient MM909.24 using standard pHLA staining to detect antigen-specific T-cells. These experiments indicated that relevant clones could be missed using standard staining protocols. Our group has recently shown that new improvements in multimer staining protocols, including staining in the presence of PKI and boosting the staining with anti-tetramer antibodies (Tungatt et al., 2015), can increase staining intensity and the likelihood of detecting relevant T-cell clones. For instance, the VB6G4.24 clone presented here, was cloned from MM909.24 TILs and is effective at killing the patient's autologous tumour. However, VB6G4.24 did not stain with standard A2-ELA tetramer staining alone; staining could be recovered when T-cells were pre-treated with PKI. Tetramer staining intensity could be further enhanced with a boosted protocol (Tungatt et al., 2015). In addition, in a recent review we have also shown the staining of the ELA-specific clone ST8.24 presented here, using a different range of multimer conditions (Dolton et al., 2015). Overall, staining with pHLA dextramers and PKI detected 3-fold more ELA-specific T-cells than standard tetramer staining. In future, the ability to dissect additional T-cell specificities in TIL infiltrates will potentially help identifying the most relevant induced T-cell responses and their correlation with clinical outcome.

During this work I also identified a number of other tumour-specific CD8 T-cell clones that were not Melan A-specific. These clones did not respond to any of the known HLA-A2-restricted peptides listed in Appendix (**Table 7.2**). It's possible that these clones responded to novel HLA A2-restricted epitopes including patient-specific neo-antigens, or that they are restricted by other HLA-I molecules. Unfortunately, I did not have the time to follow up with these clones. If I have had more time, I would have liked to attempt to delineate the HLA-restriction and peptide specificity of these tumour-specific 'orphan' clonotypes. Recently, my laboratory has devised a new way of determining HLA-restriction in such circumstances. This technique involves a complete knockout of HLA-I genes expressed by the autologous melanoma using CRISPR/Cas9 gene editing technology (Sánchez-Rivera and Jacks, 2015). Following HLA-I knockout, individual patient-autologous HLA-I genes can be added back by lentiviral transduction to test whether tumour recognition is restored. I would have also liked to explore recognition of patient-specific neo-antigens. The MM909.24 tumour is currently undergoing whole-genome exome sequencing for this purpose.

4.3.2 Cross-reactive potential of T-cell responses in melanoma TILs

The notion of T-cell cross reactivity is becoming increasingly clear from experimental evidence which shows that a high-degree of degeneracy is a normal feature of T-cell recognition, in that a single TCR may recognise more than one different peptide in the context of a single HLA-I molecule (Wooldridge et al. 2012, Sewell, 2012). Against this background, it is reasonable to hypothesise that T-cell cross-reactivity may have a role in anti-tumour immunity. Such cross-reactivity might include recognition of a tumour-associated peptide by a pathogen-specific T-cell or recognition of multiple tumour-associated peptides by a single tumour-specific T-cell. I demonstrated that MM909.24 TIL-derived T-cell clone ST8.24 might represent an example of this latter category by showing it could recognise the BST2 protein-derived peptide LLLGIGILV with a similar sensitivity to the cognate Melan-A-derived EAAGIGILTV peptide. I determined this cross-reactivity via CPL scan and a computer algorithm approach. A subsequent literature search showed that a previous study uncovered this same cross-reactivity in a different sample (Christensen et al., 2009). The finding of the same cross-reactivity by two different groups, using different samples, suggests that it might be a common occurrence. Further validation work will be required to prove that ST8.24 recognised tumour cells via both LLLGIGILV and EAAGIGILTV peptides. The possibility of single anti-tumour clones, recognising tumour via multiple peptides, opens up some interesting possibilities that may explain some previous anomalies including those within my own studies. Of particular relevance, dual recognition of LLLGIGILV and EAAGIGILTV peptides by the ST8.24 T-cell clone (and perhaps other T-cells clones) might offer an explanation for how this T-cell can simultaneously exhibit robust tumour lysis but poor staining with EAAGIGILTV pHLA tetramer. Further work will be required to test this interesting possibility.

Finally, it would be also worth exploring whether other CTLs isolated from TILs of complete regression patients exhibit tumour-reactive TCR degeneracy, and if this is correlated with *in vivo* tumour regression. Interestingly, the recognition of multiple tumour antigens by individual T-cells is likely to make it much more difficult for the tumour to escape. It remains possible that those patients that exhibit tumour regression after TIL therapy might have more cross-reactive T-cells than those where the disease continues to progress. Unfortunately, testing of such a possibility was well beyond the scope of what I could achieve during my PhD studies. Nevertheless, future studies on the potential cross-reactivity of anti-cancer T-cells are likely to be rewarding.

4.3.3 Tracking the fate of tumour-reactive TIL clones

The success of adoptive cell therapy for metastatic melanoma is likely to require long-term persistence of the adoptively transferred cells. Indeed, several studies have reported a correlation between the persistence of TILs after adoptive transfer and the successful clinical response in patients (Robbins et al., 2004; Zhou et al., 2005). However, existing TIL-based studies have not generally examined the ability of individual tumour-specific clonotypes to persist. Against this background, I dissected the TCR diversity in tumour-reactive TILs associated with *in vivo* tumour clearance, and tracked the persistence of dominant clonotypes in the patient's blood after treatment. As part of this thinking, I reasoned that the clonotypes that persist and dominate in the blood in a CR patient were most likely to be those responsible for the advantageous clinical outcome.

TCR β clonotyping was the chosen method to assess TCR diversity within the two T-cell populations (infiltrating and circulating lymphocytes). Sequencing of hundreds of clones obtained by the PCR amplification of individual cDNA sequences that include the CDR3 β region, can provide a quantitative survey of the frequency of individual T-cell clonotypes. In this chapter, I analysed the composition and persistence of tumour-reactive T-cell clones in TIL infusion products and peripheral blood of a CR melanoma patient. In summary, two T-cell clonotypes with tumour-specific activities persisted in this patient after treatment. The antigen specificity of the dominant clonotype detected in tumour-reactive TILs is yet to be identified. I have shown that a CD8 $^+$ T-cell clone isolated from the dominant population in the TILs is specific for the ELA Melan-A peptide analogue. At the time of writing, experiments are ongoing in order to clone other dominant clonotypes from the TIL infusion product and dissect their antigen specificity by the use of known melanoma-associated antigens and CPL scans. I hope to be able to update my examiners on these interesting studies during my oral examination.

Interestingly, the most dominant clonotypes in the blood after TIL therapy were not detected in the original TIL infusion product. This finding will be further discussed in Chapter 5. Surprisingly, the Melan-A specific T-cell clonotypes described at the beginning of this chapter were not detected in the TILs by TCR β sequencing. With the advent of next generation sequencing (NGS), further studies in our group are ongoing in order to repeat these experiments with increased sensitivity. By deep sequencing TCRV β loci, sequences are decoded on arrays and many millions of sequences can be read simultaneously (Metzker, 2010). Deep sequencing the TCR clonotypes of TILs and PBMCs from patient MM909.24 will allow us to detect rare CDR3 β sequences that have potentially been missed during the standard TCR β clonotyping shown above. Preliminary data suggest that there may be as many as 300 different tumour-specific clonotypes within the MM909.24 TILs. I also hope to be able to update my examiners on these studies during my viva.

In addition, my group aims to extend my studies by dissecting TCR diversity in the patient's blood at a later time points (> 12 months after TIL therapy). There are also some PBMC stored from this patient *before* therapy. A full understanding of the dynamics of T-cell responses throughout TIL therapy, will require a comparative analysis of tumour-specific clonotypes before, during (TIL infusion product) and multiple time points after treatment. These studies have now been initiated. The absence of tumour-reactive clonotypes in PBMC before treatment, would indicate that the T-cells detected in the circulation after cure are likely derived from *ex vivo* cultured and infused TILs. Theoretically, the TCR repertoire in the patient's original tumour sample (i.e. before infiltrating T-cells are isolated and expanded *ex vivo*) would also be informative, to test whether *in vitro* culture influences T-cell clone dominance. A published study has shown that *in vitro* culture can result in the preferential expansion of certain clones from a relatively small number of T-cells in the original tumour sample (Zhou et al., 2004). A comprehensive understanding of how TIL therapy works will require study of multiple patients.

I next undertook to study the response in CR patient MM909.15. Unlike MM909.24, MM909.15 is not HLA-A2+. The study of this patient allowed an examination of therapy in the absence of the known numerical dominance of HLA-A2 Melan-A-specific T-cells, and was reasoned to be more likely of uncovering new epitopes and antigens.

5 Dissection of T-cell responses in a non-HLA-A2+ melanoma patient with complete remission after TIL-therapy

5.1 Aims

Current knowledge regarding melanoma tumour antigens is still largely limited to T-cell recognition in the context of HLA-A2. This skewing is apparent in the antigen list published by Andersen and colleagues, where 45% of the epitopes are restricted by HLA-A2 with the remaining spanning over 36 different HLA-I molecules (Andersen et al., 2012). The bias in HLA-A2+ patients is further distorted by the known strong dominance of T-cell responses specific for the HLA-A2 epitope EAAGIGILTV, as described in the previous chapter. I thus thought it would be interesting to compare my studies in HLA-A2+ patient MM909.24 with those of a non-HLA-A2 patient that underwent complete lasting remission following TIL therapy.

In this chapter, the overall aim was to dissect the successful anti-melanoma T-cell response in patient MM909.15 (HLA-A3+, A31+; HLA-B8+, -B44+; HLA-C7+). In particular, melanoma T-cell responses were studied in terms of the phenotype and antigen specificity of the tumour-reactive populations. I also hypothesised that the dominant anti-melanoma responses in the patient's circulation following successful TIL therapy could be those responsible for *in vivo* tumour regression. Therefore, I also aimed to examine the antigen specificity of the dominant clones in the patient's blood after cure. Experiments for this patient were performed in parallel with those for patient MM909.24, therefore the experimental approach described at the beginning of Chapter 4 also applies here.

5.2 Results

5.2.1 Anti-tumour responses of MM909.15 TILs

Figure 5.1A provides information regarding the clinical outcome of patient MM909.15 and TIL therapy details. Data from our clinical collaborators showed the TIL infusion product received by this patient was 31.3% CD8+, 54.9% CD4+ and 10% $\gamma\delta$ TCR+. In contrast to patient MM909.24, the majority of the TIL-derived T-cells infused into this CR patient were not CD8+ T-cells. The occurrence of a significant proportion of $\gamma\delta$ T-cells was also interesting. A previous study by Donia and colleagues showed that low levels of $\gamma\delta$ T-cells can be found in melanoma infiltrates, and that higher frequencies are detected in Stage IV patients compared to Stage III melanoma (Donia et al., 2014a).

While these unconventional T-cells are very interesting, the study of this T-cell subset in melanoma infiltrates fell beyond the scope of my thesis. The role of TIL-derived $\gamma\delta$ T-cells in ACT is the subject of another PhD project in our research team being undertaken by my colleague, Mateusz Legut.

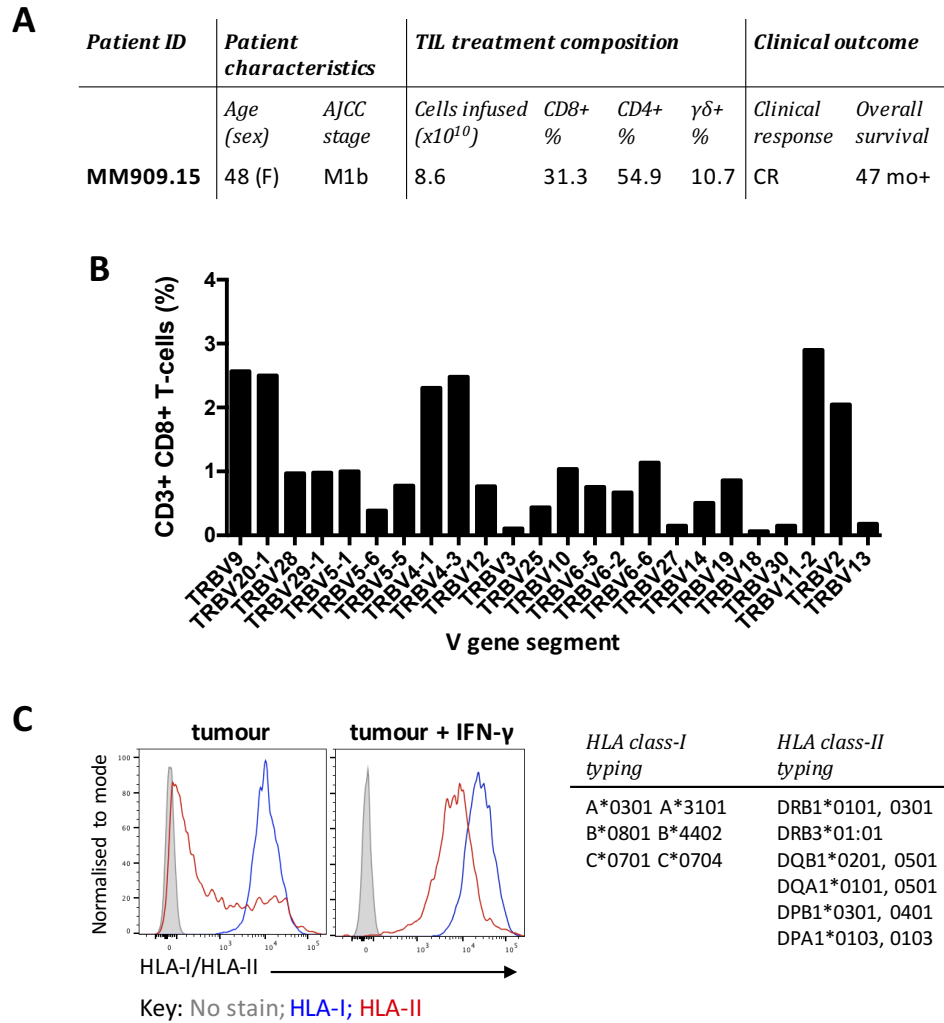


Figure 5.1. Patient MM909.15 characteristics, TIL composition and autologous tumour HLA expression.

(A) Patient characteristics, treatment details and clinical outcome. M1b stage, according to the AJCC classification, involves metastasis to the lung (or with a combination of lung and skin or subcutaneous metastases) (Balch et al., 2009). Complete response (CR) defined by RECIST guidelines as the “disappearance of all target lesions and any pathological lymph nodes must have reduction to <10 mm” (Eisenhauer et al., 2009). **(B)** TRBV antibody surface staining of MM909.15, gated on total CD3+ CD8+ viable T-cells. **(C)** Left panel shows the flow cytometric analysis of HLA-I and HLA-II expression of autologous melanoma cells. Cells were untreated or treated with low dose IFN- γ (100 IU/mL) for 72 hours. Right panel shows full HLA-I and HLA-II typing performed to the 4-digit level.

The dominant TCR V β families in MM909.15 TILs were initially analysed by flow cytometry using labelled anti-TRBV antibodies, as described in the previous chapter. Polyclonal TRBV usage was observed in MM909.15 TILs and TRBV9, TRBV20-1, TRBV4-1, TRBV4-3, TRBV11-2 and TRBV2 were the most frequent TRBV gene segments (**Figure 5.1B**). Unlike melanoma MM909.24, the MM909.15 tumour cell line constitutively express HLA-II, and over-expression is achieved by low dose IFN- γ treatment (**Figure 5.1C**). Constitutive expression of HLA-II by the MM909.15 tumour may have been responsible for the high CD4/CD8 ratio of T-cells observed within the TILs in this patient.

The reactivity of MM909.15 TILs to autologous tumour cells was initially assessed by flow cytometry using intracellular TNF- α , IFN- γ and CD107a staining and CD3, CD4 and CD8 co-labelling (**Figure 5.2B**). The CD8+ subset within MM909.15 TILs (38.1% of total CD3+ TILs) expressed both IFN- γ , TNF- α and CD107a upon stimulation with autologous tumour cells (1.97%, 2.23% and 3.7%, respectively). When gated on total CD4+ TILs (which represent 59.6% of CD3+ cells), only TNF- α tumour reactivity was detected (3.51% TNF- α + CD4+) of the three markers analysed (**Figure 5.2C**). The number of CD4+ cells that responded to tumour might have been higher for other effector readouts, but this possibility was not tested.

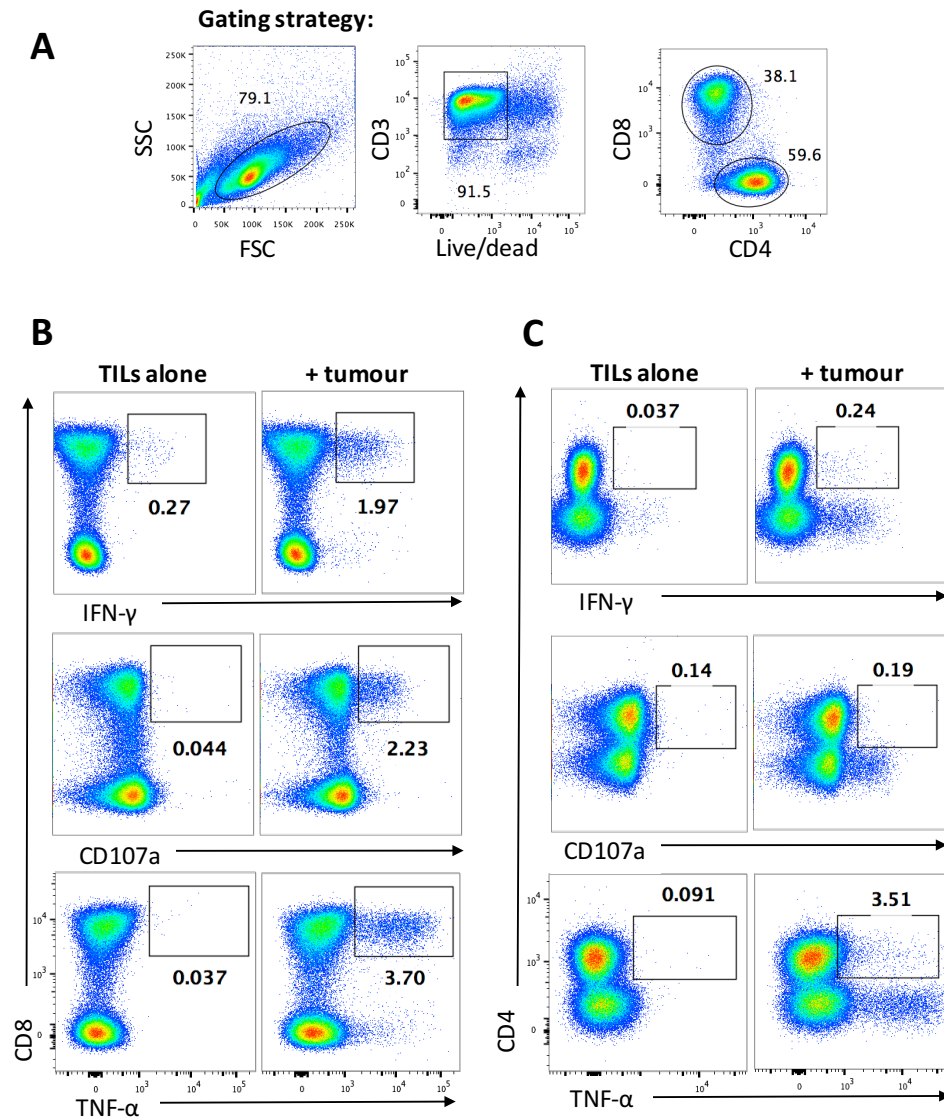


Figure 5.2. MM909.15 TILs reactivity against autologous tumour (gated on CD8 and CD4)

(A) TILs were gated on live CD3+ T-cells and CD8+ and CD4+ subsets were analysed separately. Gates were set on control sample (unstimulated TILs) stained with surface markers only. **(B)** FACS plots of ICS of CD4+ TILs expressing IFN- γ , TNF- α and CD107a after 5 hour stimulation with autologous tumour cells (E:T ratio 2:1). TILs alone were used as control. **(C)** ICS FACS plots of CD4+ TILs expressing IFN- γ , TNF- α and CD107a upon activation with autologous tumour cells. TILs alone were used as control.

To further explore the HLA-restriction of CD8⁺ TILs from patient MM909.15, I used the panel of partially matched melanoma cell lines (**Appendix: Table 7.1B**). Tumour recognition was assessed by measuring the percentage of TNF- α and CD107a positive CD8⁺ T-cells upon stimulation with these target cells. As shown in **Figure 5.3**, MM909.15 TILs recognised many melanoma cell lines in addition to the autologous tumour. Overall, these data suggest that TIL tumour reactivity spans across several different HLA-I alleles, namely HLA-A3, HLA-A31, HLA-B8 and HLA-B44.

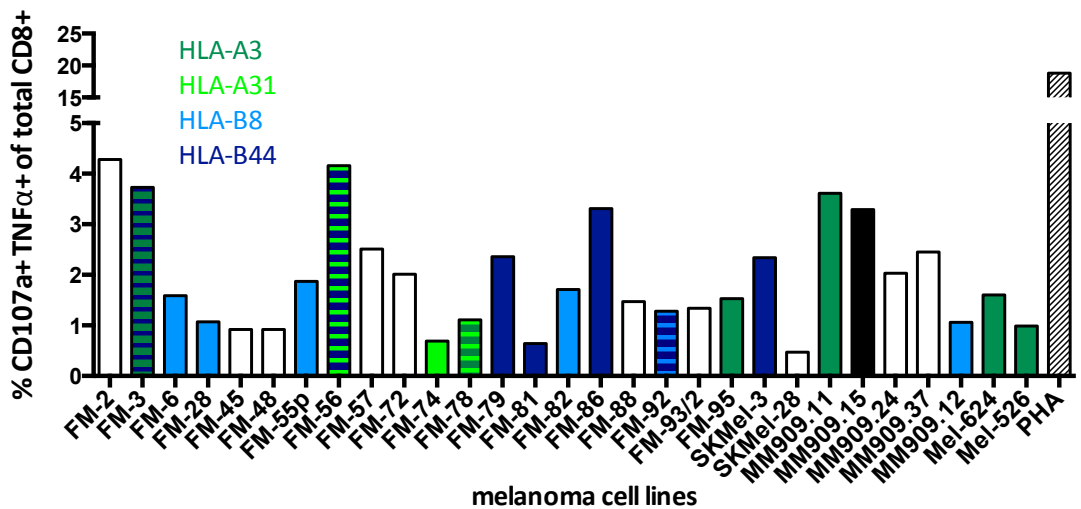


Figure 5.3. MM909.15 TILs reactivity against partially matched panel of melanoma cell lines

Bar chart shows the percentage of CD107a⁺ TNF- α ⁺ TILs upon stimulation with semi-matched melanoma cell lines (colour coded depending on the allele shared with the autologous tumour). Coloured bars show cell lines sharing at least one HLA-I allele with the autologous MM909.15 tumour. The colour-code for HLA-I expression is shown on top of the graph. Stimulation with autologous melanoma MM909.15 (black bar) and PHA (3 μ g/mL) (grey hatched bar) were used as positive controls. Gates were set on unstimulated TILs samples (negative control). Representative FACS plots are shown in Appendix (Figure 7.3). Cells were gated on live CD3⁺ CD8⁺ TILs.

I initiated my studies by looking for responses to known A3-restricted melanoma T-cell epitopes within MM909.15 TILs. A panel of 16 published A3-restricted melanoma-associated peptides were selected from the paper described in Chapter 4 (Andersen et al., 2012). The other HLA alleles expressed by patient MM909.15 were not covered by the list of known melanoma T-cell epitopes, therefore antigen specificity was assessed only in the context of one out six possible HLA alleles. A full list of the 16 A3-restricted peptides used and proteins of origin can be found in the **Appendix (Table 7.3)**. Peptide specific T-cell responses in MM909.15 TILs were quantified by an IFN- γ ELISpot assay. As shown in **Figure 5.4** out of 16 known peptides tested, the TAG –derived peptide RLSNRLLLR (RLS hereafter) elicited the highest TIL response (22 ± 7 IFN- γ SFU / 5×10^5 TILs). TAG protein isoforms are cancer-testis antigens and are widely expressed in human melanomas (Hogan et al., 2004).

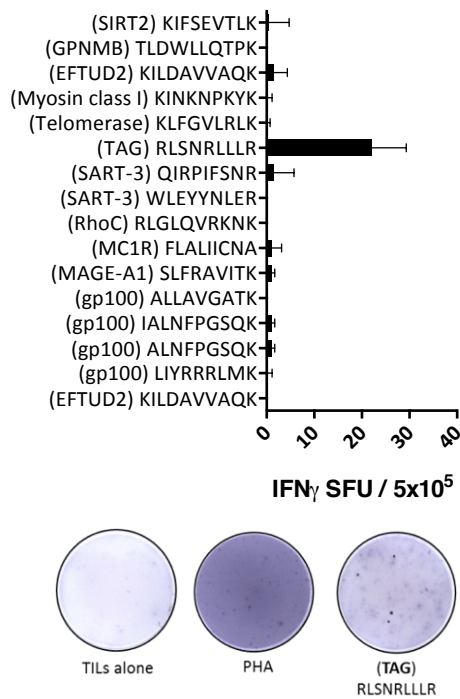


Figure 5.4. ELISpot response to 16 known A3-restricted melanoma antigens

IFN- γ ELISpot performed on 5×10^5 MM909.15 TILs stimulated in duplicate with known HLA-A3 restricted melanoma-associated peptides (10^{-6} M) for 24 hours. The number of IFN- γ secreting cells per 5×10^5 TILs is displayed on the X axis; peptide sequence and protein of origin (in brackets) are displayed on the Y axis. Each bar represents the mean spot count per well (\pm SD). Representative images of ELISpot wells are shown in the bottom panel. PHA ($3 \mu\text{g}/\text{mL}$) was used as a positive control. PHA control wells were fully saturated with spots, therefore not shown in the bar chart.

Taken together, the results shown so far highlight the heterogeneous composition of TIL cultures from the complete remission patient MM909.15. CD8+ TILs recognise several partially matched melanomas, including HLA-A3+ cell lines. In particular, TIL product MM909.15 contained relatively low frequencies of T-cells specific for the shared tumour protein TAG.

5.2.2 CD4+ T-cell response in TILs from patient MM909.15

Previous work by our collaborators and others have shown that some TIL infusion products from melanoma patients achieving tumour regression after TIL therapy, are dominated by CD4+ T-cells (Besser et al., 2009; Ellebæk et al., 2012; Pilon-Thomas et al., 2012). It is known that CD4+ T-cells exert anti-tumour functions by producing type I cytokines or by directly recognising HLA-II restricted epitopes; however rare cytolytic CD4+ T-cells have been described in melanoma (Quezada et al., 2010). Against this background, I decided to further explore the tumour reactivity of the CD4+ TIL population that represents more than 50% of the total infusion product patient MM909.15 was treated with. T-cells were gated on live CD3+ CD4+ T-cells and reactivity against a panel of melanoma cell lines was evaluated by measuring the percentage of TNF- α and CD107a positive T-cells following a 5-hour stimulation (Figure 5.5). Only 3% of MM909.15 CD4+ TILs recognise the autologous tumour cells, and reactivity against several melanoma cell lines tested in this experiment was similar. Melanoma cell line FM-2 elicited the highest T-cell response (6.6% of TNF- α + CD107a+ CD4+ TILs). The full HLA-II type of the recognised melanoma cell lines would be worth exploring in order to further dissect the class-II restriction and antigen specificity of this anti-melanoma CD4+ population.

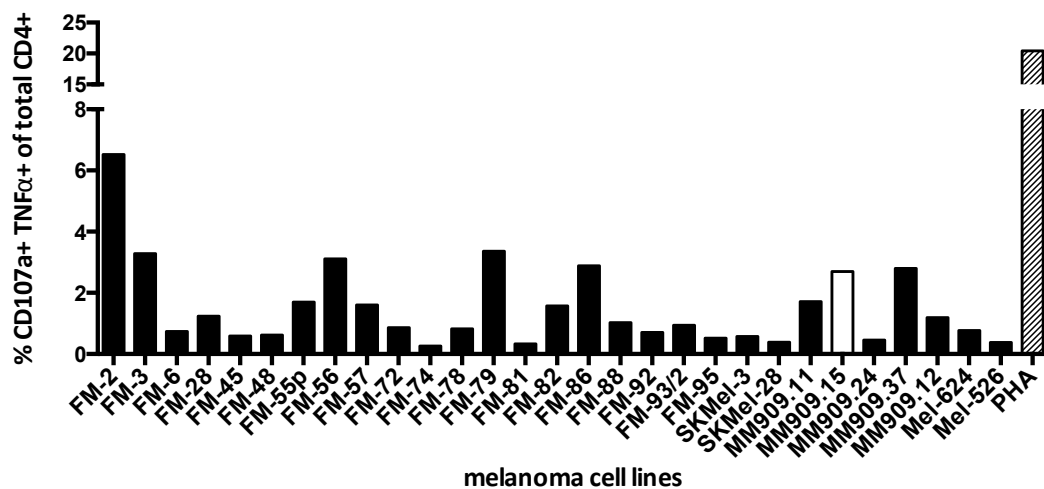


Figure 5.5. CD4+ TILs reactivity against a panel of partially matched melanoma cell lines

Bar chart shows the percentage of CD107a+ TNF- α + TILs upon stimulation with semi-matched melanoma cell lines (colour coded depending on the allele shared with the autologous tumour). Stimulation with autologous melanoma (white bar) and PHA (3 μ g/mL) (grey bar) were used as positive controls. Gates were set on unstimulated TILs samples (negative control). Representative FACS plots are shown in Appendix (Figure 7.4). Cells were gated on live CD3+ CD4+ TILs.

A CD4⁺ T-cell clone (hereafter ML30.15) was isolated from TIL cultures of patient MM909.15. Surprisingly, ML30.15 showed specific cytolytic activity when tested in a ⁵¹Chromium release assay upon 18-hour co-incubation with autologous tumour cells (**Figure 5.6A**). Reactivity against autologous melanoma was also assessed in preliminary experiments by flow cytometry by measuring the intracellular expression of IFN- γ , CD107a and TNF- α upon 5-hour stimulation with target tumour cells (**Figure 5.6B**). Cytokine production was skewed towards TNF- α (5.45%), whereas IFN- γ and the degranulation marker CD107a were detected at lower levels (1.97% and 1.07%, respectively). A further cytolytic CD4⁺ T-cell clone with a similar effector profile was isolated from TIL cultures from patient MM909.24 (data not shown). Characterisation of these rare cytotoxic CD4⁺ cells in melanoma infiltrates is worth exploring in terms of HLA restriction, killing mechanisms and antigen specificity, and is currently the basis of another project.

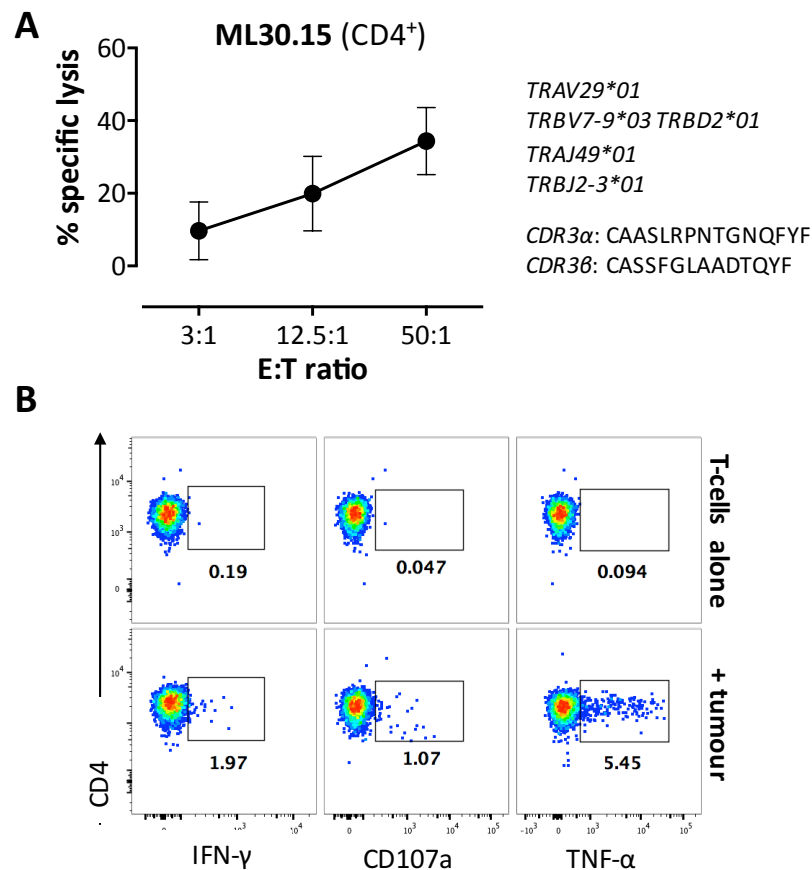


Figure 5.6. ML30.15 CD4⁺ cytotoxic clone

A) Specific lysis of autologous melanoma cells by ML30.15 CD4⁺ clone at different E:T ratios after 18 hour stimulation (left panel). Full clonotyping and CDR3 amino acid sequences are shown (right panel; courtesy of Mateusz Legut). **B)** FACS plots showing intracellular staining of the CD4⁺ clone ML30.15 to measure IFN- γ , TNF- α and CD107a production after 5-hour stimulation with autologous tumour cells (E:T ratio 2:1). Unstimulated T-cells were used as control.

5.2.3 Peptide specificity of the dominant clone in the patient blood after cure

The clonal distribution of the TCR allows detection and tracking of tumour-specific T-cells based upon their unique TCR. In light of the findings regarding T-cell clonotype persistence in the peripheral blood of patient MM909.24 after TIL therapy in Chapter 4, I used the same approach with patient MM909.15 using the TIL infusion product and patient PBMC six months after treatment. The experiment was performed directly on thawed samples which were rested overnight prior incubation with autologous melanoma cells. Tumour reactive T-cells from the TIL infusion product and PBMC were live-sorted on their ability to produce TNF- α and CD107a (5.94% and 0.41% of total CD3+ cells, respectively) upon 5-hour stimulation with autologous melanoma cells (**Figure 5.7A**). Total mRNA from sorted cells was isolated and the TCR β repertoire was amplified using the SMARTer™ RACE approach and clonotyped. TCR β clonotyping results highlight a polyclonal TRBV usage in MM909.15 TILs, where TRBV5-5 is the most frequent among tumour reactive CD3+ TILs (15.2%), followed by TRBV20-1 (10.13%), TRBV5-1 (10.1%) and TRBV7-9 (7.6%) (**Figure 5.7B**). TRBV7-9 is also expressed in the circulation six months post TIL-therapy (9.3%). Strikingly TRBV5-1 accounts for 59.8% of total tumour-reactive CD3+ PBMC.

Figure 5.7C shows the comparison of the relative frequency of TCR β CDR3 sequences among MM909.15 TIL infusion product and the corresponding tumour-reactive circulating T-cell population. Fewer clonotypes were detected in the blood compared to the infusion product (35 and 89 unique CDR3 β sequences, respectively). Overall, five distinct TCR β clonotypes from the original TIL infusion product persisted in the patient's blood six months after therapy. In particular, one of the persisting T-cells clones was found to be the dominant in the PBMC, representing 58.3% of all CDR3 β sequences expressed in the circulating tumour-reactive population.

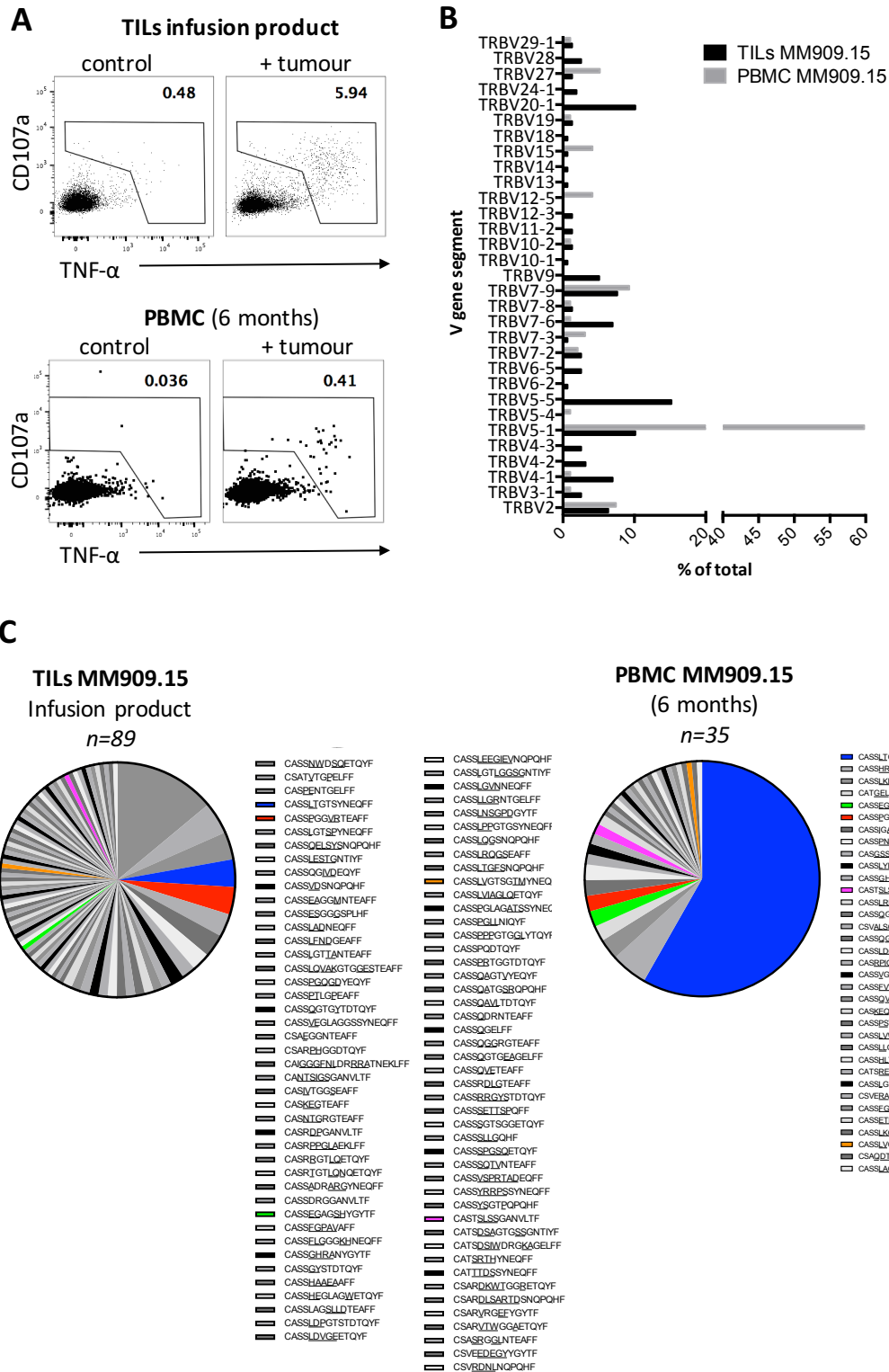


Figure 5.7. TCR β repertoire diversity in tumour-reactive TILs and PBMC from patient MM909.15

(A) Tumour reactive T-cells from TIL and PBMC were viably sorted based on the expression of both CD107a and TNF- α . Cells were gated on live CD3⁺ cells. T-cells were stimulated with autologous tumour for 5 hours in the presence of TAPI-0 (30 μ M), anti-CD107a and anti-TNF- α mAb. Control cells were not stimulated. (B) Comparison of TCRV gene usage between tumour reactive T-cells in TILs and PBMC from patient MM909.15 (C) Each pie chart represents the distribution of unique CDR3 sequences detected in TCR β repertoire from the corresponding infusion product or blood sample from patient MM909.15. Each pie segment represents the share of a distinct CDR3 β clonal sequence, thus reflects the respective frequency of each clonotype. Several grey scales are used repeatedly for different sequences because of the high level of diversity. The corresponding CDR3 amino acid sequences are listed in the order of frequency. Shared CDR3 sequences between matched TIL and PBMC samples are indicated by coloured pie segments.

T-cell cloning generated a clone with the same TCR β chain that dominates the tumour-specific response in patient MM909.15 after treatment (**Figures 5.8**). This clone was named ML33.15. The ML33.15 CD8+ TIL clone was highly cytolytic towards the MM909.15 melanoma line even at low E:T ratio in a 4- and 18-hour ⁵¹Chromium release assay (**Figure 5.8B**). To explore the antigen specificity and HLA-restriction of ML33.15, T-cells were stimulated with the above-mentioned known HLA-A3 restricted melanoma epitopes (**Table 7.3**) and MIP-1 β production was measured by ELISA (**Figure 5.8C**). ML33.15 antigen specificity was mapped to the HLA-A3 restricted RLS peptide from the TAG protein. Clone sensitivity to the TAG T-cell epitope was tested in peptide titration assay by MIP-1 β ELISA (**Figure 5.8D**).

In summary, I have shown that five different melanoma-specific TIL clonotypes persist in the circulation of a complete remission patient after TIL therapy. The dominant CD8+ CTL clone in the patient's blood was clonotyped and its antigens specificity was mapped to an HLA-A3-restricted cancer-testis TAG T-cell epitope (sequence RLSNRLLLR).

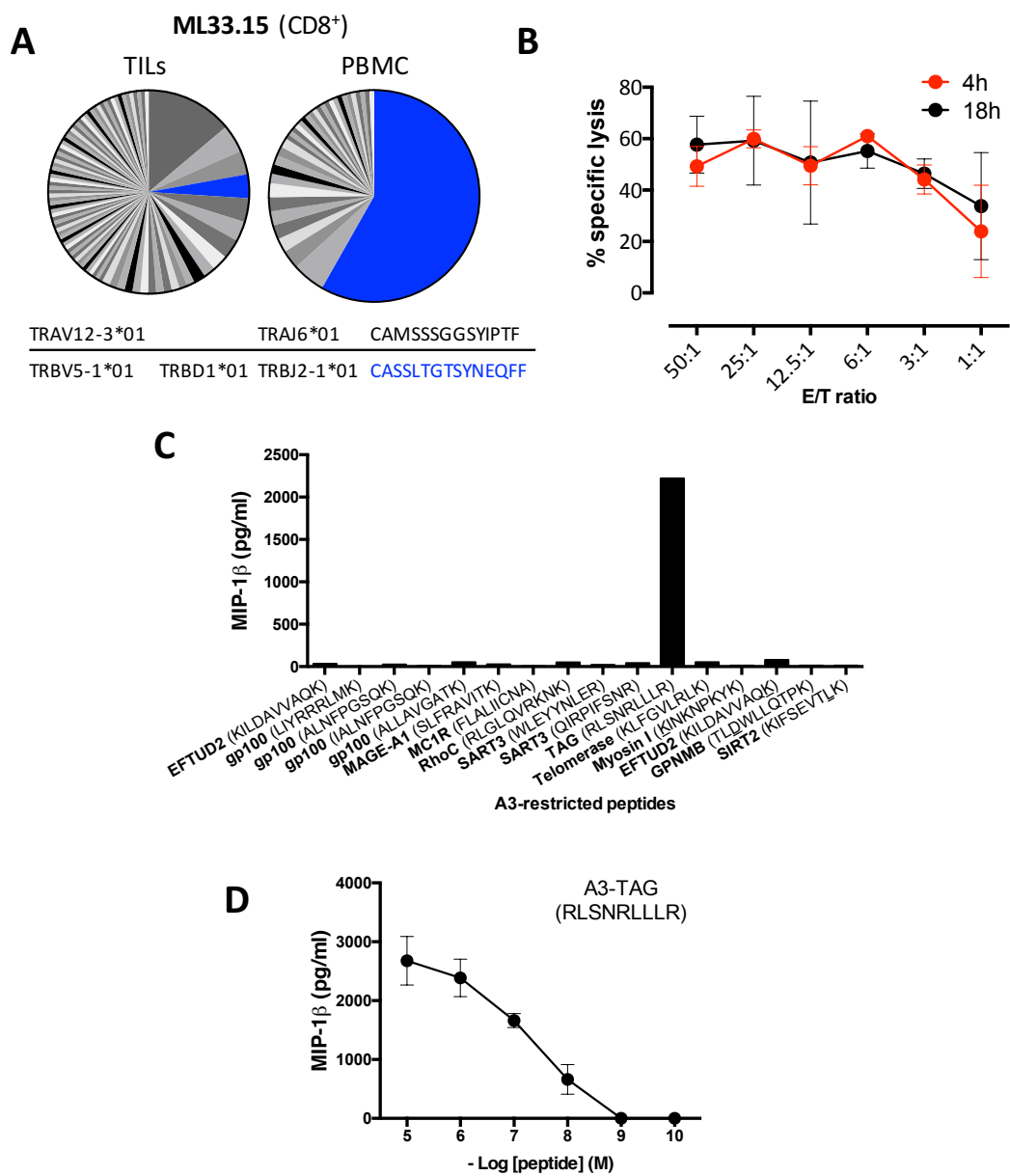


Figure 5.8. Dominant clone ML33.15 (TRBV5-1) is specific for a A3-restricted TAG peptide (RLS)

(A) ML33.15 is the dominant clone in MM909.15 PBMC after therapy and fourth most frequent in the TIL infusion product. The blue segment of each pie chart represents the share of the CDR3β sequence CASSLTGTSYNEQFF. The full clonotyping data for the ML33.15 T-cell clone is shown below (courtesy of Mateusz Legut). **(B)** Specific lysis (%) of autologous tumour cells by the CD8⁺ T-cell clone ML33.15 (E/T ratio = 5:1) after 4h and 18h, respectively. **(C)** MIP-1β ELISA A3-restricted peptides (10^{-6} M). **(D)** Clone sensitivity (dose-response) to A3-TAG peptide RLSNRLLLR.

5.3 Discussion

5.3.1 Heterogeneous cellular composition of TIL infusion products

In this chapter, I have highlighted that more than 50% of $\alpha\beta$ T-cells in the patient MM909.15 TIL infusion product were CD4+ T-cells. Previous studies have shown that at least 20% of Stage IV melanomas contain infiltrating CD4+ T-cells with specific tumour recognition (Donia et al., 2012; Friedman et al., 2012), suggesting a possible role for CD4+ cells in tumour regression after adoptive cell therapy. In addition, unlike most non-haematopoietic tumours, melanomas including the MM909.15 tumour line, can constitutively express HLA-II. Melanocytes are usually HLA-II negative (Fossati et al., 1986), suggesting that expression of HLA-II is associated with the transformation process and tumour progression (van Vreeswijk et al., 1988). Melanoma cells have been shown to process antigen and present peptides efficiently to CD4+ T cells, resulting in T-cell proliferation (Brady et al., 1996; Robila et al., 2008). However, the clinical significance of constitutive HLA-II expression in melanomas is still under debate, as HLA-II expression has been associated with both longer and shorter survival rates (Anichini et al., 2006; van Duinen et al., 1988; Zaloudik et al., 1988). In the context of TIL therapy, work from Rosenberg and colleagues has shown that co-infusion of CD8+ and CD4+ TILs is more effective than the infusion of CD8+ TILs alone (Dudley, 2002). Furthermore, it has been reported that the infusion of *in vitro* expanded autologous CD4+ T-cell clones specific for NY-ESO-1 results in long-term tumour regression in advanced melanoma patients (Hunder et al., 2008).

I also showed that CD4+ TILs from patient MM909.15 produce TNF- α upon stimulation with autologous tumour and several other other melanoma cell lines, suggesting the recognition of shared T-cell epitopes. Experiments using HLA-II blocking antibodies were not conclusive (data not shown), therefore further experiments are necessary to confirm the HLA-II restriction of this anti-melanoma CD4+ infiltrating population. In addition, a tumour-reactive CD4+ T-cell clone was isolated from TIL cultures of patient MM909.15 was shown to be cytotoxic towards the autologous tumour line. Cytotoxic CD4+ T-cell clones have been previously described in the context of anti-viral immunity (Hildemann et al., 2013; Marshall and Swain, 2011), but their role in tumour immunosurveillance is poorly understood and has only emerged in isolated papers (Perez-Diez et al., 2007; Quezada et al., 2010). It would have been interesting to study the mechanism by which cytolytic CD4 T-cells kill tumour cells by determining whether cell lysis is dominated by perforin-dependent, Fas-dependent or other mechanisms (Williams and Engelhard, 1996; Yasukawa et al., 2000). In addition, TCR gene transfer could be a strategy to address whether the anti-melanoma cytotoxicity of the ML30.15 clone is mediated by the tumour-reactive TCR. Cytokine profiling of the ML30.15 clone, was only undertaken for IFN- γ , TNF- α and CD107a upon stimulation with autologous tumour cells. However, other Th1 and Th2 cytokines should be measured to provide a full cytokine profiling of effector tumour-specific CD4+ T-cells in melanoma TILs. Previous work revealed that the proportions of different infiltrating CD4+

subtypes varies depending on the thickness and characteristics of the melanoma lesion (Conrad et al., 1999; Wagner et al., 1998). It is unclear whether this variation is cause or effect. An additional recent paper published by our collaborators analysed the functional patterns of anti-melanoma CD4+ TILs of melanoma patients in comparison to CD8+ TILs (Donia et al., 2015). Results showed that CD4+ tumour-specific T-cells were skewed towards TNF- α production in all the melanoma patients analysed (including patient MM909.15), with comparable IFN- γ and MIP-1 β production. Regulatory T-cells (Treg) are also generally CD4+ (Viguier et al., 2004). A higher percentage of Treg has been shown in TILs from metastatic melanoma lesions and can be associated with a higher risk of recurrence (Mourmouras et al., 2007; Viguier et al., 2004). It would be worth exploring if the CD4+ T-cell population that dominates MM909.15 TILs presented here express markers typically associated with this immune-suppressive Treg subtype, such as FoxP3 (Sakaguchi et al., 2001). In analysing CD4+ T-cells, it is important to remember that these cells can represent a broad population of cells that can have wide ranging immunosuppressive or immunostimulatory functions. It would therefore be worthwhile undertaking a full CD4+ T-cell profiling of the TILs present in the MM909.15 patient samples.

The heterogenic composition of melanoma TIL infusion products is highlighted not only by the different ratios of CD4+ and CD8+ conventional $\alpha\beta$ T-cells subset seen in patients, but also by the presence of a population of $\gamma\delta$ T-cells, with a prevalence of the V δ 1+ subset (Donia et al., 2012). This unconventional T-cell fraction can be significant (more than 1×10^9), as for the patient presented in this chapter (10% of infused TILs). The contribution of $\gamma\delta$ T-cells to anti-melanoma TILs has not been explored until recently. Our collaborators have described V δ 1+ T-cells derived from metastatic melanomas and characterized by an effector tumour-reactive phenotype (Donia et al., 2012). Similar findings from a cultured polyclonal V δ 1+ TIL line with *in vitro* cytotoxic capability were reported by another group (Cordova et al., 2012). Of note, other immune cells infiltrating melanomas, such as natural killer (NK) cells, usually do not expand using REP expansion methods and are therefore not commonly detected among clinical grade infusion products (Donia et al., 2012). Overall, these observations point towards interesting heterogeneity within melanoma infiltrating T-cell subsets. Detailed characterisation of these subsets awaits further experimentation.

5.3.2 T-cell responses to the TAG cancer-testis antigen

The analysis of known HLA-A3-restricted antigen specificities present in TILs from patient MM909.15 revealed T-cell reactivity against the TAG T-cell epitope RLSNRLLLR. TAG protein isoforms encode cancer-testis epitopes known to be overexpressed in melanoma cell lines and other solid tumours, including breast, ovarian and colorectal cancer (Adair et al., 2008). The TAG-derived peptide RLSNRLLLR is encoded by multiple TAG isoforms and is naturally immunogenic. Spontaneous T-cells

responses in melanoma patients against the RLSNRLLLR peptide have been previously described (Hogan et al., 2004; Linnemann et al., 2013; Yamshchikov et al., 2001).

Interestingly, T-cell reactivity against the same TAG peptide was detected in TIL cultures from a third complete remission melanoma patient analysed during my PhD project. Details on TILs from this patient (MM909.11; HLA-A3+, HLA-A1+) and a summary of melanoma reactivity are shown in **Figure 7.5** in the **Appendix**. TILs from patient MM909.11 were tested by IFN- γ ELISpot against known HLA-A1 and HLA-A3-restricted peptides. Only a response to RLS HLA-A3 restricted peptide was detected (**Appendix: Table 7.3**). TAG specific T-cell responses have also been detected in melanoma TILs by other groups (Linnemann et al., 2013; Kvistborg et al., 2012; Donia, personal communication). Strikingly, the dominant tumour-reactive clonotype in the PBMC of patient MM909.15 is specific for the RLSNRLLLR T-cell epitope. An identical RLSNRLLLR-specific clonotype has been found in another melanoma patient (Linnemann et al., 2013), suggesting that this $\alpha\beta$ TCR could be a 'public'. Public TCR CDR3 amino acid sequences have been reported in the literature (Ely et al., 2005; Venturi et al., 2008; 2006) but have not been described in the context of T-cell based adoptive cell therapy.

Overall, the dissection of the antigen specificity of the two melanoma TILs (MM909.15 and MM909.11) as presented here has an obvious limitation. T-cell reactivity against known epitopes was only measured for one out of the six possible HLA alleles. This also relates to the limited published panel of non HLA-A2 restricted T-cell epitopes (Andersen et al., 2012). However, my data suggest that TIL reactivities against known melanoma-associated antigens, such as shared cancer-testis epitopes, only account for a small fraction of the total tumour reactivity. This observation is in accordance with preliminary deep sequencing of tumour-reactive TILs from these patients, that indicates the tumour-specific T-cell population is made up of hundreds of individual clonotypes. Taken together, my results point towards the notion that T-cell responses against TAG cancer-testis melanoma antigens are shared between patients and, given their long-term persistence after therapy they could contribute to explain tumour clearance *in vivo*. Based on my data, I hypothesise that raising of a therapeutic response to HLA-A3-RLSNRLLLR in HLA-A3+ melanoma patients could result in beneficial responses.

5.3.3 Persistence of T-cell clones in the blood after cure

The activation of tumour-specific T-cells leads to clonal expansions and elevated numbers of mRNA encoding a particular TCR α and TCR β chain. Therefore, the detection of dominant clonotypes in a patient's blood after TIL therapy can be a marker of an ongoing HLA-restricted T-cell response and, indirectly, of the anti-tumour effect of adoptive TIL therapy. Against this background, I studied the TCR repertoire of reactive T-cells in both TILs and PBMC of three complete remission patients (**Figures 4.11, 5.7 and 7.6**), and made the following observations: (i) the TCR repertoire of tumour reactive cells in TIL infusion products and PBMC is broad and diverse; ii) in all three patients analysed at least two T-cell clones persisted in the blood after treatment; and iii) tumour reactive T-cells in the blood are

dominated by few clonotypes, possibly following *in situ* expansion after encounter with the tumour-antigen.

Previous studies have begun to explore the expansion and diversity of T-cell clones in melanoma patients and their role in clinical responses to TIL transfer (Berger et al., 2004; Straten et al., 1999; 2004). However, recent technological advances, such as deep next generation sequencing (Clemente et al., 2013; Mamedov et al., 2013) now allow tracking of tumour-specific T-cell clonotypes infiltrating the tumour before and after TIL therapy and monitoring of individual T-cell fate during treatment.

Of note, in the complete remission patients analysed, the TCR repertoire in the blood contained tumour-reactive clonotypes that were not detected in the original TIL infusion product. In particular, the number of CDR3 β sequences in the PBMC of patient MM909.11 was far more after than in TILs (22 and 7 unique CDR3 β sequences, respectively) (**Appendix: Figure 7.6B**). These observations may indirectly point towards epitope spreading, where T-cells with antigen specificity other than the one induced by adoptive therapy appear after tissue damage caused by the initial clone (Ribas et al., 2003). As has been reported in autoimmune diseases, this initial tissue destruction could lead to the expansion of T cells, with specificity for other melanoma antigens (Ma et al., 2013). There is also evidence of epitope spreading in some vaccination studies (Butterfield et al., 2003; Corbière et al., 2011). In order to validate this hypothesis, I would have to map the epitope that clone(s) recognises in the circulation and demonstrate via PCR specific amplification that these T-cell reactivities were not in the original infusion product. Taken together, my data highlights that a deeper knowledge of the key antigen-specificities within TIL TCR repertoires should allow a better understanding the mechanisms and complexities of tumour regression *in vivo* and improve the efficacy of T-cell based therapies for melanoma.

6 General Discussion and Conclusions

6.1 Discussion

The work outlined in my thesis is united by the common theme of immunotherapies for the treatment of advanced melanoma. Indeed, both peptide vaccination and TIL-based therapies have been among the most extensively studied strategies in both preclinical and clinical settings. In Chapter 3, I have explored the X-ray crystal structure of a TCR in complex with HLA-A2 and the gp100₂₈₀₋₂₈₈ epitope, a common target of melanoma vaccination platforms. I also undertook a thorough alanine mutagenesis study of the gp100 epitope, and performed functional analyses to assess if peptide analogues induce a specific T-cell response. From structural and functional analyses, I found that mutation of residue Glu3 into an alanine generated a molecular switch that was transmitted to neighbour residues, completely abolishing TCR binding and antigenic responses. The findings of this project have convinced me about the importance of taking into account the detailed structural information available from crystallography, combined with biophysical and binding data, when studying TCR-pHLA interactions. While sensitivity of certain TCRs to HLA and/or peptide changes in buried sites has been long appreciated, this study provides a comprehensive analysis of this phenomenon extending over a relatively long molecular distance in a cancer system of considerable current interest.

In Chapters 4 and 5, I dissected the anti-melanoma T-cell responses in long-term melanoma-free patients after adoptive TIL transfer. In the two CR patients studied in this thesis, I began by analysing the overall tumour-reactivity of TIL cultures against autologous melanoma by flow cytometry. I then proceeded to dissect a panel of TIL clones and investigate the persistence of tumour-reactive clonotypes in the patient's blood after cure and was able to map cognate T-cell specificities. I believe that the composition of T-cell clones over time, based on the detection of unique CDR sequences, offers a means to track specific T-cell reactivities that persist after TIL therapy. We are now in a prime position to understand the key antigen-specificities associated with cancer regression following TIL therapy. Gaining an understanding of the patient-specific and/or shared T-cell epitopes that mediate *in vivo* tumour clearance will allow important further investigation that may pave the way to replication of these successes in other patients and other tumour types.

My research group are exploring whether CPL scans combined with computational analysis can be integrated in an overall strategy to track T-cell clonotypes in TILs and PBMC, and map the specificities of ‘orphan’ cancer-specific T-cells (**Figure 6.1**). Regardless of their HLA-restriction, T-cell clones can be screened using autologous LCL lines and CPL scans to study the peptide landscape recognised by the cognate TCR. Cross-reactive, public or novel anti-melanoma TCRs can be then examined from a structural and biophysical point of view in order to study the TCR-pHLA molecular interaction (as shown in Chapter 3, for a gp100-specific TCR). Knowledge of the T-cell responses that persist in patients that clear their cancer will be highly informative for designing future therapeutic strategies and may allow these successes to be replicated in other patients.

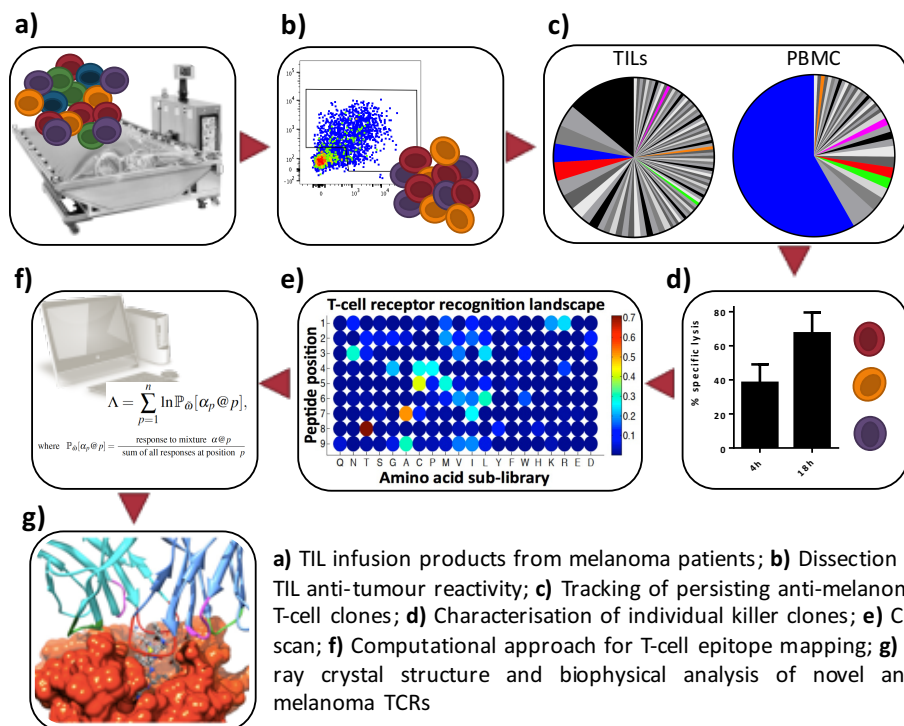


Figure 6.1. A strategy for dissecting unknown T-cell clones from anti-melanoma TIL and PBMC samples

In addition, we are exploring a new application of the cutting-edge CRISPR gene editing technology, which allows generation of tailored RNA-guided nucleases (such as Cas9) that induce DNA double-breaks at specific genomic sites (Cong et al., 2013; Mali et al., 2013; Sander and Joung, 2014). Whole-genome CRISPR libraries have been published and consist of a mixed population of lentiviral vectors containing guide-RNAs, each targeting a specific gene of the genome (Parnas et al., 2015; Wang et al., 2014). Whole-genome CRISPR libraries could be used to screen anti-melanoma TIL clones with unknown specificity to identify cognate T-cell epitope candidates. The screening process relies on the ability of cytotoxic T-cell clones to specifically lyse their target.

Briefly, the whole-genome CRISPR library is used to deliver a pool of lentiviral guide-RNAs to target melanoma cells, prior to incubation with the autologous TIL clone. Melanoma cells in which an essential gene for cognate peptide expression, processing or presentation has been knocked out, will fail to activate the specific T-cells and therefore will not be lysed. The CRISPR guide-RNAs in surviving cells can be simply amplified and sequenced to identify the genes that have been targeted, and ultimately the T-cell epitope candidate.

6.2 Future perspectives in melanoma immunotherapy

6.2.1 The role of the tumour microenvironment

Tumours have been traditionally studied as isolated entities of transformed cells, but increasing evidence supports the idea that cancer cells rather interact with the surrounding microenvironment (Steeg, 2016; Turley et al., 2015). Indeed, melanomas are composed not only of transformed melanocytes but also of the supporting stroma, which includes fibroblasts, endothelial cells, immune cells, soluble molecules, and the extracellular matrix. Extensive research in this field reveals a bidirectional and dynamic interaction between tumour cells and the microenvironment that can influence the malignant phenotype, and ultimately modulate the success of immunotherapy. Multiple immunosuppressive mechanisms can coexist in melanoma to reduce the effectiveness of T-cell immunity. These mechanisms include: expression of co-inhibitory molecules, down-regulation of co-stimulatory or HLA molecules, and increased regulatory T-cell activity (Ferrone and Marincola, 1995; Ostrand-Rosenberg, 2008; Polak et al., 2007; Real et al., 2001). Against this background, current clinical trial protocols are now trying to tip the balance towards a lower immunosuppressive microenvironment, by including antibody blockade of co-inhibitory molecules or targeting immune suppressive cells.

6.2.2 The future of peptide cancer vaccines

Therapeutic peptide cancer vaccines have generally been disappointing. Over the years several anti-melanoma vaccination platforms have been tested through clinical trials, showing a variety of success rates and highlighting issues to be addressed (Berzofsky et al., 2015; Slingluff, 2011; Tsang et al., 2015). One of the main concerns is the choice of appropriate T-cell antigens to be incorporated in the vaccine. The lack of selectivity of tumour-associated antigens can lead to autoimmunity, such as severe vitiligo, in immunised patients (Amos et al., 2011). Another major issue is the choice of the adjuvant used to boost the immunogenicity of the tumour-associated antigen.

Adjuvants are key for vaccine efficacy, but a fine balance must be found between eliciting the desired T-cell response and adverse reactions (Reed et al., 2013). Finally, data from other tumour models suggests that the use long peptides (30-mer), which include short minimal epitopes, may overcome some of the limitations of short peptide vaccines, in that they induce both CD4+ and CD8+ anti-tumour T-cell responses and better antigen presentation (Bijker et al., 2008; Sercarz and Maverakis, 2003).

Even if the selected antigen and the delivery platform have been optimised, therapeutic vaccination protocols may fail because of tumour-associated immune evasion mechanisms mentioned above. Therefore, the future of therapeutic peptide vaccines could lie in their combination with other reagents, such as immunomodulators. A promising combination is the use of a peptide vaccine administered with an anti-CTLA4 antibody. In a clinical trial in metastatic melanoma patients, a peptide vaccine in combination with IFN- α and anti-CTLA4 significantly down-regulated immunosuppression and achieved significant clinical activity (Tarhini et al., 2012). A phase III trial in advanced melanoma patients used a combination of ipilimumab and gp100 peptide vaccine; results showed that ipilimumab with or without the peptide vaccine improved the overall survival when compared to the peptide alone (Hodi et al., 2010). Dissection of successful TIL therapy, as I have done in my studies, will provide signposts to tumour antigens and peptide-HLA associated with success. These antigens will then make promising candidates for future vaccine trials.

6.2.3 Improvement of TIL therapy and future questions

Despite the overall clinical efficacy achieved with TIL-based immunotherapy, several questions remain to be addressed before this technology is routinely implemented into clinical practice. Firstly, the technical aspects of TIL therapy have room for improvement. TIL production is still a complex, laborious procedure that requires highly specialised cancer centres and a minimum of 3-4 weeks in order to expand T-cells to sufficient numbers for infusion. This time frame often results in significant patient dropout because of rapid disease progression or failure to culture and expand autologous T-cells to the numbers required for treatment (Svane and Verdegaal, 2014).

Secondly, a deeper understanding of the factors influencing clinical outcome is critical. As pointed out in Chapters 4 and 5, an important goal of current TIL investigation is to identify the subsets and phenotypes within the initial mixed TIL infiltrate that are associated with *in vivo* tumour regression. For example, a matter of controversy has been which CD8+ T-cell differentiation stage better correlates with clinical outcome by contributing to immediate melanoma killing. Several protocols for TIL generation include a two-step *in vitro* expansion (pre-REP and REP phase) which can drive further differentiation and phenotypic changes in the anti-melanoma T-cell population (Li et al., 2010; Rosenberg et al., 2008).

The use of alternative cytokines besides IL-2 (such as IL-15, IL-21 and TGF- β) are also under investigation in order to determine the most effective lymphokine combination for supporting anti-tumour T-cells over regulatory T-cells (Liu et al., 2006; Zeng et al., 2005). Understanding the role and efficacy of anti-melanoma T-cell subsets in patients could lead to their preferential *in vitro* expansion and selective administration of more effective cell combinations. In addition, immune correlates of successful anti-melanoma responses in TILs might also help as biomarkers for identifying which patients to treat. This would allow treatment of only those patients most likely to respond to TIL therapy; sparing those unlikely to respond from treatment-associated toxicities.

Thirdly, preconditioning of the patient is currently required to achieve high levels of T-cell engraftment by eradicating the patient's own immune system and making 'space' for the adoptively infused TILs. Despite being associated with better response rates (Dudley et al., 2008), non-myeloablative regimens used to precondition patients before TIL infusion, still carry significant toxicity (Dudley, 2005; Rosenberg et al., 2011). Major toxicities resulting from current ACT regimens are also related to the high-dose IL-2 administered after TIL infusion in order to support *in vivo* proliferation and persistence of the transferred T-cells.

Finally, the improvement of TIL therapy by enhancing T-cell function *in vivo* is another area of interest. TILs can either be coupled with blocking antibodies against negative co-stimulatory molecules overexpressed on tumour-specific T-cells (such as PD-1) (Chen and Han, 2015), or genetically-modified *ex vivo* in order to improve their persistence and anti-tumour reactivity *in vivo*. For example, an important aspect is whether transferred autologous T-cells migrate efficiently to the tumour site. Tumour homing has been improved in a preclinical murine melanoma model in which tumour-specific T-cells were transduced with a viral vector expressing a homing chemokine receptor (Kershaw et al., 2002; Peng et al., 2010). Besides improved trafficking, direct genetic manipulation of TIL effector function or apoptotic machinery can also be investigated (Charo et al., 2005; Cheng et al., 2002; Foster et al., 2008; Zhang et al., 2011).

6.2.3.1 *Extension to other tumour types*

TIL therapy is gradually transforming the current state of melanoma treatment. The challenge now is to extend TIL therapy to other solid tumour types beyond skin cancer. The reason why T-cell infiltrates are present in some tumour types more than others is not entirely known (Yannelli et al., 1996). Immunogenicity of a given tumour may be related to the expression of HLA-I and HLA-II molecules by a given tumour. Another influencing factor is the cancer mutational load.

Exome analysis of lung carcinoma in smokers, for example, has shown a high frequency of somatic mutations (Alexandrov et al., 2013; Lee et al., 2010). Overall, T-cell infiltration in several cancer types (such as head and neck cancer, breast cancer and colon cancer) is associated with an improved clinical outcome (Jochems and Schlom, 2011), suggesting that anti-tumour T-cells may have a therapeutic role.

6.3 Concluding remarks

Immunotherapy for cancer treatment is a rapidly growing field and has rightly earned its place in *Science's* top scientific breakthrough for 2013. It is clear that the adaptive immune system offers a viable approach to eradicating tumour cells. A key focus of my research was to study human T-cell responses against melanoma from both a molecular and cellular point of view. It is hoped that such knowledge will aid strategies to enhance current T-cell based immunotherapies by maximizing the *in vivo* specific effector function of anti-melanoma T-cell responses. As research on the role of the tumour microenvironment and the genetic makeup of the patient continues, several immunotherapeutic approaches have already shown the potential to provide real clinical benefit. The challenge for tumour immunologists is now to translate the technology into approved clinical practice for melanoma and, ultimately, to extend T-cell based treatment options to other tumours.

7 Appendix

Figure 7.1. Density plot analysis

The observed map at 1.0 sigma (shown as grey mesh around stick representations of the protein chains) after subsequent refinement using automatic non-crystallographic symmetry restraints applied by REFMAC5. (A) The model for PMEL17 TCR-A2-YLE-9V with the TCR CDR3 loops coloured blue (α chain) and orange (β chain) and the green peptide, (B) the model for A2-YLE with the peptide coloured dark green, (C) the model for A2-YLE-3A with the orange peptide, and (D) the model for A2-YLE-5A with the pink peptide.

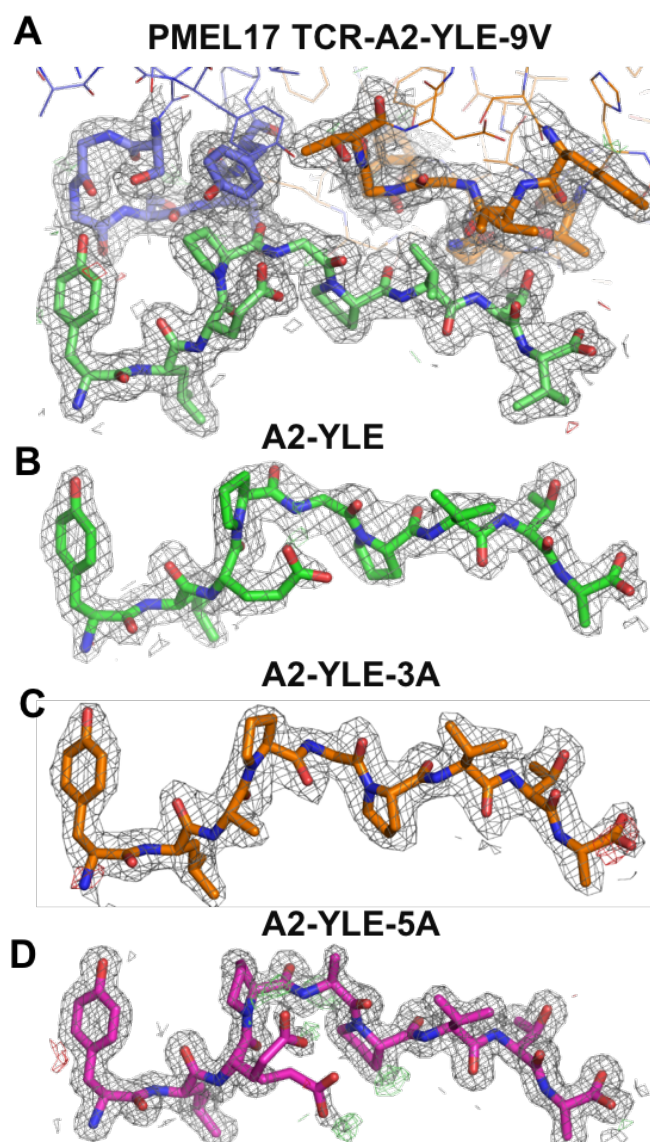


Table 7.1. Panel of melanoma cell lines

The melanoma cell line panel was kindly provided by Marco Donia (CCIT, Copenhagen). HLA class-I typing of the A and B locus is shown where available. Typing was performed at the Herlev Hospital by standard PCR on selected HLA-alleles. The autologous tumour cell lines of patient MM909.24 (**A**) and patient MM909.15 (**B**) are boxed. Colour code indicates HLA-A and HLA-B alleles shared with the corresponding autologous tumour cell line.

A			B		
<i>Cell line</i>	<i>HLA-A</i>	<i>HLA-B</i>	<i>Cell line</i>	<i>HLA-A</i>	<i>HLA-B</i>
FM-2	A1, A29	B5, B40	FM-2	A1, A29	B5, B40
FM-3	A2, A3	B7, B44	FM-3	A2, A3	B7, B44
FM-6	A1, A2	B7, B8	FM-6	A1, A2	B7, B8
FM-28	A1, A2	B8, B15	FM-28	A1, A2	B8, B15
FM-45	A23, A28	B17, B35	FM-45	A23, A28	B17, B35
FM-48	A28, A33	B15, B40	FM-48	A28, A33	B15, B40
FM-55P	A1, A2	B8, B15	FM-55P	A1, A2	B8, B15
FM-56	A28, A31	B27, B44	FM-56	A28, A31	B27, B44
FM-57	A2	B5, B7	FM-57	A2	B5, B7
FM-72	A2	B7, B18	FM-72	A2	B7, B18
FM-74	A24, A31	B15, B35	FM-74	A24, A31	B15, B35
FM-78	A3, A31	B15, B17	FM-78	A3, A31	B15, B17
FM-79	A25, A32	B18, B44	FM-79	A25, A32	B18, B44
FM-81	A2, A28	B15, B44	FM-81	A2, A28	B15, B44
FM-82	A1, A2	B8, B15	FM-82	A1, A2	B8, B15
FM-86	A2	B15, B44	FM-86	A2	B15, B44
FM-88	A2	B27, B49	FM-88	A2	B27, B49
FM-92	A1, A2	B8, B44	FM-92	A1, A2	B8, B44
FM-93/2	A2	-	FM-93/2	A2	-
FM-95	A3, A19	B5, B51	FM-95	A3, A19	B5, B51
SK-Mel-3	A24, A24	B13, B44	SK-Mel-3	A24, A24	B13, B44
SK-Mel-28	A11, A26	B40	SK-Mel-28	A11, A26	B40
Mel-526	A2, A3	B50, B62	Mel-526	A2, A3	B50, B62
Mel-624	A2, A3	B7, B14	Mel-624	A2, A3	B7, B14
MM909.11	A1, A3	-	MM909.11	A1, A3	-
MM909.15	A3, A31	B8, B44	MM909.15	A3, A31	B8, B44
MM909.24	A2, A30	B40	MM909.24	A2, A30	B40
MM909.37	A2	-	MM909.37	A2	-
MM909.09	A2, A3	-	MM909.09	A2, A3	-
MM909.12	A1, A24	B8, B55	MM909.12	A1, A24	B8, B55

Figure 7.2. MM909.24 TIL reactivity against a panel of semi-matched HLA-A2+ melanoma cell lines

FACS plots show the percentage of CD107a+ TNF- α + TILs upon stimulation with semi-matched HLA-A2+ melanoma cell lines (blue). Melanomas that share the HLA-B40 allele with tumour cells MM909.24 were also included (aqua). Cells were gated on live CD3+ CD8+ TILs. Stimulation with autologous tumour and PHA (3 μ g/mL) (bold) were used as positive controls. Stimulation with ELA peptide (10⁻⁶M) was also included in the experiment. Gates were set on unstimulated TILs (negative control).

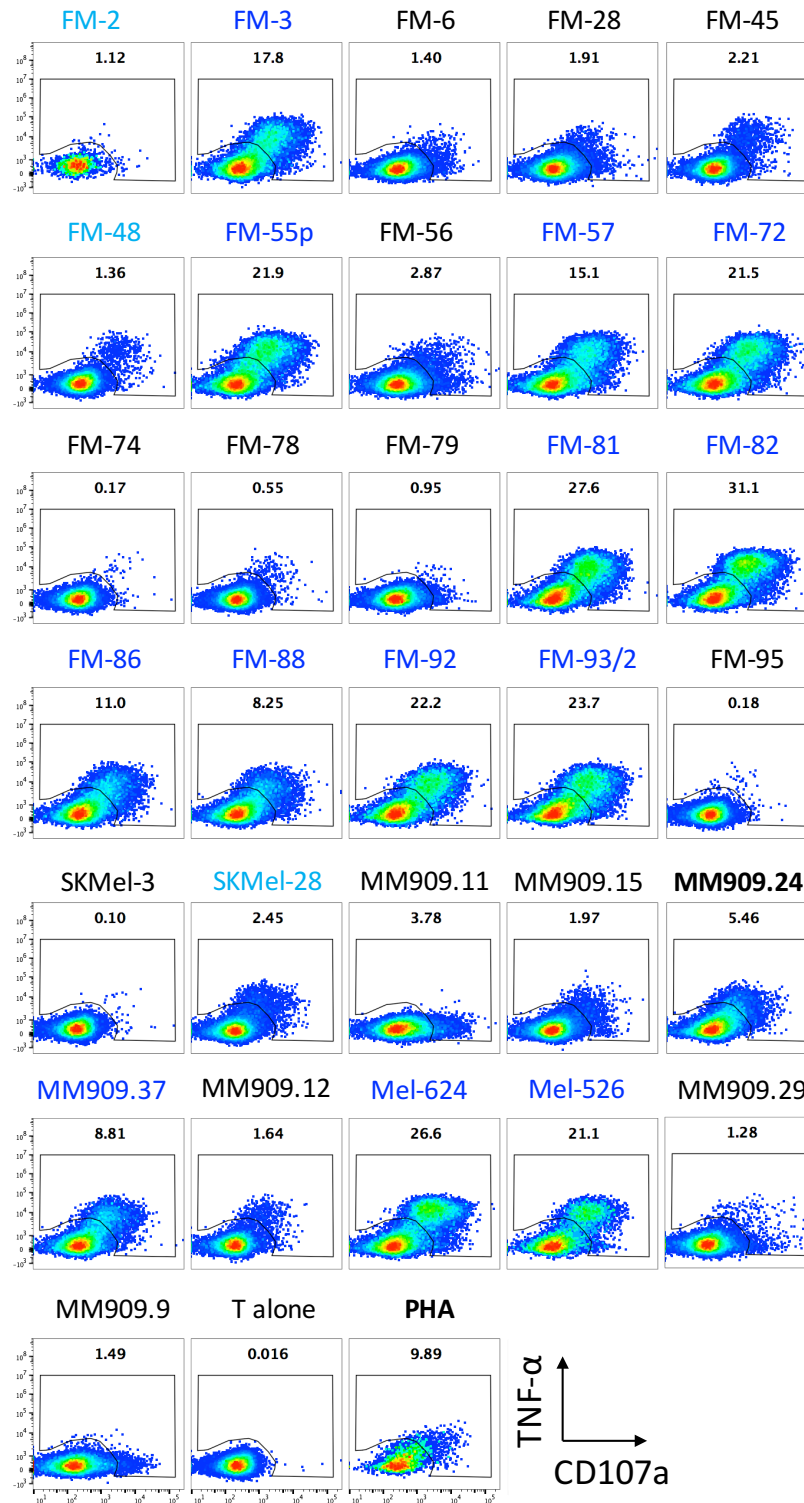


Table 7.2. List of A2-restricted melanoma-associated peptides (from Andersen et al., 2012)

#	sequence	protein
1	MVYDLYKTL	ATIC (AICRT)
2	RLDFNLIRV	
3	GLQHWVPEL	BA46 (MFG8)
4	NLFETPVEA	
5	PLDFSWLSL	Bcl-2
6	WLSLKTLLSL	
7	YLNHDHLEPWI	Bcl-xL
8	CQWGRLWQL	BING-4
9	LATEKSRWS	B-RAF
10	LATEKSRWSG	
11	FIENLKAA	Cadherin 3/P-cadherin
12	FILPVLGAV	
13	YMMPVNSEV	CDCA1/NUF2
14	KLATAQFKI	
15	ACDPHSGHFV	CDK4
16	ALVDAGVPM	CML28 (EXOSC5)
17	FMTRKLWDL	COA-1 (UBXN11)
18	RLLASLQDL	
19	LMLQNALTTM	CPSF
20	KVHPVIWLSL	
21	LLDRFLATV	Cyclin I
22	AKYLMELTM	cyclin B1
23	AGYLMELCC	
24	ILIDWLQV	
25	LLGATCMFV	cyclin D1
26	VLEGMEVV	cyclophilin B (Cyp-B)
27	KLKHYGPGWV	
28	FLWGPRAYA	DAM-6, -10 (MAGE-B1)
29	TLADFDRV	EphA2
30	IMNDMPIYM	
31	VLLLVLGAV	
32	VLAGVGFFI	
33	FMVEDETVL	EZH2
34	FINDEIFVEL	
35	VLPDVFIRCV	GnTV
36	VLPDVFIRC	
37	YLEPGVTA	gp100 / Pmel17
38	VLYRYGSFSV	
39	SLADTNSLAV	
40	MLGTHTMEV	
41	RLMKQDFSV	
42	KTWGQYWQV	
43	ITDQVPFSV	
44	IMDQVPFSV	
45	AMLGTHTMEV	
46	LLDGTATLRL	
47	RLPRIFCSC	
48	MLAVISCAV	HERV-K-MEL
49	LLDVAPSL	hsp70
50	LLLLDVAPL	
51	ALLEIASCL	IDO1
52	SLLMWITQC	LAGE-1
53	MLMAQEALAFI	
54	QLCPICRAPV	Livin (ML-IAP)
55	RLASFYDWLP	
56	SLGSPVLGL	
57	RIDITLSSV	M2BP
58	KVLEYVIKV	MAGE-A1
59	KMVVHVHFL	MAGE-A2
60	LVHFLLKY	
61	LVQENYLEY	
62	YLQLVFGIEV	
63	KVAELVHFL	MAGE-A3

64	LVFGIELMEV	
65	GVYDGREHTV	MAGE-A4
66	YLEYRQVPV*	MAGE-A6
67	GLMDVQIPT	MAGE-A8
68	KVAELVRFL	
69	ALSVMGVYV	MAGE-A9
70	GLYDGMHL	MAGE-A10
71	FLWGPALV**	MAGE-A12
72	KVLEFLAKL	MAGE-C2
73	TLDEKVAELV	
74	ALKDVEERV	
75	LLFGLALIEV	
76	VIWEVLNAV	
77	TILGIFFL	MC1R
78	ELAGIGILTV	Melan-A / MART-1
79	ILTVILGVL	
80	TLNDECWPA	Meloe-1
81	RCPKPPLA	Meloe-2
82	RLPPKPPLA	
83	WLPKILGEV	MG50
84	VLSVNVDPV	
85	TLKCDCEIL	
86	RLGPTLMCL	
87	LLLEAVPAV	
88	CMHLLLEAV	
89	MLMAQEALAF	NY-ESO-1 / LAGE-2
90	QLSLLMWIT	
91	SLLMWITQA	
92	SLLMWITQC	
93	SLLMWITQCFL	
94	IMLCLIAAV	P Polypeptide
95	YLSYGFRL	p53
96	KLCPVQLWV	
97	KTCPVQLWV	
98	LLGRNSFEV	
99	LLPENNVLSPV	
100	RMPEAAPPV	
101	SLPPPGTRV	
102	SMPPPGTRV	
103	VVPCEPEV	
104	GLAPPQHILRV	
105	IIGGGMAFT	PGK1
106	SLLQHLIGL	PRAME
107	SLYSFPEPEA	
108	ALYVDSLFFL	
109	VLDGLDVLL	
110	AMAPIKVRL	PRDX5
111	LLDDLLVSI	
112	VLHWDPETV	RAB38 / NY-MEL-1
113	LKLSGVVRL	RAGE-1
114	PLPPARNGGL	
115	YLMDTSGKV	Replication protein A
116	RLAEYQAYI	SART-3
117	LLQAEAPRL	
118	KMDAEHPPEL	secernin 1
119	AWISKPPGV	SOX10
120	SAWISKPPGV	
121	KASEKIFYV	SSX-2
122	RLQGISPKI	
123	KLQELNYNL	STAT1-alpha/B
124	FLYTLLEEV	STEAP1
125	LLGTIHAL	
126	MIAVFLPIV	
127	LMLGEFLKL	Survivin
128	ELTLGEFLKL	
129	TLPPAWQPFL	

130	SLGWLFLLL	TAG-1	
131	ILAKFLHWL	Telomerase	
132	RLVDDFLLV		
133	RLFFYRKS		
134	FLYDDNQRV	Topoisomerase II	
135	ILLRDAGLV	TRAG-3	
136	TLDSQVMSL	TRP-2	
137	FVWLHYYSV		
138	SLDDYNHLV		
139	VYDFFVWLHY		A1, A2
140	SVYDFFVWL		
141	ATTNILEHY	TRP2-6b	
142	MLLAVLYCL	tyrosinase	
143	YMDGTMSQV		
144	CLLWSFQ TSA		
145	LLSGQPASA	XBP-1	

*Sequence is shared for MAGE-A1, A2, A2, A4, A6, A10 and A12

** Sequence is shared by MAGE-A3

Table 7.3 List of A1- or A3-restricted melanoma associated peptides (from Andersen et al., 2012)

TAA resulting from mutations: The residues modified by the mutation are indicated in red.

#	sequence	protein	HLA-restriction
1	RSDSGQQARY	AIM-2	A1
2	KILDAVVAQK	EFTUD2	A3
3	LIYRRRLMK	gp100 / Pmel17	A3
4	ALNFPGSQK		A3
5	IALNFPGSQK		A3
6	ALLAVGATK		A3
7	EADPTGHSY	MAGE-A1	A1
8	SLFRAVITK		A3
9	EVDPIGHLV	MAGE-A3	A1
10	EVDPASNTY	MAGE-A4	A1
11	FLEGNEVGKTY	MART2	A1
12	FLALIICNA	MC1R	A3
13	ILD TAGREEY	N-ras	A1
14	RLGLQVRK NK	RhoC	A3
15	WLEYYNLER	SART-3	A3
16	QIRPIFSNR		A3
17	ILDSSEEDK	Sp17	A1
18	RLSNRLLLR	TAG	A3
19	KLFGVLR LK	Telomerase	A3
20	VYDFFVWLHY	TRP-2	A1, A2
21	DSDPDSFQDY	tyrosinase	A1
22	KCDICTDEY		A1
23	SSDYVIPIGTY		A1
24	KINKNP KYK	Myosin class I	A3
25	KILDAVVAQK	EFTUD2	A3
26	TLDWLLQTPK	GPNMB	A3
27	KIFSEVTLK	SIRT2	A3

Table 7.4. Overview of T-cell clones isolated from MM909.24 TIL cultures

T-cell clones isolated from MM909.24 TILs were screened and selected based on specific lysis and recognition of autologous tumour cells and ability to grow well in culture. T-cells were co-incubated overnight with autologous tumour cells (+/- IFN- γ treated for 72 hours) and supernatants were tested in a 51 Chromium release assay and MIP-1 β ELISA. The selection criteria for each T-cell clone is schematically colour coded. T-cell clones highlighted in the table correspond to those selected for further characterisation (i.e. phenotyping, clonotyping, antigen specificity).

Clone ID	51 Cr release (% lysis)	MIP-1 β (pg/mL)
1A7		
2A8		
3B11		
3D7		
4B4		
4B9		
4F2		
4G8		
4H8		
4H9		
5B2		
6A4		
6B1		
6B10		
6C10		
6D9		
6E9		
6G2		
6G4		
6G5		
6H4		
7C8		
7C11		
7D11		
7D7		
7E6		
7G3		
8B1		
8C10		
8E4		
9F4		
10F5		
10G1		
10H7		
11A4		
11A12		
11E5		
11F9		
12B10		
12C9		
12H2		
12H7		
13E10		
13E12		
13F5		
13F7		
13G3		
14D11		
14F6		
15B8		
15G3		
15H2		
16E10		
16F1		
16G12		
16H8		
16H9		
18C2		
18F9		
19B9		
19F9		
20C7		
20C9		
20C10		
20H9		
21A11		
21H6		
22A4		
22A8		
22D2		
22E4		
22E7		
22G1		
24E2		
25C1		
25D2		
25D12		
26F10		
28D7		
28E5		
28F6		
28H10		
29B4		
29F4		
29G2		
30C5		
30F8		
30F9		
31E3		
31F11		
31A8		
31A11		
32C10		
32G1		
32G10		
32H5		
33A7		
33C6		
33F3		
33F6		
33F7		
34A10		
34B9		
34C10		
34E2		
34E4		
35E1		
35E2		
35E7		
36C3		
36C7		
36E11		
36E12		
37D8		
37E3		
37E7		
37F3		
37F8		
37F12		
37G7		
38D5		
38F5		
38F12		
38H4		
39B2		
39C3		
39D6		
39F12		
39G3		
39H8		
40A3		
40A4		
40A10		
40G2		
41D9		
42B9		
42D10		
42E9		
42H10		
43A9		
43A11		
43B5		
43D7		
45B1		
45B10		
45G8		
46C9		
46C10		
46F8		
46G12		
47C11		
47F7		
48E4		
48F2		
48F11		
49C2		
50G5		
51A7		
51A10		
ST8		
ST18		
ST64		
ST81		

% specific lysis:
 < 10%
 >10% (tumour +IFN- γ)
 > 10% (untreated)

MIP-1 β production:
 < 50 pg/mL
 50 – 200 pg/mL
 > 250 pg/mL

Figure 7.3. CD8+ TILs MM909.15 reactivity against a panel of melanoma cell lines

FACS plots show the percentage of CD107a+ TNF- α + TILs upon stimulation with semi-matched melanoma cell lines. Cells were gated on live CD3+ CD8+ TILs. Stimulation with autologous tumour and PHA (3 μ g/mL) (bold) were used as positive controls. Gates were set on unstimulated TILs (negative control).

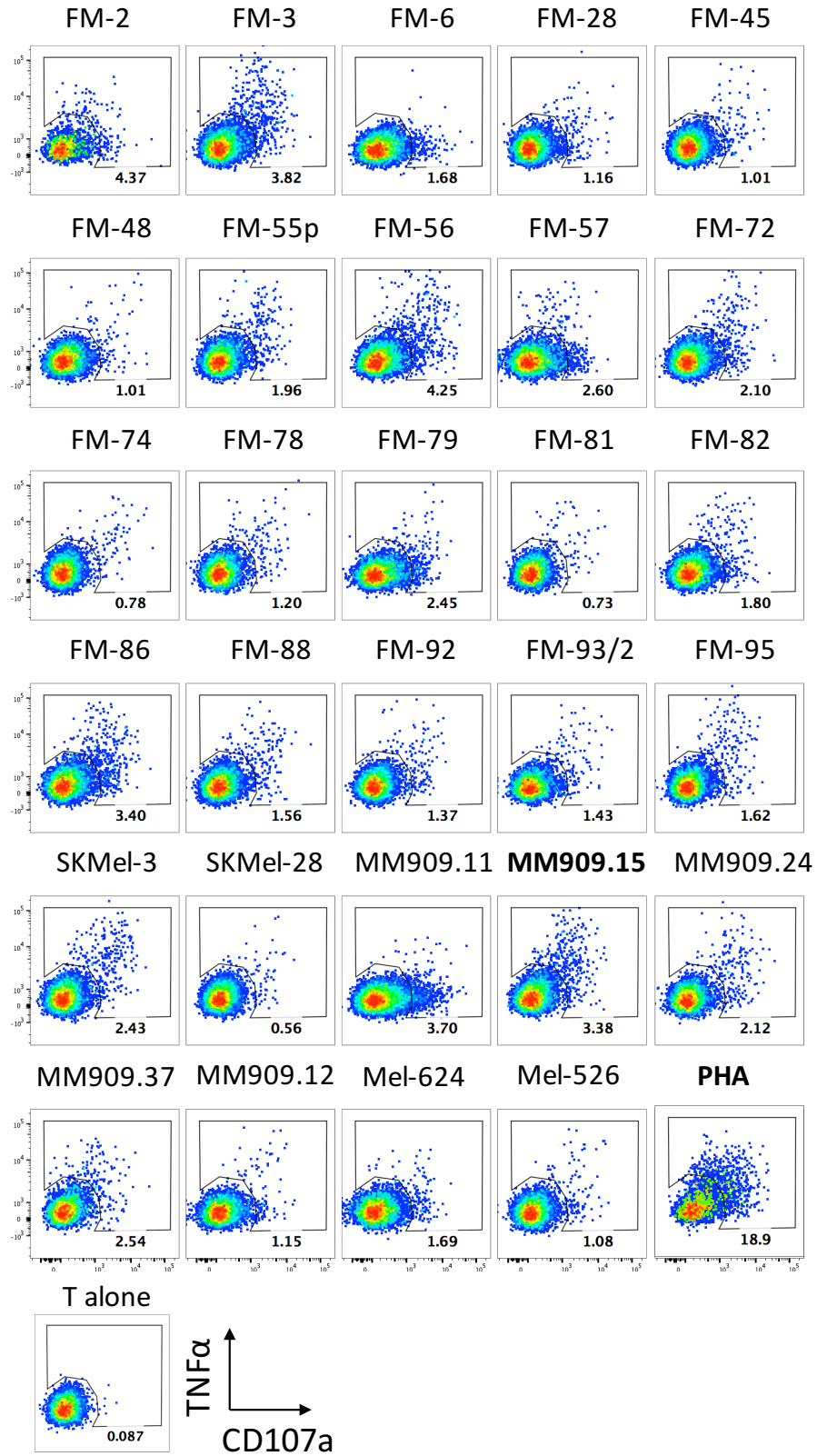


Figure 7.4. CD4+ TILs MM909.15 reactivity against a panel of melanoma cell lines

FACS plots show the percentage of CD107a+ TNF- α + TILs upon stimulation with semi-matched melanoma cell lines. Cells were gated on live CD3+ CD4+ TILs. Stimulation with autologous tumour and PHA (3 μ g/mL) (bold) were used as positive controls. Gates were set on unstimulated TILs (negative control).

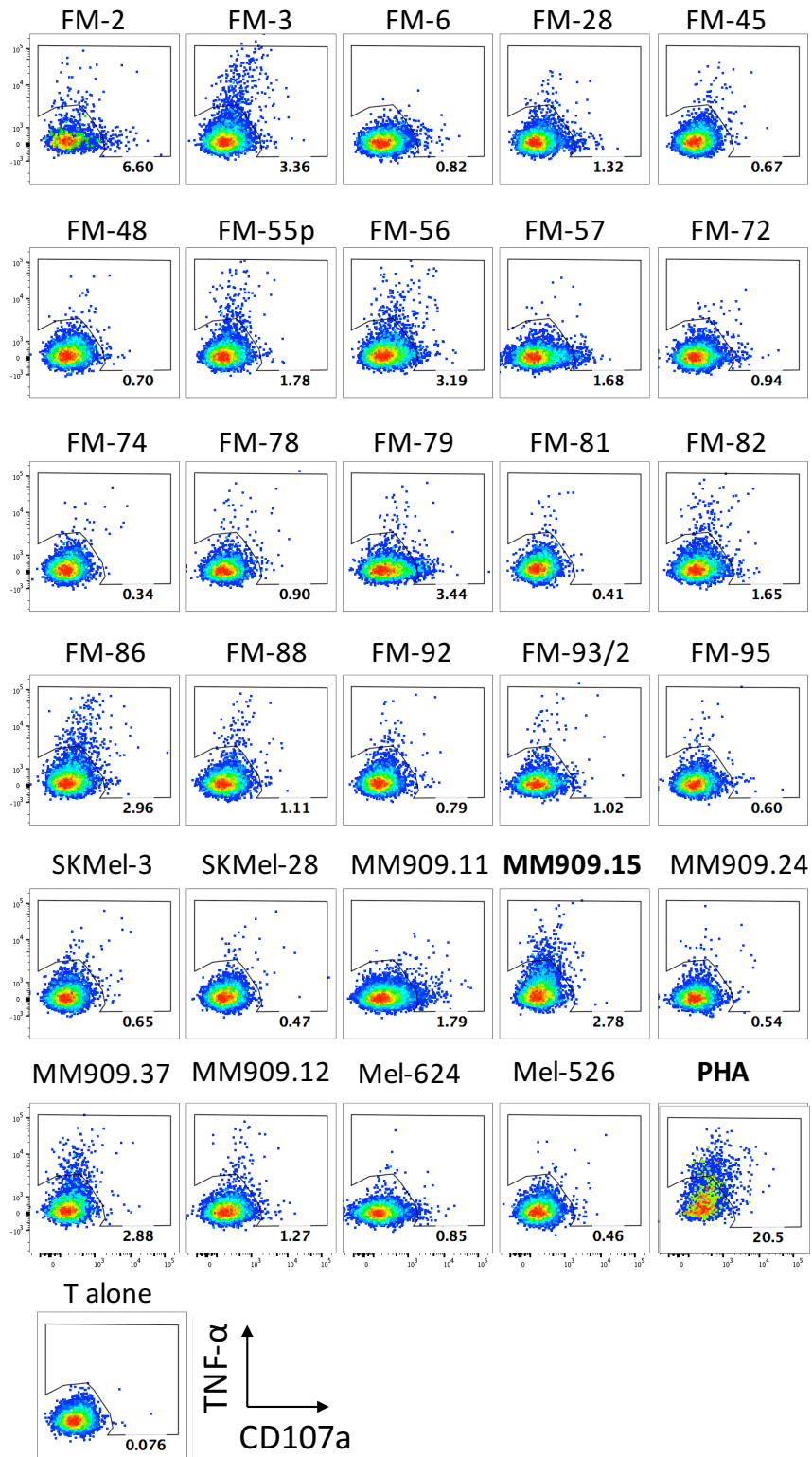


Figure 7.5. TAG T-cell reactivity detected in a complete remission HLA-A3, HLA-A1+ melanoma patient (MM909.11)

(A) Patient MM909.11 characteristics, TIL therapy details and clinical outcome. M1a stage (AJCC, Balch et al., 2009) involves distant metastasis in the skin, subcutaneous tissue, or distant lymph nodes. **(B)** HLA-I and HLA-II typing was kindly provided by Marco Donia (CCIT, Copenhagen). **(C)** CD8+ TILs MM909.11 reactivity against autologous tumour was measured by intracellular staining with IFN- γ , CD107a and TNF- α . T-cells were gated on live CD3+ and unstimulated TILs were used as control. **(D)** IFN- γ ELISpot performed on 5×10^5 MM909.11 TILs stimulated in duplicate with known HLA-A3 and HLA-A1 restricted melanoma-associated peptides (10^{-6} M) for 24 hours. The number of IFN- γ secreting cells per 5×10^5 TILs is displayed on the x axis; peptide sequence and protein of origin (in brackets) are displayed on the y axis. Each bar represents the mean spot count per well (\pm SD). Representative images of ELISpot wells are shown in the bottom panel. PHA (3 μ g/mL) was used as a positive control.

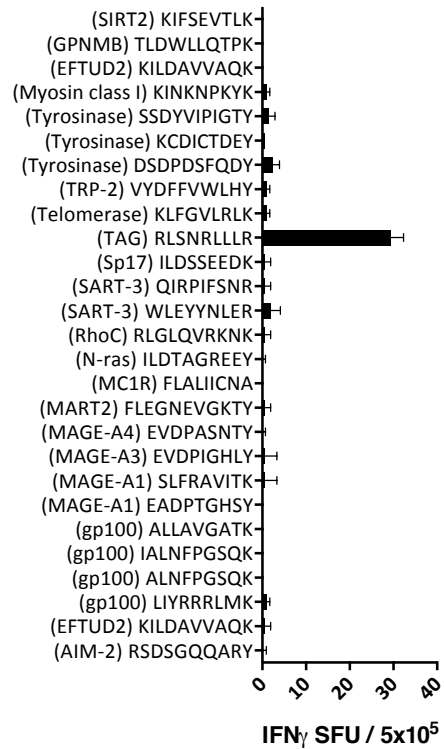
A

Patient ID	Patient characteristics		TIL treatment composition				Clinical outcome	
	Age (sex)	AJCC stage	Cells infused ($\times 10^{10}$)	CD8+ %	CD4+ %	$\gamma\delta$ + %	Clinical response	Overall survival
MM909.11	41 (M)	M1a	7.5	97	2.4	0.01	CR	30 mo+

B

HLA class-I	HLA class-II
A3, A1 B60, B62 C3	DR4, DR15, DQ6, DQ8

D



C

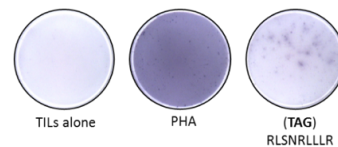
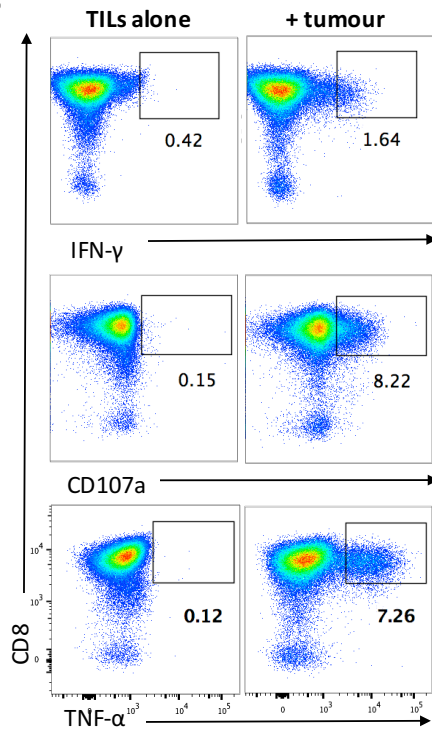
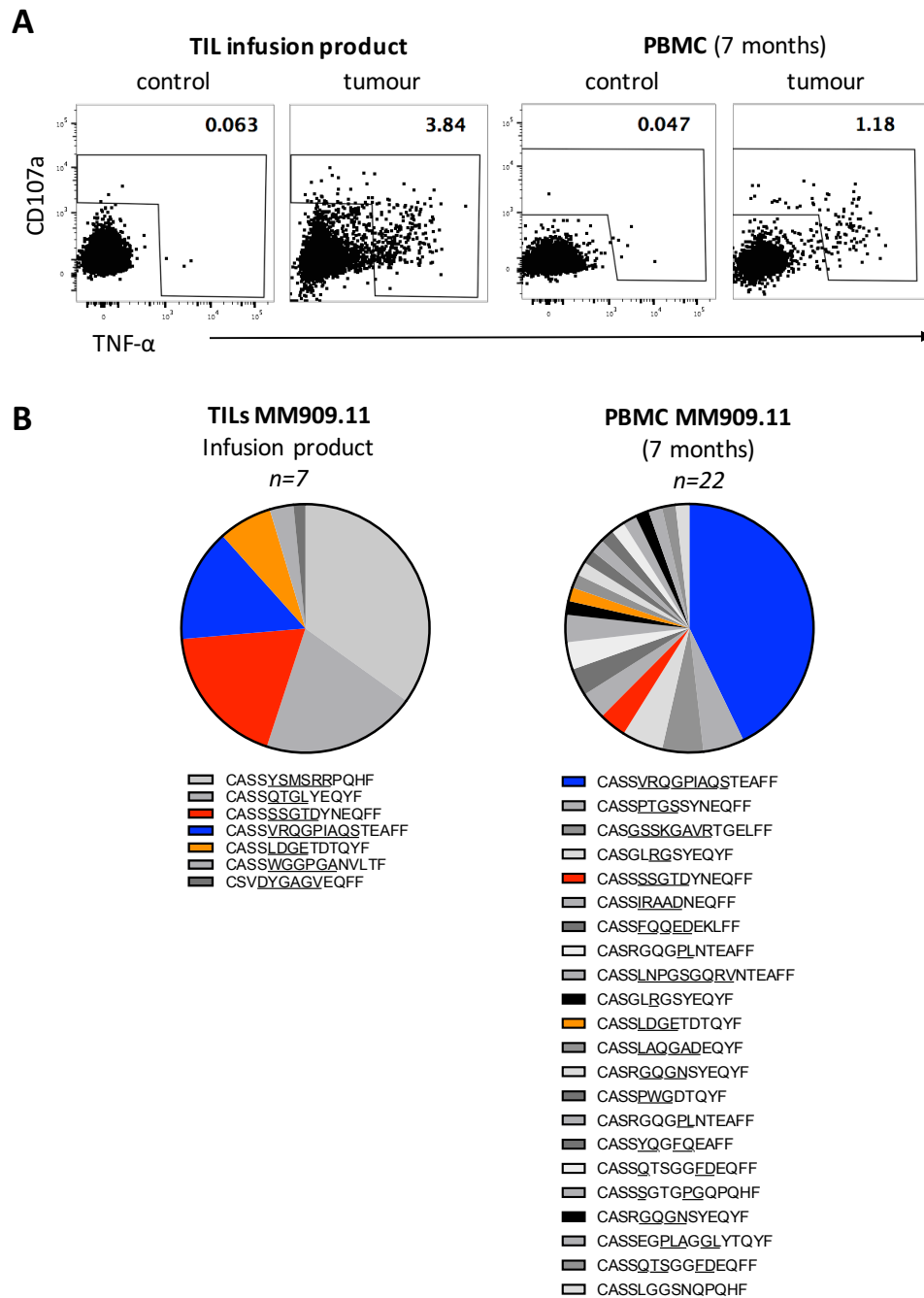


Figure 7.6. CDR3 sequences in the TCR beta repertoire of TILs and PBMC MM909.11

(A) Tumour reactive T-cells from TIL and PBMC were viably sorted based on the expression of both CD107a and TNF- α (after gating on live CD3+ cells). T-cells were stimulated with autologous tumour for 5 hours in the presence of TAPI-0 (μ M), anti-CD107a and anti-TNF- α mAb. Control cells were not stimulated. **(B)** Each pie chart represents the distribution of unique CDR3 sequences detected in TCR β repertoire from the corresponding infusion product or blood sample from patient MM909.15. Each pie segment represents the share of a distinct CDR3 β clonal sequence, thus reflects the respective frequency of each clonotype. Several grey scales are used repeatedly for different sequences because of the high level of diversity. The corresponding CDR3 amino acid sequences are listed in the order of frequency. Shared CDR3 sequences between matched TIL and PBMC samples are indicated by coloured pie segments.



References

- Adair, S.J., Carr, T.M., Fink, M.J., Slingluff, C.L., and Hogan, K.T. (2008). The TAG family of cancer/testis antigens is widely expressed in a variety of malignancies and gives rise to HLA-A2-restricted epitopes. *Journal of Immunotherapy* 31, 7–17.
- Alam, S.M., Travers, P.J., Wung, J.L., Nasholds, W., Redpath, S., Jameson, S.C., and Gascoigne, N.R. (1996). T-cell-receptor affinity and thymocyte positive selection. *Nature* 381, 616–620.
- Aleksic, M., Liddy, N., Molloy, P.E., Pumphrey, N., Vuidepot, A., Chang, K.-M., and Jakobsen, B.K. (2012). Different affinity windows for virus and cancer-specific T-cell receptors: implications for therapeutic strategies. *Eur. J. Immunol.* 42, 3174–3179.
- Alexandrov, L.B., Nik-Zainal, S., Wedge, D.C., Aparicio, S.A.J.R., Behjati, S., Biankin, A.V., Bignell, G.R., Bolli, N., Borg, A., et al. (2013). Signatures of mutational processes in human cancer. *Nature* 500, 415–421.
- Almeida, L.G., Sakabe, N.J., deOliveira, A.R., Silva, M.C.C., Mundstein, A.S., Cohen, T., Chen, Y.-T., Chua, R., Gurung, S., Gnjatic, S., et al. (2009). CTdatabase: a knowledge-base of high-throughput and curated data on cancer-testis antigens. *Nucleic Acids Research* 37, D816–D819.
- Alonso, S.R., Ortiz, P., Pollán, M., Pérez-Gómez, B., Sánchez, L., Acuña, M.J., Pajares, R., Martínez-Tello, F.J., Hortelano, C.M., Piris, M.A., et al. (2004). Progression in cutaneous malignant melanoma is associated with distinct expression profiles: a tissue microarray-based study. *The American Journal of Pathology* 164, 193–203.
- Altomonte, M., Fonsatti, E., Visintin, A., and Maio, M. (2003). Targeted therapy of solid malignancies via HLA class II antigens: a new biotherapeutic approach? *Oncogene* 22, 6564–6569.
- Amos, S.M., Duong, C.P.M., Westwood, J.A., Ritchie, D.S., Junghans, R.P., Darcy, P.K., and Kershaw, M.H. (2011). Autoimmunity associated with immunotherapy of cancer. *Blood* 118, 499–509.
- Andersen, M.H., Schrama, D., Straten, P., and Becker, J.C. (2006). Cytotoxic T cells. *J. Invest. Dermatol.* 126, 32–41.
- Andersen, R.S., Thruø, C.A., Junker, N., Lyngaa, R., Donia, M., Ellebæk, E., Svane, I.M., Schumacher, T.N., Straten, P.T., and Hadrup, S.R. (2012). Dissection of T-cell antigen specificity in human melanoma. *Cancer Research* 72, 1642–1650.
- Andersen, R., Donia, M., Ellebæk, E., Borch, T.H., Kongsted, P., Iversen, T.Z., Holmich, L.R., Hendel, H.W., Met, Ö., Andersen, M.H., et al. (2016). Long-lasting complete responses in patients with metastatic melanoma after adoptive cell therapy with tumor-infiltrating lymphocytes and an attenuated IL-2 regimen. *Clinical Cancer Research*.
- Anderson, G., Harman, B.C., Hare, K.J., and Jenkinson, E.J. (2000). Microenvironmental regulation of T cell development in the thymus. *Semin. Immunol.* 12, 457–464.
- Anderson, G., Owen, J.J., Moore, N.C., and Jenkinson, E.J. (1994). Thymic epithelial cells provide unique signals for positive selection of CD4+CD8+ thymocytes in vitro. *Journal of Experimental Medicine* 179, 2027–2031.
- Anichini, A., Mortarini, R., Nonaka, D., Molla, A., Vegetti, C., Montaldi, E., Wang, X., and Ferrone, S. (2006). Association of antigen-processing machinery and HLA antigen phenotype of melanoma cells with survival in American Joint Committee on Cancer stage III and IV melanoma patients. *Cancer Research* 66, 6405–6411.
- Antony, P.A., Piccirillo, C.A., Akpınarli, A., Finkelstein, S.E., Speiss, P.J., Surman, D.R., Palmer, D.C., Chan, C.-C., Klebanoff, C.A., Overwijk, W.W., et al. (2005). CD8+ T cell immunity against a tumor/self-antigen is augmented by CD4+ T helper cells and hindered by naturally occurring T regulatory cells. *The Journal of Immunology* 174, 2591–2601.
- Apetoh, L., Ghiringhelli, F., Tesniere, A., Criollo, A., Ortiz, C., Lidereau, R., Mariette, C., Chaput, N., Mira, J.-P., Delaloge, S., et al. (2007a). The interaction between HMGB1 and TLR4 dictates the outcome of anticancer chemotherapy and radiotherapy. *Immunol. Rev.* 220, 47–59.
- Arden, B., Clark, S., Kabelitz, D., and Mak, T. (1995). Human T-cell receptor variable gene segment families. *Immunogenetics* 42, 455–500.
- Armstrong, K.M., and Baker, B.M. (2007). A comprehensive calorimetric investigation of an entropically driven T cell receptor-peptide/major histocompatibility complex interaction. *Biophys. J.* 93, 597–609.
- Ashton-Rickardt, P.G., and Tonegawa, S. (1994). A differential-avidity model for T-cell selection. *Immunol. Today* 15, 362–366.
- Atkins, M.B., Lotze, M.T., Dutcher, J.P., Fisher, R.I., Weiss, G., Margolin, K., Abrams, J., Sznol, M., Parkinson, D., Hawkins, M., et al. (1999). High-dose recombinant interleukin 2 therapy for patients with metastatic melanoma: analysis of 270 patients treated between 1985 and 1993. *J. Clin. Oncol.* 17, 2105–2116.

- Ayyoub, M., Dojcinovic, D., Pignon, P., Raimbaud, I., Schmidt, J., Luescher, I., and Valmori, D. (2010). Monitoring of NY-ESO-1 specific CD4+ T cells using molecularly defined MHC class II/His-tag-peptide tetramers. *Proceedings of the National Academy of Sciences* *107*, 7437–7442.
- Ayyoub, M., Merlo, A., Hesdorffer, C.S., Rimoldi, D., Speiser, D., Cerottini, J.-C., Chen, Y.-T., Old, L.J., Stevanovic, S., and Valmori, D. (2005). CD4+ T cell responses to SSX-4 in melanoma patients. *The Journal of Immunology* *174*, 5092–5099.
- Ayyoub, M., Zippelius, A., Pittet, M.J., Rimoldi, D., Valmori, D., Cerottini, J.-C., Romero, P., Lejeune, F., Liénard, D., and Speiser, D.E. (2003). Activation of human melanoma reactive CD8+ T cells by vaccination with an immunogenic peptide analog derived from Melan-A/melanoma antigen recognized by T cells-1. *Clinical Cancer Research* *9*, 669–677.
- Bailey, S. (1994). The Ccp4 Suite - Programs For Protein Crystallography. *Acta Crystallographica. Section D, Biological Crystallography* *50*, 760–763.
- Balch, C., Gershenwald, J., Soong, S.-J., Thompson, J., Atkins, M., Byrd, D., Buzaid, A., Cochran, A., Coit, D., Ding, S., et al. (2009). Final version of 2009 AJCC melanoma staging and classification. *Journal of Clinical Oncology : Official Journal of the American Society of Clinical Oncology* *27*, 6199–6206.
- Banham, A.H., and Smith, G.L. (1993). Characterization of vaccinia virus gene B12R. *Journal of General Virology* *74*, 2807–2812.
- Barrow, C., Browning, J., MacGregor, D., Davis, I.D., Sturrock, S., Jungbluth, A.A., and Cebon, J. (2006). Tumor antigen expression in melanoma varies according to antigen and stage. *Clinical Cancer Research* *12*, 764–771.
- Barry, M., and Bleackley, R.C. (2002). Cytotoxic T lymphocytes: all roads lead to death. *Nature Rev Immunol* *2*, 401–409.
- Bednarek, M.A., Sauma, S.Y., Gammon, M.C., Porter, G., Tamhankar, S., Williamson, A.R., and Zweerink, H.J. (1991). The minimum peptide epitope from the influenza virus matrix protein. Extra and intracellular loading of HLA-A2. *The Journal of Immunology* *147*, 4047–4053.
- Bell, J.L., Wächter, K., Mühleck, B., Pazaitis, N., Köhn, M., Lederer, M., and Hüttelmaier, S. (2013). Insulin-like growth factor 2 mRNA-binding proteins (IGF2BPs): post-transcriptional drivers of cancer progression? *Cell. Mol. Life Sci.* *70*, 2657–2675.
- Bennett, S.R., Carbone, F.R., Karamalis, F., Flavell, R.A., Miller, J.F., and Heath, W.R. (1998). Help for cytotoxic-T-cell responses is mediated by CD40 signalling. *Nature* *393*, 478–480.
- Bennett, S.R., Carbone, F.R., Karamalis, F., Miller, J.F., and Heath, W.R. (1997). Induction of a CD8+ cytotoxic T lymphocyte response by cross-priming requires cognate CD4+ T cell help. *Journal of Experimental Medicine* *186*, 65–70.
- Berger, T.G., Haendle, I., Schrama, D., Lüftl, M., Bauer, N., Pedersen, L.Ø., Schuler-Thurner, B., Hohenberger, W., Straten, P.T., Schuler, G., et al. (2004). Circulation and homing of melanoma-reactive T cells to both cutaneous and visceral metastases after vaccination with monocyte-derived dendritic cells. *Int. J. Cancer* *111*, 229–237.
- Berwick, M., Buller, D.B., Cust, A., Gallagher, R., Lee, T.K., Meyskens, F., Pandey, S., Thomas, N.E., Veierød, M.B., and Ward, S. (2016). Melanoma Epidemiology and Prevention. *Cancer Treat. Res.* *167*, 17–49.
- Berzofsky, J.A., Wood, L.V., and Terabe, M. (2015). Strategies for Improving Vaccines to Elicit T Cells to Treat Cancer. In *Developments in T Cell Based Cancer Immunotherapies*, P.A. Ascierto, D.F. Stronck, and E. Wang, eds. (Springer International Publishing), pp. 29–52.
- Besser, M.J., Shapira-Frommer, R., Treves, A.J., Zippel, D., Itzhaki, O., Schallmach, E., Kubi, A., Shalmon, B., Hardan, I., Catane, R., et al. (2009). Minimally Cultured or Selected Autologous Tumor-infiltrating Lymphocytes After a Lympho-depleting Chemotherapy Regimen in Metastatic Melanoma Patients. *Journal of Immunotherapy* *32*, 415–423.
- Betts, M.R., Brenchley, J.M., Price, D.A., De Rosa, S.C., Douek, D.C., Roederer, M., and Koup, R.A. (2003). Sensitive and viable identification of antigen-specific CD8+ T cells by a flow cytometric assay for degranulation. *Journal of Immunological Methods* *281*, 65–78.
- Bevan, M.J. (1977). Killer cells reactive to altered-self antigens can also be alloreactive. *Proceedings of the National Academy of Sciences* *74*, 2094–2098.
- Bianchi, V., Bulek, A., Fuller, A., Lloyd, A., Attaf, M., Rizkallah, P.J., Dolton, G., Sewell, A.K., and Cole, D.K. (2016). A molecular switch abrogates gp100 TCR-targeting of a human melanoma antigen. *J. Biol. Chem.* *291*, jbc.M115.707414–jbc.M115.708959.
- Bijker, M.S., van den Eeden, S.J.F., Franken, K.L., Melief, C.J.M., van der Burg, S.H., and Offringa, R. (2008). Superior induction of anti-tumor CTL immunity by extended peptide vaccines involves prolonged, DC-focused antigen presentation. *Eur. J. Immunol.* *38*, 1033–1042.

- Blanchard, T., Srivastava, P.K., and Duan, F. (2013). Vaccines against advanced melanoma. *Clin. Dermatol.* *31*, 179–190.
- Bloom, M.B., Perry-Lalley, D., Robbins, P.F., Li, Y., El-Gamil, M., Rosenberg, S.A., and Yang, J.C. (1997). Identification of tyrosinase-related protein 2 as a tumor rejection antigen for the B16 melanoma. *Journal of Experimental Medicine* *185*, 453–459.
- Boehmer, von, H. (2005). Unique features of the pre-T-cell receptor alpha-chain: not just a surrogate. *Nature Rev Immunol* *5*, 571–577.
- Boland, G.M., and Gershenwald, J.E. (2016). Principles of Melanoma Staging. *Cancer Treat. Res.* *167*, 131–148.
- Boniface, J.J., Reich, Z., Lyons, D.S., and Davis, M.M. (1999). Thermodynamics of T cell receptor binding to peptide-MHC: evidence for a general mechanism of molecular scanning. *Proceedings of the National Academy of Sciences* *96*, 11446–11451.
- Boniol, M., Autier, P., Boyle, P., and Gandini, S. (2012). Cutaneous melanoma attributable to sunbed use: systematic review and meta-analysis. *Bmj* *345*, e4757–e4757.
- Boon, T., Coulie, P., Eynde, B., and Bruggen, P. (2006). Human T cell responses against melanoma. *24*, 175–208.
- Borbulevych, O.Y., Piepenbrink, K.H., Gloor, B.E., Scott, D.R., Sommese, R.F., Cole, D.K., Sewell, A.K., and Baker, B.M. (2009). T cell receptor cross-reactivity directed by antigen-dependent tuning of peptide-MHC molecular flexibility. *Immunity* *31*, 885–896.
- Borbulevych, O.Y., Santhanagopalan, S.M., Hossain, M., and Baker, B.M. (2011). TCRs used in cancer gene therapy cross-react with MART-1/Melan-A tumor antigens via distinct mechanisms. *Journal Immunology* *187*, 2453–2463.
- Born, W., Yagüe, J., Palmer, E., Kappler, J., and Marrack, P. (1985). Rearrangement of T-cell receptor beta-chain genes during T-cell development. *Proceedings of the National Academy of Sciences* *82*, 2925–2929.
- Boulter, J.M., Glick, M., Todorov, P.T., Baston, E., Sami, M., Rizkallah, P., and Jakobsen, B.K. (2003). Stable, soluble T-cell receptor molecules for crystallization and therapeutics. *Protein Engineering Design and Selection* *16*, 707–711.
- Bouvier, M., and Wiley, D.C. (1994). Importance of peptide amino and carboxyl termini to the stability of MHC class I molecules. *Science* *265*, 398–402.
- Brady, M.S., Eckels, D.D., Ree, S.Y., Schultheiss, K.E., and Lee, J.S. (1996). MHC class II-mediated antigen presentation by melanoma cells. *J Immunother Emphasis Tumor Immunol* *19*, 387–397.
- Brady, M.S., Lee, F., Petrie, H., Eckels, D.D., and Lee, J.S. (2000). CD4(+) T cells kill HLA-class-II-antigen-positive melanoma cells presenting peptide in vitro. *Cancer Immunol Immunother* *48*, 621–626.
- Braumüller, H., Wieder, T., Brenner, E., Aßmann, S., Hahn, M., Alkhaled, M., Schilbach, K., Essmann, F., Kneilling, M., Griessinger, C., et al. (2013). T-helper-1-cell cytokines drive cancer into senescence. *Nature* *494*, 361–365.
- Brichard, V., van Pel, A., Wolfel, T., Wolfel, C., De Plaen, E., Lethé, B., Coulie, P., and Boon, T. (1993). The tyrosinase gene codes for an antigen recognized by autologous cytolytic T lymphocytes on HLA-A2 melanomas. *Journal of Experimental Medicine* *178*, 489–495.
- Bridgeman, J.S., Sewell, A.K., Miles, J.J., Price, D.A., and Cole, D.K. (2011). Structural and biophysical determinants of $\alpha\beta$ T-cell antigen recognition. *Immunology* *135*, 9–18.
- Brunet, J.F., Denizot, F., Luciani, M.F., Roux-Dosseto, M., Suzan, M., Mattei, M.G., and Golstein, P. (1987). A new member of the immunoglobulin superfamily—CTLA-4. *Nature* *328*, 267–270.
- Bulek, A.M., Madura, F., Fuller, A., Holland, C.J., Schauenburg, A.J.A., Sewell, A.K., Rizkallah, P.J., and Cole, D.K. (2012). TCR/pMHC Optimized Protein crystallization Screen. *Journal of Immunological Methods* *382*, 203–210.
- Burnet, F.M. (1970). The concept of immunological surveillance. *Prog Exp Tumor Res* *13*, 1–27.
- Burrows, J.M., Bell, M.J., Brennan, R., Miles, J.J., Khanna, R., and Burrows, S.R. (2008). Preferential binding of unusually long peptides to MHC class I and its influence on the selection of target peptides for T cell recognition. *Mol. Immunol.* *45*, 1818–1824.
- Butterfield, L.H., Ribas, A., Dissette, V.B., Amarnani, S.N., Vu, H.T., Oseguera, D., Wang, H.-J., Elashoff, R.M., McBride, W.H., Mukherji, B., et al. (2003). Determinant spreading associated with clinical response in dendritic cell-based immunotherapy for malignant melanoma. *Clinical Cancer Research* *9*, 998–1008.

Cai, D., Cao, J., Li, Z., Zheng, X., Yao, Y., Li, W., and Yuan, Z. (2009). Up-regulation of bone marrow stromal protein 2 (BST2) in breast cancer with bone metastasis. *BMC Cancer* 9, 102.

Carpenter, A.C., and Bosselut, R. (2010). Decision checkpoints in the thymus. *Nature Immunology* 11, 666–673.

Carreno, B.M., Magrini, V., Becker-Hapak, M., Kaabinejadian, S., Hundal, J., Petti, A.A., Ly, A., Lie, W.R., Hildebrand, W.H., Mardis, E.R., et al. (2015). A dendritic cell vaccine increases the breadth and diversity of melanoma neoantigen-specific T cells. *Science* 348, 803–808.

Carson, R.T., Vignali, K.M., Woodland, D.L., and Vignali, D.A. (1997). T cell receptor recognition of MHC class II-bound peptide flanking residues enhances immunogenicity and results in altered TCR V region usage. *Immunity* 7, 387–399.

Castle, J.C., Kreiter, S., Diekmann, J., Löwer, M., van de Roemer, N., de Graaf, J., Selmi, A., Diken, M., Boegel, S., Paret, C., et al. (2012). Exploiting the mutanome for tumor vaccination. *Cancer Research* 72, 1081–1091.

Charo, J., Finkelstein, S.E., Grewal, N., Restifo, N.P., Robbins, P.F., and Rosenberg, S.A. (2005). Bcl-2 overexpression enhances tumor-specific T-cell survival. *Cancer Research* 65, 2001–2008.

Chen, J.L. (2005). Structural and kinetic basis for heightened immunogenicity of T cell vaccines. *Journal of Experimental Medicine* 201, 1243–1255.

Chen, L., and Han, X. (2015). Anti-PD-1/PD-L1 therapy of human cancer: past, present, and future. *J. Clin. Invest.* 125, 3384–3391.

Cheng, L.E., Ohlén, C., Nelson, B.H., and Greenberg, P.D. (2002). Enhanced signaling through the IL-2 receptor in CD8+ T cells regulated by antigen recognition results in preferential proliferation and expansion of responding CD8+ T cells rather than promotion of cell death. *Proceedings of the National Academy of Sciences* 99, 3001–3006.

Chinnasamy, D., Yu, Z., Theoret, M.R., Zhao, Y., Shrimali, R.K., Morgan, R.A., Feldman, S.A., Restifo, N.P., and Rosenberg, S.A. (2010). Gene therapy using genetically modified lymphocytes targeting VEGFR-2 inhibits the growth of vascularized syngenic tumors in mice. *J. Clin. Invest.* 120, 3953–3968.

Chinnasamy, N., Wargo, J.A., Yu, Z., Rao, M., Frankel, T.L., Riley, J.P., Hong, J.J., Parkhurst, M.R., Feldman, S.A., Schrupp, D.S., et al. (2011). A TCR targeting the HLA-A*0201-restricted epitope of MAGE-A3 recognizes multiple epitopes of the MAGE-A antigen superfamily in several types of cancer. *J. Immunol.* 186, 685–696.

Chothia, C., Boswell, D.R., and Lesk, A.M. (1988). The outline structure of the T-cell alpha beta receptor. *Embo J.* 7, 3745–3755.

Christensen, O., Lupu, A., Schmidt, S., Condomines, M., Belle, S., Maier, A., Hose, D., Neuber, B., Moos, M., Kleist, C., et al. (2009). Melan-A/MART1 analog peptide triggers anti-myeloma T-cells through crossreactivity with HM1.24. *J. Immunother.* 32, 613–621.

Clark, W.H., Elder, D.E., Guerry, D., Epstein, M.N., Greene, M.H., and Van Horn, M. (1984). A study of tumor progression: the precursor lesions of superficial spreading and nodular melanoma. *Hum. Pathol.* 15, 1147–1165.

Clay, T.M., Custer, M.C., McKee, M.D., Parkhurst, M., Robbins, P.F., Kerstann, K., Wunderlich, J., Rosenberg, S.A., and Nishimura, M.I. (1999). Changes in the fine specificity of gp100(209-217)-reactive T cells in patients following vaccination with a peptide modified at an HLA-A2.1 anchor residue. *The Journal of Immunology* 162, 1749–1755.

Clemente, M.J., Przychodzen, B., Jerez, A., Dienes, B.E., Afable, M.G., Hussein, H., Rajala, H.L.M., Wlodarski, M.W., Mustjoki, S., and Maciejewski, J.P. (2013). Deep sequencing of the T-cell receptor repertoire in CD8+ T-large granular lymphocyte leukemia identifies signature landscapes. *Blood* 122, 4077–4085.

Cole, D.K., Edwards, E.S., Wynn, K.K., Clement, M., Miles, J.J., Ladell, K., Ekeruche, J., Gostick, E., Adams, K.J., Skowera, A., et al. (2010). Modification of MHC anchor residues generates heteroclitic peptides that alter TCR binding and T cell recognition. *Journal Immunology* 185, 2600–2610.

Cole, D.K., Pumphrey, N.J., Boulter, J.M., Sami, M., Bell, J.I., Gostick, E., Price, D.A., Gao, G.F., Sewell, A.K., and Jakobsen, B.K. (2007). Human TCR-binding affinity is governed by MHC class restriction. *The Journal of Immunology* 178, 5727–5734.

Cole, D., Yuan, F., Rizkallah, P., Miles, J., Gostick, E., Price, D., Gao, G., Jakobsen, B., and Sewell, A. (2009). Germ line-governed recognition of a cancer epitope by an immunodominant human T-cell receptor. *The Journal of Biological Chemistry* 284, 27281–27289.

Cong, L., Ran, F.A., Cox, D., Lin, S., Barretto, R., Habib, N., Hsu, P.D., Wu, X., Jiang, W., Marraffini, L.A., et al. (2013). Multiplex genome engineering using CRISPR/Cas systems. *Science* 339, 819–823.

- Conrad, N., Leis, P., Orengo, I., Medrano, E.E., Hayes, T.G., Baer, S., and Rosen, T. (1999). Multiple primary melanoma. *Dermatol Surg* 25, 576–581.
- Corbière, V., Chapiro, J., Stroobant, V., Ma, W., Lurquin, C., Lethé, B., van Baren, N., Van den Eynde, B.J., Boon, T., and Coulie, P.G. (2011). Antigen spreading contributes to MAGE vaccination-induced regression of melanoma metastases. *Cancer Research* 71, 1253–1262.
- Cordova, A., Toia, F., Mendola, C., Orlando, V., Meraviglia, S., Rinaldi, G., Todaro, M., Cicero, G., Zichichi, L., Donni, P., et al. (2012). Characterization of human $\gamma\delta$ T lymphocytes infiltrating primary malignant melanomas. *PLoS One* 7, e49878.
- Cormier, J.N., Salgaller, M.L., Prevette, T., Barracchini, K.C., Rivoltini, L., Restifo, N.P., Rosenberg, S.A., and Marincola, F.M. (1997). Enhancement of cellular immunity in melanoma patients immunized with a peptide from MART-1/Melan A. *Cancer J Sci Am* 3, 37–44.
- Couzin-Frankel, J. (2013). Breakthrough of the year 2013. *Cancer immunotherapy. Science* 342, 1432–1433.
- Cox, M.A., Kahan, S.M., and Zajac, A.J. (2013). Anti-viral CD8 T cells and the cytokines that they love. *Virology* 435, 157–169.
- Crowe, P.D., Walter, B.N., Mohler, K.M., Otten-Evans, C., Black, R.A., and Ware, C.F. (1995). A metalloprotease inhibitor blocks shedding of the 80-kD TNF receptor and TNF processing in T lymphocytes. *Journal of Experimental Medicine* 181, 1205–1210.
- Damsky, W.E., Theodosakis, N., and Bosenberg, M. (2014). Melanoma metastasis: new concepts and evolving paradigms. *Oncogene* 33, 2413–2422.
- Davies, H., Bignell, G.R., Cox, C., Stephens, P., Edkins, S., Clegg, S., Teague, J., Woffendin, H., Garnett, M.J., Bottomley, W., et al. (2002). Mutations of the BRAF gene in human cancer. *Nature* 417, 949–954.
- Davis, M.M., and Bjorkman, P.J. (1988). T-cell antigen receptor genes and T-cell recognition. *Nature* 334, 395–402.
- Deng, L., Langley, R.J., Brown, P.H., Xu, G., Teng, L., Wang, Q., Gonzales, M.I., Callender, G.G., Nishimura, M.I., Topalian, S.L., et al. (2007). Structural basis for the recognition of mutant self by a tumor-specific, MHC class II-restricted T cell receptor. *Nature Immunology* 8, 398–408.
- Diamond, D.J., York, J., Sun, J.Y., Wright, C.L., and Forman, S.J. (1997). Development of a candidate HLA A*0201 restricted peptide-based vaccine against human cytomegalovirus infection. *Blood* 90, 1751–1767.
- Dietrich, P.-Y., Le Gal, F.-A., Dutoit, V., Pittet, M.J., Trautman, L., Zippelius, A., Cognet, I., Widmer, V., Walker, P.R., Michielin, O., et al. (2003). Prevalent role of TCR alpha-chain in the selection of the preimmune repertoire specific for a human tumor-associated self-antigen. *Journal Immunology* 170, 5103–5109.
- Dolton, G., Tungatt, K., Lloyd, A., Bianchi, V., Theaker, S.M., Trimby, A., Holland, C.J., Donia, M., Godkin, A.J., Cole, D.K., et al. (2015). More tricks with tetramers: a practical guide to staining T cells with peptide-MHC multimers. *Immunology* 146, 11–22.
- Donia, M., Junker, N., Ellebaek, E., Andersen, M.H., Straten, P.T., and Svane, I.M. (2012). Characterization and Comparison of 'Standard' and 'Young' Tumour-Infiltrating Lymphocytes for Adoptive Cell Therapy at a Danish Translational Research Institution. *Scandinavian Journal of Immunology* 75, 157–167.
- Donia, M., Andersen, R., Kjeldsen, J.W., Fagone, P., Munir, S., Nicoletti, F., Andersen, M.H., Straten, P., and Svane, I.M. (2015). Aberrant Expression of MHC Class II in Melanoma Attracts Inflammatory Tumor-Specific CD4+ T- Cells, Which Dampen CD8+ T-cell Antitumor Reactivity. *Cancer Research* 75, 3747–3759.
- Donia, M., Ellebaek, E., Andersen, M.H., Straten, P.T., and Svane, I.M. (2014a). Analysis of V δ 1 T cells in clinical grade melanoma-infiltrating lymphocytes. *Oncoimmunology* 1, 1297–1304.
- Donia, M., Hansen, M., Sendrup, S.L., Iversen, T.Z., Ellebaek, E., Andersen, M.H., Straten, P.T., and Svane, I.M. (2013). Methods to Improve Adoptive T-Cell Therapy for Melanoma: IFN- γ Enhances Anticancer Responses of Cell Products for Infusion. *Journal of Investigative Dermatology* 133, 545–552.
- Donia, M., Larsen, S.M., Met, Ö., and Svane, I.M. (2014b). Simplified protocol for clinical-grade tumor-infiltrating lymphocyte manufacturing with use of the Wave bioreactor. *Cytotherapy* 16, 1117–1120.
- Drake, C.G., Lipson, E.J., and Brahmer, J.R. (2014). Breathing new life into immunotherapy: review of melanoma, lung and kidney cancer. *Nat Rev Clin Oncol* 11, 24–37.
- Dudley, M.E. (2002). Cancer Regression and Autoimmunity in Patients After Clonal Repopulation with Antitumor Lymphocytes. *Science* 298, 850–854.

- Dudley, M.E. (2005). Adoptive Cell Transfer Therapy Following Non-Myeloablative but Lymphodepleting Chemotherapy for the Treatment of Patients With Refractory Metastatic Melanoma. *J. Clin. Oncol.* *23*, 2346–2357.
- Dudley, M.E., Gross, C.A., Langhan, M.M., Garcia, M.R., Sherry, R.M., Yang, J.C., Phan, G.Q., Kammula, U.S., Hughes, M.S., Citrin, D.E., et al. (2010). CD8+ enriched “young” tumor infiltrating lymphocytes can mediate regression of metastatic melanoma. *Clinical Cancer Research* *16*, 6122–6131.
- Dudley, M.E., Yang, J.C., Sherry, R., Hughes, M.S., Royal, R., Kammula, U., Robbins, P.F., Huang, J., Citrin, D.E., Leitman, S.F., et al. (2008). Adoptive cell therapy for patients with metastatic melanoma: evaluation of intensive myeloablative chemoradiation preparative regimens. *J. Clin. Oncol.* *26*, 5233–5239.
- Eisenhauer, E.A., Therasse, P., Bogaerts, J., Schwartz, L.H., Sargent, D., Ford, R., Dancey, J., Arbuck, S., Gwyther, S., Mooney, M., et al. (2009). New response evaluation criteria in solid tumours: Revised RECIST guideline (version 1.1). *European Journal of Cancer* *45*, 228–247.
- Ellebæk, E., Iversen, T., Junker, N., Donia, M., Engell-Noerregaard, L., Met, Ö., Hölmich, L., Andersen, R., Hadrup, S., Andersen, M., et al. (2012). Adoptive cell therapy with autologous tumor infiltrating lymphocytes and low-dose Interleukin-2 in metastatic melanoma patients. *J Transl Med* *10*, 169.
- Ely, L.K., Kjer-Nielsen, L., McCluskey, J., and Rossjohn, J. (2005). Structural studies on the alphabeta T-cell receptor. *IUBMB Life* *57*, 575–582.
- Emery, C.M., Vijayendran, K.G., Zipser, M.C., Sawyer, A.M., Niu, L., Kim, J.J., Hatton, C., Chopra, R., Oberholzer, P.A., Karpova, M.B., et al. (2009). MEK1 mutations confer resistance to MEK and B-RAF inhibition. *Proc. Natl. Acad. Sci. U.S.A.* *106*, 20411–20416.
- Emsley, P., and Cowtan, K. (2004). Coot: model-building tools for molecular graphics. *Acta Crystallographica. Section D, Biological Crystallography* *60*, 2126–2132.
- Erdmann, F., Lortet-Tieulent, J., Schüz, J., Zeeb, H., Greinert, R., Breitbart, E.W., and Bray, F. (2012). International trends in the incidence of malignant melanoma 1953-2008-are recent generations at higher or lower risk? *Int. J. Cancer* *132*, 385–400.
- Ewen, C.L., Kane, K.P., and Bleackley, R.C. (2012). A quarter century of granzymes. *Cell Death Differ.* *19*, 28–35.
- Fang, H., Ang, B., Xu, X., Huang, X., Wu, Y., Sun, Y., Wang, W., Li, N., Cao, X., and Wan, T. (2014). TLR4 is essential for dendritic cell activation and anti-tumor T-cell response enhancement by DAMPs released from chemically stressed cancer cells. *Cell. Mol. Immunol.* *11*, 150–159.
- Fang, H., Wu, Y., Huang, X., Wang, W., Ang, B., Cao, X., and Wan, T. (2011). Toll-like receptor 4 (TLR4) is essential for Hsp70-like protein 1 (HSP70L1) to activate dendritic cells and induce Th1 response. *J. Biol. Chem.* *286*, 30393–30400.
- Ferrone, S., and Marincola, F.M. (1995). Loss of HLA class I antigens by melanoma cells: molecular mechanisms, functional significance and clinical relevance. *Immunol. Today* *16*, 487–494.
- FitzGerald, M.G., Harkin, D.P., Silva-Arrieta, S., MacDonald, D.J., Lucchina, L.C., Unsal, H., O'Neill, E., Koh, J., Finkelstein, D.M., Isselbacher, K.J., et al. (1996). Prevalence of germ-line mutations in p16, p19ARF, and CDK4 in familial melanoma: analysis of a clinic-based population. *Proc. Natl. Acad. Sci. U.S.A.* *93*, 8541–8545.
- Fitzpatrick, T.B., Seiji, M., and McGugan, A.D. (1961). Melanin Pigmentation. *N. Engl. J. Med.* *265*, 328–332.
- Folch, G., and Lefranc, M.P. (2000). The human T cell receptor beta variable (TRBV) genes. *Exp. Clin. Immunogenet.* *17*, 42–54.
- Fossati, G., Anichini, A., Taramelli, D., Balsari, A., Gambacorti-Passerini, C., Kirkwood, J.M., and Parmiani, G. (1986). Immune response to autologous human melanoma: implication of class I and II MHC products. *Biochim. Biophys. Acta* *865*, 235–251.
- Foster, A.E., Dotti, G., Lu, A., Khalil, M., Brenner, M.K., Heslop, H.E., Rooney, C.M., and Bollard, C.M. (2008). Antitumor activity of EBV-specific T lymphocytes transduced with a dominant negative TGF-beta receptor. *Journal of Immunotherapy* *31*, 500–505.
- Friedman, K.M., Prieto, P.A., Devillier, L.E., Gross, C.A., Yang, J.C., Wunderlich, J.R., Rosenberg, S.A., and Dudley, M.E. (2012). Tumor-specific CD4+ melanoma tumor-infiltrating lymphocytes. *J. Immunother.* *35*, 400–408.
- Gandini, S., Sera, F., Cattaruzza, M.S., Pasquini, P., Picconi, O., Boyle, P., and Melchi, C.F. (2005). Meta-analysis of risk factors for cutaneous melanoma: II. Sun exposure. *European Journal of Cancer* *41*, 45–60.
- Gao, F.G., Khammanivong, V., Liu, W.J., Leggett, G.R., Frazer, I.H., and Fernando, G.J.P. (2002). Antigen-specific CD4+ T-cell help

is required to activate a memory CD8+ T cell to a fully functional tumor killer cell. *Cancer Research* 62, 6438–6441.

Garbe, C., Peris, K., Hauschild, A., Saiag, P., Middleton, M., Spatz, A., Grob, J.-J., Malvehy, J., Newton-Bishop, J., Alex, et al. (2010). Diagnosis and treatment of melanoma: European consensus-based interdisciplinary guideline. *European Journal of Cancer* 46, 270–283.

Garbe, C., Peris, K., Hauschild, A., Saiag, P., Middleton, M., Spatz, A., Grob, J.-J., Malvehy, J., Newton-Bishop, J., Stratigos, A., et al. (2012). Diagnosis and treatment of melanoma. European consensus-based interdisciplinary guideline--Update 2012. *Eur. J. Cancer* 48, 2375–2390.

Garcia, K.C., Adams, J.J., Feng, D., and Ely, L.K. (2009). The molecular basis of TCR germline bias for MHC is surprisingly simple. *Nature Immunology* 10, 143–147.

Gargett, T., Fraser, C.K., Dotti, G., Yvon, E.S., and Brown, M.P. (2015). BRAF and MEK inhibition variably affect GD2-specific chimeric antigen receptor (CAR) T-cell function in vitro. *J. Immunother.* 38, 12–23.

Gattinoni, L. (2005). Acquisition of full effector function in vitro paradoxically impairs the in vivo antitumor efficacy of adoptively transferred CD8+ T cells. *J. Clin. Invest.* 115, 1616–1626.

Germain, R.N. (1994). MHC-dependent antigen processing and peptide presentation: providing ligands for T lymphocyte activation. *Cell* 76, 287–299.

Gershenwald, J.E., Soong, S.-J., Balch, C.M., and Committee, O.B.O.T.A.J.C.O.C.A.M.S. (2010). 2010 TNM Staging System for Cutaneous Melanoma...and Beyond. *Ann Surg Oncol* 17, 1475–1477.

Gilham, D.E., Anderson, J., Bridgeman, J.S., Hawkins, R.E., Exley, M.A., Stauss, H., Maher, J., Pule, M., Sewell, A.K., Bendle, G., et al. (2015). Adoptive T-Cell Therapy for Cancer in the United Kingdom: A Review of Activity for the British Society of Gene and Cell Therapy Annual Meeting 2015. *Human Gene Therapy* 26, 276–285.

Gillespie, A.M., Rodgers, S., Wilson, A.P., Tidy, J., Rees, R.C., Coleman, R.E., and Murray, A.K. (1998). MAGE, BAGE and GAGE: tumour antigen expression in benign and malignant ovarian tissue. *Br. J. Cancer* 78, 816–821.

Giudicelli, V., Brochet, X., and Lefranc, M.-P. (2011). IMGT/V-QUEST: IMGT standardized analysis of the immunoglobulin (IG) and T cell receptor (TR) nucleotide sequences. *Cold Spring Harb Protoc* 2011, 695–715.

Gnjatic, S., Atanackovic, D., Jäger, E., Matsuo, M., Selvakumar, A., Altorki, N.K., Maki, R.G., Dupont, B., Ritter, G., Chen, Y.-T., et al. (2003). Survey of naturally occurring CD4+ T cell responses against NY-ESO-1 in cancer patients: correlation with antibody responses. *Proceedings of the National Academy of Sciences* 100, 8862–8867.

Godfrey, D.I., Uldrich, A.P., McCluskey, J., Rossjohn, J., and Moody, D.B. (2015). The burgeoning family of unconventional T cells. *Nature Immunology* 16, 1114–1123.

Godkin, A., Friede, T., Davenport, M., Stevanovic, S., Willis, A., Jewell, D., Hill, A., and Rammensee, H.G. (1997). Use of eluted peptide sequence data to identify the binding characteristics of peptides to the insulin-dependent diabetes susceptibility allele HLA-DQ8 (DQ 3.2). *International Immunology* 9, 905–911.

Goff, S.L., Smith, F.O., Klapper, J.A., Sherry, R., Wunderlich, J.R., Steinberg, S.M., White, D., Rosenberg, S.A., Dudley, M.E., and Yang, J.C. (2010). Tumor infiltrating lymphocyte therapy for metastatic melanoma: analysis of tumors resected for TIL. *J. Immunother.* 33, 840–847.

Gras, S., Burrows, S.R., Turner, S.J., Sewell, A.K., McCluskey, J., and Rossjohn, J. (2012). A structural voyage toward an understanding of the MHC-I-restricted immune response: lessons learned and much to be learned. *Immunological Reviews* 250, 61–81.

Guillaume, B., Chapiro, J., Stroobant, V., Colau, D., Van Holle, B., Parvizi, G., Bousquet-Dubouch, M.-P., Théate, I., Parmentier, N., and Van den Eynde, B.J. (2010). Two abundant proteasome subtypes that uniquely process some antigens presented by HLA class I molecules. *Proc. Natl. Acad. Sci. U.S.A.* 107, 18599–18604.

Haen, S.P., and Rammensee, H.-G. (2013). The repertoire of human tumor-associated epitopes — identification and selection of antigens and their application in clinical trials. *Current Opinion in Immunology* 25, 277–283.

Hammer, G.E., Gonzalez, F., James, E., Nolla, H., and Shastri, N. (2007). In the absence of aminopeptidase ERAAP, MHC class I molecules present many unstable and highly immunogenic peptides. *Nat Immunol* 8, 101–108.

Harding, C.V., and Unanue, E.R. (1990). Cellular mechanisms of antigen processing and the function of class I and II major histocompatibility complex molecules. *Cell Regul.* 1, 499–509.

- Haynes, B.F., and Heinly, C.S. (1995). Early human T cell development: analysis of the human thymus at the time of initial entry of hematopoietic stem cells into the fetal thymic microenvironment. *Journal of Experimental Medicine* *181*, 1445–1458.
- Heath, W.R., and Carbone, F.R. (2001). Cross-presentation in viral immunity and self-tolerance. *Nature Rev Immunol* *1*, 126–134.
- Henkart, P.A. (1994). Lymphocyte-mediated cytotoxicity: two pathways and multiple effector molecules. *Immunity* *1*, 343–346.
- Hernandez, C., Huebener, P., and Schwabe, R.F. (2016). Damage-associated molecular patterns in cancer: a double-edged sword. *Oncogene*.
- Hildemann, S.K., Eberlein, J., Davenport, B., Nguyen, T.T., Victorino, F., and Homann, D. (2013). High Efficiency of Antiviral CD4+ Killer T Cells. *PLoS One* *8*, e60420.
- Hinrichs, C.S., and Rosenberg, S.A. (2013). Exploiting the curative potential of adoptive T-cell therapy for cancer. *Immunol. Rev.* *257*, 56–71.
- Hinrichs, C.S., Borman, Z.A., Gattinoni, L., Yu, Z., Burns, W.R., Huang, J., Klebanoff, C.A., Johnson, L.A., Kerkar, S.P., Yang, S., et al. (2011). Human effector CD8+ T cells derived from naive rather than memory subsets possess superior traits for adoptive immunotherapy. *Blood* *117*, 808–814.
- Hodi, F.S. (2006). Well-defined melanoma antigens as progression markers for melanoma: insights into differential expression and host response based on stage. *Clinical Cancer Research* *12*, 673–678.
- Hodi, F.S., O'Day, S.J., McDermott, D.F., Weber, R.W., Sosman, J.A., Haanen, J.B., Gonzalez, R., Robert, C., Schadendorf, D., Hassel, J.C., et al. (2010). Improved survival with ipilimumab in patients with metastatic melanoma. *N. Engl. J. Med.* *363*, 711–723.
- Hodis, E., Watson, I.R., Kryukov, G.V., Arold, S.T., Imielinski, M., Theurillat, J.-P., Nickerson, E., Auclair, D., Li, L., Place, C., et al. (2012). A landscape of driver mutations in melanoma. *Cell* *150*, 251–263.
- Hogan, K.T., Coppola, M.A., Gatlin, C.L., Thompson, L.W., Shabanowitz, J., Hunt, D.F., Engelhard, V.H., Ross, M.M., and Slingluff, C.L. (2004). Identification of novel and widely expressed cancer/testis gene isoforms that elicit spontaneous cytotoxic T-lymphocyte reactivity to melanoma. *Cancer Research* *64*, 1157–1163.
- Hogquist, K.A., Jameson, S.C., and Bevan, M.J. (1994). The ligand for positive selection of T lymphocytes in the thymus. *Curr. Opin. Immunol.* *6*, 273–278.
- Holland, C.J., Cole, D.K., and Godkin, A. (2013). Re-Directing CD4(+) T Cell Responses with the Flanking Residues of MHC Class II-Bound Peptides: The Core is Not Enough. *Front. Immunol.* *4*, 172.
- Howard, K., and Mehnert, J.M. (2016). *Melanoma* (Cham: Springer International Publishing).
- Hu, Q., Bazemore Walker, C.R., Giraio, C., Opferman, J.T., Sun, J., Shabanowitz, J., Hunt, D.F., and Ashton-Rickardt, P.G. (1997). Specific recognition of thymic self-peptides induces the positive selection of cytotoxic T lymphocytes. *Immunity* *7*, 221–231.
- Huang, J., El-Gamil, M., Dudley, M.E., Li, Y.F., Rosenberg, S.A., and Robbins, P.F. (2004). T cells associated with tumor regression recognize frameshifted products of the CDKN2A tumor suppressor gene locus and a mutated HLA class I gene product. *The Journal of Immunology* *172*, 6057–6064.
- Huang, T., Zhuge, J., and Zhang, W.W. (2013). Sensitive detection of BRAF V600E mutation by Amplification Refractory Mutation System (ARMS)-PCR. *Biomark Res* *1*, 3.
- Hundemer, M., Schmidt, S., Condomines, M., Lupu, A., Hose, D., Moos, M., Cremer, F., Kleist, C., Terness, P., Belle, S., et al. (2006). Identification of a new HLA-A2-restricted T-cell epitope within HM1.24 as immunotherapy target for multiple myeloma. *Exp. Hematol.* *34*, 486–496.
- Hunder, N.N., Wallen, H., Cao, J., Hendricks, D.W., Reilly, J.Z., Rodmyre, R., Jungbluth, A., Gnjjatic, S., Thompson, J.A., and Yee, C. (2008). Treatment of metastatic melanoma with autologous CD4+ T cells against NY-ESO-1. *N. Engl. J. Med.* *358*, 2698–2703.
- Ikeda, H., Lethé, B., Lehmann, F., van Baren, N., Baurain, J.F., De Smet, C., Chambost, H., Vitale, M., Moretta, A., Boon, T., et al. (1997). Characterization of an antigen that is recognized on a melanoma showing partial HLA loss by CTL expressing an NK inhibitory receptor. *Immunity* *6*, 199–208.
- Irving, M., Zoete, V., Hebeisen, M., Schmid, D., Baumgartner, P., Guillaume, P., Romero, P., Speiser, D., Luescher, I., Rufer, N., et al. (2012). Interplay between T Cell Receptor Binding Kinetics and the Level of Cognate Peptide Presented by Major

- Histocompatibility Complexes Governs CD8+ T Cell Responsiveness. *Journal of Biological Chemistry* 287, 23068–23078.
- Ishida, Y., Agata, Y., Shibahara, K., and Honjo, T. (1992). Induced expression of PD-1, a novel member of the immunoglobulin gene superfamily, upon programmed cell death. *Embo J.* 11, 3887–3895.
- Itzhaki, O., Hovav, E., Ziporen, Y., Levy, D., Kubi, A., Zikich, D., Hershkovitz, L., Treves, A.J., Shalmon, B., Zippel, D., et al. (2011). Establishment and large-scale expansion of minimally cultured “young” tumor infiltrating lymphocytes for adoptive transfer therapy. *J. Immunother.* 34, 212–220.
- Janeway, C., and Murphy, K. (2011). *Janeway's Immunobiology* (8th edition) (Gardland Science).
- Janssen, E.M., Lemmens, E.E., Wolfe, T., Christen, U., Herrath, von, M.G., and Schoenberger, S.P. (2003). CD4+ T cells are required for secondary expansion and memory in CD8+ T lymphocytes. *Nature* 421, 852–856.
- Jäger, E., Chen, Y.T., Drijfhout, J.W., Karbach, J., Ringhoffer, M., Jäger, D., Arand, M., Wada, H., Noguchi, Y., Stockert, E., et al. (1998). Simultaneous humoral and cellular immune response against cancer-testis antigen NY-ESO-1: definition of human histocompatibility leukocyte antigen (HLA)-A2-binding peptide epitopes. *Journal of Experimental Medicine* 187, 265–270.
- Jiang, S., and Dong, C. (2013). A complex issue on CD4(+) T-cell subsets. *Immunol. Rev.* 252, 5–11.
- Jochems, C., and Schlom, J. (2011). Tumor-infiltrating immune cells and prognosis: the potential link between conventional cancer therapy and immunity. *Exp. Biol. Med. (Maywood)* 236, 567–579.
- Johnson, L.A., Morgan, R.A., Dudley, M.E., Cassard, L., Yang, J.C., Hughes, M.S., Kammula, U.S., Royal, R.E., Sherry, R.M., Wunderlich, J.R., et al. (2009). Gene therapy with human and mouse T-cell receptors mediates cancer regression and targets normal tissues expressing cognate antigen. *Blood* 114, 535–546.
- Joseph, R.W., Peddareddigari, V.R., Liu, P., Miller, P.W., Overwijk, W.W., Bekele, N.B., Ross, M.I., Lee, J.E., Gershenwald, J.E., Lucci, A., et al. (2011). Impact of clinical and pathologic features on tumor-infiltrating lymphocyte expansion from surgically excised melanoma metastases for adoptive T-cell therapy. *Clinical Cancer Research* 17, 4882–4891.
- Joyce, J.A., and Fearon, D.T. (2015). T cell exclusion, immune privilege, and the tumor microenvironment. *Science* 348, 74–80.
- Kalialis, L.V., Drzewiecki, K.T., and Klyver, H. (2009). Spontaneous regression of metastases from melanoma: review of the literature. *Melanoma Res.* 19, 275–282.
- Kawakami, Y., Dang, N., Wang, X., Tupesis, J., Robbins, P.F., Wang, R.F., Wunderlich, J.R., Yannelli, J.R., and Rosenberg, S.A. (2000). Recognition of shared melanoma antigens in association with major HLA-A alleles by tumor infiltrating T lymphocytes from 123 patients with melanoma. *Journal of Immunotherapy* 23, 17–27.
- Kawakami, Y., Eliyahu, S., Delgado, C.H., Robbins, P.F., Rivoltini, L., Topalian, S.L., Miki, T., and Rosenberg, S.A. (1994a). Cloning of the gene coding for a shared human melanoma antigen recognized by autologous T cells infiltrating into tumor. *Proceedings of the National Academy of Sciences of the United States of America* 91, 3515–3519.
- Kawakami, Y., Eliyahu, S., Delgado, C.H., Robbins, P.F., Sakaguchi, K., Appella, E., Yannelli, J.R., Adema, G.J., Miki, T., and Rosenberg, S.A. (1994b). Identification of a human melanoma antigen recognized by tumor-infiltrating lymphocytes associated with in vivo tumor rejection. *Proceedings of the National Academy of Sciences* 91, 6458–6462.
- Kawakami, Y., Eliyahu, S., Jennings, C., Sakaguchi, K., Kang, X., Southwood, S., Robbins, P., Sette, A., Appella, E., and Rosenberg, S. (1995). Recognition of multiple epitopes in the human melanoma antigen gp100 by tumor-infiltrating T lymphocytes associated with in vivo tumor regression. *Journal Immunology* 154, 3961–3968.
- Kawakami, Y., Eliyahu, S., Sakaguchi, K., Robbins, P.F., Rivoltini, L., Yannelli, J.R., Appella, E., and Rosenberg, S.A. (1994c). Identification of the immunodominant peptides of the MART-1 human melanoma antigen recognized by the majority of HLA-A2-restricted tumor infiltrating lymphocytes. *Journal of Experimental Medicine* 180, 347–352.
- Keir, M.E., Butte, M.J., Freeman, G.J., and Sharpe, A.H. (2008). PD-1 and its ligands in tolerance and immunity. *Annu. Rev. Immunol.* 26, 677–704.
- Kershaw, M.H., Wang, G., Westwood, J.A., Pachynski, R.K., Tiffany, H.L., Marincola, F.M., Wang, E., Young, H.A., Murphy, P.M., and Hwu, P. (2002). Redirecting migration of T cells to chemokine secreted from tumors by genetic modification with CXCR2. *Human Gene Therapy* 13, 1971–1980.
- Kim, H.-J., and Cantor, H. (2014). CD4 T-cell subsets and tumor immunity: the helpful and the not-so-helpful. *Cancer Immunology Research* 2, 91–98.

- Kim, T., Amaria, R.N., Spencer, C., Reuben, A., Cooper, Z.A., and Wargo, J.A. (2014). Combining targeted therapy and immune checkpoint inhibitors in the treatment of metastatic melanoma. *Cancer Biol Med* *11*, 237–246.
- Klebanoff, C.A., Acquavella, N., Yu, Z., and Restifo, N.P. (2011). Therapeutic cancer vaccines: are we there yet? *Immunol. Rev.* *239*, 27–44.
- Kloetzel, P.-M. (2004). The proteasome and MHC class I antigen processing. *Biochim. Biophys. Acta* *1695*, 225–233.
- Knuth, A., Danowski, B., Oettgen, H.F., and Old, L.J. (1984). T-cell-mediated cytotoxicity against autologous malignant melanoma: analysis with interleukin 2-dependent T-cell cultures. *Proceedings of the National Academy of Sciences* *81*, 3511–3515.
- Koshenkov, V.P., Broucek, J., and Kaufman, H.L. (2016). Surgical Management of Melanoma. *Cancer Treat. Res.* *167*, 149–179.
- Kreiter, S., Vormehr, M., van de Roemer, N., Diken, M., Löwer, M., Diekmann, J., Boegel, S., Schrörs, B., Vascotto, F., Castle, J.C., et al. (2015). Mutant MHC class II epitopes drive therapeutic immune responses to cancer. *Nature* *520*, 692–696.
- Kroemer, G., Galluzzi, L., Kepp, O., and Zitvogel, L. (2013). Immunogenic Cell Death in Cancer Therapy. *Annu. Rev. Immunol.* *31*, 51–72.
- Krogsgaard, M., Prado, N., Adams, E.J., He, X.-L., Chow, D.-C., Wilson, D.B., Garcia, K.C., and Davis, M.M. (2003). Evidence that structural rearrangements and/or flexibility during TCR binding can contribute to T cell activation. *Mol. Cell* *12*, 1367–1378.
- Kvistborg, P., Shu, C.J., Heemskerk, B., Fankhauser, M., Thru, C.A., Toebes, M., van Rooij, N., Linnemann, C., van Buuren, M.M., Urbanus, J.H., et al. (2012). TIL therapy broadens the tumor-reactive CD8+ T cell compartment in melanoma patients. *Oncol Immunology* *1*, 409–418.
- Kyewski, B., and Derbinski, J. (2004). Self-representation in the thymus: an extended view. *Nature Rev Immunol* *4*, 688–698.
- La Gruta, N.L., Turner, S.J., and Doherty, P.C. (2004). Hierarchies in cytokine expression profiles for acute and resolving influenza virus-specific CD8+ T cell responses: correlation of cytokine profile and TCR avidity. *The Journal of Immunology* *172*, 5553–5560.
- Lanitis, E., Irving, M., and Coukos, G. (2015). Targeting the tumor vasculature to enhance T cell activity. *Current Opinion in Immunology* *33*, 55–63.
- Laugel, B., Price, D.A., Milicic, A., and Sewell, A.K. (2007). CD8 exerts differential effects on the deployment of cytotoxic T lymphocyte effector functions. *Eur. J. Immunol.* *37*, 905–913.
- Lawrence, M.S., Stojanov, P., Polak, P., Kryukov, G.V., Cibulskis, K., Sivachenko, A., Carter, S.L., Stewart, C., Mermel, C.H., Roberts, S.A., et al. (2013). Mutational heterogeneity in cancer and the search for new cancer-associated genes. *Nature* *499*, 214–218.
- Lechler, R., Aichinger, G., and Lightstone, L. (1996). The endogenous pathway of MHC class II antigen presentation. *Immunol. Rev.* *151*, 51–79.
- Lee, K.H., Wang, E., Nielsen, M.B., Wunderlich, J., Migueles, S., Connors, M., Steinberg, S.M., Rosenberg, S.A., and Marincola, F.M. (1999). Increased vaccine-specific T cell frequency after peptide-based vaccination correlates with increased susceptibility to in vitro stimulation but does not lead to tumor regression. *The Journal of Immunology* *163*, 6292–6300.
- Lee, W., Jiang, Z., Liu, J., Haverty, P.M., Guan, Y., Stinson, J., Yue, P., Zhang, Y., Pant, K.P., Bhatt, D., et al. (2010). The mutation spectrum revealed by paired genome sequences from a lung cancer patient. *Nature* *465*, 473–477.
- Lefranc, M.P., Giudicelli, V., Ginestoux, C., Bodmer, J., Muller, W., Bontrop, R., Lemaître, M., Malik, A., Barbie, V., and Chaume, D. (1999). IMGT, the international ImMunoGeneTics database. *Nucleic Acids Research* *27*, 209–212.
- LeibundGut-Landmann, S., Waldburger, J.-M., Reis e Sousa, C., Acha-Orbea, H., and Reith, W. (2004). MHC class II expression is differentially regulated in plasmacytoid and conventional dendritic cells. *Nat Immunol* *5*, 899–908.
- Lennerz, V., Fatho, M., Gentilini, C., Frye, R.A., Lifke, A., Ferel, D., Wolfel, C., Huber, C., and Wolfel, T. (2005). The response of autologous T cells to a human melanoma is dominated by mutated neoantigens. *Proceedings of the National Academy of Sciences* *102*, 16013–16018.
- Lesterhuis, W.J., Schreiber, G., Scharenborg, N.M., Brouwer, H.M.-L.H., Gerritsen, M.-J.P., Croockewit, S., Coulie, P.G., Torensma, R., Adema, G.J., Figdor, C.G., et al. (2011). Wild-type and modified gp100 peptide-pulsed dendritic cell vaccination of advanced melanoma patients can lead to long-term clinical responses independent of the peptide used. *Cancer Immunol Immunother* *60*, 249–260.

- Leung, A.M., Hari, D.M., and Morton, D.L. (2012). Surgery for distant melanoma metastasis. *Cancer J* 18, 176–184.
- Li, H., Ye, C., Ji, G., and Han, J. (2012). Determinants of public T cell responses. *Cell Research* 22, 33–42.
- Li, Y., Liu, S., Hernandez, J., Vence, L., Hwu, P., and Radvanyi, L. (2010). MART-1-specific melanoma tumor-infiltrating lymphocytes maintaining CD28 expression have improved survival and expansion capability following antigenic restimulation in vitro. *J. Immunol.* 184, 452–465.
- Li MO, Sarkisian MR, Mehal WZ, Rakic P, Flavell RA. (2003). Phosphatidylserine receptor is required for clearance of apoptotic cells. *Science* 302:1560–63
- Lind, E.F., Prockop, S.E., Porritt, H.E., and Petrie, H.T. (2001). Mapping precursor movement through the postnatal thymus reveals specific microenvironments supporting defined stages of early lymphoid development. *Journal of Experimental Medicine* 194, 127–134.
- Lines, J.L., Pantazi, E., Mak, J., Sempere, L.F., Wang, L., O'Connell, S., Ceeraz, S., Suriawinata, A.A., Yan, S., Ernstoff, M.S., et al. (2014). VISTA is an immune checkpoint molecule for human T cells. *Cancer Research* 74, 1924–1932.
- Linette, G.P., Stadtmauer, E.A., Maus, M.V., Rapoport, A.P., Levine, B.L., Emery, L., Litzky, L., Bagg, A., Carreno, B.M., Cimino, P.J., et al. (2013). Cardiovascular toxicity and titin cross-reactivity of affinity-enhanced T cells in myeloma and melanoma. *Blood* 122, 863–871.
- Linnemann, C., Heemskerk, B., Kvistborg, P., Kluijn, R.J.C., Bolotin, D.A., Chen, X., Bresser, K., Nieuwland, M., Schotte, R., Michels, S., et al. (2013). High-throughput identification of antigen-specific TCRs by TCR gene capture. *Nat. Med.* 19, 1534–1541.
- Linnemann, C., van Buuren, M.M., Bies, L., Verdegaal, E.M.E., Schotte, R., Calis, J.J.A., Behjati, S., Velds, A., Hilkmann, H., Atmioui, D.E., et al. (2014). High-throughput epitope discovery reveals frequent recognition of neo-antigens by CD4+ T cells in human melanoma. *Nat. Med.* 21, 81–85.
- Lippolis, J.D., White, F.M., Marto, J.A., Luckey, C.J., Bullock, T.N.J., Shabanowitz, J., Hunt, D.F., and Engelhard, V.H. (2002). Analysis of MHC class II antigen processing by quantitation of peptides that constitute nested sets. *The Journal of Immunology* 169, 5089–5097.
- Lissina, A., Ladell, K., Skowera, A., Clement, M., Edwards, E., Seggewiss, R., van den Berg, H.A., Gostick, E., Gallagher, K., Jones, E., et al. (2009). Protein kinase inhibitors substantially improve the physical detection of T-cells with peptide-MHC tetramers. *Journal of Immunological Methods* 340, 11–24.
- Liu, J., Yuan, Y., Chen, W., Putra, J., Suriawinata, A.A., Schenk, A.D., Miller, H.E., Guleria, I., Barth, R.J., Huang, Y.H., et al. (2015). Immune-checkpoint proteins VISTA and PD-1 nonredundantly regulate murine T-cell responses. *Proc. Natl. Acad. Sci. U.S.A.* 112, 6682–6687.
- Liu, S., Riley, J., Rosenberg, S., and Parkhurst, M. (2006). Comparison of common gamma-chain cytokines, interleukin-2, interleukin-7, and interleukin-15 for the in vitro generation of human tumor-reactive T lymphocytes for adoptive cell transfer therapy. *Journal of Immunotherapy* 29, 284–293.
- Liuzzi, A.R., McLaren, J.E., Price, D.A., and Eberl, M. (2015). Early innate responses to pathogens: pattern recognition by unconventional human T-cells. *Curr. Opin. Immunol.* 36, 31–37.
- Lu, Y.C., Yao, X., Li, Y.F., El-Gamil, M., Dudley, M.E., Yang, J.C., Almeida, J.R., Douek, D.C., Samuels, Y., Rosenberg, S.A., et al. (2013). Mutated PPP1R3B Is Recognized by T Cells Used To Treat a Melanoma Patient Who Experienced a Durable Complete Tumor Regression. *The Journal of Immunology* 190, 6034–6042.
- Ma, C., Cheung, A.F., Chodon, T., Koya, R.C., Wu, Z., Ng, C., Avramis, E., Cochran, A.J., Witte, O.N., Baltimore, D., et al. (2013). Multifunctional T-cell Analyses to Study Response and Progression in Adoptive Cell Transfer Immunotherapy. *Cancer Discovery* 3, 418–429.
- Madura, F., Rizkallah, P.J., Holland, C.J., Fuller, A., Bulek, A., Godkin, A.J., Schauenburg, A.J., Cole, D.K., and Sewell, A.K. (2015). Structural basis for ineffective T-cell responses to MHC anchor residue-improved “heteroclitic” peptides. *Eur. J. Immunol.* 45, 584–591.
- Mali, P., Yang, L., Esvelt, K.M., Aach, J., Guell, M., DiCarlo, J.E., Norville, J.E., and Church, G.M. (2013). RNA-guided human genome engineering via Cas9. *Science* 339, 823–826.
- Malissen, B., Grégoire, C., Malissen, M., and Roncagalli, R. (2014). Integrative biology of T cell activation. *Nat Immunol* 15, 790–797.
- Mamedov, I.Z., Britanova, O.V., Zvyagin, I.V., Turchaninova, M.A., Bolotin, D.A., Putintseva, E.V., Lebedev, Y.B., and Chudakov,

- D.M. (2013). Preparing unbiased T-cell receptor and antibody cDNA libraries for the deep next generation sequencing profiling. *Frontiers in Immunology* *4*, 456.
- Marchand, M., van Baren, N., Weynants, P., Brichard, V., Dréno, B., Tessier, M.H., Rankin, E., Parmiani, G., Arienti, F., Humblet, Y., et al. (1999). Tumor regressions observed in patients with metastatic melanoma treated with an antigenic peptide encoded by gene MAGE-3 and presented by HLA-A1. *Int. J. Cancer* *80*, 219–230.
- Marincola, F.M., Jaffee, E.M., Hicklin, D.J., and Ferrone, S. (2000). Escape of human solid tumors from T-cell recognition: molecular mechanisms and functional significance. *Adv. Immunol.* *74*, 181–273.
- Marincola, F.M., Rivoltini, L., Salgaller, M.L., Player, M., and Rosenberg, S.A. (1996). Differential anti-MART-1/MelanA CTL activity in peripheral blood of HLA-A2 melanoma patients in comparison to healthy donors: evidence of in vivo priming by tumor cells. *J Immunother Emphasis Tumor Immunol* *19*, 266–277.
- Marrack, P., Rubtsova, K., Scott-Browne, J., and Kappler, J.W. (2008). T cell receptor specificity for major histocompatibility complex proteins. *Curr. Opin. Immunol.* *20*, 203–207.
- Marshall, N.B., and Swain, S.L. (2011). Cytotoxic CD4 T cells in antiviral immunity. *J. Biomed. Biotechnol.* *2011*, 954602–954608.
- Mason, D. (1998). A very high level of crossreactivity is an essential feature of the T-cell receptor. *Immunol. Today* *19*, 395–404.
- Mazzocchi, A., Belli, F., Mascheroni, L., Vegetti, C., Parmiani, G., and Anichini, A. (1994). Frequency of cytotoxic T lymphocyte precursors (CTLp) interacting with autologous tumor via the T-cell receptor: limiting dilution analysis of specific CTLp in peripheral blood and tumor-invaded lymph nodes of melanoma patients. *Int. J. Cancer* *58*, 330–339.
- Márquez-Rodas, I., Cerezuela, P., Soria, A., Berrocal, A., Riso, A., González-Cao, M., and Martín-Algarra, S. (2015). Immune checkpoint inhibitors: therapeutic advances in melanoma. *Ann Transl Med* *3*, 267.
- McCoy, A., Grosse-Kunstleve, R., Adams, P., Winn, M., Storoni, L., and Read, R. (2007). Phaser crystallographic software. *Journal of Applied Crystallography* *40*, 658–674.
- McCoy, K.D., and Le Gros, G. (1999). The role of CTLA-4 in the regulation of T cell immune responses. *Immunol. Cell Biol.* *77*, 1–10.
- McGargill, M.A., Derbinski, J.M., and Hogquist, K.A. (2000). Receptor editing in developing T cells. *Nat Immunol* *1*, 336–341.
- McGranahan, N., Furness, A.J.S., Rosenthal, R., Ramskov, S., Lyngaa, R., Saini, S.K., Jamal-Hanjani, M., Wilson, G.A., Birkbak, N.J., Hiley, C.T., et al. (2016). Clonal neoantigens elicit T cell immunoreactivity and sensitivity to immune checkpoint blockade. *Science* *351*, 1463–1469.
- McMahan, R.H. (2006). Relating TCR-peptide-MHC affinity to immunogenicity for the design of tumor vaccines. *J. Clin. Invest.* *116*, 2543–2551.
- Melief, C.J.M., van Hall, T., Arens, R., Ossendorp, F., and van der Burg, S.H. (2015). Therapeutic cancer vaccines. *J. Clin. Invest.* *125*, 3401–3412.
- Mellman, I., Coukos, G., and Dranoff, G. (2011). Cancer immunotherapy comes of age. *Nature* *480*, 480–489.
- Mendez, R., Aptsiauri, N., del Campo, A., Maleno, I., Cabrera, T., Ruiz-Cabello, F., Garrido, F., and Garcia-Lora, A. (2009). HLA and melanoma: multiple alterations in HLA class I and II expression in human melanoma cell lines from ESTDAB cell bank. *Cancer Immunology, Immunotherapy* *58*, 1507–1515.
- Mescher, M.F., Curtsinger, J.M., Agarwal, P., Casey, K.A., Gerner, M., Hammerbeck, C.D., Popescu, F., and Xiao, Z. (2006). Signals required for programming effector and memory development by CD8+ T cells. *Immunol. Rev.* *211*, 81–92.
- Metzker, M.L. (2010). Sequencing technologies - the next generation. *Nat. Rev. Genet.* *11*, 31–46.
- Miles, J.J., Douek, D.C., and Price, D.A. (2011a). Bias in the $\alpha\beta$ T-cell repertoire: implications for disease pathogenesis and vaccination. *Immunol. Cell Biol.* *89*, 375–387.
- Miles, K.M., Miles, J.J., Madura, F., Sewell, A.K., and Cole, D.K. (2011b). Real time detection of peptide-MHC dissociation reveals that improvement of primary MHC-binding residues can have a minimal, or no, effect on stability. *Molecular Immunology* *48*, 728–732.
- Miller, J.F. (1961). Analysis of the thymus influence in leukaemogenesis. *Nature* *191*, 248–249.

- Moretti, S., Massobrio, R., Brogelli, L., Novelli, M., Giannotti, B., and Bernengo, M.G. (1990). Ki67 antigen expression correlates with tumor progression and HLA-DR antigen expression in melanocytic lesions. *J. Invest. Dermatol.* *95*, 320–324.
- Morgan, R.A., Chinnasamy, N., Abate-Daga, D., Gros, A., Robbins, P.F., Zheng, Z., Dudley, M.E., Feldman, S.A., Yang, J.C., Sherry, R.M., et al. (2013). Cancer regression and neurological toxicity following anti-MAGE-A3 TCR gene therapy. *J. Immunother.* *36*, 133–151.
- Morgan, R.A., Dudley, M.E., Wunderlich, J.R., Hughes, M.S., Yang, J.C., Sherry, R.M., Royal, R.E., Topalian, S.L., Kammula, U.S., Restifo, N.P., et al. (2006). Cancer regression in patients after transfer of genetically engineered lymphocytes. *Science* *314*, 126–129.
- Moudgil, K.D., Wang, J., Yeung, V.P., and Sercarz, E.E. (1998). Heterogeneity of the T cell response to immunodominant determinants within hen eggwhite lysozyme of individual syngeneic hybrid F1 mice: implications for autoimmunity and infection. *The Journal of Immunology* *161*, 6046–6053.
- Mourmouras, V., Biagioli, M., Miracco, C., Luzi, P., Tosi, P., Cosci, E., Monciatti, I., Mannucci, S., and Rubegni, P. (2007). Utility of tumour-infiltrating CD25+FOXP3+ regulatory T cell evaluation in predicting local recurrence in vertical growth phase cutaneous melanoma. *Oncology Reports*.
- Mukherji, B., and MacAlister, T.J. (1983). Clonal analysis of cytotoxic T cell response against human melanoma. *Journal of Experimental Medicine* *158*, 240–245.
- Murshudov, G.N., Vagin, A.A., and Dodson, E.J. (1997). Refinement of macromolecular structures by the maximum-likelihood method. *Acta Crystallographica. Section D, Biological Crystallography* *53*, 240–255.
- Nazarian, R., Shi, H., Wang, Q., Kong, X., Koya, R.C., Lee, H., Chen, Z., Lee, M.-K., Attar, N., Sazegar, H., et al. (2010). Melanomas acquire resistance to B-RAF(V600E) inhibition by RTK or N-RAS upregulation. *Nature* *468*, 973–977.
- Nishimura, T., Iwakabe, K., Sekimoto, M., Ohmi, Y., Yahata, T., Nakui, M., Sato, T., Habu, S., Tashiro, H., Sato, M., et al. (1999). Distinct role of antigen-specific T helper type 1 (Th1) and Th2 cells in tumor eradication in vivo. *Journal of Experimental Medicine* *190*, 617–627.
- Novellino, L., Castelli, C., and Parmiani, G. (2005). A listing of human tumor antigens recognized by T cells: March 2004 update. *Cancer Immunol Immunother* *54*, 187–207.
- Oettinger, M.A., Schatz, D.G., Gorka, C., and Baltimore, D. (1990). RAG-1 and RAG-2, adjacent genes that synergistically activate V(D)J recombination. *Science* *248*, 1517–1523.
- Ophir, E., Bobisse, S., Coukos, G., Alex, Harari, A., Harari, R., Kandalaft, L.E., K, L.E., and alaft (2015). Personalized approaches to active immunotherapy in cancer. *Biochimica Et Biophysica Acta* –.
- Ostrand-Rosenberg, S. (2008). Immune surveillance: a balance between protumor and antitumor immunity. *Curr. Opin. Genet. Dev.* *18*, 11–18.
- Overwijk, W.W., and Restifo, N.P. (2000). Autoimmunity and the immunotherapy of cancer: targeting the "self" to destroy the "other". *Crit. Rev. Immunol.* *20*, 433–450.
- Overwijk, W.W., Tsung, A., Irvine, K.R., Parkhurst, M.R., Goletz, T.J., Tsung, K., Carroll, M.W., Liu, C., Moss, B., Rosenberg, S.A., et al. (1998). gp100/pm17 is a murine tumor rejection antigen: induction of "self"-reactive, tumoricidal T cells using high-affinity, altered peptide ligand. *Journal of Experimental Medicine* *188*, 277–286.
- Pamer, E., and Cresswell, P. (1998). Mechanisms of MHC class I--restricted antigen processing. *Annu. Rev. Immunol.* *16*, 323–358.
- Pardoll, D.M. (2012). The blockade of immune checkpoints in cancer immunotherapy. *Nat Rev Cancer* *12*, 252–264.
- Parish, I.A., and Kaech, S.M. (2009). Diversity in CD8(+) T cell differentiation. *Curr. Opin. Immunol.* *21*, 291–297.
- Parker, K., Bednarek, M., Hull, L., Utz, U., Cunningham, B., Zweierink, H., Biddison, W., and Coligan, J. (1992). Sequence motifs important for peptide binding to the human MHC class I molecule, HLA-A2. *Journal Immunology* *149*, 3580–3587.
- Parkhurst, M.R., Salgaller, M.L., Southwood, S., Robbins, P.F., Sette, A., Rosenberg, S.A., and Kawakami, Y. (1996). Improved induction of melanoma-reactive CTL with peptides from the melanoma antigen gp100 modified at HLA-A*0201-binding residues. *The Journal of Immunology* *157*, 2539–2548.
- Parnas, O., Jovanovic, M., Eisenhaure, T.M., Herbst, R.H., Dixit, A., Ye, C.J., Przybylski, D., Platt, R.J., Tirosh, I., Sanjana, N.E., et

- al. (2015). A Genome-wide CRISPR Screen in Primary Immune Cells to Dissect Regulatory Networks. *Cell* *162*, 675–686.
- Pass, H.A., Schwarz, S.L., Wunderlich, J.R., and Rosenberg, S.A. (1998). Immunization of patients with melanoma peptide vaccines: immunologic assessment using the ELISPOT assay. *Cancer J Sci Am* *4*, 316–323.
- Paulos, C.M., Wrzesinski, C., Kaiser, A., Hinrichs, C.S., Chieppa, M., Cassard, L., Palmer, D.C., Boni, A., Muranski, P., Yu, Z., et al. (2007). Microbial translocation augments the function of adoptively transferred self/tumor-specific CD8⁺ T cells via TLR4 signaling. *J. Clin. Invest.* *117*, 2197–2204.
- Peng, W., Ye, Y., Rabinovich, B.A., Liu, C., Lou, Y., Zhang, M., Whittington, M., Yang, Y., Overwijk, W.W., Lizée, G., et al. (2010). Transduction of tumor-specific T cells with CXCR2 chemokine receptor improves migration to tumor and antitumor immune responses. *Clinical Cancer Research* *16*, 5458–5468.
- Perez-Diez, A., Joncker, N.T., Choi, K., Chan, W.F.N., Anderson, C.C., Lantz, O., and Matzinger, P. (2007). CD4 cells can be more efficient at tumor rejection than CD8 cells. *Blood* *109*, 5346–5354.
- Phan, G.Q., Attia, P., Steinberg, S.M., White, D.E., and Rosenberg, S.A. (2001). Factors associated with response to high-dose interleukin-2 in patients with metastatic melanoma. *J. Clin. Oncol.* *19*, 3477–3482.
- Pilon-Thomas, S., Kuhn, L., Ellwanger, S., Janssen, W., Royster, E., Marzban, S., Kudchadkar, R., Zager, J., Gibney, G., Sondak, V.K., et al. (2012). Efficacy of adoptive cell transfer of tumor-infiltrating lymphocytes after lymphopenia induction for metastatic melanoma. *J. Immunother.* *35*, 615–620.
- Pinto, S., Sommermeyer, D., Michel, C., Wilde, S., Schendel, D., Uckert, W., Blankenstein, T., and Kyewski, B. (2014). Misinitiation of intrathymic MART-1 transcription and biased TCR usage explain the high frequency of MART-1-specific T cells. *Eur. J. Immunol.* *44*, 2811–2821.
- Pittet, M.J., Speiser, D.E., Liénard, D., Valmori, D., Guillaume, P., Dutoit, V., Rimoldi, D., Lejeune, F., Cerottini, J.C., and Romero, P. (2001). Expansion and functional maturation of human tumor antigen-specific CD8⁺ T cells after vaccination with antigenic peptide. *Clinical Cancer Research* *7*, 796s–803s.
- Plonka, P.M., Passeron, T., Brenner, M., Tobin, D.J., Shibahara, S., Thomas, A., Slominski, A., Kadakara, A.L., Hershkovitz, D., Peters, E., et al. (2009). What are melanocytes really doing all day long...? *Experimental Dermatology* *18*, 799–819.
- Polak, M.E., Borthwick, N.J., Gabriel, F.G., Johnson, P., Higgins, B., Hurren, J., McCormick, D., Jager, M.J., and Cree, I.A. (2007). Mechanisms of local immunosuppression in cutaneous melanoma. *Br. J. Cancer* *96*, 1879–1887.
- Potts, W.K., and Slev, P.R. (1995). Pathogen-based models favoring MHC genetic diversity. *Immunol. Rev.* *143*, 181–197.
- Price, D.A., Sewell, A.K., Dong, T., Tan, R., Goulder, P.J., Rowland-Jones, S.L., and Phillips, R.E. (1998). Antigen-specific release of beta-chemokines by anti-HIV-1 cytotoxic T lymphocytes. *Curr. Biol.* *8*, 355–358.
- Probst-Kepper, M., Stroobant, V., Kridel, R., Gaugler, B., Landry, C., Brasseur, F., Cosyns, J.P., Weyand, B., Boon, T., and Van Den Eynde, B.J. (2001). An alternative open reading frame of the human macrophage colony-stimulating factor gene is independently translated and codes for an antigenic peptide of 14 amino acids recognized by tumor-infiltrating CD8 T lymphocytes. *Journal of Experimental Medicine* *193*, 1189–1198.
- Quezada, S.A., Simpson, T.R., Peggs, K.S., Merghoub, T., Vider, J., Fan, X., Blasberg, R., Yagita, H., Muranski, P., Antony, P.A., et al. (2010). Tumor-reactive CD4⁺ T cells develop cytotoxic activity and eradicate large established melanoma after transfer into lymphopenic hosts. *Journal of Experimental Medicine* *207*, 637–650.
- Radka, S.F., Charron, D.J., and Brodsky, F.M. (1986). Class II molecules of the major histocompatibility complex considered as differentiation markers. *Hum. Immunol.* *16*, 390–400.
- Radvanyi, L.G., Bernatchez, C., Zhang, M., Fox, P.S., Miller, P., Chacon, J., Wu, R., Lizée, G., Mahoney, S., Alvarado, G., et al. (2012). Specific Lymphocyte Subsets Predict Response to Adoptive Cell Therapy Using Expanded Autologous Tumor-Infiltrating Lymphocytes in Metastatic Melanoma Patients. *Clinical Cancer Research* *18*, 6758–6770.
- Raman, M.C.C., Rizkallah, P.J., Simmons, R., Donnellan, Z., Dukes, J., Bossi, G., Le Provost, G.S., Todorov, P., Baston, E., Hickman, E., et al. (2016). Direct molecular mimicry enables off-target cardiovascular toxicity by an enhanced affinity TCR designed for cancer immunotherapy. *Sci Rep* *6*, 18851.
- Rammensee, H.G., Fink, P.J., and Bevan, M.J. (1984). Functional clonal deletion of class I-specific cytotoxic T lymphocytes by veto cells that express antigen. *The Journal of Immunology* *133*, 2390–2396.
- Rammensee, H.G., Friede, T., and Stevanović, S. (1995). MHC ligands and peptide motifs: first listing. *Immunogenetics* *41*, 178–228.

- Raposo, G., and Marks, M.S. (2007). Melanosomes — dark organelles enlighten endosomal membrane transport. *Nature Reviews Molecular Cell Biology* 8, 786–797.
- Ratner, A., and Clark, W.R. (1993). Role of TNF-alpha in CD8+ cytotoxic T lymphocyte-mediated lysis. *The Journal of Immunology* 150, 4303–4314.
- Real, L.M., Jimenez, P., Kirkin, A., Serrano, A., García, A., Cantón, J., Zeuthen, J., Garrido, F., and Ruiz-Cabello, F. (2001). Multiple mechanisms of immune evasion can coexist in melanoma tumor cell lines derived from the same patient. *Cancer Immunol Immunother* 49, 621–628.
- Reed, S.G., Orr, M.T., and Fox, C.B. (2013). Key roles of adjuvants in modern vaccines. *Nat Cancer Rev* 19, 1597–1608.
- Reith, W., LeibundGut-Landmann, S., and Waldburger, J.-M. (2005). Regulation of MHC class II gene expression by the class II transactivator. *Nature Rev Immunol* 5, 793–806.
- Ribas, A., Timmerman, J.M., Butterfield, L.H., and Economou, J.S. (2003). Determinant spreading and tumor responses after peptide-based cancer immunotherapy. *Trends Immunol.* 24, 58–61.
- Riberdy, J.M., Newcomb, J.R., Surman, M.J., Barbosa, J.A., and Cresswell, P. (1992). HLA-DR molecules from an antigen-processing mutant cell line are associated with invariant chain peptides. *Nature* 360, 474–477.
- Ritter, A.T., Asano, Y., Stinchcombe, J.C., Dieckmann, N.M.G., Chen, B.-C., Gawden-Bone, C., van Engelenburg, S., Legant, W., Gao, L., Davidson, M.W., et al. (2015). Actin depletion initiates events leading to granule secretion at the immunological synapse. *Immunity* 42, 864–876.
- Rivoltini, L., Kawakami, Y., Sakaguchi, K., Southwood, S., Sette, A., Robbins, P.F., Marincola, F.M., Salgaller, M.L., Yannelli, J.R., and Appella, E. (1995). Induction of tumor-reactive CTL from peripheral blood and tumor-infiltrating lymphocytes of melanoma patients by in vitro stimulation with an immunodominant peptide of the human melanoma antigen MART-1. *Journal Immunology* 154, 2257–2265.
- Rivoltini, L., Squarcina, P., Loftus, D.J., Castelli, C., Tarsini, P., Mazzocchi, A., Rini, F., Viggiano, V., Belli, F., and Parmiani, G. (1999). A superagonist variant of peptide MART1/Melan A27-35 elicits anti-melanoma CD8+ T cells with enhanced functional characteristics: implication for more effective immunotherapy. *Cancer Research* 59, 301–306.
- Robbins, P.F., Dudley, M.E., Wunderlich, J., El-Gamil, M., Li, Y.F., Zhou, J., Huang, J., Powell, D.J., and Rosenberg, S.A. (2004). Cutting edge: persistence of transferred lymphocyte clonotypes correlates with cancer regression in patients receiving cell transfer therapy. *The Journal of Immunology* 173, 7125–7130.
- Robbins, P.F., El-Gamil, M., Li, Y.F., Zeng, G., Dudley, M., and Rosenberg, S.A. (2002). Multiple HLA class II-restricted melanocyte differentiation antigens are recognized by tumor-infiltrating lymphocytes from a patient with melanoma. *The Journal of Immunology* 169, 6036–6047.
- Robbins, P.F., Li, Y.F., El-Gamil, M., Zhao, Y., Wargo, J.A., Zheng, Z., Xu, H., Morgan, R.A., Feldman, S.A., Johnson, L.A., et al. (2008). Single and dual amino acid substitutions in TCR CDRs can enhance antigen-specific T cell functions. *Journal Immunology* 180, 6116–6131.
- Robbins, P.F., Lu, Y.-C., El-Gamil, M., Li, Y.F., Gross, C., Gartner, J., Lin, J.C., Teer, J.K., Clifton, P., Tycksen, E., et al. (2013). Mining exomic sequencing data to identify mutated antigens recognized by adoptively transferred tumor-reactive T cells. *Nat Cancer Rev* 19, 747–752.
- Robbins, P.F., Morgan, R.A., Feldman, S.A., Yang, J.C., Sherry, R.M., Dudley, M.E., Wunderlich, J.R., Nahvi, A.V., Helman, L.J., Mackall, C.L., et al. (2011). Tumor regression in patients with metastatic synovial cell sarcoma and melanoma using genetically engineered lymphocytes reactive with NY-ESO-1. *J. Clin. Oncol.* 29, 917–924.
- Robert, C., Ribas, A., Wolchok, J.D., Hodi, F.S., Hamid, O., Kefford, R., Weber, J.S., Joshua, A.M., Hwu, W.-J., Gangadhar, T.C., et al. (2014). Anti-programmed-death-receptor-1 treatment with pembrolizumab in ipilimumab-refractory advanced melanoma: a randomised dose-comparison cohort of a phase 1 trial. *Lancet* 384, 1109–1117.
- Robert, C., Thomas, L., Bondarenko, I., O'Day, S., Weber, J., Garbe, C., Lebbé, C., Baurain, J.-F., Testori, A., Grob, J.-J., et al. (2011). Ipilimumab plus Dacarbazine for Previously Untreated Metastatic Melanoma. *N. Engl. J. Med.* 364, 2517–2526.
- Robila, V., Ostankovitch, M., Altrich-Vanlith, M.L., Alex, Theos, A.C., Theos, E.C., Drover, S., Marks, M.S., Restifo, N., and Engelhard, V.H. (2008). MHC class II presentation of gp100 epitopes in melanoma cells requires the function of conventional endosomes and is influenced by melanosomes. *Journal Immunology* 181, 7843–7852.
- Robinson, J., and Marsh, S.G.E. (2003). HLA informatics. Accessing HLA sequences from sequence databases. *Methods Mol. Biol.* 210, 3–21.

- Romero, P., Dunbar, P.R., Valmori, D., Pittet, M., Ogg, G.S., Rimoldi, D., Chen, J.L., Liénard, D., Cerottini, J.C., and Cerundolo, V. (1998). Ex vivo staining of metastatic lymph nodes by class I major histocompatibility complex tetramers reveals high numbers of antigen-experienced tumor-specific cytolytic T lymphocytes. *Journal of Experimental Medicine* *188*, 1641–1650.
- Romero, P., Gervois, N., Schneider, J., Escobar, P., Valmori, D., Pannetier, C., Steinle, A., Wolfel, T., Liénard, D., Brichard, V., et al. (1997). Cytolytic T lymphocyte recognition of the immunodominant HLA-A*0201-restricted Melan-A/MART-1 antigenic peptide in melanoma. *The Journal of Immunology* *159*, 2366–2374.
- Romero, P., Cerottini, J.-C., and Speiser, D.E. (2006). The human T cell response to melanoma antigens. *Advances in Immunology* *92*, 187–224.
- Romero, P., Valmori, D., Pittet, M.J., Zippelius, A., Rimoldi, D., Lévy, F., Dutoit, V., Ayyoub, M., Rubio-Godoy, V., Michelin, O., et al. (2002). Antigenicity and immunogenicity of Melan-A/MART-1 derived peptides as targets for tumor reactive CTL in human melanoma. *Immunol. Rev.* *188*, 81–96.
- Rosenberg, S.A., Packard, B.S., Aebersold, P.M., Solomon, D., Topalian, S.L., Toy, S.T., Simon, P., Lotze, M.T., Yang, J.C., and Seipp, C.A. (1988). Use of tumor-infiltrating lymphocytes and interleukin-2 in the immunotherapy of patients with metastatic melanoma. A preliminary report. *N. Engl. J. Med.* *319*, 1676–1680.
- Rosenberg, S.A., Yang, J.C., Schwartzentruber, D.J., Hwu, P., Marincola, F.M., Topalian, S.L., Seipp, C.A., Einhorn, J.H., White, D.E., and Steinberg, S.M. (1999). Prospective randomized trial of the treatment of patients with metastatic melanoma using chemotherapy with cisplatin, dacarbazine, and tamoxifen alone or in combination with interleukin-2 and interferon alfa-2b. *J. Clin. Oncol.* *17*, 968–975.
- Rosenberg, S.A., Yang, J.C., Sherry, R.M., Kammula, U.S., Hughes, M.S., Phan, G.Q., Citrin, D.E., Restifo, N.P., Robbins, P.F., Wunderlich, J.R., et al. (2011). Durable Complete Responses in Heavily Pretreated Patients with Metastatic Melanoma Using T-Cell Transfer Immunotherapy. *Clinical Cancer Research* *17*, 4550–4557.
- Rosenberg, S.A., Yannelli, J.R., Yang, J.C., Topalian, S.L., Schwartzentruber, D.J., Weber, J.S., Parkinson, D.R., Seipp, C.A., Einhorn, J.H., and White, D.E. (1994). Treatment of patients with metastatic melanoma with autologous tumor-infiltrating lymphocytes and interleukin 2. *J. Natl. Cancer Inst.* *86*, 1159–1166.
- Rosenberg, S.A., Yang, J.C., and Restifo, N.P. (2004). Cancer immunotherapy: moving beyond current vaccines. *Nature Medicine* *10*, 909–915.
- Rosenberg, S.A., Restifo, N.P., Yang, J.C., Morgan, R.A., and Dudley, M.E. (2008). Adoptive cell transfer: a clinical path to effective cancer immunotherapy. *Nature Reviews Cancer* *8*, 299–308.
- Rothenberg, E.V., Moore, J.E., and Yui, M.A. (2008). Launching the T-cell-lineage developmental programme. *Nature Rev Immunol* *8*, 9–21.
- Rudolph, M.G., Stanfield, R.L., and Wilson, I.A. (2006). How TCRs bind MHCs, peptides, and coreceptors. *Annu. Rev. Immunol.* *24*, 419–466.
- Ruiter, D.J., Bergman, W., Welvaart, K., Scheffer, E., van Vloten, W.A., Russo, C., and Ferrone, S. (1984). Immunohistochemical analysis of malignant melanomas and nevocellular nevi with monoclonal antibodies to distinct monomorphic determinants of HLA antigens. *Cancer Research* *44*, 3930–3935.
- Ruppert, J., Sidney, J., Celis, E., Kubo, R.T., Grey, H.M., and Sette, A. (1993). Prominent role of secondary anchor residues in peptide binding to HLA-A2.1 molecules. *Cell* *74*, 929–937.
- Sakaguchi, S., Sakaguchi, N., Shimizu, J., Yamazaki, S., Sakihama, T., Itoh, M., Kuniyasu, Y., Nomura, T., Toda, M., and Takahashi, T. (2001). Immunologic tolerance maintained by CD25+ CD4+ regulatory T cells: their common role in controlling autoimmunity, tumor immunity, and transplantation tolerance. *Immunol. Rev.* *182*, 18–32.
- Sakaguchi, S. (2004). Naturally arising CD4+ regulatory t cells for immunologic self-tolerance and negative control of immune responses. *Annu. Rev. Immunol.* *22*, 531–562.
- Salgaller, M.L., Marincola, F.M., Cormier, J.N., and Rosenberg, S.A. (1996). Immunization against epitopes in the human melanoma antigen gp100 following patient immunization with synthetic peptides. *Cancer Research* *56*, 4749–4757.
- Sander, J.D., and Joung, J.K. (2014). CRISPR-Cas systems for editing, regulating and targeting genomes. *Nat. Biotechnol.* *32*, 347–355.
- Sanderson, C.J. (1976). The mechanism of T cell mediated cytotoxicity. I. The release of different cell components. *Proc. R. Soc. Lond., B, Biol. Sci.* *192*, 221–239.

- Sánchez-Rivera, F.J., and Jacks, T. (2015). Applications of the CRISPR–Cas9 system in cancer biology. *Nat Rev Cancer* 15, 387–395.
- Scaffidi P, Misteli T, Bianchi ME. (2002). Release of chromatin protein HMGB1 by necrotic cells triggers inflammation. *Nature* 418:191–95
- Schatz, D.G., Oettinger, M.A., and Baltimore, D. (1989). The V(D)J recombination activating gene, RAG-1. *Cell* 59, 1035–1048.
- Scheibenbogen, C., Schmittel, A., Keilholz, U., Allgäuer, T., Hofmann, U., Max, R., Thiel, E., and Schadendorf, D. (2000). Phase 2 trial of vaccination with tyrosinase peptides and granulocyte-macrophage colony-stimulating factor in patients with metastatic melanoma. *Journal of Immunotherapy* 23, 275–281.
- Schmid, D.A., Irving, M.B., Posevitz, V., Hebeisen, M., Posevitz-Fejfar, A., Sarria, J.-C.F., Gomez-Eerland, R., Thome, M., Schumacher, T.N.M., Romero, P., et al. (2010). Evidence for a TCR affinity threshold delimiting maximal CD8 T cell function. *J. Immunol.* 184, 4936–4946.
- Schmidt, S.M., Schag, K., Müller, M.R., Weck, M.M., Appel, S., Kanz, L., Grünebach, F., and Brossart, P. (2003). Survivin is a shared tumor-associated antigen expressed in a broad variety of malignancies and recognized by specific cytotoxic T cells. *Blood* 102, 571–576.
- Schumacher, T.N., and Schreiber, R.D. (2015). Neoantigens in cancer immunotherapy. *Science* 348, 69–74.
- Seliger, B., Ruiz-Cabello, F., and Garrido, F. (2008). IFN inducibility of major histocompatibility antigens in tumors. *Adv. Cancer Res.* 101, 249–276.
- Serana, F., Sottini, A., Caimi, L., Palermo, B., Natali, P.G., Nisticò, P., and Imberti, L. (2009). Identification of a public CDR3 motif and a biased utilization of T-cell receptor V beta and J beta chains in HLA-A2/Melan-A-specific T-cell clonotypes of melanoma patients. *J Transl Med* 7, 21.
- Sercarz, E.E., and Maverakis, E. (2003). Mhc-guided processing: binding of large antigen fragments. *Nature Rev Immunol* 3, 621–629.
- Serrone, L., Zeuli, M., Sega, F.M., and Cognetti, F. (2000). Dacarbazine-based chemotherapy for metastatic melanoma: thirty-year experience overview. *J. Exp. Clin. Cancer Res.* 19, 21–34.
- Serwold, T., Gonzalez, F., Kim, J., Jacob, R., and Shastri, N. (2002). ERAAP customizes peptides for MHC class I molecules in the endoplasmic reticulum. *Nature* 419, 480–483.
- Sewell, A.K. (2012). Why must T cells be cross-reactive? *Nature Rev Immunol* 12, 669–677.
- Silva-Santos, B., Serre, K., and Norell, H. (2015). $\gamma\delta$ T cells in cancer. *Nature Rev Immunol* 15, 683–691.
- Simpson, A.J.G., Caballero, O.L., Jungbluth, A., Chen, Y.-T., and Old, L.J. (2005). Cancer/testis antigens, gametogenesis and cancer. *Nat Rev Cancer* 5, 615–625.
- Skipper, J.C.A., Gulden, P.H., Hendrickson, R.C., Harthun, N., Caldwell, J.A., Shabanowitz, J., Engelhard, V.H., Hunt, D.F., and Slingluff, C.L. (1999). Mass-spectrometric evaluation of HLA-A*0201-associated peptides identifies dominant naturally processed forms of CTL epitopes from MART-1 and gp100. *Int. J. Cancer* 82, 669–677.
- Slifka, M.K., Rodriguez, F., and Whitton, J.L. (1999). Rapid on/off cycling of cytokine production by virus-specific CD8+ T cells. *Nature* 401, 76–79.
- Slingluff, C.L. (2011). The Present and Future of Peptide Vaccines for Cancer. *The Cancer Journal* 17, 343–350.
- Solit, D.B., and Rosen, N. (2011). Resistance to BRAF inhibition in melanomas. *N. Engl. J. Med.* 364, 772–774.
- Somerville, R.P., Devillier, L., Parkhurst, M.R., Rosenberg, S.A., and Dudley, M.E. (2012). Clinical scale rapid expansion of lymphocytes for adoptive cell transfer therapy in the WAVE® bioreactor. *Journal of Translational Medicine* 10, 69.
- Speir, J.A., Stevens, J., Joly, E., Butcher, G.W., and Wilson, I.A. (2001). Two different, highly exposed, bulged structures for an unusually long peptide bound to rat MHC class I RT1-Aa. *Immunity* 14, 81–92.
- Speiser, D.E., Baumgaertner, P., Voelter, V., Devevre, E., Barbey, C., Rufer, N., and Romero, P. (2008). Unmodified self antigen triggers human CD8 T cells with stronger tumor reactivity than altered antigen. *Proceedings of the National Academy of Sciences of the United States of America* 105, 3849–3854.

- Speiser, D.E., Liénard, D., Rufer, N., Rubio-Godoy, V., Rimoldi, D., Lejeune, F., Krieg, A.M., Cerottini, J.-C., and Romero, P. (2005). Rapid and strong human CD8⁺ T cell responses to vaccination with peptide, IFA, and CpG oligodeoxynucleotide 7909. *J. Clin. Invest.* *115*, 739–746.
- Steeg, P.S. (2016). Targeting metastasis. *Nat Cancer Rev* *16*, 201–218.
- Steimle, V., Siegrist, C.A., Mottet, A., Lisowska-Grospierre, B., and Mach, B. (1994). Regulation of MHC class II expression by interferon-gamma mediated by the transactivator gene CIITA. *Science* *265*, 106–109.
- Stern, L.J., and Wiley, D.C. (1994). Antigenic peptide binding by class I and class II histocompatibility proteins. *Structure* *2*, 245–251.
- Straten, P.T., Guldberg, P., Grønbaek, K., Hansen, M.R., Kirkin, A.F., Seremet, T., Zeuthen, J., and Becker, J.C. (1999). In situ T cell responses against melanoma comprise high numbers of locally expanded T cell clonotypes. *Journal Immunology* *163*, 443–447.
- Straten, P.T., Schrama, D., Andersen, M.H., and Becker, J.C. (2004). T-cell clonotypes in cancer. *Journal of Translational Medicine* *2*, 11.
- Studier, F.W., Rosenberg, A.H., Dunn, J.J., and Dubendorff, J.W. (1990). Use of T7 RNA polymerase to direct expression of cloned genes. *Meth. Enzymol.* *185*, 60–89.
- Svane, I.M., and Verdegaal, E.M. (2014). Achievements and challenges of adoptive T cell therapy with tumor-infiltrating or blood-derived lymphocytes for metastatic melanoma: what is needed to achieve standard of care? *Cancer Immunology, Immunotherapy* : CII *63*, 1081–1091.
- Szomolay, B., Liu, J., Brown, P.E., Miles, J.J., Clement, M., Llewellyn-Lacey, S., Dolton, G., Ekeruche-Makinde, J., Lissina, A., Schauburg, A.J., et al. (2016). Identification of human viral protein-derived ligands recognized by individual MHCI-restricted T-cell receptors. *Immunol. Cell Biol.*
- Takahama, Y. (2006). Journey through the thymus: stromal guides for T-cell development and selection. *Nature Rev Immunol* *6*, 127–135.
- Tan, M.P., Gerry, A.B., Brewer, J.E., Melchiori, L., Bridgeman, J.S., Bennett, A.D., Pumphrey, N.J., Jakobsen, B.K., Price, D.A., Ladell, K., et al. (2015). T cell receptor binding affinity governs the functional profile of cancer-specific CD8⁺ T cells. *Clin. Exp. Immunol.* *180*, 255–270.
- Tarhini, A.A., Cherian, J., Moschos, S.J., Tawbi, H.A., Shuai, Y., Gooding, W.E., Sander, C., and Kirkwood, J.M. (2012). Safety and efficacy of combination immunotherapy with interferon alfa-2b and tremelimumab in patients with stage IV melanoma. *J. Clin. Oncol.* *30*, 322–328.
- Théry, C., Brachet, V., Regnault, A., Rescigno, M., Ricciardi-Castagnoli, P., Bonnerot, C., and Amigorena, S. (1998). MHC class II transport from lysosomal compartments to the cell surface is determined by stable peptide binding, but not by the cytosolic domains of the alpha- and beta-chains. *The Journal of Immunology* *161*, 2106–2113.
- Thiery, J., Keefe, D., Boulant, S., Boucrot, E., Walch, M., Martinvalet, D., Goping, I.S., Bleackley, R.C., Kirchhausen, T., and Lieberman, J. (2011). Perforin pores in the endosomal membrane trigger the release of endocytosed granzyme B into the cytosol of target cells. *Nat Immunol* *12*, 770–777.
- Thomas, L. (1982). On immunosurveillance in human cancer. *Yale J Biol Med* *55*, 329–333.
- Tickle, I.J., Laskowski, R.A., and Moss, D.S. (2000). Rfree and the rfree ratio. II. Calculation Of the expected values and variances of cross-validation statistics in macromolecular least-squares refinement. *Acta Crystallographica. Section D, Biological Crystallography* *56*, 442–450.
- Tonegawa, S. (1983). Somatic generation of antibody diversity. *Nature* *302*, 575–581.
- Topalian, S.L., Gonzales, M.I., Parkhurst, M., Li, Y.F., Southwood, S., Sette, A., Rosenberg, S.A., and Robbins, P.F. (1996). Melanoma-specific CD4⁺ T cells recognize nonmutated HLA-DR-restricted tyrosinase epitopes. *Journal of Experimental Medicine* *183*, 1965–1971.
- Topalian, S.L., Hodi, F.S., Brahmer, J.R., Gettinger, S.N., Smith, D.C., McDermott, D.F., Powderly, J.D., Carvajal, R.D., Sosman, J.A., Atkins, M.B., et al. (2012). Safety, Activity, and Immune Correlates of Anti-PD-1 Antibody in Cancer. *N. Engl. J. Med.* *366*, 2443–2454.
- Trajanoski, Z., Maccalli, C., Mennonna, D., Casorati, G., Parmiani, G., and Dellabona, P. (2015). Somatically mutated tumor antigens in the quest for a more efficacious patient-oriented immunotherapy of cancer. *Cancer Immunol Immunother* *64*, 99–104.

- Tran, E., Turcotte, S., Gros, A., Robbins, P.F., Lu, Y.C., Dudley, M.E., Wunderlich, J.R., Somerville, R.P., Hogan, K., Hinrichs, C.S., et al. (2014). Cancer Immunotherapy Based on Mutation-Specific CD4+ T Cells in a Patient with Epithelial Cancer. *Science* *344*, 641–645.
- Tran, K.Q., Zhou, J., Durlinger, K.H., Langhan, M.M., Shelton, T.E., Wunderlich, J.R., Robbins, P.F., Rosenberg, S.A., and Dudley, M.E. (2008). Minimally cultured tumor-infiltrating lymphocytes display optimal characteristics for adoptive cell therapy. *J. Immunother.* *31*, 742–751.
- Trautmann, L., Labarrière, N., Jotereau, F., Karanikas, V., Gervois, N., Connerotte, T., Coulie, P., and Bonneville, M. (2002). Dominant TCR V alpha usage by virus and tumor-reactive T cells with wide affinity ranges for their specific antigens. *European Journal of Immunology* *32*, 3181–3190.
- Traversari, C., van der Bruggen, P., Van den Eynde, B., Hainaut, P., Lemoine, C., Ohta, N., Old, L., and Boon, T. (1992). Transfection and expression of a gene coding for a human melanoma antigen recognized by autologous cytolytic T lymphocytes. *Immunogenetics* *35*, 145–152.
- Tsang, K.Y., Jochems, C., and Schlom, J. (2015). Insights on Peptide Vaccines in Cancer Immunotherapy. In *Developments in T Cell Based Cancer Immunotherapies*, P.A. Ascierto, D.F. Stronck, and E. Wang, eds. (Springer International Publishing), pp. 1–27.
- Tungatt, K., Bianchi, V., Crowther, M.D., Powell, W.E., Schauenburg, A.J., Trimby, A., Donia, M., Miles, J.J., Holland, C.J., Cole, D.K., et al. (2015). Antibody stabilization of peptide-MHC multimers reveals functional T cells bearing extremely low-affinity TCRs. *J. Immunol.* *194*, 463–474.
- Turley, S.J., Cremasco, V., and Astarita, J.L. (2015). Immunological hallmarks of stromal cells in the tumour microenvironment. *Nature Rev Immunol* *15*, 669–682.
- Turner, S.J., Doherty, P.C., McCluskey, J., and Rossjohn, J. (2006). Structural determinants of T-cell receptor bias in immunity. *Nature Rev Immunol* *6*, 883–894.
- Tynan, F.E., Burrows, S.R., Buckle, A.M., Clements, C.S., Borg, N.A., Miles, J.J., Beddoe, T., Whisstock, J.C., Wilce, M.C., Silins, S.L., et al. (2005). T cell receptor recognition of a “super-bulged” major histocompatibility complex class I-bound peptide. *Nature Immunology* *6*, 1114–1122.
- Ullenhag, G.J., Sadeghi, A.M., Carlsson, B., Ahlström, H., Mosavi, F., Wagenius, G., and Tötterman, T.H. (2011). Adoptive T-cell therapy for malignant melanoma patients with TILs obtained by ultrasound-guided needle biopsy. *Cancer Immunol Immunother* *61*, 725–732.
- Valmori, D., Fonteneau, J.F., Lizana, C.M., Gervois, N., Liénard, D., Rimoldi, D., Jongeneel, V., Jotereau, F., Cerottini, J.C., and Romero, P. (1998). Enhanced generation of specific tumor-reactive CTL in vitro by selected Melan-A/MART-1 immunodominant peptide analogues. *The Journal of Immunology* *160*, 1750–1758.
- van den Berg, J.H., Gomez-Eerland, R., van de Wiel, B., Hulshoff, L., van den Broek, D., Bins, A., Tan, H.L., Harper, J.V., Hassan, N.J., Jakobsen, B.K., et al. (2015). Case Report of a Fatal Serious Adverse Event Upon Administration of T Cells Transduced With a MART-1-specific T-cell Receptor. 1–10.
- Van den Eynde, B.J., and van der Bruggen, P. (1997). T cell defined tumor antigens. *Curr. Opin. Immunol.* *9*, 684–693.
- van der Bruggen, P., Bastin, J., Gajewski, T., Coulie, P.G., Boël, P., De Smet, C., Traversari, C., Townsend, A., and Boon, T. (1994). A peptide encoded by human gene MAGE-3 and presented by HLA-A2 induces cytolytic T lymphocytes that recognize tumor cells expressing MAGE-3. *Eur. J. Immunol.* *24*, 3038–3043.
- van der Bruggen, P., Traversari, C., Chomez, P., Lurquin, C., De Plaen, E., Van den Eynde, B., Knuth, A., and Boon, T. (1991). A gene encoding an antigen recognized by cytolytic T lymphocytes on a human melanoma. *Science* *254*, 1643–1647.
- van der Merwe, P.A., and Davis, S.J. (2003). Molecular interactions mediating T cell antigen recognition. *Annu. Rev. Immunol.* *21*, 659–684.
- van Duinen, S.G., Ruiter, D.J., Broecker, E.B., van der Velde, E.A., Sorg, C., Welvaart, K., and Ferrone, S. (1988). Level of HLA antigens in locoregional metastases and clinical course of the disease in patients with melanoma. *Cancer Research* *48*, 1019–1025.
- van Rooij, N., van Buuren, M.M., Philips, D., Velds, A., Toebes, M., Heemskerk, B., van Dijk, L.J.A., Behjati, S., Hilkmann, H., Atmioui, el, D., et al. (2013). Tumor Exome Analysis Reveals Neoantigen-Specific T-Cell Reactivity in an Ipilimumab-Responsive Melanoma. *J. Clin. Oncol.* *31*, e439–e442.
- van Vreeswijk, H., Ruiter, D.J., Bröcker, E.B., Welvaart, K., and Ferrone, S. (1988). Differential expression of HLA-DR, DQ, and DP

antigens in primary and metastatic melanoma. *J. Invest. Dermatol.* *90*, 755–760.

Varela-Rohena, A., Carpenito, C., Perez, E.E., Richardson, M., Parry, R.V., Milone, M., Scholler, J., Hao, X., Mexas, A., Carroll, R.G., et al. (2008). Genetic engineering of T cells for adoptive immunotherapy. *Immunologic Research* *42*, 166–181.

Venturi, V., Kedzierska, K., Price, D.A., Doherty, P.C., Douek, D.C., Turner, S.J., and Davenport, M.P. (2006). Sharing of T cell receptors in antigen-specific responses is driven by convergent recombination. *Proceedings of the National Academy of Sciences* *103*, 18691–18696.

Venturi, V., Price, D.A., Douek, D.C., and Davenport, M.P. (2008). The molecular basis for public T-cell responses? *Nature Rev Immunol* *8*, 231–238.

Vigneron, N., and Van den Eynde, B.J. (2014). Proteasome subtypes and regulators in the processing of antigenic peptides presented by class I molecules of the major histocompatibility complex. *Biomolecules* *4*, 994–1025.

Vigneron, N., Stroobant, V., van den Eynde, B.J., and van der Bruggen, P. (2013). Database of T cell-defined human tumor antigens: the 2013 update. *Cancer Immunity* *13*, 15.

Viguier, M., Lemaitre, F., Verola, O., Cho, M.S., Gorochov, G., Dubertret, L., Bachelez, H., Kourilsky, P., and Ferradini, L. (2004). Foxp3 Expressing CD4+CD25high Regulatory T Cells Are Overrepresented in Human Metastatic Melanoma Lymph Nodes and Inhibit the Function of Infiltrating T Cells. *The Journal of Immunology* *173*, 1444–1453.

Vogelstein, B., Papadopoulos, N., Velculescu, V.E., Zhou, S., Diaz, L.A., and Kinzler, K.W. (2013). Cancer genome landscapes. *Science* *339*, 1546–1558.

Vonderheide, R.H., Hahn, W.C., Schultze, J.L., and Nadler, L.M. (1999). The telomerase catalytic subunit is a widely expressed tumor-associated antigen recognized by cytotoxic T lymphocytes. *Immunity* *10*, 673–679.

Vonderheide, R.H., and June, C.H. (2013). Engineering T cells for cancer: our synthetic future. *Immunol. Rev.* *257*, 7–13.

Voskoboinik, I., Dunstone, M.A., Baran, K., Whisstock, J.C., and Trapani, J.A. (2010). Perforin: structure, function, and role in human immunopathology. *Immunol. Rev.* *235*, 35–54.

Wagner, S.N., Schultewolter, T., Wagner, C., Briedigkeit, L., Becker, J.C., Kwasnicka, H.M., and Goos, M. (1998). Immune response against human primary malignant melanoma: a distinct cytokine mRNA profile associated with spontaneous regression. *Lab. Invest.* *78*, 541–550.

Wagner, S.N., Wagner, C., Schultewolter, T., and Goos, M. (1997). Analysis of Pmel17/gp100 expression in primary human tissue specimens: implications for melanoma immuno- and gene-therapy. *Cancer Immunology, Immunotherapy* : *CII* *44*, 239–247.

Wang, H.Y., Lee, D.A., Peng, G., Guo, Z., Li, Y., Kiniwa, Y., Shevach, E.M., and Wang, R.F. (2004). Tumor-specific human CD4+ regulatory T cells and their ligands: implications for immunotherapy. *Immunity* *20*, 107–118.

Wang, L., Rubinstein, R., Lines, J.L., Wasiuk, A., Ahonen, C., Guo, Y., Lu, L.-F., Gondek, D., Wang, Y., Fava, R.A., et al. (2011). VISTA, a novel mouse Ig superfamily ligand that negatively regulates T cell responses. *J. Exp. Med.* *208*, 577–592.

Wang, R.F., Robbins, P.F., Kawakami, Y., Kang, X.Q., and Rosenberg, S.A. (1995). Identification of a gene encoding a melanoma tumor antigen recognized by HLA-A31-restricted tumor-infiltrating lymphocytes. *Journal of Experimental Medicine* *181*, 799–804.

Wang, R.F. (2006). Immune suppression by tumor-specific CD4+ regulatory T-cells in cancer. *Semin. Cancer Biol.* *16*, 73–79.

Wang, T., Wang, T., Wei, J.J., Wei, J.J., Sabatini, D.M., Sabatini, D.M., Lander, E.S., and Lander, E.S. (2014). Genetic screens in human cells using the CRISPR-Cas9 system. *Science* *343*, 80–84.

Weber, J.S., Hua, F.L., Spears, L., Marty, V., Kuniyoshi, C., and Celis, E. (1999). A phase I trial of an HLA-A1 restricted MAGE-3 epitope peptide with incomplete Freund's adjuvant in patients with resected high-risk melanoma. *Journal of Immunotherapy* *22*, 431–440.

Weber, J.S., D'Angelo, S.P., Minor, D., Hodi, F.S., Gutzmer, R., Neyns, B., Hoeller, C., Khushalani, N.I., Miller, W.H., Lao, C.D., et al. (2015). Nivolumab versus chemotherapy in patients with advanced melanoma who progressed after anti-CTLA-4 treatment (CheckMate 037): a randomised, controlled, open-label, phase 3 trial. *Lancet Oncol.* *16*, 375–384.

Weidanz, J.A., Nguyen, T., Woodburn, T., Neethling, F.A., Chiriva-Internati, M., Hildebrand, W.H., and Lustgarten, J. (2006). Levels of specific peptide-HLA class I complex predicts tumor cell susceptibility to CTL killing. *The Journal of Immunology* *177*, 5088–5097.

- Wenzel, J., Bekisch, B., Uerlich, M., Haller, O., Bieber, T., and Tüting, T. (2005). Type I interferon-associated recruitment of cytotoxic lymphocytes: a common mechanism in regressive melanocytic lesions. *Am. J. Clin. Pathol.* *124*, 37–48.
- Wieckowski, S., Baumgaertner, P., Corthesy, P., Voelter, V., Romero, P., Speiser, D.E., and Rufer, N. (2009). Fine structural variations of alphabetaTCRs selected by vaccination with natural versus altered self-antigen in melanoma patients. *Journal Immunology* *183*, 5397–5406.
- Willcox, B.E., Gao, G.F., Wyer, J.R., Ladbury, J.E., Bell, J.I., Jakobsen, B.K., and van der Merwe, P.A. (1999). TCR binding to peptide-MHC stabilizes a flexible recognition interface. *Immunity* *10*, 357–365.
- Williams, N.S., and Engelhard, V.H. (1996). Identification of a population of CD4+ CTL that utilizes a perforin- rather than a Fas ligand-dependent cytotoxic mechanism. *The Journal of Immunology* *156*, 153–159.
- Winter, G. (2010). xia2: an expert system for macromolecular crystallography data reduction. *Journal of Applied Crystallography* *43*, 186–190.
- Wooldridge, L., Ekeruche-Makinde, J., van den Berg, H.A., Skowera, A., Miles, J.J., Tan, M.P., Dolton, G., Clement, M., Llewellyn-Lacey, S., Price, D.A., et al. (2012). A single autoimmune T cell receptor recognizes more than a million different peptides. *J. Biol. Chem.* *287*, 1168–1177.
- Wyer, J., Willcox, B., Gao, G., Gerth, U., Davis, S., Bell, J., Merwe, P., and Jakobsen, B. (1999). T cell receptor and coreceptor CD8 alphaalpha bind peptide-MHC independently and with distinct kinetics. *Immunity* *10*, 219–225.
- Xing, Y., and Hogquist, K.A. (2012). T-cell tolerance: central and peripheral. *Cold Spring Harb Perspect Biol* *4*, a006957–a006957.
- Yamasaki, S., Ishikawa, E., Sakuma, M., Ogata, K., Sakata-Sogawa, K., Hiroshima, M., Wiest, D.L., Tokunaga, M., and Saito, T. (2006). Mechanistic basis of pre-T cell receptor-mediated autonomous signaling critical for thymocyte development. *Nat Immunol* *7*, 67–75.
- Yamshchikov, G., Thompson, L., Ross, W.G., Galavotti, H., Aquila, W., Deacon, D., Caldwell, J., Patterson, J.W., Hunt, D.F., and Slingluff, C.L. (2001). Analysis of a natural immune response against tumor antigens in a melanoma survivor: lessons applicable to clinical trial evaluations. *Clinical Cancer Research* *7*, 909s–916s.
- Yannelli, J.R., Hyatt, C., McConnell, S., Hines, K., Jacknin, L., Parker, L., Sanders, M., and Rosenberg, S.A. (1996). Growth of tumor-infiltrating lymphocytes from human solid cancers: summary of a 5-year experience. *Int. J. Cancer* *65*, 413–421.
- Yao, X., Ahmadzadeh, M., Lu, Y.-C., Liewehr, D.J., Dudley, M.E., Liu, F., Schrumpp, D.S., Steinberg, S.M., Rosenberg, S.A., and Robbins, P.F. (2012). Levels of peripheral CD4(+)FoxP3(+) regulatory T cells are negatively associated with clinical response to adoptive immunotherapy of human cancer. *Blood* *119*, 5688–5696.
- Yasukawa, M., Ohminami, H., Arai, J., Kasahara, Y., Ishida, Y., and Fujita, S. (2000). Granule exocytosis, and not the fas/fas ligand system, is the main pathway of cytotoxicity mediated by alloantigen-specific CD4(+) as well as CD8(+) cytotoxic T lymphocytes in humans. *Blood* *95*, 2352–2355.
- Yee, C., Thompson, J.A., Byrd, D., Riddell, S.R., Roche, P., Celis, E., and Greenberg, P.D. (2002). Adoptive T cell therapy using antigen-specific CD8+ T cell clones for the treatment of patients with metastatic melanoma: in vivo persistence, migration, and antitumor effect of transferred T cells. *Proceedings of the National Academy of Sciences* *99*, 16168–16173.
- Yi, E.H., Yoo, H., Noh, K.H., Han, S., Lee, H., Lee, J.-K., Won, C., Kim, B.-H., Kim, M.-H., Cho, C.-H., et al. (2013). BST-2 is a potential activator of invasion and migration in tamoxifen-resistant breast cancer cells. *Biochem. Biophys. Res. Commun.* *435*, 685–690.
- Yui, M.A., and Rothenberg, E.V. (2014). Developmental gene networks: a triathlon on the course to T cell identity. *Nature Rev Immunol* *14*, 529–545.
- Zaloudik, J., Moore, M., Ghosh, A.K., Mechl, Z., and Rejthar, A. (1988). DNA content and MHC class II antigen expression in malignant melanoma: clinical course. *J. Clin. Pathol.* *41*, 1078–1084.
- Zarnitsyna, V.I., Evavold, B.D., Schoettle, L.N., Blattman, J.N., and Antia, R. (2013). Estimating the diversity, completeness, and cross-reactivity of the T cell repertoire. *Front. Immunol.* *4*, 485.
- Zarour, H.M., Kirkwood, J.M., Kierstead, L.S., Herr, W., Brusic, V., Slingluff, C.L., Sidney, J., Sette, A., and Storkus, W.J. (2000). Melan-A/MART-1(51-73) represents an immunogenic HLA-DR4-restricted epitope recognized by melanoma-reactive CD4(+) T cells. *Proceedings of the National Academy of Sciences* *97*, 400–405.
- Zeng, R., Spolski, R., Finkelstein, S.E., Oh, S., Kovanen, P.E., Hinrichs, C.S., Pise-Masison, C.A., Radonovich, M.F., Brady, J.N., Restifo, N.P., et al. (2005). Synergy of IL-21 and IL-15 in regulating CD8+ T cell expansion and function. *Journal of Experimental Medicine* *201*, 139–148.

Zhang, L., Kerkar, S.P., Yu, Z., Zheng, Z., Yang, S., Restifo, N.P., Rosenberg, S.A., and Morgan, R.A. (2011). Improving adoptive T cell therapy by targeting and controlling IL-12 expression to the tumor environment. *Mol Ther* *19*, 751–759.

Zhou, J., Dudley, M.E., Rosenberg, S.A., and Robbins, P.F. (2004). Selective growth, in vitro and in vivo, of individual T cell clones from tumor-infiltrating lymphocytes obtained from patients with melanoma. *The Journal of Immunology* *173*, 7622–7629.

Zhou, J., Dudley, M.E., Rosenberg, S.A., and Robbins, P.F. (2005). Persistence of multiple tumor-specific T-cell clones is associated with complete tumor regression in a melanoma patient receiving adoptive cell transfer therapy. *Journal of Immunotherapy* *28*, 53–62.

Zhu, J., and Paul, W.E. (2008). CD4 T cells: fates, functions, and faults. *Blood* *112*, 1557–1569.

Zhu, Y.Y., Machleder, E.M., Chenchik, A., Li, R., and Siebert, P.D. (2001). Reverse transcriptase template switching: a SMART approach for full-length cDNA library construction. *BioTechniques* *30*, 892–897.

Zinkernagel, R.M., and Doherty, P.C. (1997). The discovery of MHC restriction. *Immunol. Today* *18*, 14–17.